THE FEASIBILITY OF PERVAPORATION IN THE PURIFICATION OF ETHANOL

A thesis presented in partial fulfilment of the requirements for the degree of Doctor of Philosophy in Process and Environmental Technology at Massey University.

Lílian de Barros Ferreira

1998

All animals, except man, know that the principal business of life is to enjoy it.

S. Butler.

Abstract

This study investigated how pervaporation could be incorporated into hybrid schemes for purifying ethanol produced from whey of fusel oils and whether this could be achieved at a lower energy cost than distillation alone whilst maintaining product quality within specification. In order to achieve these objectives the project included: investigation of fundamental pervaporation mechanisms and the influence of operation parameters, simulation of the distillation train at the New Zealand Distillery Co. Ltd. (NZDCL) including pervaporation relationships developed during this study, and pinch analysis of the NZDCL.

Aqueous solutions of 5 to 20% w/w ethanol with approximately 1% w/w of a mixture of *n*-propanol, *i*-butanol, *n*-butanol, *i*-amyl alcohol and ethyl acetate were pervaporated through a disk apparatus fitted with either poly-ether-block-amide (PEBA) or poly(dimethyl siloxane) membranes. Similar solutions were sorbed into PEBA beads for the study of sorption.

A new, semi-empirical relationship between enrichment factor of alcohols during pervaporation and their molecular size and activity coefficient in the feed stream was proposed. It was observed that for organophilic membranes, sorption generally sets the enrichment factor while the influence of diffusion becomes relevant only when the distribution range of the size of the molecules involved is quite large. In consequence, it is recommended that the study of sorption and diffusion relationships between solvents and dense polymers be given priority as they are relevant for the fast development of this technology.

During pervaporation, the temperature of the feed affected mainly the process economics, as an increase in temperature resulted in an exponential increase in the total flux, without significantly changing the product composition.

The flux of the minor components studied was independent of the total flux through the membrane except for the *i*-amyl alcohol, which had its flux influenced by the total flux possibly due to its higher concentration.

For the removal of fusels from the fermentation broth with organophilic membranes, all three commercially available membranes investigated presented similar enrichment factors and, compared to evaporation, did not significantly improve the separation of fusels from ethanol. The membranes investigated differed amongst each other with respect to their total flux; the higher the flux through the membrane, the lower the membrane area required for a specific separation.

Hydrophilic membranes were used to remove the water fraction at an earlier stage of distillation. Simulation and experiments of the new process showed that it was possible to reduce design complexity and energy expenditure by approximately ten percent. This process could become economically feasible if membrane price dropped by over 60%.

Pinch analysis and simulation results of distillation were combined to investigate immediate opportunities to reduce energy usage at NZDCL. Changes in the heat exchanger network and in the distillation feed temperature could reduce production costs (steam usage) without compromising product quality and plant flexibility.

Acknowledgements

I would like to thank my supervisors *John Mawson* and *Don Cleland* for the opportunity to do this work and for their trust, guidance, and support throughout my studies, I thank *Stephen White* and *Prof. Ross Taylor* (Clarkson University, USA) for the constructive criticism and for sharing their knowledge in moments of need.

I would also like to thank *Moacir Kaminski*, professor at the Federal University of Paraná, Brazil, and *Edgar Liebold*, of BASF Ludwigshafen - AG, Germany, for their unconditional friendship, support, and help in the technical or personal aspects of this thesis.

This thesis could not have been completed without the dedication of all staff at the New Zealand Distillery Co. Ltd., that collected samples and helped me throughout the project by providing information freely and accurately; the technical staff at the Institute of Technology and Engineering at Massey University, that built and kept all experimental apparatus in running condition; and the Library staff.

Many a Wednesday or Thursday evening was spent in the company of *Stephanie* and *Camille*, who kept me sane, in touch with the world around, and motivated to bring this work to completion.

I thank my parents and sister, *Henrique, Heloisa* and *Eliane*, for their love and trust. Last but not least, I would like to thank *Stephen van Eyk* for sharing his wisdom through the ups and downs of the past four years, supporting me with his love, understanding, and endless faith.

This project was supported financially by the New Zealand Distillery Co. Ltd., the ECNZ, the BoP Electricity, and by Massey University. Pervaporation membranes were generously supplied by GFT/Deutche Carbone AG and GKSS Forschungszentrum, Germany. Membrane polymers were supplied by GKSS and Elf-Atochem (Pty) Australia.

TABLE OF CONTENTS

List of Figures

Chapter V

Chapter VII

Chapter IX

Chapter X

Chapter XI

Appendix B

Appendix C

List of Tables

Chapter II

Chapter IV

Chapter V

Appendix A

Chapter 1

INTRODUCTION

Since 1980, the ethanol consumed in New Zealand has been produced from the fermentation of deproteinated whey, a former waste product of the dairy industry. Significant export opportunities exist if the New Zealand production capacity increases.

As in all ethanol fermentation processes, whey fermentation produces a small amount (less than one percent of the total ethanol produced) of higher alcohols, known as fusel oils, and esters that impart aroma to the product. For high-grades of industrial ethanol and for neutral spirits, the presence of this aroma fraction is undesired. During distillation, steam injection provides the energy required for the concentration of ethanol and helps in the removal of the fusel oils. Overall, it is estimated that steam consumption for distillation constitutes a quarter of the total production cost of whey ethanol, with perhaps half of this energy spent at the stages required for fusel oil removal (Mawson, 1987).

Throughout the chemical industry it is estimated that approximately fifty percent of all capital investment and running costs are associated with separation. Distillation alone accounts for fifteen percent of the industrial energy consumption (Fell, 1997). Since the oil crisis in 1974, the chemical industry has been continuously aware of the need for energy conservation if it is to remain competitive and meet the increasing environmental regulations, in particular the reduction of carbon dioxide emission.

The New Zealand Distillery Co. Ltd. (NZDCL) whey facility was established at Edgecumbe, NZ, in 1982. Since 1977, while still based in Auckland and processing grain, the company committed to actively pursuing a reduction in energy consumption. In 1980, in anticipation of its move to Edgecumbe, the company reached an agreement with the neighbouring dairy company to purchase the steam required for its process, thus allowing their boilers to run at optimum rates. It was also the first distilling company in New

Zealand to implement a heat exchanger network and a flash cooling train that aimed at the recovery of heat and steam, thus reducing the total steam usage by at least twenty percent.

In recent times, the company installed a pervaporation unit for the dehydration of ethanol past its azeotropic point. Consistent to its commitment to research and development in process optimization, the present study was commissioned to investigate whether pervaporation could be incorporated into hybrid schemes for purifying ethanol at an earlier stage in the process and whether this could be achieved at a lower energy cost than distillation alone whilst maintaining product quality within specification. In order to achieve these objectives the project included: a fundamental investigation of pervaporation mechanisms and the influence of operation parameters, wrapped with simulation of the distillation train at New Zealand Distillery Co. Ltd. (NZDCL) with and without pervaporation, and pinch analysis of the NZDCL process.

This study was divided into four parts. In Part One, the fundamentals of pervaporation are reviewed and the experimental results relative to pervaporation mechanisms are reported and discussed. In Part Two the impact of introducing a pervaporation unit to the distillation scheme is evaluated and relevant techniques used for this evaluation, such as distillation modelling and heat integration analysis, are also addressed. Part Three comprises the conclusions of the study. Lastly, Part Four is a compilation of all Appendices.

Part One

FUNDAMENTALS

Chapter II

LITERATURE REVIEW: FUNDAMENTALS

II.1 BACKGROUND

Pervaporation is a separation process based on the selective transport of feed components across a membrane followed by evaporation of the permeate on the product side of the membrane. The term pervaporation was first introduced by Kober (1917) who, unable to explain the evaporation from a liquid contained in a sealed collodion bag, concluded that the liquid was transported through the membrane and evaporated into the atmosphere.

However, it took almost seven decades for the first commercial pervaporation plant to be commissioned. As pervaporation performance is a consequence of membrane selectivity and membrane thickness, the introduction of pervaporation was necessarily linked to the development of membranes. Thus Wijmans *et al.* (1994) noted that "[the pervaporation mechanisms were] ... first studied in a systematic fashion by Binning, Lee, and co-workers at the American Oil in the early 1950s...[, however] membrane fabrication technology at that time did not allow production of the high-performance membranes and modules required for a commercially competitive process." It is only in the last decade that highly selective membranes have become commercially available and since then, the study of pervaporation mechanisms has been seized upon with renewed interest.

II.2 PERVAPORATION TERMINOLOGY

The terminology used in this study will follow the guidelines set by Böddeker (1990). Flux, selectivity, and energy consumption are the main parameters employed in the assessment of pervaporation performance. Flux, defined as the product of the permeability and the driving force, is usually taken to be inversely proportional to the membrane thickness. Throughout

this study, membrane thickness will be taken to be the dry thickness, regardless of the degree of swelling of the membrane.

In pervaporation, selectivity is usually expressed by the separation factor (α) or by the enrichment factor (β). The separation factor (α) resembles the relative volatility of the components of binary liquid mixtures:

$$\alpha_{ij} = \frac{\left(\frac{c_i}{c_j}\right)^p}{\left(\frac{c_i}{c_j}\right)^f} \qquad [II.1]$$

where, c concentration;

f feed;

i preferentially permeating species;

j non-preferentially permeating species;

p permeate.

The enrichment factor (β) is the ratio of the concentration of the preferentially permeating species in the permeate to that in the feed (Equation II.2) and it is related to the solute rejection (R) used to describe reverse osmosis (RO) performance:

$$\beta = \frac{c_i^p}{c_i^f} \qquad [II.2]$$

$$\beta = 1 - R \qquad [II.3]$$

II.3 Overview of mechanisms

Figure II.1 schematically depicts a pervaporation unit. The feed stream is pre-heated prior to entering the membrane cell and the energy stored in the feed stream is used in the evaporation of the permeate on the product side of the membrane. Inside the membrane cell, the feed is separated from the permeate by a dense, non-porous membrane. Transport of feed components across the membrane results from a difference in chemical potential between the feed-side and the permeate-side of the membrane and from the different affinities of components for the membrane. In order to maintain the driving force of the process (i.e. the difference in chemical potential across the membrane), the permeate is removed from the product side of the membrane by a vacuum pump as soon as it desorbs; alternatively a sweep gas, such as nitrogen or water vapour, may be used. The permeate may then be condensed downstream before further processing.

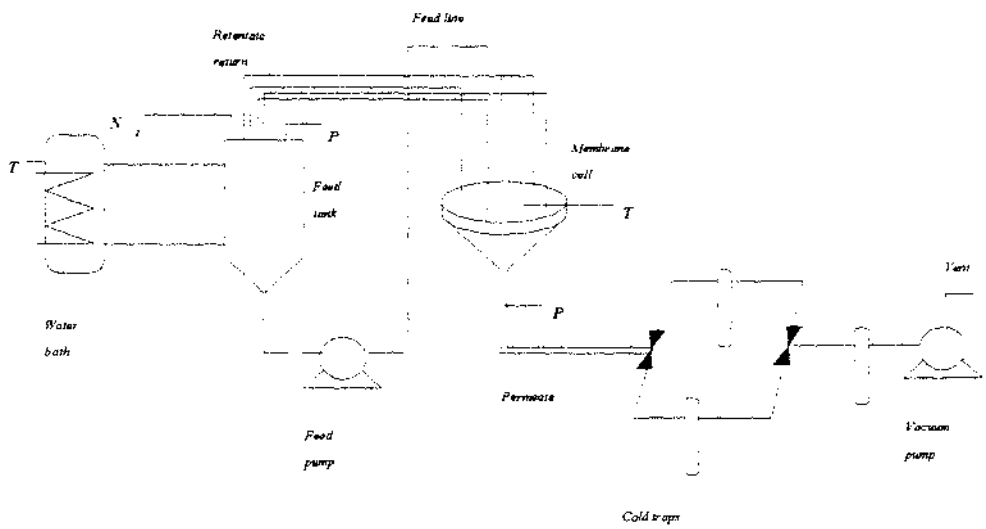

Figure II.1 Schematic drawing of a pervaporation rig.
T: temperature measurement; P: pressure measurement.

Beaumelle & Marin (1994) described pervaporation as a succession of seven stages:

(1) diffusion from the liquid bulk to the membrane interphase;

(2) sorption into the membrane;

(3) diffusion across the non-porous, polymeric layer;

(4) desorption;

(5) transport of the vapour across the porous support;

(6) transport of the vapour to the condenser;

(7) condensation of the permeate.

Item (1) describes mass transfer resistance on the feed side of the membrane - transport across the boundary layer; items (2) to (4) relate to transport through the membrane; and items (5) to (7) comprise mass transfer resistance on the permeate side of the membrane.

II.3.1 THE RESISTANCE-IN-SERIES MODEL

As a consequence of separating the pervaporation mechanisms into such distinct stages, it is customary to represent the pervaporation process using a resistance-in-series model, by summing all resistances to the transport of a molecule from the bulk of the feed stream to the condenser. The flux across the membrane is described as proportional to the driving force and inversely proportional to the sum of all resistances involved (Equations II.4 and II.5), and the resistances to transport are defined as the inverses of the mass transfer coefficients (Equation II.6) (Mulder, 1991).

$$J = \frac{\Delta\mu}{R_{TOT}} \qquad [II.4]$$

$$R_{TOT} = R_{bl} + R_m + R_p + R_c \qquad [II.5]$$

$$R = \frac{1}{k} \qquad [II.6]$$

where, J flux;

k mass transfer coefficient;

R resistance to transport;

R_{TOT} sum of all resistances to transport;

R_m resistance to transport across the membrane;

R_p resistance to transport across the porous support;

R_c resistance to transport across the vacuum line;

$\Delta\mu$ driving force.

II.3.1.1 MASS TRANSFER RESISTANCE ON THE FEED SIDE

The resistance to diffusion of the feed components from the liquid bulk to the membrane interface (stage 1) results in a difference in the composition at the membrane interface from the bulk composition (Böddeker, 1990). This phenomenon is known as concentration polarization. To date, there are no precise guidelines for the levels of operating parameters that will induce concentration polarization. However, concentration polarization is a consequence of separation and its severity is increased by low feed concentration, low feed flow rate, and high membrane selectivity. A detailed discussion of concentration polarization can be found in Karlsson (1996).

For concentration polarization, the mass transfer coefficient across the boundary layer can be calculated via a semi-empirical Sherwood correlation. The Sherwood constants for pervaporation systems can be found in Colman & Mitchell (1991), Mulder (1991), Rautenbach *et al.* (1991), Beaumelle *et al.* (1993), Field (1993), Ji *et al.* (1994a), Rautenbach & Helmuls (1994), and Karlsson (1996).

Ji *et al.* (1994b) observed that in the pervaporation of dilute, aqueous solutions of methylene chloride, toluene, and trichloroethane the resistance of the boundary layer accounted for 48% of the total resistance. In this experiment, a reduction in the feed flow rate resulted in an increase in the boundary layer resistance, which was followed by a reduction of the organic components concentrations at the membrane interface. To maintain the same level of separation prior to the reduction of the feed flow rate it was necessary to increase the membrane area, thus increasing the costs of the equipment. For a fixed Reynolds number, a decrease in membrane thickness resulted in an increase in the permeability of the membrane (higher flux). This further reduced the concentration of theorganic components

at the membrane interface, thus increasing the concentration polarization and decreasing the membrane selectivity towards organic components.

Although the common belief assumes that the boundary layer resistance tends to occur with laminar flow (Feng & Huang, 1994), data from Lamer *et al.* (1994) showed that for the faster permeating species, the boundary layer resistance was not negligible even at turbulent feed conditions. A comparison of the pervaporation of dilute, aqueous solutions of ethyl hexanoate and ethyl ethanoate showed that for the former, the faster permeating component, the boundary layer resistance could be as high as 30% of the total resistance to transport even at turbulent feed conditions, while for the latter, the boundary layer resistance remained below 2%.

Gref *et al.* (1992) also noted that concentration polarization may occur under high feed concentrations, provided that the membrane presents high selectivity and permeability to the preferentially permeating species. This conclusion was derived from observation of the pervaporation of a mixture of *n*-octanol in water at 4.7 % (w/w). The membrane used (cellulose acetate) gave a selectivity (α) of over 2000 for *n*-octanol. This result was supported by the observations of Ji *et al.* (1994b) for the pervaporation of toluene and methylene chloride through organophilic membranes. It means that efforts to increase membrane permeability by reducing membrane thickness may result in reduction of permeation of the faster permeating species in relation to the total flux due to an increase in concentration polarization at the boundary layer.

Rautenbach & Helmus (1994) pointed out that failure to account for the occurrence of concentration polarization and transport resistance through the porous support may cause an overestimation of the separation potential of a membrane. With laminar flow, the actual pervaporation fluxes can be reduced up to 60% compared to those predicted based on the resistance through the membrane only.

In general, concentration polarization can be reduced by changes in the module dimensions, by creating turbulence, or by breaking the boundary layer with pulsating flow, baffles and oscillatory flow (Colman & Mitchell, 1991; Mulder, 1991; Field, 1993; Karlsson, 1996).

Colman & Mitchell (1991) stated that the introduction of baffles can produce at a Reynolds number of 100 a separation equivalent to a Reynolds number of 10,000.

II.3.1.2 Resistance to transport across the membrane

Transport across the membrane is usually described as a combination of steps 2, 3 and 4 (sorption, diffusion and desorption), although desorption does not contribute to the transport resistances. The mechanism and equations developed to describe this process are reviewed in Section II.3.2.

II.3.1.3 Mass transfer resistance across the porous support and the vacuum line

Transport of vapour across a porous support might result in pressure losses which contribute to the reduction of the driving force. As a consequence of this pressure loss, the pressure at the membrane interface (vapour side) is higher than the pressure created by the vacuum pump and may reduce the permeate flow, which would in turn change the selectivity of the membrane. Therefore, failure to account for the effects of transport in the porous support could result in an overestimate of fluxes across the membrane.

The porous support is usually modelled as a number of capillaries in parallel, inside which either a viscous or a molecular flow pattern is assumed. Rautenbach & Albrecht (1984) described the correlations used to calculate the flow through the porous support, including corrections for the presence of tortuosities in the capillaries.

Lastly, the design of the vacuum line (linking the condenser to the pervaporation module) and operating parameters (condenser temperature and permeate pressure) become relevant when pervaporation is carried at low feed temperatures, such as 300 K, even at low permeate pressures (< 500 Pa). Under such conditions the permeate flux decreases with an increase in condenser temperature and with an increase in distance between the condenser and the

membrane. These influences are stronger the higher the permeate pressure. This behaviour was observed and modelled by Beaumelle & Marin (1994) for a mixture of water and ethanol permeating through poly(dimethyl siloxane) (PDMS).

In most cases vacuum is applied at the permeate side of the membrane and the activity of species *i* at the permeate side of the membrane tends to zero. When the permeate pressure cannot be considered negligible the equation developed by Watson & Payne (1990) applies:

$$\frac{p_i^p}{p_j^p} = \frac{P_i\, c_i^f}{P_j\, c_j^f}\left(1 - \frac{p_i^p}{p_i^f}\right) + \frac{p_i^p}{p_j^f} \qquad [II.7]$$

where, *i,j* binary solvents;

p partial pressure;

P permeability.

In Equation II.7, viscous flow at the membrane - vapour interface is assumed. If molecular flow occurs, Equation II.7 should be corrected by multiplying the right hand side by the square root of the ratio of the molecular weights of the permeating species, which means that a further enrichment in favour of the high molecular weight permeating species will take place (Watson & Payne, 1990).

Equation II.7 is useful in evaluating the effect of the partial pressure at the permeate side of the membrane on selectivity and flux. If the partial pressure of species *i* at the permeate side of the membrane tends to zero, then the equation shows that the separation process is controlled by the membrane. If the partial pressure of species *i* at the permeate side of the membrane is close its vapour equilibrium pressure then the separation process is controlled by the vapour liquid equilibrium (VLE). Equation II.7 reflects the general belief that the higher the permeate pressure, the lower the membrane selectivity. Watson & Payne (1990) successfully tested the validity of the above equation on systems containing 0.05% (v/v) *n*-octanol or 10% (v/v) methanol in water, permeating through a poly(dimethyl siloxane) (PDMS) membrane.

Néel *et al.* (1985) analysed the permeation of a mixture of *n*-hexane and *n*-heptane over a pressure range of zero to 16 kPa (120 mmHg). Besides the loss of selectivity, an increase in the permeate pressure over 6.7 kPa (50 mmHg) resulted in a decrease in the overall rate of permeation. This behaviour was observed only if the faster permeating species was the less volatile component of the mixture. If the faster permeating species was the more volatile component of the mixture, an increase in the permeate pressure resulted in an increase in selectivity. This result is in agreement with the mechanism represented by Equation II.7, where at higher permeate pressures the vapour liquid equilibrium controls the separation process.

Other anomalous behaviour regarding the effect of the permeate pressure on the pervaporation process were observed by Ji *et al.* (1994a; 1994b), for the pervaporation of a mixture of water and organic solvent (toluene, trichloroethylene (TCE) and methylene chloride - 500 ppm each) in a hollow-fibre module coated with PDMS. Over a permeate pressure range of 500 to 3300 Pa, a lower flux for toluene and methylene chloride was observed at the higher permeate pressures, as expected, whereas the fluxes of TCE could be kept at the same level regardless of the value of the permeate pressure. The behaviour of TCE could not be explained. For toluene and methylene chloride, Ji *et al.* (1994b) observed that when the permeate pressure was close to zero Pa the permeability was linearly related to the flux, but this linear relation did not hold at higher permeate pressures. It was then assumed that at high permeate pressures flow coupling occurred in the vapour phase. In this case, the boundary layer diffusive fraction of the flow dominated mass transfer, thus reducing the flows, while at lower pressures the convective flow represented the main contribution for the vapour transport. The behaviour of toluene and methylene chloride was most likely to be a consequence of a reduction in the driving force across the membrane due to an increase in downstream partial pressure of the permeating species.

II.3.1.4 SUMMARY OF THE EFFECTS OF EXTERNAL MASS TRANSFER RESISTANCES

Overall, the prediction of pervaporation transport will be overestimated if external mass transfer resistances are ignored. Such overestimation could compromise the feasibility of a particular separation by pervaporation or invalidate the design of new modules. Both an increase in the partial pressure of the vapour permeate or the occurrence of concentration polarization on the feed side of the membrane have the potential for greatly decreasing the membrane selectivity and flux. As a rule-of-thumb, the effects of concentration polarization might be minimized by increasing the turbulence on the feed side of the membrane, and the effects of transport resistances on the permeate side of the membrane might be minimized by selection of an appropriate vacuum pump and proper design of the membrane chamber and piping system.

II.3.2 MEMBRANE TRANSPORT MECHANISMS

In membrane technology, two mechanisms have been proposed to describe the transport through the membrane: the solution-diffusion model and the pore flow mechanism. Okada & Matsuura (1991; 1992) proposed a pore flow mechanism based on the results of pervaporation experiments with cellulose membranes of different pore sizes with various binary organic mixtures. However, Zhang & Drioli (1995) criticized this mechanism from the point of view that the process described is not pervaporation but vacuum membrane distillation. Pervaporation uses non-porous, dense membranes, while the pore flow mechanism is more appropriate for micro-porous membranes.

Mason & Lonsdale (1990) tried to unify all theories that may be used in the membrane transport under a statistical-mechanical theory. This assumes that the liquid can be described in terms of a local state, i.e., by values of variables like pressure, temperature, density, and composition, and that the local state deviates slightly from a local equilibrium state. In consequence, the expansion of the distribution function leads to a linear transport equation, i.e., fluxes are proportional to gradients. In this model, the membrane is assumed

homogeneous and is considered a component of the mixture. The transport coefficients represent values within the membrane and they may depend on position, direction of flow, or deformation within the membrane. To date, no comparison between this model and experimental data has been reported.

Descriptions of the solution-diffusion model based on Fick's law, the Maxwell-Stephan Equation, and the Thermodynamics of Irreversible Processes (TIP) can be found in the literature and each are discussed below. In general, because of their low concentration, transport of each solute through the membrane is independent of the presence of other components and a model based on Fick's law describes the transport satisfactorily, thus being the most widely used. In this section, a brief description of each model is presented. Given the historical significance of the solution-diffusion model based on Fick's law and its application to the experimental results of Chapters IV and V, this model will be explored in greater depth.

II.3.2.1 The Maxwell-Stephan equation

In the Maxwell-Stephan equation the non-idealities of transport are accounted for in the expression for the driving force (Wesseling & Krishna, 1990). As a consequence the diffusion coefficient is independent of the composition and of the frame of reference, i.e., whether the membrane is stationary or not (Wesseling & Krishna, 1990). The Maxwell-Stephan equation states that a driving force is necessary to maintain the velocity of a component against the resistance of the membrane and the flow of the other compounds of a mixture (Heintz & Stephan, 1994a). Thus it is a diffusion equation that accounts for the convective flow (Bitter, 1991) and has the advantage of including the effects of flow coupling in its basic formulation.

One of the main difficulties in using the Maxwell-Stephan equation is in finding an appropriate correlation for calculating the necessary diffusion coefficients. Krishna & Taylor (1986) pointed out that the diffusion coefficients calculated for a binary mixture are different from the coefficients of a ternary mixture. The main reason is that intermolecular forces

between a third species and the binary mixture changes the interactions between the species in the binary mixture. As a universal equation for diffusion is still lacking, each system must be evaluated separately.

Bitter (1991) and van den Berg & Smolders (1992) suggested that the Vigne equation could be used to estimate the diffusivity of a given component in a multicomponent mixture. The advantage of using this procedure was that only pure component diffusivities needed to be calculated. Bitter (1991) applied this procedure to the simulation of pervaporation of water-glycerol. Since the Vigne equation was developed for ideal solutions, it was necessary to introduce corrections based on pure component viscosity, molecular size, and shape factors to account for non-idealities. For polar components, or for mixtures where differences in molecular size were significant, the relationship between the viscosity of the pure components and the viscosity of the mixture required an empirical viscosity correction factor to be accurate. Therefore, for mixtures that deviate from ideal behaviour, the ease in using the Vigne equation is overshadowed by the need to make a large number of viscosity measurements to determine the correction factor.

The Maxwell-Stephan equation was also used by Heintz & Stephan (1994a) to model the pervaporation of water and ethanol through poly(vinyl alcohol) (PVA) membranes. The model was accurate for low permeate pressures, but the equation did not account for the effects of high permeate pressure.

Koops *et al.* (1994) stated that the Maxwell-Stephan equation was not appropriate for the simulation of systems where the flux ratio between a fast and a slow permeating species was constant but selectivity decreased with a decrease of membrane thickness. This is because the equation associates the loss of selectivity with an increase in friction between the faster permeating species and the other components of the system. On the other hand, they considered the Maxwell-Stephan equation appropriate for the simulation of non-ideal behaviour caused by flow coupling.

These studies highlighted the advantages of the Mawell-Stephan equation in dealing with flow coupling and non-idealities of sorption. However, the use of this model is labourious

since the flux term is not explicit and the lack of a universal theory for diffusivity requires extensive experimental data to fit all parameters. Furthermore, the Mawell-Stephan equation is not suitable for modelling systems which have a high permeate pressure and it is not able to evaluate the effects of changes in the membrane thickness.

II.3.2.2 THERMODYNAMICS OF IRREVERSIBLE PROCESSES (TIP)

In the TIP, the influence of coupling effects is addressed by phenomenological parameters that do not require knowledge of the mechanisms inside the membrane and are easily fitted from experimental data. In comparison to the Maxwell-Stephan equation, the main advantages of representing transport through a membrane by the TIP are the explicit evaluation of flow coupling and the ability to model the effects of the permeate pressure (Molina *et al.*, 1997).

Thermodynamic equilibrium does not exist in a system in which transport is occurring (Meares, 1976), therefore classical thermodynamics can only offer a description through the second law. This states that any process can only proceed spontaneously in one direction and the variation of entropy is used to determine the feasibility of a process occurring spontaneously (Bitter, 1991). The rate of entropy variation with time at a constant temperature measures the rate of dissipation of free energy (Meares, 1976), which can be related to the sum of the product of flow and its conjugated driving force for each species (Kedem, 1989). It follows that close to equilibrium the driving force is linearly related to the flux.

From the TIP, Kedem (1989) developed a theoretical model from which the contribution of both diffusion and convection in the transport through membranes can be evaluated. In this modification, the influence of convection on flux is measured by a drag coefficient (Q):

$$J_i = P_i \left(- \frac{d\phi_i}{dz} + Q p_i J_j \right) \qquad [II.8]$$

$$Q = - \frac{R_{ij}}{RT} = - \frac{R_{ji}}{RT} \qquad [II.9]$$

$$P_i = \frac{RT}{p_i R_{ii}} \qquad [II.10]$$

where, J_i flux of species i through the membrane;

P_i permeability of species i;

p_i partial pressure of species i;

R universal gas constant;

R_{ii} straight coefficient in Onsager equation;

R_{ij} cross coefficient in Onsager equation;

T temperature;

z membrane thickness.

Although the TIP is easier to use than the Maxwell-Stephan equation as the flux term is explicit, the Maxwell-Stephan approach is often preferred since it provides better insight to the mechanisms occurring inside the membrane. However, whenever separation is influenced by the permeate pressure, the TIP provides a better description of the phenomenon.

II.3.2.3 THE SOLUTION-DIFFUSION MODEL

The solution-diffusion model is that most widely used to represent the pervaporation process. Separation is represented as a consequence of preferential sorption of permeating component into the membrane and preferential diffusion through the membrane followed by desorption (steps 2, 3 and 4; Section II.3). Usually the permeating component encounters no resistance to desorption (Mulder, 1991); it follows that selective sorption and selective diffusion determine the separation ability of the process. In this section the solution-diffusion model

will be evaluated. The individual roles, mechanisms and models of sorption and diffusion will be considered separately in subsequent sections.

The solution-diffusion model assumes that Fickian transport occurs, i.e., the flux of the permeating component (J_i) across the membrane is proportional to a driving force. The driving force is usually represented by a gradient in chemical potential ($\nabla\mu$). The chemical potential was defined by Sonntag & Van Wylen (1982) as the variation of the system's total Gibbs energy (G) divided by the variation of the number of moles of species i (n_i) at constant temperature (T), pressure (P), and the number of moles of other species (n_j):

$$\mu = \left(\frac{\Delta G^t}{\Delta n_i} \right)_{T,\, P,\, n_j} \qquad [II.11]$$

According to Smith & Van Ness (1980), the Gibbs free energy is defined as:

$$d\,G^t = S^t\,d\,T + V^t\,d\,P \qquad [II.12]$$

where, S entropy;

V molar volume.

Under isothermal conditions the first term on the right hand side of Equation II.12 disappears. The pressure in the second term can be expressed as a combination of the osmotic (π) and hydrostatic pressure (P), but in pervaporation the contribution of the hydrostatic pressure is negligible. The osmotic pressure is a function of fugacity (f), giving Equation II.14, but when dealing with liquids, it is more convenient to use activity (a) (Equation II.15):

$$d\mu_i = V_i\,(d\pi + d\,P) \qquad [II.13]$$

$$d\pi = \frac{R\,T}{V_i}\,d\ln\,f_i \qquad [II.14]$$

$$d\mu_i = R\,T\,d\ln a_i \qquad [II.15]$$

where, R universal gas constant.

Tsujita (1992) developed the equation used in the solution-diffusion model from the definition of flux as a product of concentration (c) of component i inside the membrane (m) and velocity (u), where velocity was defined as the driving force ($\Delta\mu$) divided by a friction coefficient (f_c), which is related to the diffusion coefficient (D) according to Einstein's equation (Equation II.18).

$$J_i = u_i\,c_i^m \qquad [II.16]$$

$$u_i = -\frac{\Delta\mu_i}{f_c} \qquad [II.17]$$

$$D_i = \frac{R\,T}{f_c} \qquad [II.18]$$

Thus, defining the driving force as a gradient in the chemical potential across the membrane and combining Equations II.15 through II.18, the equation for the solution-diffusion model is obtained:

$$J_i = -D_i\,c_i^m\,\nabla\ln a_i \qquad [II.19]$$

For the pure component i, if solubility (S) is defined as the ratio of the average concentration of species i inside the membrane to the concentration of species i in the feed, and the permeability (P) as the product of solubility and the diffusion coefficient, Equation II.19 reduces to Equation II.22:

$$J_i = -P_i\,\nabla c_i^f \qquad [II.20]$$

$$S = \frac{c_i^m}{c_i^f} \qquad [II.21]$$

$$P_i = S_i D_i \qquad [II.22]$$

where, c^f concentration in the feed stream;

c^m concentration in the membrane

In Equation II.20, it is assumed that the coordinates of the system are at the extremes of the membrane. Rautenbach & Albrecht (1980) showed that better predictions can be obtained by using a stationary coordinate system, where a convection term is included in the expression of the solution-diffusion model. The starting point for the development of the solution-diffusion law is still Fick's law of diffusion (Paul & Ebra-Lima, 1970; Rautenbach & Albrecht, 1985):

$$J_i = w_i (J_i + J_m) - \rho D_i \nabla w_i \qquad [II.23]$$

where, w_i mass fraction of i inside the membrane;

$\rho = \Sigma \rho_i$ density of the membrane plus the permeate.

For dilute systems $\rho = \rho_m$ (density of the membrane). In general the membrane is static and J_m is equal to zero.

In its basic format (Equation II.19), the solution-diffusion model assumes that the permeating species do not interact with each other and that equilibrium exists at the interface between the membrane and the feed solution. The model also assumes that the diffusion and the partition coefficients are independent of concentration, i.e. Henry's law applies (Meares, 1976). The latter generally does not hold for non-dilute, multicomponent solutions and equations that deal with the non-idealities of sorption and diffusion need to be applied to correctly estimate these coefficients.

The importance of using a concentration dependent mean diffusion coefficient was demonstrated by Mulder & Smolders (1984). In the modelling of the water-ethanol-cellulose acetate (CA) system, the simulation predicted the concentration of ethanol becoming zero inside the membrane. Also Rautenbach & Albrecht (1980; 1985) in their study of the pervaporation of benzene and cyclohexane in polyethylene stated the need to introduce concentration dependent diffusion coefficients. A more detailed discussion on sorption and diffusion coefficients is presented in Sections II.3.2.4 and II.3.2.5.

The validity of the solution-diffusion model was questioned by Tusel & Brüshke (1985). In a pervaporation experiment using two different membranes and a mixture of water and ethanol, the sorption isotherms calculated for each membrane over an activity range of 0.1 to 1 predicted different selectivities for both membranes. The pervaporation experiments however showed similar permeabilities for the membranes. This result implied that diffusivity was not only dependent on composition and concentration of the permeating mixture, but also on the polymer type. Tusel & Brüshke (1985) also pointed out that the solution-diffusion model failed to predict the separation of ternary systems from binary experimental data. Although the solution-diffusion model is simple and easy to use, its limitations restrict its use to systems for which experimental results are already available since any extrapolations are not reliable. The above results reinforces the need for a universal theory of diffusivity, for with the currently available tools, any generalizations derived from experimental results are bound to be challenged with exceptions to the rule.

In comparison to the solution-diffusion model, in systems where flow coupling occurs, better accuracy in the prediction of fluxes is achieved by using the Maxwell-Stephan equation, as shown by Rautenbach & Albrecht (1980;1985) for systems with large concentration gradients inside the membrane. Alternatively, a deviation coefficient can be introduced into the solution-diffusion model to account for the occurrence of flow coupling among permeating species (Drioli *et al.*, 1993). This deviation coefficient was defined as a ratio between the real flux and the ideal flux (calculated without coupling), which also enabled the evaluation of the importance of the coupling in the separation process, but must be calculated for each set of conditions.

Radovanovic *et al.* (1990) developed a formulation of the solution-diffusion model based on the assumption that molecular clustering reduced the diffusivity of pure components but enhanced the transport of the slow component depending on the degree of swelling. Their hypothesis was that water clusters immobilized in the silicone rubber membrane broke down in the presence of ethanol and formed a mobile ethanol-water dimer which enhanced the overall water flux.

Wijmans & Baker (1993) developed a model thermodynamically equivalent to the solution-diffusion model. This new model assumed that pervaporation could be modelled as a sequence of two steps:

(1) evaporation of the liquid feed to produce a saturated vapour phase;

(2) permeation of the vapour through the membrane, driven by a partial pressure gradient.

The model of Wijmans & Baker (1993) enabled the performance of the membrane to be separated from the operating conditions and to be compared to other separation methods, since the contribution of the vapour liquid equilibrium (VLE) and the membrane are explicit in the mathematical formulation.

The modifications to the solution-diffusion model suggested by Rautenbach & Albrecht (1985), Radovanovic *et al.* (1990), and Wijmans & Baker (1993) improved the understanding and analysis of the pervaporation phenomenon. Nevertheless, they did not overcome the limitations of the original formulation. Equations II.19 and II.20 apply to systems of pure components, or when sorption may be described by Henry's Law and the sorbed components diffuse through the membrane independently of each other's presence. These shortcomings might be reduced by including the non-ideal behaviour of the feed solution in the estimations of the solubility and diffusivity coefficients. So far, the solution-diffusion model has been preferred over the Maxwell-Stephan equation and the TIP approach because it is simpler to solve and requires less experimental data for fitting the diffusion coefficients, and it gives satisfactory insight to the transport mechanisms of pervaporation, respectively.

II.3.2.4 SORPTION MODELS

In pervaporation it is common practice to assume that equilibrium exists at the membrane-feed interface. Therefore, the main interest is to establish the mechanisms and relations that govern the isothermal sorption curves. At present there are few mechanisms developed to explain the sorption phenomenon; more often empirical equations are developed for each case studied and in most cases the shape of the experimental curve should indicate the type of mechanism to be expected. The study of the sorption of liquids in polymers is further complicated because the rule of addition cannot be applied (Hauser *et al.*, 1989a; Heintz *et al.*, 1991), that is, sorption data from a pure solvent in a polymer cannot be used to predict the sorption behaviour of this solvent in the same polymer when it participates in a mixture of solvents.

Vieth (1988) and Tsujita (1992) reviewed some of the mechanisms usually encountered in the study of sorption in polymers. In the rubbery state, solvents distribute randomly inside the polymer (Rogers, 1985), consequently a linear relationship between pressure and concentration inside the polymer is observed (Vieth, 1988; Tsujita, 1992). In the glassy state, polymers generally follow a sorption mechanism which combines Henry's law and Langmuir's mechanism (Vieth, 1988; Tsujita, 1992). Langmuir's mechanism describes single molecular layer sorption, while multilayer sorption was described by Brunauer, Emmett and Teller (BET) from an expansion of the Langmuir expression (Tsujita, 1992). When multilayer sorption occurs at high vapour pressures, the sorption curve has a sigmoidal shape (Tsujita, 1992).

Although from the above discussion a linear relationship for sorption of lower alcohols (methanol, ethanol and *n*-propanol) in zeolites and zeolite-filled membranes would be expected, Bartels-Caspers *et al.* (1992) observed that the shape of the sorption curve matched the Langmuir mechanism. On the other hand, a system composed of water and ethanol in a PVA/PAN composite membrane followed a BET mechanism, as expected for glassy polymers.

Attempts to model the behaviour of sorption in membrane-solvent systems fall into two categories: correlation or predictive equations. In the first case, empirical equations are developed to describe the behaviour of the solvent-membrane system based on experimental data (Hauser *et al.*, 1989a; Bartels-Caspers *et al.*, 1992; Ennecking *et al.*, 1993), but cannot be extended beyond the range of the experiment for which they were developed. Predictive equations, as their name suggests, should provide good forecasts for a large set of conditions even when they have been generated from limited experimental data. So far, three predictive equations have been tested for solvent-membrane systems: the solution theory of Heidelbrand (Lee *et al.*, 1989), UNIQUAC (Ennecking *et al.*, 1993, 1996; Heintz & Stephan, 1994a), and the Flory-Huggins equation (Bitter, 1984, 1987, 1991; Mulder and Smolders, 1986; Rhim and Huang, 1989; Favre *et al.*, 1993, 1994, 1996).

Although Lee *et al.* (1989) suggested the use of the solution theory developed by Heidelbrand for the prediction of sorption of solvents in polymers, this relationship accounts only for the contribution of the enthalpy of mixing. Since the entropy of mixing is not taken into account, this theory is only valid for pure component sorption and is of little practical value.

Flory and Huggins (Flory, 1953; Bitter, 1984) developed an expression for the prediction of equilibrium sorption in polymer solutions based on the entropy of mixing, polymer size and system composition. A lattice model was used, where the segments of the polymer and the solvent molecules occupy single sites (Mulder & Smolders, 1986). Bitter (1991) pointed out that the Flory-Huggins theory is only valid for adiabatic absorption, since the enthalpy of mixing is not included in the original formulation. The theory showed a good fit for dilute polymer solutions in non-polar, single solvents (Bitter, 1991).

Successful applications of the Flory-Huggins theory in the description of mixtures of solvent sorption into membrane materials include benzene and *n*-hexane in polyethylene (PE) (Huang & Rhim, 1991). For water and ethanol sorbed in PVA (Heintz *et al.*, 1991), in cellulose acetate, polyacrylonitrile and polysulfone membranes (Mulder *et al.*, 1985a) good agreement between experiment data and calculated values was obtained only when using a concentration-dependent interaction parameter, as well as including the contribution of the

enthalpy of mixing. Although the use of concentration-dependent interaction parameters was first suggested by Heil & Prausnitz (1966), the latter also criticised the use of more than two interaction parameters. Thus Favre *et al.* (1993) later observed "Following Prausnitz, it can be said at this point that the eventual need to use more than two empirical parameters for the correct description of the polymer-solvent isotherm ..., reduces considerably the usefulness of the Flory-Huggins equation."

Regardless of such criticism, Bitter (1984) attempted to improve the Flory-Huggins theory by including the enthalpy of mixing and a term to account for the loss of molecular chain flexibility during swelling. The inclusion of the enthalpy of mixing, as used in the solution theory of Heidelbrand, was suggested by Heil & Prausnitz (1966) so that systems with strong molecular interactions could be modelled. The loss of molecular chain flexibility was reflected in the use of a variable coordination number (Bitter, 1984).

In a comprehensive review carried out by Favre *et al.* (1993), it was concluded that the Flory-Huggins equation is not adequate for the prediction of sorption of poor solvents (polar compounds) into membrane materials such as polydimethyl siloxane (PDMS), because "... [poor solvents] are more susceptible to aggregate formation than good solvents... and can consequently be suspected to be prone to clustering in the PDMS matrix. ...[The Flory-Huggins equation] assumes super flexibility of the polymer chain leading to a complete mixing situation and no exclusion volume. Underestimation of the heterogeneity of the system is probably responsible for the ... deviations [observed between experimental and predicted data]." Heil and Prausnitz (1966) had arrived at a similar conclusion for solutions of dilute polymers in polar solutions.

Even modifications of the Flory-Huggins equation to account for elastic forces contributions, modified entropic contributions, and enthalpic contributions have proven unsatisfactory (Favre *et al.*, 1993). Furthermore, most modifications of the Flory-Huggins equation required that an increased number of parameters be estimated (Heil and Prausnitz, 1966; Mulder and Smolders, 1984, 1986; Bitter, 1984, 1987; Favre *et al.*, 1993), which besides the raising criticism noted above, also reflected adversely on the number of experiments required to generate the interaction parameters.

The universal quasi-chemical equation (UNIQUAC) developed by Abrams and Prausnitz (1975) also predicts the excess Gibbs energy of multicomponent mixtures based on the lattice theory, using parameters extracted from binary mixtures. Since both enthalpic and entropic contributions are taken into account, this methodology is applicable for polar and non-polar solvents. Provided that a liquid mixture is in equilibrium with a polymeric system, the activity coefficients of the sorbed mixture can be calculated from the UNIQUAC equation. It follows that sorption experiments with binary solvent solutions and data acquired from vapour liquid equilibrium experiments should enable the prediction of the concentration of multi-component mixtures inside the polymer.

While the Flory-Huggins equation requires knowledge of the volume fractions of all components in the membrane phase for a given membrane-solvent system, the UNIQUAC equation set, as modified by Ennecking *et al.* (1993), requires knowledge of the mass fractions. As the degree of swelling of a membrane in contact with a liquid is often unknown, it is generally impossible to calculate the volume fractions for membrane-solvent systems without incurring considerable error. On the other hand, mass fraction measurements are independent of changes in the volume of the membrane and therefore are more reliable.

Use of the UNIQUAC equation in the prediction of sorption behaviour in membrane-solvent systems has so far been limited to the work of Ennecking *et al.* (1993, 1996), and Heintz & Stephan (1994a). The required solvent-solvent interaction parameters are well documented (Gmehling & Onken, 1977) and only membrane-solvent binary interaction parameters need be estimated experimentally. Ennecking *et al.*(1993) first generated these binary interaction parameters for systems comprising of a polyurethane (PU) membrane in contact with a solution of cyclohexane and benzene, and PU membrane in contact with cyclohexene and toluene. Later, these parameters were used to predict sorption of a ternary solvent mixture (benzene, cyclohexene, and cyclohexane) in contact with PU membrane. Parameters for predicting sorption of the same ternary mixture in poly(ether-*block*-amide) (PEBA) membranes were also determined (Ennecking *et al.*, 1996). Heintz & Stephan (1994a) reported binary parameters for poly(vinyl alcohol) (PVA) membranes and various aqueous/organic mixtures. The organic compounds used were methanol, ethanol, *n*-propanol, *i*-propanol, tetrahydrofuran (THF), and dioxane. It was found that in order to fit the sorption

isotherm of water, the binary interaction parameter for water/PVA had to be made dependent on the activity of water. Although both studies claim that the UNIQUAC approach is adequate to predict sorption characteristics, prediction errors were not published.

So far, the main difficulty in developing a model for the prediction of sorption of solvents into dense polymers is the lack of a universal theory for solid-liquid equilibrium and the need to perform large quantities of experiments. However, it is generally accepted that the effect of temperature on the sorption of solvents by membrane materials can be described by an Arrhenius expression:

$$S = S_o \, e^{\left(\frac{-E_a}{R\,T}\right)} \qquad [II.24]$$

where, S amount sorbed by the membrane material;

S_o constant;

R universal constant of gases;

T temperature;

E_a activation energy.

If the process is exothermic, ΔH is negative (Feng & Huang, 1996). When either the Flory-Huggins or the UNIQUAC equation is used, the temperature effect is usually incorporated in the binary interaction parameter.

In pervaporation of organophilic components through rubbery polymers, sorption and permeation often have similar selectivities (Mulder *et al*, 1983). Therefore, in a process where sorption is the rate determining step, the component with the lowest ΔH should permeate preferentially.

II.3.2.5 DIFFUSION MODELS

As pointed out by Wesseling & Krishna (1990), in the Fickian description of the solution-diffusion model the non-idealities of mixtures are accounted for by the diffusion coefficient. In pervaporation, both predictive and empirical equations for diffusivity have been used with limited success. Table II.1 summarizes the main predictive models developed for diffusion of liquids through polymers used in pervaporation; a review of empirical models can be found in Fleming & Slater (1992b) and Mulder (1991).

Table II.1 Predictive models for diffusion of liquids through polymers used in pervaporation.

Predictive Models		
Stokes-Einstein Equation	$D = \frac{R\,T}{6\pi\eta r}$	[II.25]
Free-Volume Theory	$D_T = R\,T\,A_f\,exp\left(\frac{-B}{v_f\,(0,T)}\right)$	[II.26]
Monte Carlo Method	$D = D_o\,e^{\frac{-E}{R\,T}}$	[II.27]

The simplest approach in the prediction of the diffusion coefficient is to consider the diffusion term independent of composition and concentration. This assumption is valid for systems where Henry's law applies (Rogers, 1985). In this case, diffusion becomes a function of molecular size and the Stokes-Einstein equation applies (Equation II.25), with the diffusivity of a species decreasing with an increase in radius (size) and increase in viscosity (friction). The relation between diffusivity and viscosity was observed by Paul & Ebra-Lima (1970) and Aptel *et al.* (1974) in the pervaporation of a series of pure components, but other mechanisms acted in the permeation of binary mixtures (Aptel *et al.*, 1974).

When thick membranes are used, the permeation of dilute systems is controlled by the diffusivity alone (Bode, 1990; Raghunath & Huang, 1992). Raghunath & Huang (1992) plotted the feed concentration versus flux for very dilute organic-aqueous solutions (toluene and phenol) permeating through poly(ethylene *bock* amine) (PEBA) and PDMS for two extreme membrane thicknesses (0.013 and 0.1 cm for PDMS; 0.004 and 0.02 cm for PEBA). The plots were almost linear, which enabled the use of concentration independent diffusion coefficients to model the system.

Bitter (1984) attempted to model the diffusivity of very dilute multicomponent systems by reducing the multi-component mixture to a pseudo-binary mixture. The equations developed were based on the diffusivities of the components at infinite dilution. Good agreement of the predicted permeabilities with the experimental data was found for the permeation of *n*-heptane and *i*-octane over the whole concentration range.

As the above results highlight, the use of concentration independent diffusion coefficients is restricted to systems of very dilute feed concentrations, where the flow of the components inside the membrane can be considered independent. Most systems however present non-idealities and do not behave according to Henry's law, as thermodynamic and kinetic interactions between the polymer and permeating component, and between permeating components, play an important role. Consequently, the diffusion coefficient can no longer be described as a constant and non-idealities must be incorporated into the diffusion term.

The free volume theory (Equation II.26) was developed by Fujita from the Cohen-Turnbull theory (Tsujita, 1992). In this theory, diffusion results from a redistribution of the free volume inside the liquid and not as a result of an activation of some sort, as in the description of diffusion for fluids that conform to Brownian motion (Kumins & Kwein, 1968). In the free volume theory, it is assumed that the introduction of a penetrant increases the free volume of the polymer, which is the space available between molecules for transport of the penetrant. The free volume is thus a function of the polymer's chain mobility, i.e., the thermal energy available. Details on the free volume theory formulation can be found in Mulder (1991).

Fels & Huang (1971) attempted to predict the diffusivity of binary mixtures from the permeation results obtained with pure components using the free volume theory. Their experiments were performed with *n*-hexane and benzene permeating through polyethylene (PE) and showed that the diffusivities of the binary mixture could only be adequately predicted if the fitted parameter that represents the contribution of the penetrant to the free volume in the polymer was dependent on the presence of all components of the permeating mixture. Huang & Rhim (1991) also noted that the free volume theory, when applied to the system *n*-hexane/benzene/PE, failed to account for flow coupling and thermodynamic interactions if only data from pure components were used to predict the behaviour of the binary mixture.

Gōto *et al.* (1995) attempted to predict the transient permeability of binary mixtures from steady state data of single components. Their work was based on the Monte Carlo method, where diffusion is dependent on the probability statistics as a function of an activation energy term and a concentration gradient (Equation II.27). The experiments were performed with a mixture of ethanol and methanol over a poly(acrylonitrile) (PAN) membrane. The calculations provided good agreement with the steady state experimental data, but the calculated transient data deviated from the experimental data, probably due to the lack of a term to account for the effects of swelling in the membrane. Compared to other methodologies, the Monte Carlo method has the disadvantage of requiring powerful computation hardware and long computation times.

The study of diffusion can be further complicated by the dependency of the diffusion coefficient on time (Park, 1968). The increase of the diffusion coefficient with time is a result of a relaxation process and is characteristic of the glassy state. Other factors that influence diffusion include crystallinity (Bitter, 1984; Park, 1986; Mulder, 1991; van den Berg & Smolders, 1992), membrane swelling (Bitter, 1984), clustering (Park, 1986), and the presence of fillers (Park, 1986).

The traditional methods for the measurement of the diffusion coefficient are based on sorption kinetics (Crank, 1956; Crank & Park, 1968; Felder & Huvard, 1980; Comyn, 1985; Rogers, 1985; Park, 1986; Heintz *et al.*, 1991; Mulder, 1991), on the time lag method from

transient diffusion experiments (Crank & Park, 1968; Felder & Huvard, 1980; Rogers, 1985; Vieth, 1988; Watson & Payne, 1990), permeation experiments (Crank, 1956; Crank & Park, 1968; Felder, 1980), and on knowledge of the concentration profile (Crank, 1956; Crank & Park, 1968). The method of sorption kinetics can only be applied in the gaseous phase and attempts to extrapolate data for liquid diffusion from gaseous measurements often result in an underestimation of the real value. Since liquids have a higher affinity for the polymer than the gas phase, the degree of swelling of the polymer will be higher in the presence of liquids than in the presence of gases (Heintz *et al.*, 1991). The time lag method assumes Fickian diffusion (Vieth, 1988). This method should therefore be applied for systems which have a linear response to changes of membrane thickness (Watson & Payne, 1990). Bode (1990) derived a simple method to estimate the concentration profile inside the membrane from permeation experiments and the profiles thus calculated enable the estimate of the diffusion coefficient. However, the method requires a considerable amount of experimental work and so far has been applied only to pure components. Fels & Huang (1971) recommend the use of permeation experiments for the evaluation of diffusivity coefficients for liquid mixtures. Although the latter is the most reliable methodology currently available, its accuracy depends on how well sorption can be measured or predicted.

II.3.3 The influence of feed temperature on membrane selectivity and flux

Beaumelle *et al.* (1993) hypothesized that the effect of temperature on membrane selectivity depended on which phenomenon governed the selectivity. If the process was governed by sorption, then the selectivity should decrease when the temperature increased. On the other hand, if the process was governed by diffusion, the variation in selectivity would depend on the relative values of activation energy for diffusion of each component. A higher activation energy of diffusion of the preferential component should lead to an increase in selectivity with temperature (Nguyen, 1986). The effect of temperature on selectivity is highly dependent on the system and the above discussion should be used as a guideline only. Furthermore, whenever concentration polarization occurs, the influence of temperature on

selectivity will depend on its effect on the individual mass transfer coefficients of the components of the feed (Karlsson, 1996)

Feng & Huang (1996) noted that the permeation flux increases with an increase in temperature, because the effect of temperature on saturated vapour pressure is more significant than its effect on sorption or diffusion, and that the flux increase follows an Arrhenius-like relationship (Böddeker *et al.*, 1991; Beaumelle *et al.*, 1992, 1993). It follows that as the permeation flux increases, the temperature of the feed stream along the membrane decreases and, due to the greater rate of evaporation, a larger heat supply needs to be provided to maintain performance.

II.3.4 Supply of the evaporation enthalpy

In pervaporation, the evaporation of the permeate is an essential step and the heat flux drawn from the feed provides the energy necessary for this phase change at the permeate membrane surface. Consequently, temperature gradients develop orthogonally to the membrane and also in the direction of flow, and the temperature drop between the bulk flow and the membrane surface depends mainly on the flux of the preferentially permeating component. (Rautenbach & Albrecht, 1989).

Karlsson & Tragård (1995) modelled the heat transfer process as a sequence of the following steps:

(1) absorption of the liquid permeating components at the feed membrane interface;
(2) diffusion of the permeating components through the membrane;
(3) desorption of the permeating components into a liquid permeate at the same state as the feed;
(4) vaporization of the permeating components forming a vapour at equilibrium pressure;
(5) expansion of the vapour from the equilibrium pressure to the operating permeate pressure.

In this representation the heats of absorption and desorption are equal and the heat of vaporization is a function of temperature and composition. The expansion may be isothermal or adiabatic; if adiabatic the expansion heat is equal to zero.

Karlsson & Tragård (1995) assumed that the heat consumption occurred at the membrane-permeate interface. In this case an analogy with mass transfer could be drawn. As the heat required in the process must be supplied by the feed, the following steps should be introduced in a resistance-in-series model:

(1) heat transfer from the bulk feed through the liquid feed boundary layer;

(2) heat transfer through the polymer membrane from the feed side to the permeate side;

(3) consumption of heat at the membrane interface.

If the first step is rate limiting then the flux through the membrane is reduced as a consequence of a reduction in heat supply, which is associated to a temperature gradient from bulk to the membrane surface This phenomenon is termed temperature polarization (Karlsson & Tragård, 1995) and was observed in the study of pure water permeating through poly(dimethyl siloxane) membranes (Karlsson, 1996). The occurrence of a temperature gradient between the feed and the permeate was also hinted at by Néel (1985).

II.4 Summary

As will be shown when applications are considered (Part II), pervaporation first entered the market as an option for solvent dehydration in substitution to extractive distillation (Ballweg *et al.*, 1982). Since then, new membranes have been developed that permeate organic components preferentially to water. To date, the development of industrial scale processes for organic removal by pervaporation is limited by the degree of selectivity of the organophilic membranes.

In pervaporation transport is accomplished by the maintenance of a chemical potential gradient across the membrane. Usually transport through the membrane is described by a solution-diffusion mechanism, with the presence of non-idealities requiring the use of more

complex equations for the sorption and diffusion terms (Mulder, 1991). Flow coupling is generally addressed by the Maxwell-Stephan equation or the Thermodynamics of Irreversible Processes. Depending on module design and operation, resistances in fluid transport in the feed and vapour lines may determine enrichment and separation rate; in this case, the process is better described by a resistance-in-series model.

To date, no single equation or mechanism has been able to satisfactorily describe or predict the behaviour of pervaporation in every instance. Part of this limitation might be attributed to the lack of a universal theory of the sorption of liquids into dense membranes or of the diffusion of solvents through membranes. Often empirical equations are employed for sorption and diffusion whenever the solution-diffusion model applies and complex, non-ideal mixtures must be modelled. It is therefore of great importance to start evaluating the influence of basic membrane and feed mixture properties on the sorption and transport phenomena. It is also of significant interest to the industry to evaluate how well this knowledge may be immediately applied in the prediction or correlation of membrane performance.

Chapter III

RESEARCH OBJECTIVES

As introduced in Chapter I, the NZDCL is commited to examining new opportunities for energy savings in the production of industrial ethanol and it was decided to evaluate whether a pervaporation-aided distillation scheme could further improve the economics of ethanol production. The research objectives pertinent to distillation are listed in Chapter VIII of Part Two - Applications; here the objectives relating to the fundamental aspects of pervaporation are delineated In this light, one of the main objectives set for this project were:

- to evaluate whether organophilic membranes developed for pervaporation provide an alternative method for the purification and for concentration of industrial ethanol;

Therefore, the specific aims of this research were:

- *to model multicomponent mixtures in pervaporation.*

  In order to efficiently assess the impact of linking pervaporation into distillation, a mathematical model of the pervaporation process is required. As the transport of multicomponent mixtures through pervaporation membranes is little understood, experiments needed to be designed to evaluate the influence of operating parameters such as membrane type, temperature, feed composition, and feed flow rate on the process. Furthermore, it was necessary to evaluate whether flow coupling or concentration polarization occurred and, if present, how they could be better accounted for in a mathematical model.

- *to evaluate the impact of basic feed and membrane properties on the sorption and transport behaviour.*

  Assuming that the solution-diffusion model applied to this process, it was necessary to investigate the influence of sorption and diffusion on the ability of the membranes

to separate the components of interest. It was also deemed important to evaluate how basic information on the properties of the membrane type and feed solution could be used for the prediction or correlation of the behaviour of pervaporation.

Chapter IV

PERVAPORATION EXPERIMENTS

IV. 1 INTRODUCTION

Pervaporation competes with traditional separation techniques such as distillation, air stripping, carbon adsorption, and extraction, among others. In general, the deciding factors in the selection of a separation technique are reliability, ability to achieve the desired degree of separation, and total cost (capital and operational). Pervaporation has been successfully used for the dehydration of solvents past their azeotropic point in over one hundred plants around the world established during the last fifteen years, which indicates the maturity, competitiviness, and reliability of this technique. The capital and operational costs are a function of the price of the membrane, the module, and auxiliary equipment, such as pumps and heat exchangers; of flux, which defines the membrane area required; of membrane life-time; and of energy use.

In pervaporation, the separation ability is determined by the selective affinity of the membrane material for each component of the feed mixture and a variety of polymeric materials are available for the manufacture of membranes. In this chapter, the performance of three commercially available, hydrophobic pervaporation membranes (Table IV.1) in an application involving separation of fusels from ethanol and water is examined. The membranes used, their active layer material, and their supplier are listed in Table IV.1. The thickness of the active layer and the total thickness of each membrane are shown in Table IV.2.

In this chapter, the influence of operation parameters, such as temperature, concentration, and flow regime, on the flux and enrichment factors are considered for each membrane tested.

Table IV.1 Commercial, hydrophobic membranes used in experiments.

Membrane Type	Active layer material	Supplier
GFT 1000[1]	poly(vinyl alcohol)	GFT/Deutsche Carbone AG, Germany
GFT 1060	poly(dimethyl siloxane)	GFT/Deutsche Carbone AG, Germany
GFT 1070	poly(dimethyl siloxane) + silicalite	GFT/Deutsche Carbone AG, Germany
PEBA	poly-ether-*block*-amide	GKSS, Germany.

[1]dehydration membrane (hydrophilic).

Table IV.2 Membrane thickness. The total thickness of the membranes was measured using a Vernier caliper.

Membrane Type	Total thickness (μm)	Thickness of active layer (μm)
PEBA	200	58[1]
GFT 1060	170	10[2]
GFT 1070	200	30[3]

[1]Pingel, 1995; [2]Karlsson *et al.*, 1995; [3]Baudot & Marin, 1996.

Experimental results are explained in terms of the mechanisms and relationships of pervaporation reviewed in Chapter II. Note that although the name fusel oil, or fusels, normally refers to higher alcohols such as propanol, butanol, and *i*-amyl alcohol, in this study it may also include ethyl acetate.

IV.2 Materials and methods

IV.2.1 Disc pervaporation apparatus

Figure IV.1 shows the pervaporation apparatus which was used for all preliminary experiments and to evaluate the influence of feed temperature and feed composition on separation. Figure IV.2 is a photograph of this equipment during operation.

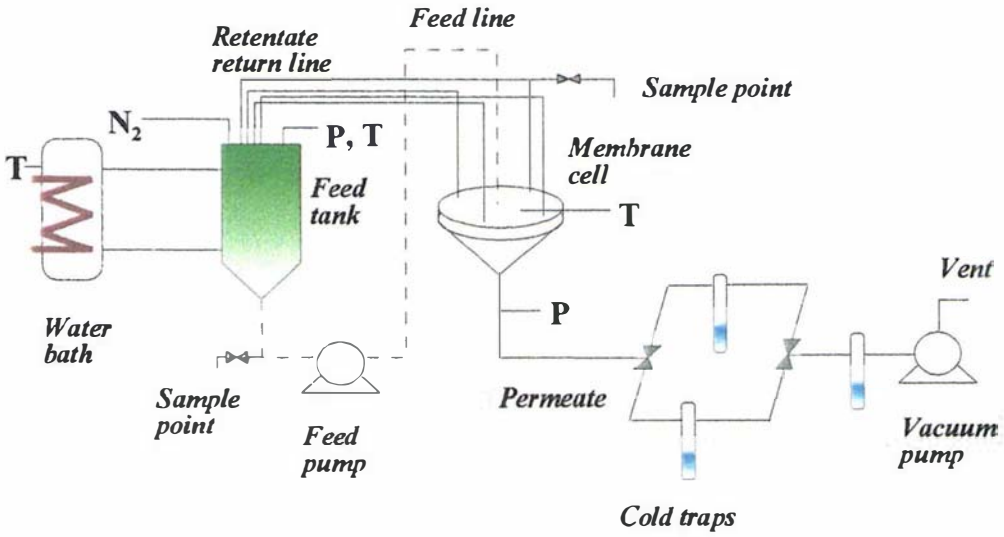

Figure IV.1 Schematic diagram of the first pervaporation apparatus. T: temperature measurement; P: pressure measurement.

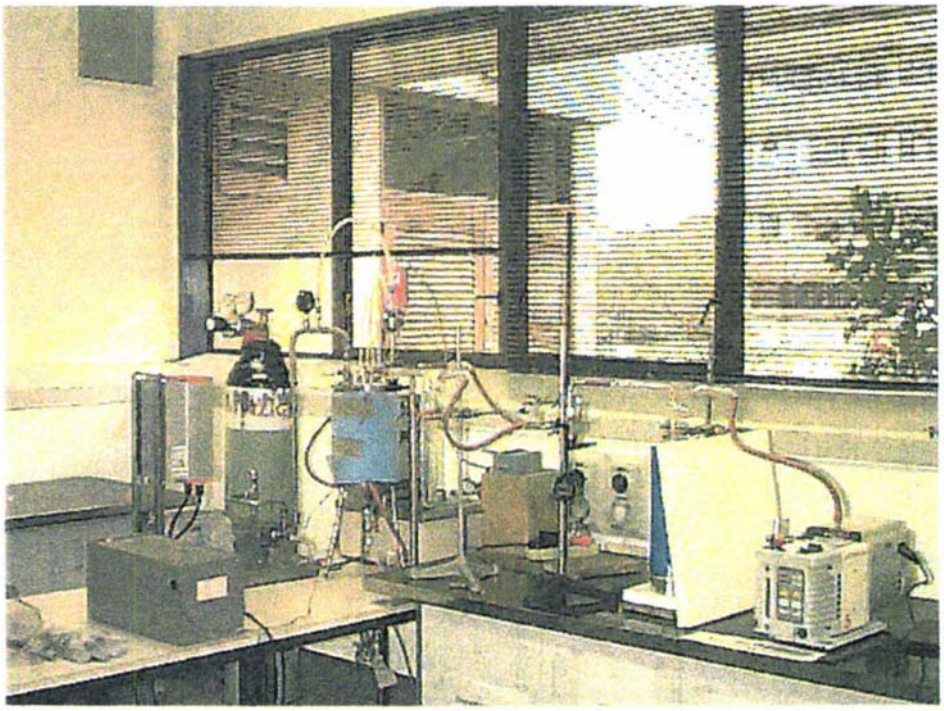

Figure IV.2 Photograph of the first pervaporation apparatus during operation.

IV.2.1.1 Experimental procedure and results, Experiment I

In Experiment I, the objective was to evaluate the influence of feed composition on the separation obtained with pervaporation and to compare the performance of the three organophilic membranes available (Table IV.1). Three feed concentrations were used, approximately corresponding to the feed to BC1, pinch point in BC2 and product of BC2 (Tables IV.3 to IV.5) - these terms are clearly explained in Figures IX.1 and IX.2 and Chapter X. The product concentration listed in Tables IV.3 to IV.5 is the average of triplicates.

Table IV.3 Total flux, feed and product concentration for Experiment I with GFT 1060. The balance is water. EtOH: ethanol; EtOAc: ethyl acetate; nPrOH: *n*-propanol; iBuOH: *i*-butanol; iAmOH: *i*-amyl alcohol.

		Feed Mass Fraction	Product Concentration (w/w)	Product Concentration (w/w)	Product Concentration (w/w)
low ethanol concentration	**EtOH**	0.01	5.64%	5.33%	5.87%
	EtOAc	2.3e-06	0.01%	0.01%	0.00%
	nPrOH	9.6e-06	0.01%	0.01%	0.01%
	iBuOH	8.5e-06	0.02%	0.02%	0.02%
	iAmOH	3.1e-06	0.04%	0.03%	0.04%
	Total Flux	***($g.m^{-2}.h^{-1}$)***	*1481*	*1285*	*1285*
medium ethanol concentration	**EtOH**	0.32	47.09%	45.08%	44.71%
	EtOAc	9.4e-03	7.22%	6.81%	6.78%
	nPrOH	9.1e-03	1.61%	1.53%	1.51%
	iBuOH	9.4e-03	1.85%	1.77%	1.75%
	iAmOH	9.9e-03	1.98%	1.89%	1.87%
	Total Flux	***($g.m^{-2}.h^{-1}$)***	*3562*	*3481*	*3430*
high ethanol concentration	**EtOH**	0.90	82.89%	85.04%	85.04%
	EtOAc	9.4e-04	0.26%	0.27%	0.27%
	nPrOH	1.7e-03	0.13%	0.14%	0.14%
	iBuOH	2.4e-03	0.16%	0.16%	0.16%
	iAmOH	2.0e-03	0.10%	0.10%	0.10%
	Total Flux	***($g.m^{-2}.h^{-1}$)***	*5355*	*5337*	*5447*

Table IV.4 Total flux, feed and product concentrations for Experiment I with PEBA. The balance is water. EtOH: ethanol; EtOAc: ethyl acetate; nPrOH: *n*-propanol; iBuOH: *i*-butanol; iAmOH: *i*-amyl alcohol.

		Feed Mass Fraction	Product Concentration (w/w)	Product Concentration (w/w)	Product Concentration (w/w)
low	**EtOH**	0.01	8.62%	9.28%	
ethanol	**EtOAc**	1.1e-05	0.03%	0.02%	
concentration	**nPrOH**	5.7e-06	0.01%	0.01%	
	iBuOH	1.0e-05	0.02%	0.02%	
	iAmOH	3.2e-06	0.08%	0.08%	
	Total Flux	***($g.m^{-2}.h^{-1}$)***	*209*	*206*	
medium	**EtOH**	0.31	35.07%	35.68%	45.96%
ethanol	**EtOAc**	9.2e-03	3.77%	3.54%	4.39%
concentration	**nPrOH**	8.7e-03	1.45%	1.50%	1.69%
	iBuOH	8.9e-03	1.89%	1.95%	2.19%
	iAmOH	9.4e-03	2.43%	2.47%	2.78%
	Total Flux	***($g.m^{-2}.h^{-1}$)***	*1072*	*1069*	*1069*
high	**EtOH**	0.93	92.16%	96.54%	87.72%
ethanol	**EtOAc**	9.3e-04	0.14%	0.14%	0.13%
concentration	**nPrOH**	1.7e-03	0.16%	0.17%	0.15%
	iBuOH	2.4e-03	0.20%	0.21%	0.19%
	iAmOH	2.0e-03	0.15%	0.16%	0.15%
	Total Flux	***($g.m^{-2}.h^{-1}$)***	*3614*	*3597*	*3626*

Table IV.5 Total flux, feed and product concentration for Experiment I with GFT 1070. The balance is water. EtOH: ethanol; EtOAc: ethyl acetate; nPrOH: *n*-propanol; iBuOH: *i*-butanol; iAmOH: *i*-amyl alcohol.

		Feed Mass Fraction	Product Concentration (w/w)	Product Concentration (w/w)	Product Concentration (w/w)
low	**EtOH**	0.01	10.61%	10.63%	10.39%
ethanol	**EtOAc**	1.5e-05	0.14%	0.08%	0.06%
concentration	**nPrOH**	9.9e-06	0.01%	0.01%	0.01%
	iBuOH	1.3e-05	0.03%	0.03%	0.03%
	iAmOH	6.1e-06	0.09%	0.09%	0.09%
	Total Flux	***(g.m^{-2}.h^{-1})***	*373*	*363*	*353*
medium	**EtOH**	0.37	39.94%	39.71%	39.80%
ethanol	**EtOAc**	4.0e-03	5.12%	5.07%	5.22%
concentration	**nPrOH**	4.5e-03	1.00%	1.01%	1.00%
	iBuOH	4.6e-03	1.34%	1.34%	1.35%
	iAmOH	4.7e-03	1.59%	1.52%	1.59%
	Total Flux	***(g.m^{-2}.h^{-1})***	*749*	*765*	*934*
high	**EtOH**	0.96	91.77%	97.22%	92.86%
ethanol	**EtOAc**	0.09%	0.35%	0.37%	0.36%
concentration	**nPrOH**	0.18%	0.15%	0.17%	0.16%
	iBuOH	0.25%	0.19%	0.20%	0.19%
	iAmOH	0.21%	0.12%	0.14%	0.13%
	Total Flux	***(g.m^{-2}.h^{-1})***	*1683*	*1677*	*1804*

The feed was held in an approximately 4.5 litre, insulated, jacketed vessel, which was pressurized to 0.5 atm (g) with nitrogen. The feed was pumped at a rate of approximately 50 l.h^{-1} to the top centre of the membrane cell using a diaphragm pump (Metripump E2/D90S) It was then recirculated to the feed vessel through four radial exits in the periphery of the cell (Figures IV.3 and IV.4).

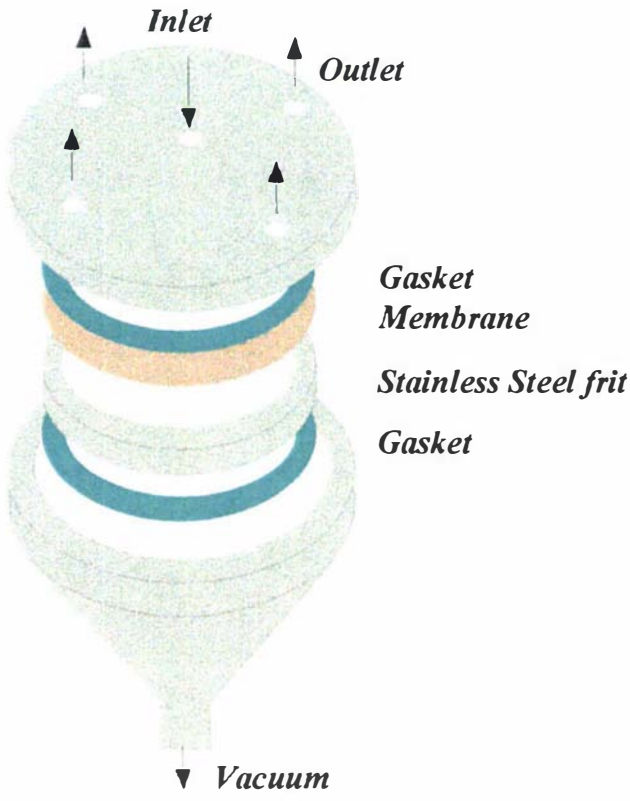

Figure IV.3 Detail of membrane cell of the first pervaporation apparatus.

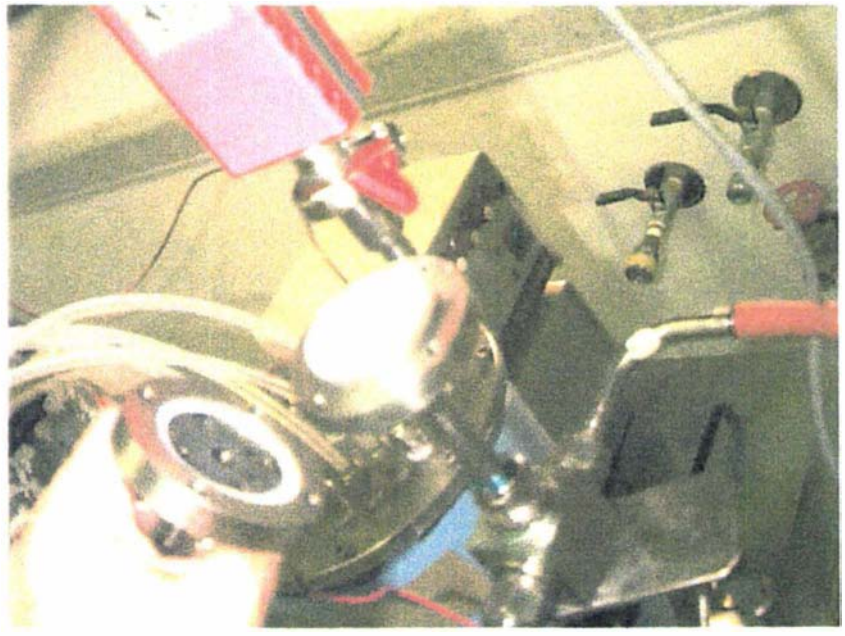

Figure IV.4 Photograph of the membrane cell.

During experiments, a vacuum pressure of less than 1 mbar.a was created on the permeate side of the membrane by condensation of the vapour in conjunction with a vacuum pump (Edwards RV5), which operated continuously. Immediately after the permeate chamber, the vacuum pressure was measured by an active Pirani gauge (Edwards). The gauge was calibrated to measure between 1 and 100 mbar.a of pressure, however, readings indicated that the pressure achieved for all tests run was well below 1 mbar.a.

The permeate was collected in cold traps, which were cooled to -196°C by liquid nitrogen. Immediately after the membrane cell, two cold traps operated in parallel. By alternating the flow of permeate between the two cold traps it was possible to operate the equipment continuously. A third trap in series with the first two acted as a safety trap to prevent any solvent from reaching the vacuum pump (Figure IV.5).

Figure IV.5 Photograph of safety trap and vacuum pump.

In order to guarantee the physical integrity of the membranes, the vacuum was turned on before the recirculation pump was started. Next the feed tank was heated. Three hours after initiating the heating and circulating of the feed, collection of the permeate was started. Three consecutive samples were collected, each collection lasted between 1 and 15 h, depending on the permeate flow. Samples of the feed were taken at regular intervals so that three samples were collected during each experimental run. For the twenty six samples analysed, the variation in the reproducibility of the product concentration was on average below 5% and the variation in the reproducibility of the total product flow rates was on average below 3%, which indicated that the samples were taken at steady-state. A set of five runs performed in distinct days showed that a variation in the reproducibility of maximum 15% should be expected for all components except ethyl acetate (<35%).

The temperature at the feed vessel was controlled by a water circulator (Julabo Labortechnik GmbH) and set to maintain a temperature of 70±1 °C at the membrane cell, where the temperature was monitored by a Honeywell chart recorder using thermocouples.

The flow through the membrane was calculated by dividing the change in weight of the cold traps by the operation time (accuracy of the scale: ± 0.02 g). The composition of the permeate was analysed by gas chromatography (Section IV.2.2). Occasionally the permeate collected separated into two phases. Whenever this occurred, the mixture was weighed and diluted with a known amount of ethanol until a single phase was obtained.

All parts were made of teflon, stainless steel or glass, and teflon gaskets were used. The piping between the feed vessel and the membrane cell was constructed of stainless steel with $^1/_8$" O.D. The membrane cell comprised a circular unit with 47 mm effective diameter, corresponding to an area of 17 cm^2, where the membrane was supported by a stainless-steel frit (Figures IV.3 and IV.4). There was a 2 mm gap between the frit and the top of the cell. The tubing linking the cold traps from the membrane cell to the vacuum pump was made of vacuum-resistant rubber. All reagents used were of analytical grade (AR) and were used without further purification. The water used was treated by a Milli-Q system (Millipore Corp.).

IV.2.1.2 Experimental procedure and results, Experiment II

Experiment II was designed to evaluate the influence of feed temperature and/or composition in the total and component fluxes. The conditions for Experiment II were similar to those described for Experiment I, except:

- an Oberdorfer Chemseal series size 'I' pump was used to introduce the feed at a flow rate of approximately 35 $l.h^{-1}$ for most of the trials. The pump used in Experiment I and early Experiment II trials had to be replaced due to leakages in the diaphragm.

- for the GFT 1060 and PEBA membranes, all experimental runs were performed at 75±1°C at the membrane cell. Each run was repeated at least three times on different days.

- for the GFT 1070 membrane, each run was carried out at four temperatures: 60, 65, 70, and 75°C. Each set of tests was repeated at least three times in a random sequence.

- the membranes were replaced for each temperature set.

- the feed composition comprised dilutions between 5 and 20% (w/w) ethanol with a fixed ethanol:fusels ratio (Tables IV.6 and IV.9) . Trials with these diluted solutions were undertaken according to the schemes described in Tables IV.6 and IV.9.

- approximately 4 ml of permeate sample was collected for each trial. The collection period lasted between two to four hours.

- samples of the feed were collected before and after each run.

Table IV.6 Feed concentration (w/w) and experiment design for evaluation of PEBA and GFT 1060 membranes, Experiment II.

order	set*	water	ethanol	*i*-propanol	*n*-propanol	*i*-butanol	*n*-butanol	*i*-amyl alcohol	ethyl acetate
5	**5**	94%	5%	0.0007%	0.09%	0.02%	0.002%	0.5%	0.005%
2	**7.5**	92%	7.6%	0.0003%	0.14%	0.04%	0.003%	0.7%	0.008%
4	**10**	89%	10%	0.0007%	0.18%	0.05%	0.004%	1.0%	0.011%
1	**15**	83%	15%	0.001%	0.27%	0.07%	0.006%	1.4%	0.016%
3	**20**	77%	20%	0.001%	0.36%	0.10%	0.008%	1.9%	0.025%

*: nominal ethanol concentration.

Table IV.7 Product flux ($g.m^{-2}.h^{-1}$) for evaluation of PEBA membrane, Experiment II.

Order	set*	EtOH	nPrOH	iBuOH	nBuOH	iAmOH	EtOAc	water	total
1	**15**	396	17.77	6.94	0.50	150.9	1.12	271	844
2	**7.5**	205	4.91	1.84	0.13	71.0	0.13	243	526
3	**20**	415	17.82	6.79	0.43	160.9	1.14	461	1064
4	**10**	241	9.24	4.25	0.27	100.1	0.86	340	696
5	**5**	164	2.88	1.37	0.08	52.8	0.14	213	435

*: nominal ethanol concentration.

Table IV.8 Product flux ($g.m^{-2}.h^{-1}$) for evaluation of GFT 1060 membrane, Experiment II.

Order	set*	EtOH	nPrOH	iBuOH	nBuOH	iAmOH	EtOAc	water	total
1	**15**	1136	47.57	16.68	1.12	404	6.30	1776	3387
2	**7.5**	938	28.97	10 99	0.65	305	2.12	1319	2604
3	**20**	1148	41.03	13.95	0.87	304	4.86	2180	3692
4	**10**	1059	38.95	16.40	0.98	405	7.32	1344	2871
5	**5**	772	13.03	5.21	0.30	179	0.89	969	1939

*: nominal ethanol concentration.

Table IV.9 Feed concentration (w/w) and experiment design for GFT 1070 membrane, Experiment II.

order	set[&]	water	ethanol	*i*-propanol	*n*-propanol	*i*-butanol	*n*-butanol	*i*-amyl alcohol	ethyl acetate
3	**5***	94%	5%	0.0003%	0.09%	0.02%	0.002%	0.5%	0.02%
5	**5**	94%	5%	0.0004%	0.09%	0.02%	0.002%	0.5%	0.01%
6	**5**	94%	5%	0.0003%	0.09%	0.02%	0.002%	0.5%	0.01%
11	**7.5**	92%	7.6%	0.0003%	0.14%	0.04%	0.003%	0.7%	0.01%
2	**10***	89%	10%	0.0007%	0.18%	0.05%	0.004%	1.0%	0.01%
7	**10**	89%	10%	0.0007%	0.18%	0.05%	0.004%	1.0%	0.01%
9	**10**	89%	10%	0.004%	0.18%	0.05%	0.005%	1.0%	0.01%
4	**15***	83%	15%	0.002%	0.27%	0.07%	0.005%	1.4%	0.02%
8	**15**	83%	15%	0.001%	0.27%	0.07%	0.006%	1.4%	0.02%
10	**15**	83%	15%	0.001 %	0.27%	0.07%	0.006%	1.4%	0.02%
12	**20**	77%	20%	0.001%	0.36%	0.10%	0.008%	1.9%	0.03%
1	**90***	7%	83%	0.005 %	1.55%	0.38%	0.030%	7.9%	0.09%

* diaphragm pump. [&]: nominal ethanol concentration.

Table IV.10 Product flux ($g.m^{-2}.h^{-1}$) for GFT 1070 membrane, Experiment II.

T (°C)	EtOH	n-PrOH	i-BuOH	n-BuOH	i-AmOH	EtOAc	Water	Total
60	142	4.54	2.29	0.12	55.21	1.37	322	527
	107	2.93	1.60	0.09	55.21	3.16	242	412
	251	9.85	4.31	0.20	100.70	3.35	232	602
	107	5.38	2.76	0.14	72.95	1.32	198	388
	101	3.86	2.02	0.12	61.47	1.13	238	408
	143	6.78	3.47	0.23	67.56	2.45	262	485
	165	8.35	3.89	0.28	72.61	3.35	282	536
	128	6.33	3.29	0.26	60.93	2.11	242	442
	144	7.01	3.56	0.28	66.56	2.12	257	480
	236	11.63	5.02	0.34	99.48	2.93	205	561
	116	5.14	2.46	0.14	55.20	1.33	237	417
	217	10.79	4.49	0.25	85.34	3.13	239	561
65	200	6.90	4.16	0.21	89.07	2.37	355	657
	146	3.22	1.25	0.09	70.45	3.53	325	550
	292	11.35	4.88	0.29	114.23	3.10	261	687
	112	4.43	2.38	0.14	71.05	1.03	299	490
	125	4.12	2.06	0.13	66.68	0.72	168	367
	200	9.31	4.62	0.29	91.23	2.61	310	618
	226	11.33	5.10	0.35	95.63	3.14	328	669
	191	9.62	4.66	0.36	85.30	1.21	247	539
	220	11.38	4.98	0.36	94.10	3.76	345	680
	177	6.99	3.04	0.17	73.49	0.97	259	521
	230	11.31	4.68	0.33	88.90	2.85	385	723
70	247	8.45	4.93	0.25	106.07	2.47	416	785
	197	4.61	1.89	0.15	81.19	3.73	384	673
	364	13.69	5.78	0.30	137.92	3.89	365	890
	169	5.45	2.87	0.17	94.11	1.46	363	637
	186	5.48	2.83	0.17	94.94	1.56	146	437
	247	11.35	5.46	0.34	108.88	2.19	356	731
	274	13.41	5.95	0.40	114.24	4.21	404	816
	249	11.87	5.67	0.43	108.85	1.58	302	679
	295	14.92	6.25	0.43	121.38	3.41	387	828
	207	8.94	4.13	0.22	92.61	2.53	377	691
	320	15.43	6.26	0.35	123.28	4.63	470	940
75	296	9.54	5.57	0.29	128.59	2.93	530	973
	214	4.75	2.61	0.17	97.99	5.77	482	807
	447	16.12	6.78	0.36	166.36	5.08	425	1067
	158	6.27	3.31	0.20	92.08	0.97	425	686
	207	7.37	3.52	0.21	70.06	0.83	190	478
	305	13.68	6.31	0.38	128.78	1.99	417	874
	306	13.83	6.28	0.38	127.71	1.41	392	847
	307	13.71	6.18	0.36	126.93	1.31	378	834
	335	15.85	6.81	0.44	133.79	3.16	436	931
	345	16.61	7.01	0.45	136.11	2.68	439	946
	304	13.92	6.30	0.46	124.54	0.94	381	831
	348	17.12	7.13	0.47	141.02	4.34	480	999
	231	9.86	4.56	0.25	104.12	2.07	415	766
	411	19.91	7.89	0.42	155.10	4.81	435	1034

IV.2.1.3 Experimental procedure and results, Experiment III

Experiment III was designed to evaluate the influence of ethanol compositions in the partial fluxes of the minor components. The conditions for Experiment III were similar to those described for Experiment I, except:

- teflon piping of $^{3}/_{8}$" O.D. and $^{1}/_{4}$" O.D. was used for the feed and exit lines of the membrane cell, respectively. It was shown that the previous set of piping was causing excessive pressure losses. This new piping resulted in preferential flow through one of the exit piping, which caused a reduction in the area available for permeation and consequently reduced the total flux through the membrane. There were no significant changes in the product composition.

- all tests were performed at 70±1 °C.

- the feed had a set concentration of fusels and a varying concentration of ethanol (Table IV.11).

- all tests were performed with GFT 1070 only.

Table IV.11 Percentage feed concentration (w/w) or mass fraction and experiment design for GFT 1070 membrane, Experiment III.

Order	(nominal) ethanol	*i*-propanol	ethyl acetate	*n*-propanol	*i*-butanol	*n*-butanol	*i*-amyl alcohol	water
1	0%	6E-06	0.01%	0 17%	0.04%	4E-05	0.92%	99%
2	10%	6E-06	0.01%	0.17%	0.04%	4E-05	1.07%	86%
3	15%	6E-06	0.01%	0.17%	0.04%	4E-05	0.98%	84%
4	2.5%	6E-06	0.01%	0.18%	0.04%	4E-05	1.03%	96%
5	20%	6E-06	0.01%	0.20%	0.05%	4E-05	1.12%	82%
6	17.5%	6E-06	0.01%	0.16%	0.04%	4E-05	0.94%	83%
7	12.5%	6E-06	0.01%	0.18%	0.04%	4E-05	1.05%	85%
8	5%	6E-06	0.01%	0.18%	0.04%	4E-05	1.02%	94%
9	7.5%	6E-06	0.01%	0.19%	0.04%	4E-05	1.09%	90%
10	17.5%	6E-06	0.01%	0.19%	0.04%	4E-05	1.05%	83%
11	2.5%	6E-06	0.01%	0.19%	0.04%	4E-05	1.06%	96%
12	0.%	6E-06	0.01%	0.18%	0.04%	4E-05	0.96%	98%
13	2.5%	6E-06	0.01%	0.20%	0.05%	4E-05	1.16%	96%
14	5%	6E-06	0.01%	0 19%	0.05%	4E-05	1.11%	93%
15	7.5%	6E-06	0.01%	0.19%	0.04%	4E-05	1.08%	91%
16	10%	6E-06	0.01%	0.20%	0.05%	4E-05	1.12%	89%
17	12.5%	6E-06	0.01%	0.20%	0.05%	4E-05	1.13%	86%
18	15%	6E-06	0.01%	0.20%	0.04%	4E-05	1.13%	84%
19	17.5%	6E-06	0.01%	0.20%	0.04%	4E-05	1.09%	82%
20	20%	6E-06	0.01%	0.19%	0 04%	4E-05	1.06%	81%
21	20%	6E-06	0.01%	0.19%	0.04%	4E-05	1.01%	81%
22	0%	6E-06	0.01%	0.20%	0.04%	4E-05	0.97%	98%
23	17.5%	6E-06	0.01%	0.20%	0.05%	4E-05	1.06%	84%
24	2.5%	6E-06	0.01%	0.19%	0.04%	4E-05	1.07%	96%
25	15%	6E-06	0.01%	0.21%	0.05%	4E-05	1.19%	84%
26	5%	6E-06	0.01%	0.19%	0.04%	4E-05	1.06%	94%
27	12.5%	6E-06	0.01%	0.18%	0.05%	4E-05	1.00%	86%
28	7.5%	6E-06	0.01%	0.20%	0.04%	4E-05	1.12%	91%
29	10%	6E-06	0.01%	0.20%	0.05%	4E-05	1.13%	89%

Table IV.12 Product flux ($g.m^{-2}.h^{-1}$) for GFT 1070 membrane, Experiment III.

Nominal Ethanol Conc. (% w/w)	Total	EtOH	nPrOH	iBuOH	nBuOH	iAmOH	EtOAc	water
0	97	2.5	1.27	0.73	0.05	23.98	0.17	68.0
10	134	31.4	1.16	0.64	0.04	21.05	0.14	79.2
15	147	53.9	1.21	0.59	0.04	21.00	0.12	69.9
2.5	99	0.4	1.32	0.76	0.06	29.14	0.18	67.6
20	155	68.2	1.04	0.48	0.04	16.55	0.09	68.2
17.5	147	56.7	1.09	0.52	0.04	18.72	0.11	69.9
12.5	132	37.3	1.15	0.58	0.04	21.07	0.14	71.6
5	112	27.9	1.42	0.78	0.06	30.50	0.14	51.4
7.5	117	38.9	1.80	0.95	0.07	29.61	0.21	45.0
17.5	144	67.1	1.20	0.57	0.04	19.87	0.11	54.9
2.5	97	17.6	1.25	0.70	0.05	24.86	0.10	52.4
0	81	9.2	1.22	0.68	0.05	24.57	0.14	44.7
2.5	97	19.3	1.53	0.85	0.06	26.92	0.22	48.1
5	103	26.4	1.30	0.72	0.05	25.56	0.17	49.1
7.5	108	27.8	1.28	0.69	0.05	23.64	0.17	54.8
10	111	50.6	1.18	0.61	0.04	23.31	0.12	35.4
12.5	123	46.0	1.24	0.63	0.04	21.79	0.15	53.1
15	139	58.2	1.20	0.58	0.04	20.04	0.13	58.6
17.5	139	64.8	1.10	0.52	0.03	17.74	0.10	54.6
20	152	77.2	1.12	0.50	0.03	16.70	0.11	56.1
20	148	72.8	1.02	0.46	0.03	15.30	0.09	58.6
0	86	9.0	1.48	0.74	0.05	25.73	0.18	49.3
17.5	142	63.5	1.11	0.53	0.03	18.60	0.10	57.9
2.5	97	21.1	1.46	0.74	0.05	26.20	0.14	47.7
15	137	49.2	1.22	0.60	0.04	21.14	0.14	64.8
5	101	32.3	1.26	0.68	0.05	17.62	0.17	48.9
12.5	130	46.0	1.18	0.59	0.04	9.71	0.15	72.8
7.5	110	31.2	1.13	0.60	0.04	25.11	0.09	51.9
10	112	37.0	1.49	0.71	0.05	23.64	0.17	49.0

IV.2.1.4 Experimental procedure and results, Experiment IV

A cross-flow pervaporation apparatus was built for the study of feed flow effects. It differed from the disk pervaporation apparatus (Experiment III) in the design of the membrane cell (Figure IV.6). In the membrane chamber the feed flowed along a rectangular channel of 2x20 mm, in cross flow to the permeate. The entrance and exit channels were approximately 30 mm long and had the same width and depth as the membrane chamber; they were designed to minimise entrance and exit effects on the flow. The top plate of the filter could be heated to keep the feed temperature along the membrane chamber constant and uniform. During experiments, four thermocouples placed along the membrane chamber at the level of the feed flow and two thermocouples placed at the inlet and outlet, respectively provided temperature measurement.

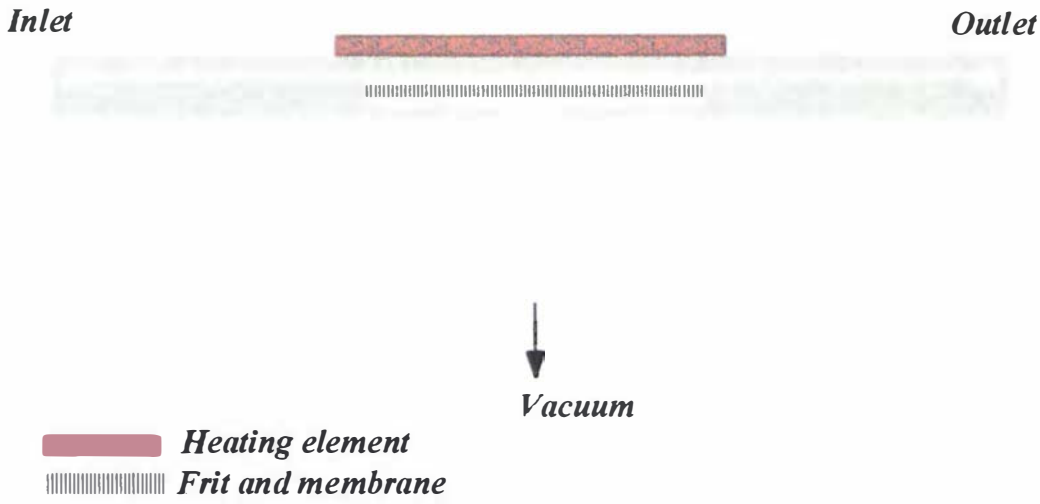

Figure IV.6 Detail of cross-flow membrane cell.

The experiments were conducted with GFT 1070 at 65°C. Table IV.13 lists the total feed flow rates and the mass fractions of each component of the mixture. Table IV.14 lists the total product flux and the mass fractions of each component.

Table IV.13 Feed flow rates ($l.h^{-1}$) and feed mass fractions employed in Experiment IV.

Flow rate	EtOH	iPrOH	EtOAc	nPrOH	iBuOH	nBuOH	iAmOH	water
200	0.14	1.5e-05	8.1e-05	1.8e-03	3.6e-04	5.4e-05	8.0e-03	0.85
33	0.14	1.5e-05	8.1e-05	1.8e-03	3.6e-04	5.4e-05	8.0e-03	0.85
33	0.13	1.0e-05	2.2e-05	1.6e-03	3.3e-04	3.3e-05	6.7e-03	0.86
200	0.13	1.1e-05	2.6e-05	1.6e-03	3.2e-04	3.6e-05	6.7e-03	0.86
33	0.13	1.2e-05	5.5e-05	1.7e-03	3.8e-04	4.3e-05	8.3e-03	0.86
33	0.20	3.9e-05	1.1e-04	2.8e-03	6.4e-04	7.9e-05	1.4e-02	0.78
33	0.20	4.1e-05	8.8e-05	2.8e-03	6.5e-04	7.7e-05	1.4e-02	0.78

Table IV.14 Total product flux ($g.m^{-2}.h^{-1}$) and mass fraction of product components, Experiment IV.

Flux	EtOH	iPrOH	EtOAc	nPrOH	iBuOH	nBuOH	iAmOH	water
675	0.28		2.9e-03	1.2e-02	4.7e-03	5.8e-04	0.15	0.55
666	0.31	6.0e-05	1.5e-03	1.3e-02	4.7e-03	5.6e-04	0.14	0.53
642	0.30		1.1e-03	1.2e-02	4.4e-03	5.5e-04	0.14	0.54
637	0.28		1.4e-03	1.1e-02	4.4e-03	5.6e-04	0.14	0.56
914	0.25	3.0e-05	1.9e-03	8.9e-03	3.5e-03	4.5e-04	0.12	0.62
859	0.31	1.2e-04	3.7e-03	1.5e-02	5.9e-03	7.4e-04	0.15	0.51
876	0.30	1.3e-04	2.7e-03	1.4e-02	5.7e-03	7.5e-04	0.15	0.53

IV.2.2 ANALYTICAL PROCEDURES

A Carlo Erba gas chromatograph (Model GC 6000 vega series 2, Carlo Erba Strumentazione) fitted with a flame ionization detector, auto sampler (AS 550) and a 2 m x 2 mm ID glass column filled with 80/120 Carbopack B/ 6.6% Carbowax®20M (Supelco, Inc.) was used for the identification of organic compounds and measurement of their concentration. Nitrogen, the carrier gas, flowed at a rate of 20 ml/min. The temperatures of the injector and detector were 210°C and 220°C, respectively, and the column temperature was varied from 80 to 200°C at 4°C/min. The sample volume injected varied

from 0.3 to 0.6 μl. The pressures of oxygen and hydrogen were set at 180 and 150 kPa, respectively.

Quantification of the concentrations was accomplished using a Hitachi Chromato-integrator (Hitachi Ltd. Model D2500) to measure the peak areas. The concentrations were calculated by measuring the relative areas of each component and internal standard peaks, and comparing these with the standard solutions. Standard solutions were prepared at concentrations near the concentration expected for the solution under investigation with 2,4-dimethyl-3-pentanone used as an internal standard at a concentration of 1μl.ml^{-1}.

Quantitative determination of organic compounds could be achieved down to a level of 5 ppm. In a study of 56 solutions, which were each analysed three or more times, the reproducibility of measurements for compounds with concentration above 150 ppm (w/w) averaged 5% for all the solutions injected. At this same level of concentration, the difference between the calculated and the known concentration of 21 solutions was 5.5% on average. At concentrations lower than 150 ppm the difference between known and calculated concentration increased rapidly and generally averaged 90%. Most samples analysed had a solvent concentration of 1% (w/w) or higher.

IV.3 THE INFLUENCE OF CONCENTRATION ON FLUX

The solution-diffusion model is the most accepted mechanism for the description of pervaporation flux (Chapter II).At low feed concentrations (a few ppm), the models used for prediction or correlation of flux must include mechanisms to account for the occurrence of concentration polarization. At high concentrations, flow coupling between components that are sorbed into the membrane must be investigated.

Throughout this project, the total feed concentration of the organic components was never below 1% (w/w) and care was taken to maintain the feed flow rate at the highest level possible. Therefore, concentration polarization was unlikely. During Experiment IV no influence of changes in feed flow rate could be observed. Two sets of feed mass fractions were studied and the feed pump was operated at its lowest (33 $l.h^{-1}$) and highest (200 $l.h^{-1}$) flow rates. Furthermore, the total fluxes measured in Experiment IV were comparable to the total fluxes achieved in Experiment II under similar temperature and feed concentrations. For example, despite the different feed flow rates and filter configuration, for an ethanol feed concentration of 15% w/w the total flux varied between 670-690 $g.m^{-2}.h^{-1}$ and for an ethanol feed concentration of 20% w/w the total flux was approximately 725 $g.m^{-2}.h^{-1}$. These results indicated that at the feed flow rates and concentrations studied, the permeate flux and concentration was not affected by the filter configuration and feed flow rate. However, the possibility of flow coupling between organic species could not be ignored.

The starting point for assessing the occurrence of flow coupling was Equation IV.1 developed by Kedem (1989) and discussed in Section II.3.2.2.

$$J_i = P_i \left(- \frac{dp_i}{p_i \, dz} + Q_i \, J_j \right) \qquad [IV.1]$$

where, for each component i, J_j partial flux of species j, $j \neq i$, in $g.m^{-2}.h^{-1}$;

p partial pressure in bar;

P permeability in $g.m^{-1}.h^{-1}$;

Q drag factor.

For liquids it is more convenient to work with activity instead of partial pressures and making the contribution of each species to the flow coupling explicit, for which Equation IV.1 becomes:

$$J_i = - P_i \frac{\partial \ln a_i}{\partial z} + \sum_{j \neq i} (Q_i' J_j) \qquad [IV.2]$$

where, for each component i, $Q_i' = Q_i P_i$

For a membrane of z thickness and under high vacuum on the permeate side, Equation IV.2 simplifies to:

$$J_i = \frac{P_i}{z} (\ln a_i - 0) + \sum_{j \neq i} (Q_i' J_j) \qquad [IV.3]$$

Within a limited concentration range, the partial flux at any concentration can be calculated from the relationship:

$$J_i = J_o + \frac{P_i}{z} \ln a_i + \sum_{j \neq i} (Q_i' J_j) \qquad [IV.4]$$

where, for each component i, J_j partial flux of species $j \neq i$, at the activity a_i, in $g.m^{-2}.h^{-1}$;

J_o diffusion flux of pure i in the feed in $g.m^{-2}.h^{-1}$.

Equation IV.4 must be solved simultaneously for all components unless experimental data for every J_j is available. If only the influence of ethanol coupling is considered, Equation IV.4 can be further simplified to:

$$J_i = J_o + P_i' \ln a_i + Q_i' J_{ethanol} \qquad [IV.5]$$

where, P_i' ratio of the permeability to the membrane thickness.

Alternatively, for highly swollen membranes, flow coupling could be based on total flux (J_T) through the membrane. In this case, a similar equation to IV.5 can be written:

$$J_i = J_o + P_i' \ln a_i + Q_i'' J_T \qquad [IV.6]$$

where, the first two terms on the right hand side account for the diffusional flux and the last term on the right hand side accounts for the influence of the total flux.

IV.3.1 Analysis of experimental results

In order to evaluate the influence of coupling on the flux of minor organic components in the presence of ethanol, the results for two sets of experiments were analysed. In Experiment II the ratio of fusels concentration to ethanol concentration was kept constant while the ethanol concentration varied by dilution with water between approximately 5 and 20% (w/w). In Experiment III the fusels concentration was kept constant while the ethanol concentration varied between 0 and 20% (w/w). In Experiment III, the ethanol concentration was the only concentration to be varied; firstly, because it was the major organic component in all feed mixtures and therefore the most likely to participate in coupling; secondly, there was a strong correlation between the feed concentration of the organic components in the feed because of the use of solutions obtained by dilution in Experiment II. This correlation of the feed concentration could also have influenced the partial fluxes and thus affected the analysis of the occurrence of coupling between the partial flux of ethanol and the partial flux of the fusels in Experiment II. Experiment III was performed to address this issue.

Measured fluxes from Experiments II and III for GFT 1070 (Tables III.10 and II.12) were fitted by the solution-diffusion, linear Equation IV.7:

$$J_i = J_o + P_i' \ln a_i \qquad [IV.7]$$

where, P_i' ratio of the permeability by the membrane thickness.

They were also fitted by the ethanol and total flux coupling (Equations IV.5 and IV.6) using the *fsolve* and *leastsq* functions of MatLab® (Mathworks, Inc., USA) and analysed with the inferential statistical procedures for multiple regression described by Koopmans (1987). All fitted parameters are given in Tables IV.15 through IV.19 and Figures IV.7 through IV.37. Tables IV.15 through IV.19 show relevant statistics, and fitted parameters for all organic compounds at the various temperatures studied. Figures IV.7 through IV.31 show the experimental data and fitted lines for each compound at each temperature.

The statistical analysis of the coupling/convection model was performed to judge whether:

- the model explained the behaviour of the raw data;
- the extra variable for coupling or convection was statistically significant.

The model hypothesis was assessed using an F-test and the variable hypothesis was assessed by a t-test.

Table IV.15 Summary of fitted parameters and linear, multivariable statistics for evaluation of flow coupling effects in pervaporation (Experiment II, 60°C).

Model		EtOH	nPrOH	iBuOH	nBuOH	iAmOH	EtOAc
	n	12	12	12	12	12	12
Equation	J_o	371.7	52.3	22.0	2.2	156.4	15.7
IV.7	P	131.5	8.8	3.2	0.2	37.1	2.0
	r^2	0.72	0.72	0.62	0.58	0.12	0.66
	H_1: P≠0	Y	Y	Y	Y	N	Y
Equation	J_o		-1.1e-07	1.2e-07	1.8e-10	-2.7e-07	1.5e-05
IV.5	P		-2.8e-10	1.6e-09	7.2e-12	-1.6e-08	-7.0e-08
	Q		4.4e-02	2.1e-02	1.3e-03	4.6e-01	1.5e-02
	r^2		0.86	0.79	0.60	0.66	0.63
	H_1: P≠0		Y	Y	Y	Y	Y
	H_1: Q≠0		Y	Y	Y	Y	Y
Equation	J_o		1.1e-09	5.1e-09	-1.2e-10	-2.0e-07	-1.5e-08
IV.6	P		-7.2e-11	-1.4e-10	-1.2e-12	-5.4e-08	-2.4e-10
	Q		1.4e-02	6.7e-03	4.2e-04	1.5e-01	4.8e-03
	r^2		0.65	0.67	0.59	0.68	0.61
	H_1: P≠0		Y	Y	Y	Y	Y
	H_1: Q≠0		N	N	N	N	N

EtOH: ethanol; nPrOH: *n*-propanol; iBuOH: *i*-butanol; nBuOH: *n*-butanol; iAmOH: *i*-amyl alcohol; n: number of observations; Y: yes; N: no.

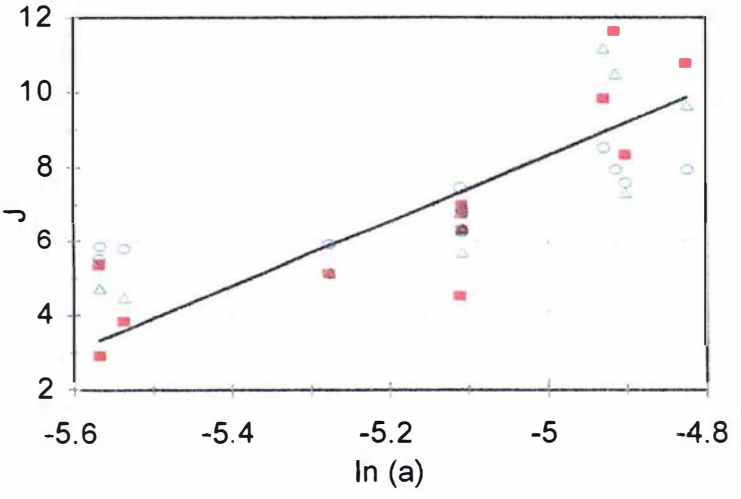

Figure IV.7 Experimental data and predicted flux for *n*-propanol at 60°C through GFT 1070, Experiment II. *J*: flux in $g.m^{-2}.h^{-1}$; ■: raw data; —: Eq. IV.7; △ : Eq. IV.5; ○ : Eq. IV.6.

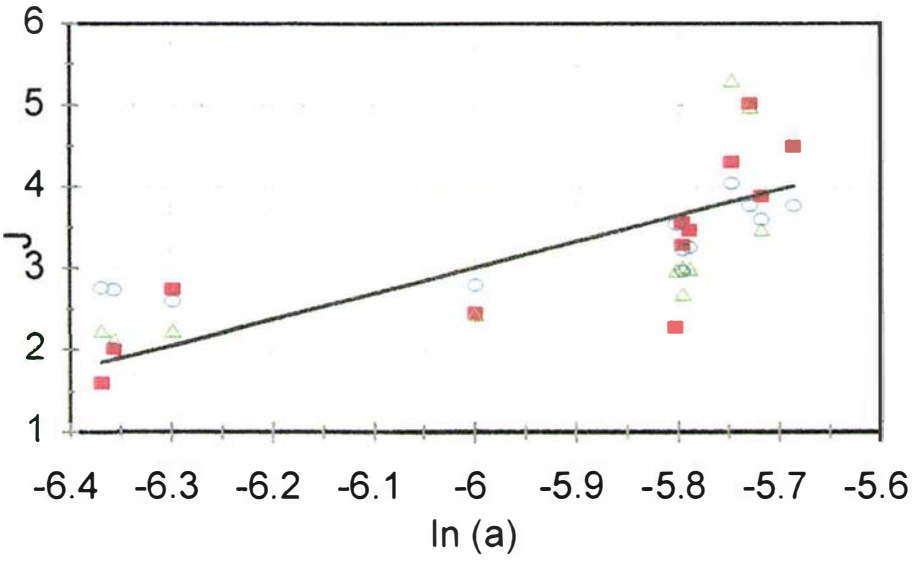

Figure IV.8 Experimental data and predicted flux for *i*-butanol at 60°C through GFT 1070, Experiment II. *J*: flux in $g.m^{-2}.h^{-1}$; ■: raw data; —: Eq. IV.7; △ : Eq. IV.5; ○ : Eq. IV.6.

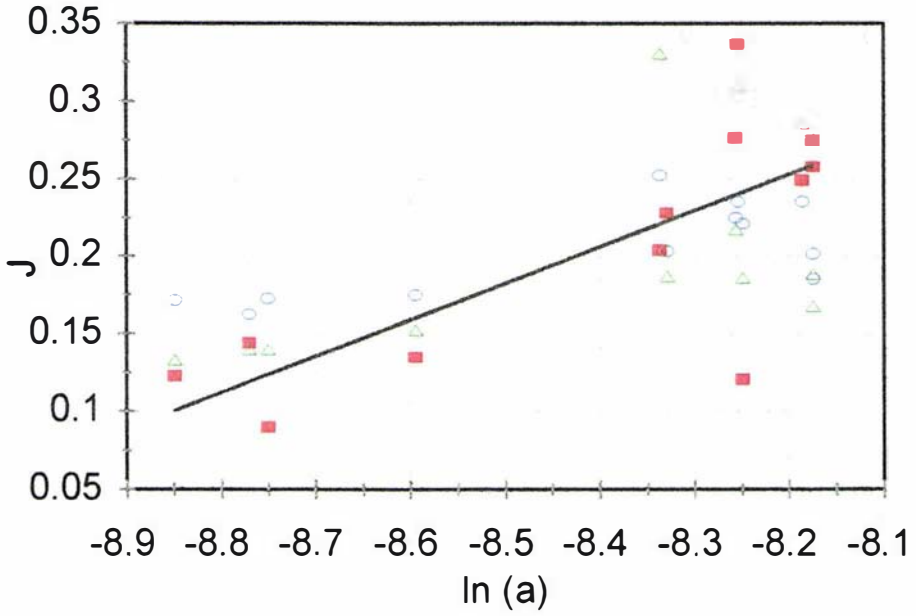

Figure IV.9 Experimental data and predicted flux for *n*-butanol at 60°C through GFT 1070, Experiment II. *J*: flux in $g.m^{-2}.h^{-1}$; ■: raw data; —: Eq. IV.7; △ : Eq. IV.5; ○ : Eq. IV.6.

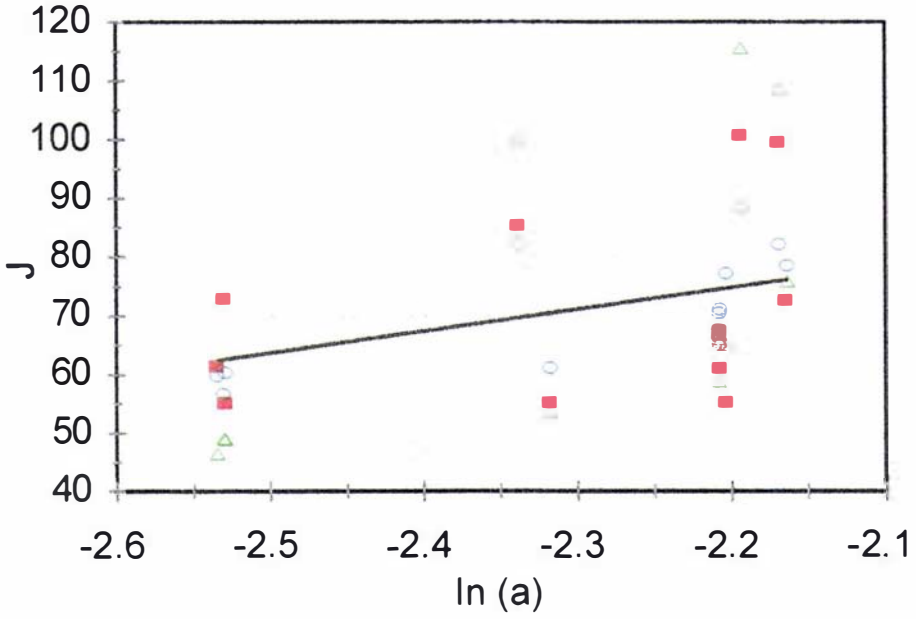

Figure IV.10 Experimental data and predicted flux for *i*-amyl alcohol at 60°C through GFT 1070, Experiment II. *J*: flux in $g.m^{-2}.h^{-1}$; ■: raw data; —: Eq. IV.7; △ : Eq. IV.5; ○ : Eq. IV.6.

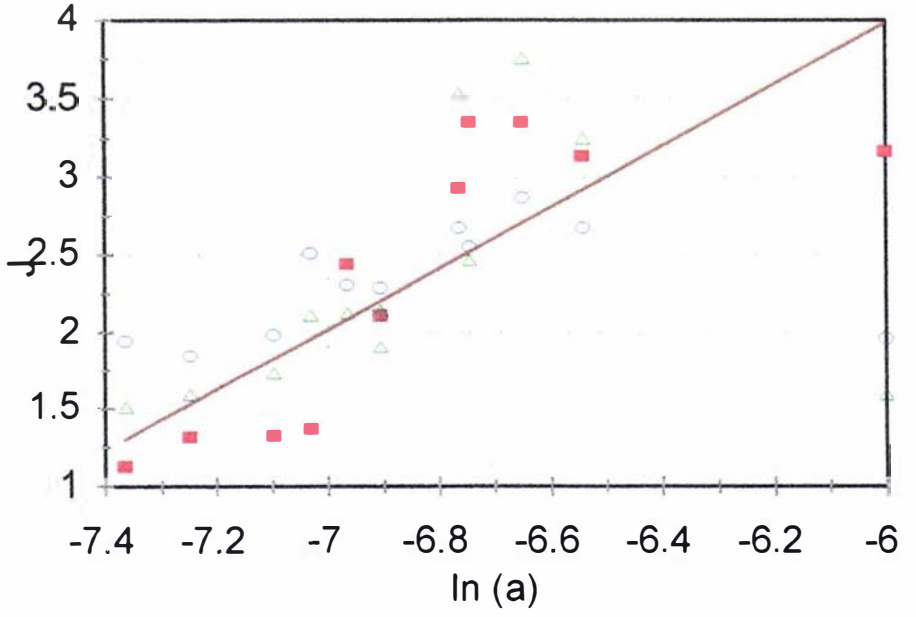

Figure IV.11 Experimental data and predicted flux for ethyl acetate at 60°C through GFT 1070, Experiment II. *J*: flux in $g.m^{-2}.h^{-1}$; ■: raw data; —: Eq. IV.7; △ : Eq. IV.5; ○ : Eq. IV.6.

Table IV.16 Summary of fitted parameters and linear, multivariable statistics for evaluation of flow coupling effects in pervaporation (Experiment II, 65°C).

Model		EtOH	nPrOH	iBuOH	nBuOH	iAmOH	EtOAc
	n	11	11	11	11	11	11
Equation	J_o	412.1	64.6	32.4	3.3	252.8	18.1
IV.7	P	132.3	10.9	4.8	0.4	72.3	2.3
	r^2	0.82	0.94	0.95	0.83	0.68	0.60
	H_1: P≠0	Y	Y	Y	Y	Y	Y
Equation	J_o		9.0e-12	1.2e-12	-6.3e-11	-1.1e-06	-8.1e-11
IV.5	P		7.3e-13	6.7e-13	6.1e-13	3.5e-07	-2.4e-12
	Q		4.2e-02	2.0e-02	1.3e-03	4.4e-01	1.2e-02
	r^2		0.79	0.76	0.69	0.65	0.61
	H_1: P≠0		Y	Y	Y	Y	Y
	H_1: Q≠0		N	Y	N	Y	N
Equation	J_o		3.8e-07	-2.5e-09	-2.0e-10	-6.5e-09	2.9e-12
IV.6	P		5.0e-08	6.7e-11	2.5e-12	7.6e-09	7.5e-13
	Q		1.4e-02	6.4e-03	4.2e-04	1.4e-01	3.9e-03
	r^2		0.67	0.67	0.63	0.70	0.64
	H_1: P≠0		Y	Y	Y	Y	Y
	H_1: Q≠0		N	N	N	Y	N

EtOH: ethanol; nPrOH: *n*-propanol; iBuOH: *i*-butanol; nBuOH: *n*-butanol; iAmOH: *i*-amyl alcohol.n: number of observations; Y: yes; N: no.

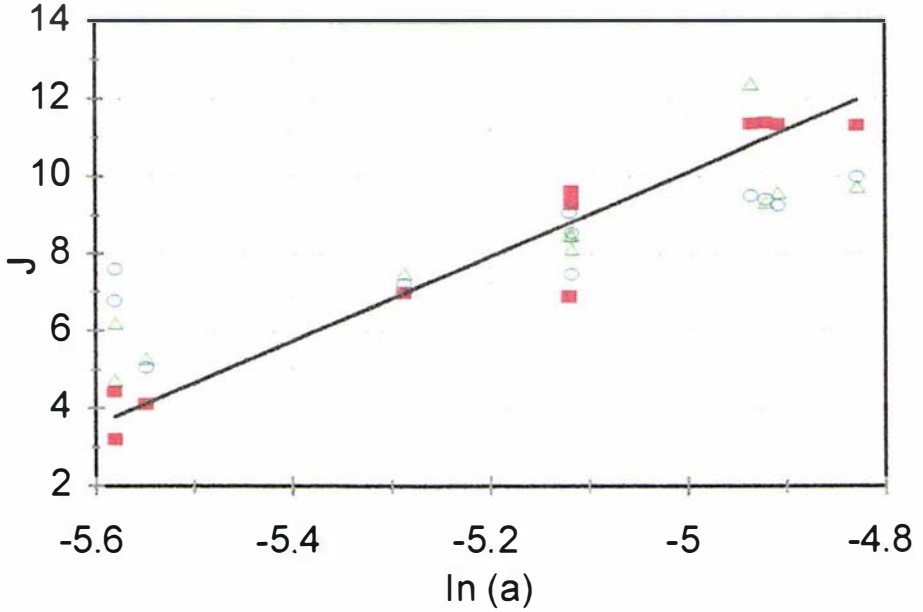

Figure IV.12 Experimental data and predicted flux for *n*-propanol at 65°C through GFT 1070, Experiment II. *J*: flux in $g.m^{-2}.h^{-1}$; ■: raw data; —: Eq. IV.7; △ : Eq. IV.5; ○ : Eq. IV.6.

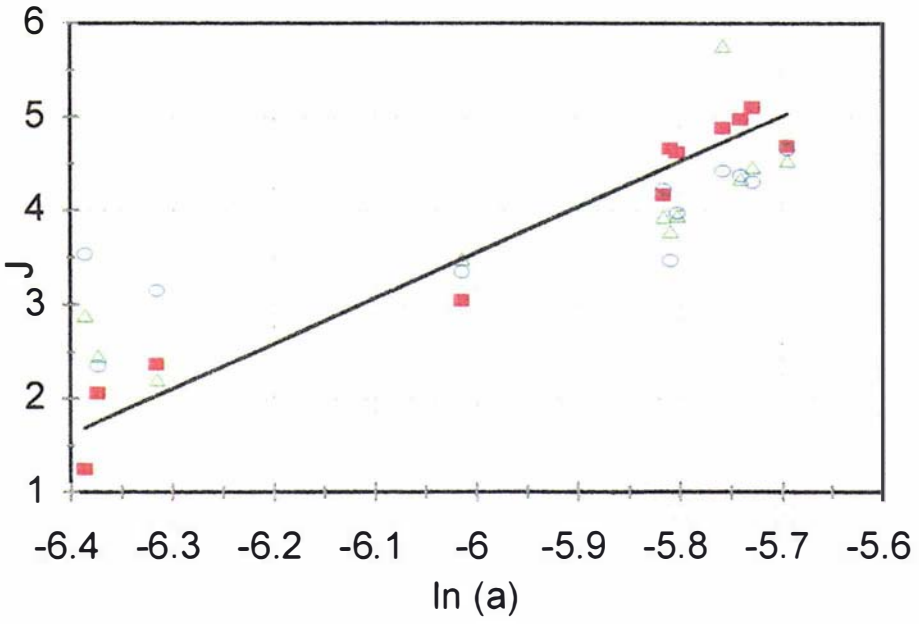

Figure IV.13 Experimental data and predicted flux for *i*-butanol at 65°C through GFT 1070, Experiment II. *J*: flux in $g.m^{-2}.h^{-1}$; ■: raw data; —: Eq. IV.7; △ : Eq. IV.5; ○ : Eq. IV.6.

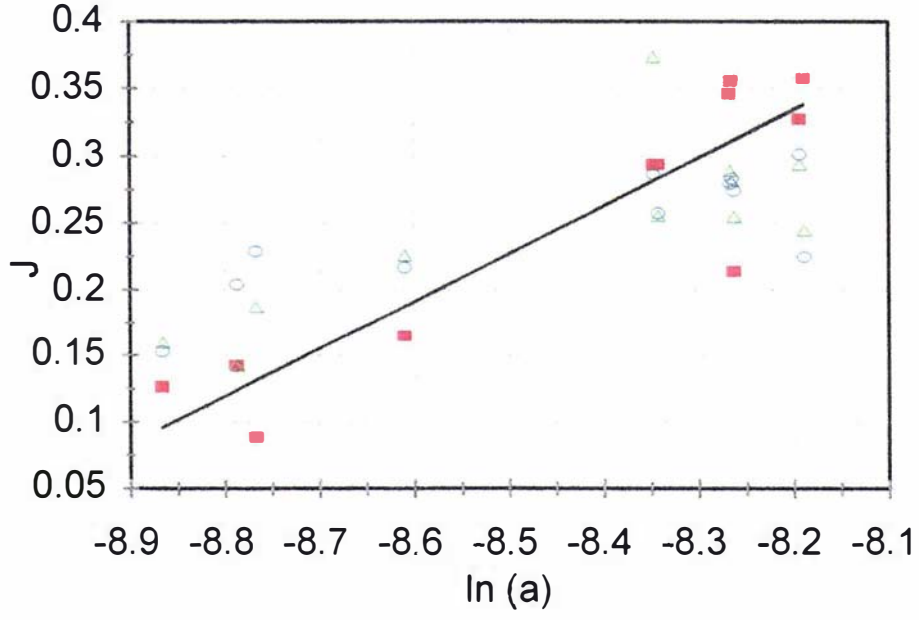

Figure IV.14 Experimental data and predicted flux for *n*-butanol at 65°C through GFT 1070, Experiment II. *J*: flux in $g.m^{-2}.h^{-1}$; ■: raw data; —: Eq. IV.7; △ : Eq. IV.5; ○ : Eq. IV.6.

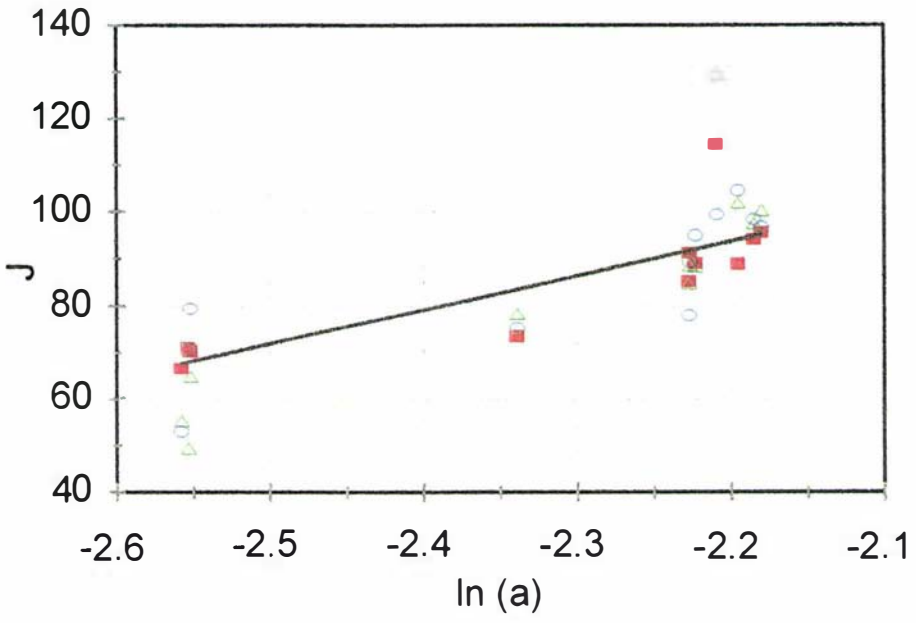

Figure IV.15 Experimental data and predicted flux for *i*-amyl alcohol at 65°C through GFT 1070, Experiment II. *J*: flux in $g.m^{-2}.h^{-1}$; ■: raw data; —: Eq. IV.7; △ : Eq. IV.5; ○ : Eq. IV.6.

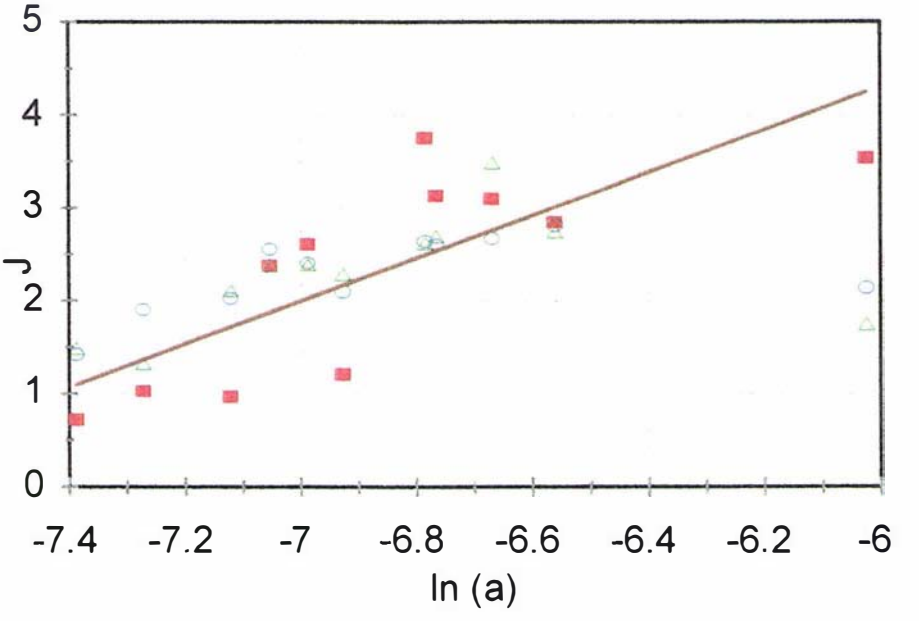

Figure IV.16 Experimental data and predicted flux for ethyl acetate at 65°C through GFT 1070, Experiment II. *J*: flux in $g.m^{-2}.h^{-1}$; ■: raw data; —: Eq. IV.7; △ : Eq. IV.5; ○ : Eq. IV.6.

Table IV.17 Summary of fitted parameters and linear, multivariable statistics for evaluation of flow coupling effects in pervaporation (Experiment II, 70°C).

Model		EtOH	nPrOH	iBuOH	nBuOH	iAmOH	EtOAc
	n	11	11	11	11	11	11
Equation	J_0	504.7	80.0	37.3	3.3	293.2	18.6
IV.7	P	153.0	13.4	5.5	0.4	79.6	2.3
	r^2	0.83	0.94	0.96	0.78	0.63	0.56
	H_1: P≠0	Y	Y	Y	Y	Y	Y
Equation	J_0		-2.7e-08	3.0e-09	5.2e-09	1.6e-06	-4.5e-09
IV.5	P		-1.2e-10	2.1e-11	5.2e-12	-2.3e-08	4.8e-11
	Q		4.1e-02	1.9e-02	1.2e-03	4.3e-01	1.1e-02
	r^2		0.77	0.75	0.64	0.67	0.65
	H_1: P≠0		Y	Y	Y	Y	Y
	H_1: Q≠0		N	Y	N	Y	N
Equation	J_0		-1.5e-11	6.5e-09	-2.3e-07	3.7e-07	-1.5e-08
IV.6	P		6.9e-13	-2.4e-12	-3.1e-09	4.6e-09	2.6e-11
	Q		1.4e-02	6.4e-03	4.0e-04	1.5e-01	3.9e-03
	r^2		0.69	0.68	0.60	0.60	0.67
	H_1: P≠0		Y	Y	Y	Y	Y
	H_1: Q≠0		N	N	N	Y	N

EtOH: ethanol; nPrOH: *n*-propanol; iBuOH: *i*-butanol; nBuOH: *n*-butanol; iAmOH: *i*-amyl alcohol.n: number of observations; Y: yes; N: no.

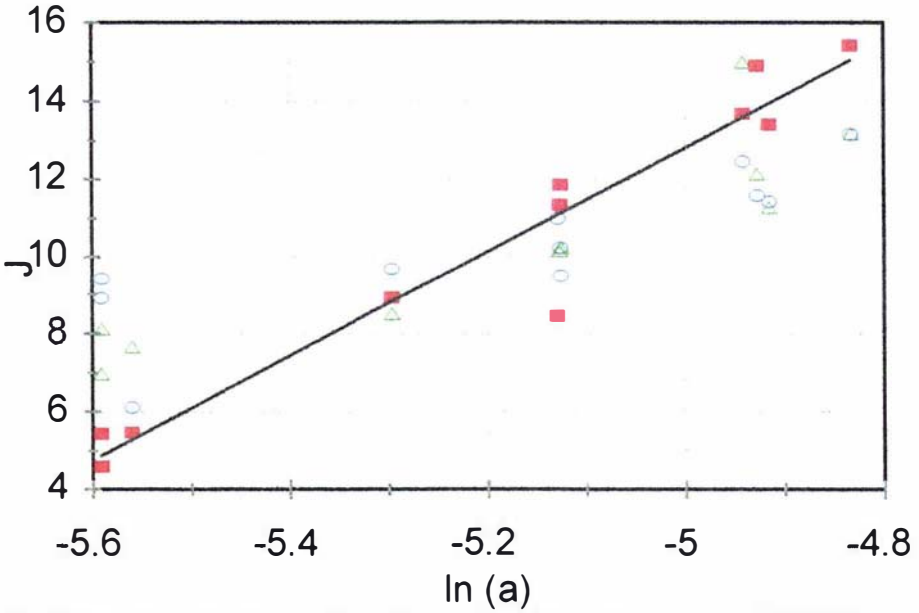

Figure IV.17 Experimental data and predicted flux for *n*-propanol at 70°C through GFT 1070, Experiment II. *J*: flux in $g.m^{-2}.h^{-1}$; ■: raw data; —: Eq. IV.7; △ : Eq. IV.5; ○ : Eq. IV.6.

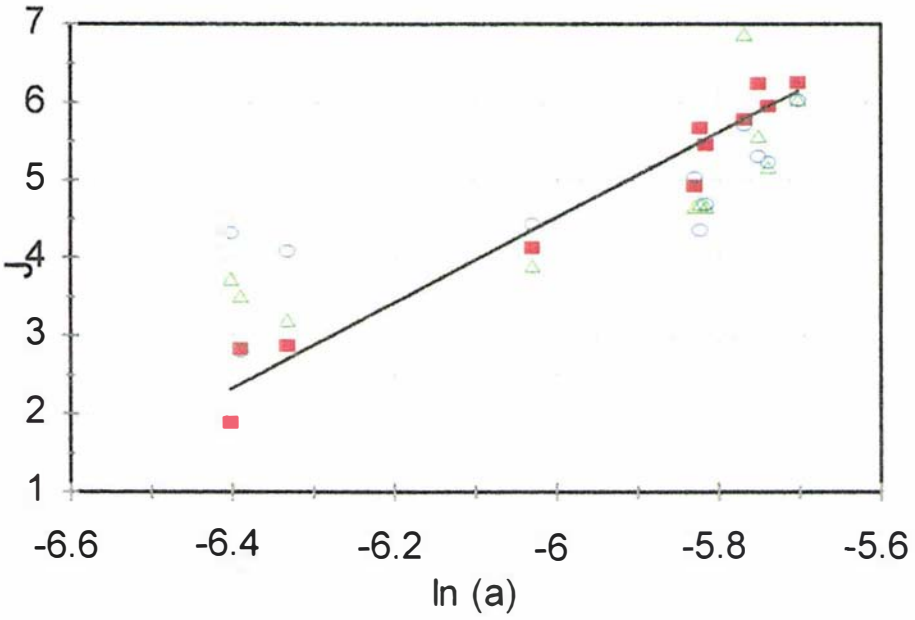

Figure IV.18 Experimental data and predicted flux for *i*-butanol at 70°C through GFT 1070, Experiment II. *J*: flux in $g.m^{-2}.h^{-1}$; ■: raw data; —: Eq. IV.7; △ : Eq. IV.5; ○ : Eq. IV.6.

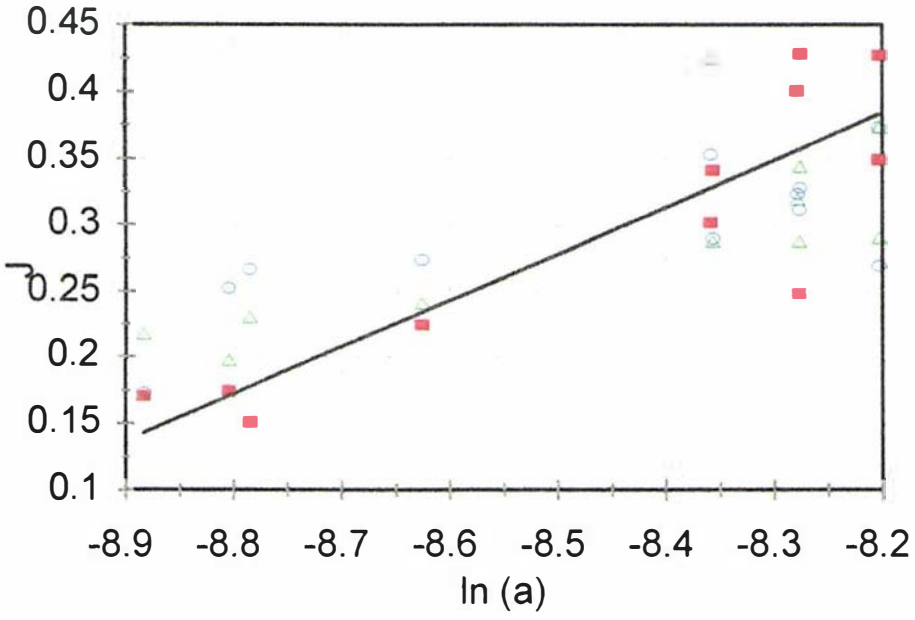

Figure IV.19 Experimental data and predicted flux for *n*-butanol at 70°C through GFT 1070, Experiment II. *J*: flux in $g.m^{-2}.h^{-1}$; ■: raw data; —: Eq. IV.7; △ : Eq. IV.5; ○ : Eq. IV.6.

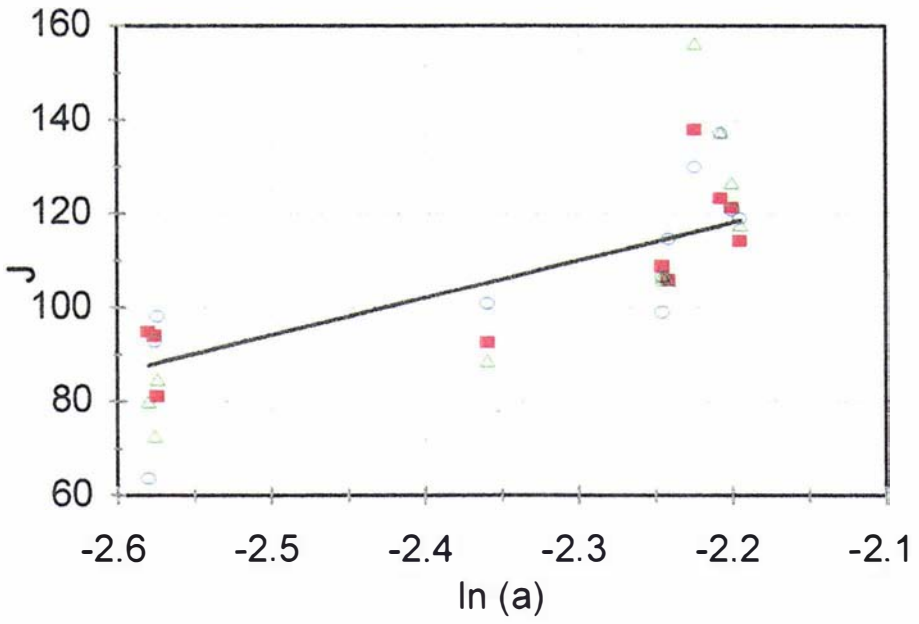

Figure IV.20 Experimental data and predicted flux for *i*-amyl alcohol at 70°C through GFT 1070, Experiment II. *J*: flux in $g.m^{-2}.h^{-1}$; ■: raw data; —: Eq. IV.7; △ : Eq. IV.5; ○ : Eq. IV.6.

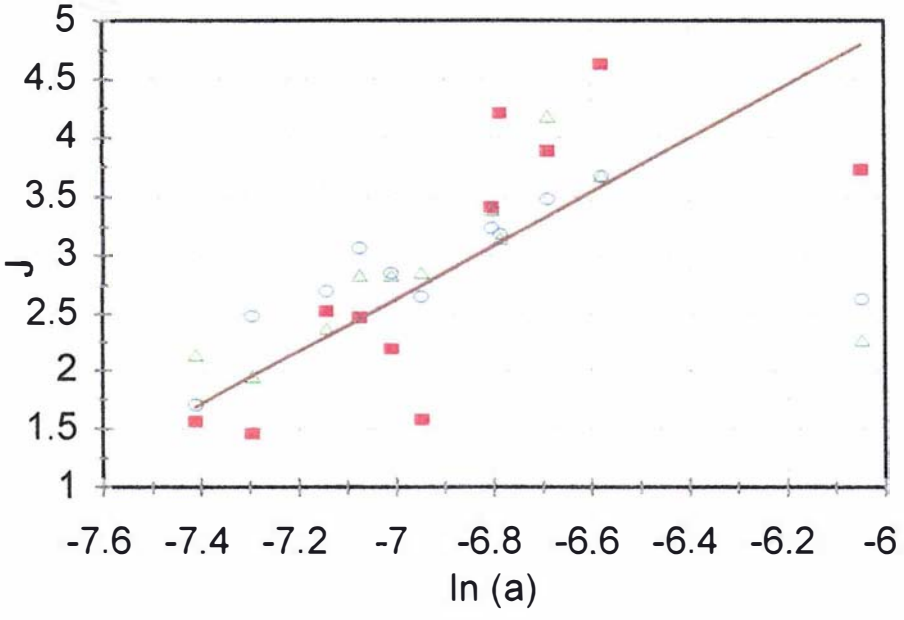

Figure IV.21 Experimental data and predicted flux for ethyl acetate at 70°C through GFT 1070, Experiment II. *J*: flux in $g.m^{-2}.h^{-1}$; ■: raw data; —: Eq. IV.7; △ : Eq. IV.5; ○ : Eq. IV.6.

Table IV.18 Summary of fitted parameters and linear, multivariable statistics for evaluation of flow coupling effects in pervaporation (Experiment II, 75°C).

Model		EtOH	nPrOH	iBuOH	nBuOH	iAmOH	EtOAc
	n	14	14	14	14	14	14
Equation	J_0	670.2	97.6	41.5	3.7	461.2	32.3
IV.7	P	225.7	16.4	6.0	0.4	145.0	4.3
	r^2	0.87	0.92	0.94	0.82	0.77	0.73
	H_1: P≠0	Y	Y	Y	Y	Y	Y
Equation	J_0		5.1e-10	4.4e-08	1.9e-13	-7.1e-11	-2.4e-10
IV.5	P		8.5e-12	-3.4e-10	9.3e-13	-1.7e-11	-1.8e-12
	Q		4.2e-02	1.9e-02	1.1e-03	4.1e-01	9.1e-03
	r^2		0.82	0.83	0.70	0.83	0.57
	H_1: P≠0		Y	Y	Y	Y	Y
	H_1: Q≠0		Y	Y	Y	Y	N
Equation	J_0		1.3e-07	-2.7e-11	-9.4e-08	1.3e-07	3.2e-09
IV.6	P		8.6e-10	-4.6e-13	-1.3e-09	2.6e-09	4.2e-10
	Q		1.5e-02	6.6e-03	4.0e-04	1.4e-01	3.2e-03
	r^2		0.66	0.70	0.63	0.91	0.58
	H_1: P≠0		Y	Y	Y	Y	Y
	H_1: Q≠0		N	Y	N	Y	N

EtOH: ethanol; nPrOH: *n*-propanol; iBuOH: *i*-butanol; nBuOH: *n*-butanol; iAmOH: *i*-amyl alcohol.n: number of observations; Y: yes; N: no.

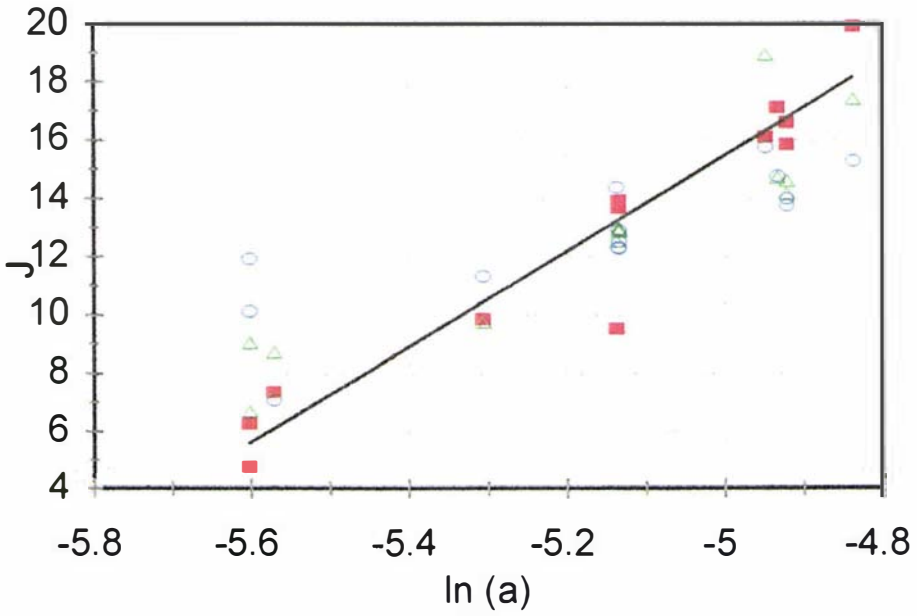

Figure IV.22 Experimental data and predicted flux for *n*-propanol at 75°C through GFT 1070, Experiment II. *J*: flux in $g.m^{-2}.h^{-1}$; ■: raw data; —: Eq. IV.7; △ : Eq. IV.5; ○ : Eq. IV.6.

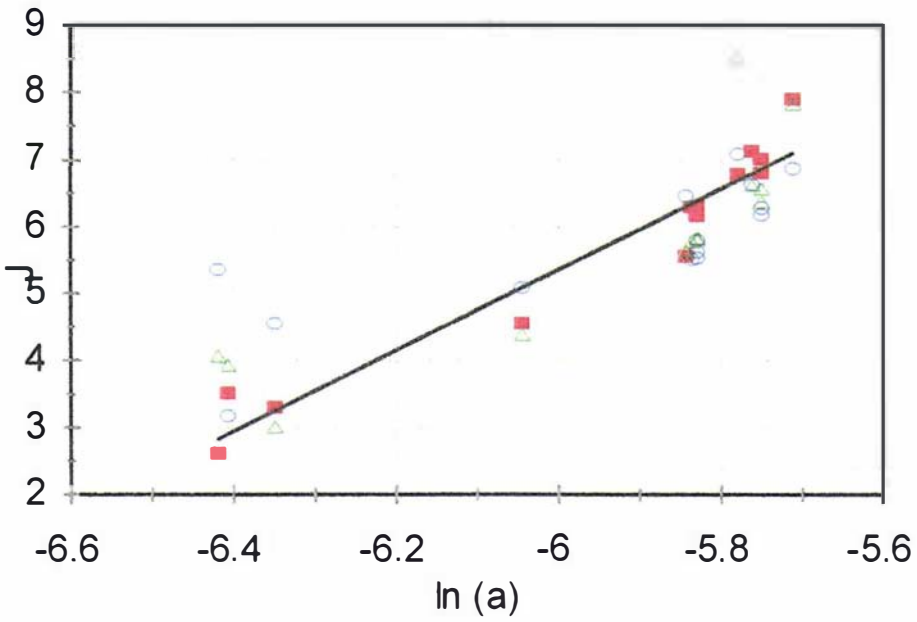

Figure IV.23 Experimental data and predicted flux for *i*-butanol at 75°C through GFT 1070, Experiment II. *J*: flux in $g.m^{-2}.h^{-1}$; ■: raw data; —: Eq. IV.7; △ : Eq. IV.5; ○ : Eq. IV.6.

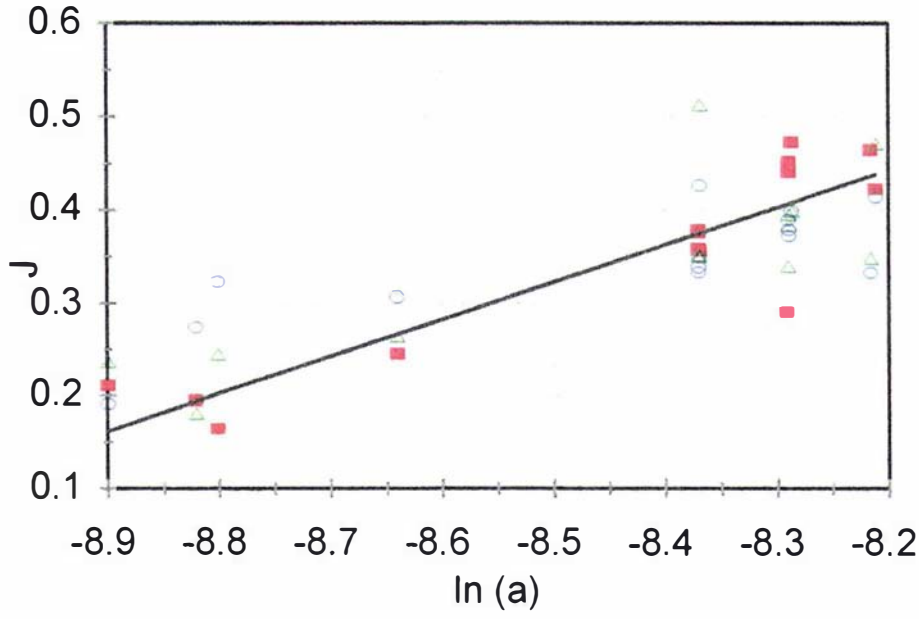

Figure IV.24 Experimental data and predicted flux for *n*-butanol at 75°C through GFT 1070, Experiment II. *J*: flux in $g.m^{-2}.h^{-1}$; ■: raw data; —: Eq. IV.7; △ : Eq. IV.5; ○ : Eq. IV.6.

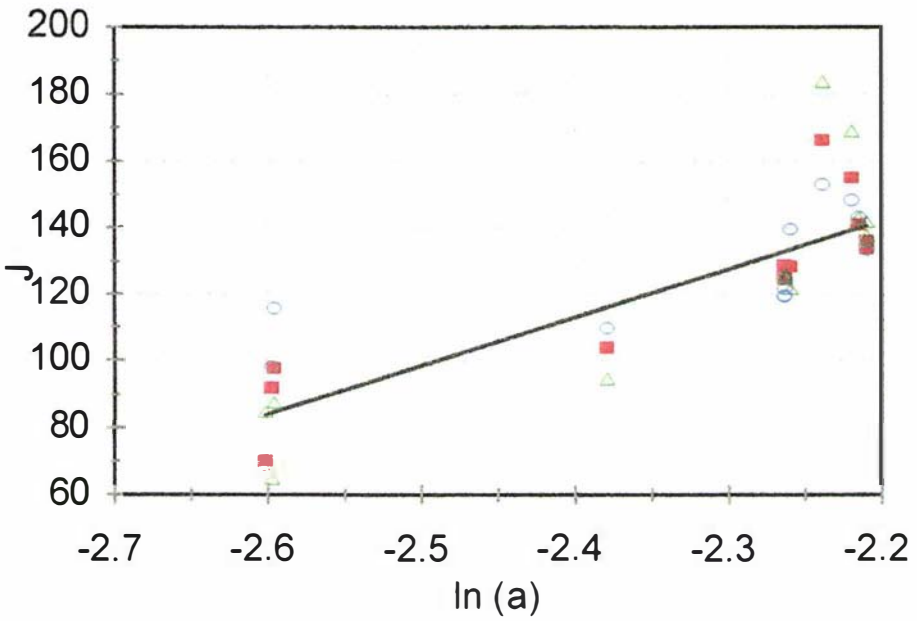

Figure IV.25 Experimental data and predicted flux for *i*-amyl alcohol at 75°C through GFT 1070, Experiment II. *J*: flux in $g.m^{-2}.h^{-1}$; ■: raw data; —: Eq. IV.7; △ : Eq. IV.5; ○ : Eq. IV.6.

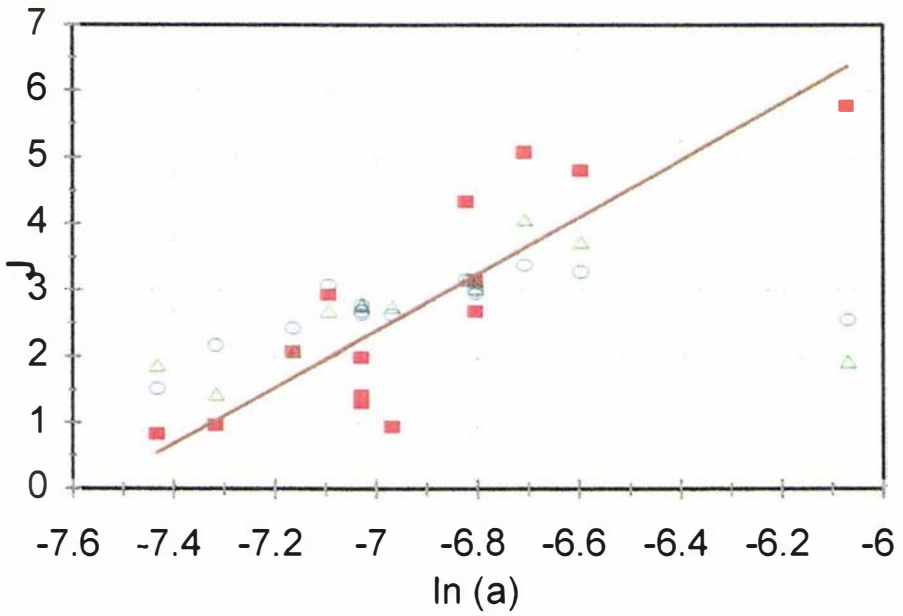

Figure IV.26 Experimental data and predicted flux for ethyl acetate at 75°C through GFT 1070, Experiment II. *J*: flux in $g.m^{-2}.h^{-1}$; ■: raw data; —: Eq. IV.7; △ : Eq. IV.5; ○ : Eq. IV.6.

Table IV.19 Summary of fitted parameters and linear, multivariable statistics for evaluation of flow coupling effects in pervaporation (Experiment III, 70°C). J_o and P are in $g.m^{-2}.h^{-1}$.

Model		EtOH	nPrOH	iBuOH	nBuOH	iAmOH	EtOAc
	n	29	29	29	29	29	29
Equation	J_o	61.2	3.38	2.40	0.22	43.2	0.68
IV.7	P	10.8	0.43	0.29	0.02	9.36	0.08
	r^2	0.52	0.36	0.58	0.61	0.53	0.34
	H_1: P≠0		Y	Y	Y	Y	Y
Equation	J_o		3.35	1.76	0.14	39.6	0.19
IV.5	P		0.40	0.18	0.01	7.92	-9.36e-05
	Q		-1.7e-04	-1.8e-03	-1.6e-04	-2.7e-02	-9.8e-04
	r^2		0.61	0.72	0.72	0.68	0.59
	H_1: P≠0		Y	Y	Y	Y	Y
	H_1: Q≠0		N	N	Y	N	Y
Equation	J_o		3.42	2.02	0.27	43.2	0.04
IV.6	P		0.43	0.21	0.03	17.3	-0.03
	Q		1.3e-04	-1.2e-03	1.1e-04	1.4e-01	-6.5e-04
	r^2		0.61	0.71	0.72	0.69	0.56
	H_1: P≠0		Y	Y	Y	Y	Y
	H_1: Q≠0		N	N	N	Y	Y

n: number of observations; Y: yes; N: no. EtOH: ethanol; nPrOH: *n*-propanol; iBuOH: *i*-butanol; nBuOH: *n*-butanol; iAmOH: *i*-amyl alcohol.

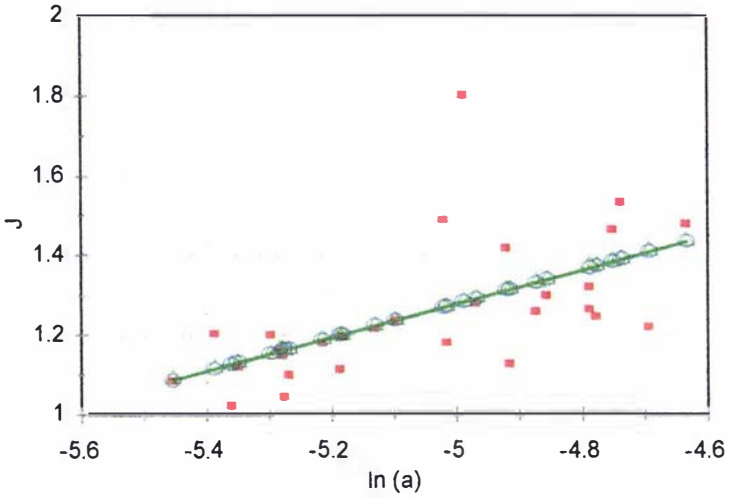

Figure IV.27 Experimental data and predicted flux for *n*-propanol at 70°C through GFT 1070, Experiment III. *J*: flux in $g.m^{-2}.h^{-1}$; ■: raw data; —: Eq. IV.7; ○ : Eq. IV.5; △: Eq. IV.6.

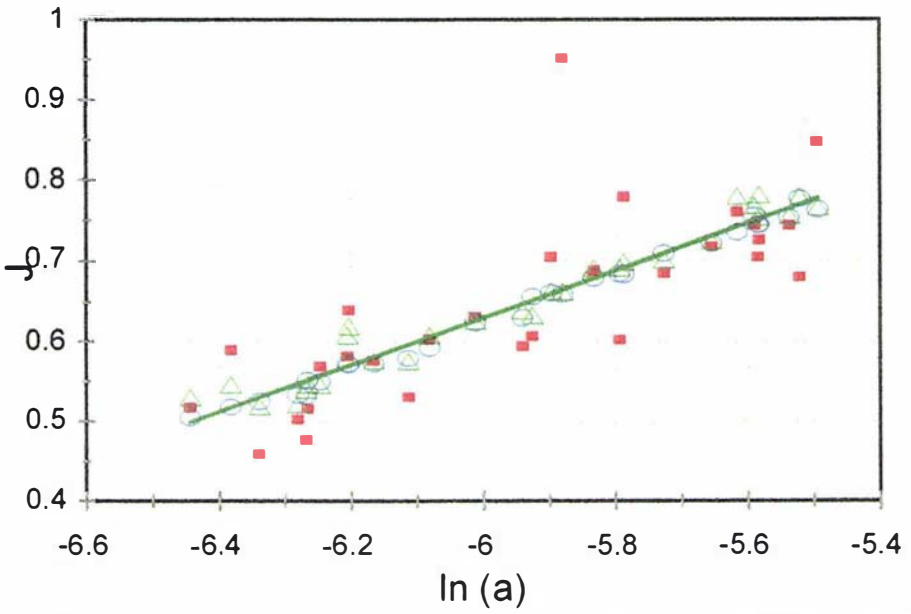

Figure IV.28 Experimental data and predicted flux for *i*-butanol at 70°C through GFT 1070, Experiment III. *J*: flux in $g.m^{-2}.h^{-1}$; ■: raw data; —: Eq. IV.7; ○ : Eq. IV.5; △: Eq. IV.6.

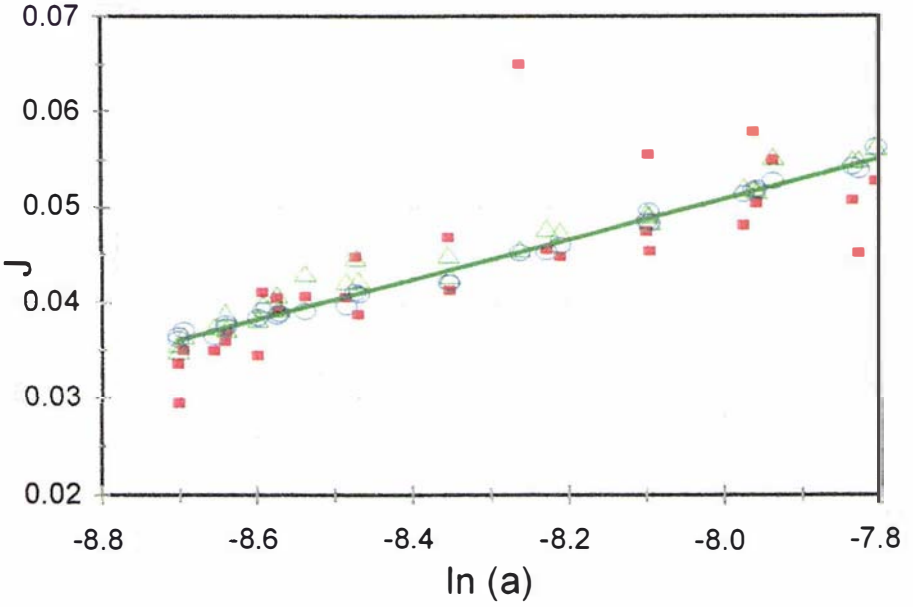

Figure IV.29 Experimental data and predicted flux for *n*-butanol at 70°C through GFT 1070, Experiment III. *J*: flux in $g.m^{-2}.h^{-1}$; ■: raw data; —: Eq. IV.7; ○ : Eq. IV.5; △: Eq. IV.6.

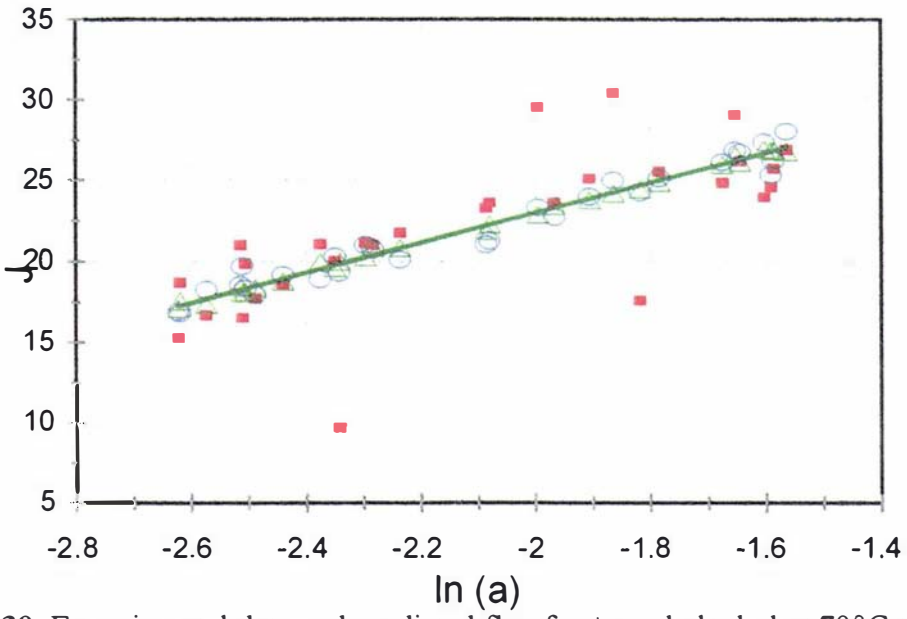

Figure IV.30 Experimental data and predicted flux for *i*-amyl alcohol at 70°C through GFT 1070, Experiment III. *J*: flux in $g.m^{-2}.h^{-1}$; ■: raw data; —: Eq. IV.7; ○ : Eq. IV.5; △: Eq. IV.6.

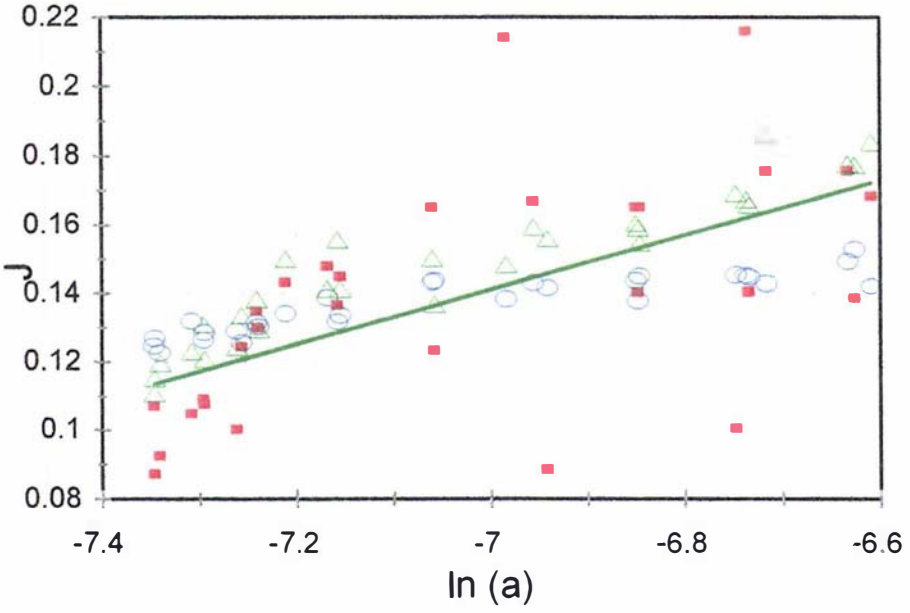

Figure IV.31 Experimental data and predicted flux for ethyl acetate at 70°C through GFT 1070, Experiment III. *J*: flux in $g.m^{-2}.h^{-1}$; ■: raw data; —: Eq. IV.7; ○ : Eq. IV.5; △: Eq. IV.6.

As explained in Section IV.2.1.3, the feed and return pipings of the membrane cell were changed between Experiment II and III. With the larger piping diameter (Experiment III), it was observed that preferential flow occurred through one of the axial exits, the other three had minimal flow. As a consequence, the effective membrane area available for pervaporation decreased by an unknown value. However, on calculating the flux of Experiment III, it was assumed that the whole membrane area was available, and, therefore, the flux values of Experiment III should only be considered qualitatively. Experiment IV confirmed the accuracy of the flux values obtained with Experiment II and the separation trends observed in Experiment III were similar as those observed in Experiments I and II as shown in the enrichment factor plots of Section IV.2. For a temperature of 70°C and a nominal ethanol feed concentration of 15% (w/w), in Experiment II (Table IV.10) it was shown that the total flux varied between 679 and 810 $g.m^{-2}.h^{-1}$; under similar feed conditions, the total flux in Experiment IV (Table IV.14) varied between 666 and 675 $g.m^{-2}.h^{-1}$; however, in Experiment III (Table IV.12), the total flux calculated varied between 137 and 147 $g.m^{-2}.h^{-1}$. In this light, Experiments II and III were analysed separately.

In Tables IV.15 through IV.19, for Experiment II with GFT 1070, the linear model (Equation IV.7) explained the behaviour of all organic components at all temperatures, except for *i*-amyl alcohol at 60°C. The poor fit was probably caused by the large uncertainty in the experimental data as shown in Figures IV.7 through IV.31. The introduction of an extra variable for flow coupling did not improve the model fit (r^2) significantly for most organic components. For *i*-amyl alcohol the improvement was in most cases marginal. However, visual analysis of Figures IV.10, IV.15, IV.20 and IV.25 in contrast to Figures IV.7 through IV.31 for the other organic components might suggest that Equation IV.5 could provide a better fit of the raw data of *i*-amyl alcohol than the linear model.

Experiment II was not conclusive as to whether the ethanol or the total flux best described the effect of flow coupling on the flux of *i*-amyl alcohol. In Experiment II, the concentration of ethanol and the minor organic components was kept at a constant

ratio.The aim of Experiment III was to discriminate between the influence of ethanol flux or total flux in the partial flux of *i*-amyl alcohol. Therefore, during the experiment, the feed concentration of ethanol varied between 0 and 20% (w/w) while the total and individual feed concentrations of the fusels was kept constant.

Figure IV.32 shows that there was a strong correlation between the total flux and the ethanol partial flux for Experiment III, which indicates that it is not possible to separate the influence of either flux. The statistical analysis of the partial flux of *i*-amyl alcohol confirmed this observation (Table IV.19), for given the small difference in the values of the correlation coefficient ($r^2 = 0.68$ for Equation IV.5 and 0.69 for Equation IV.6), it was also not conclusive whether the flux of ethanol or the total flux was the major influence in coupling.

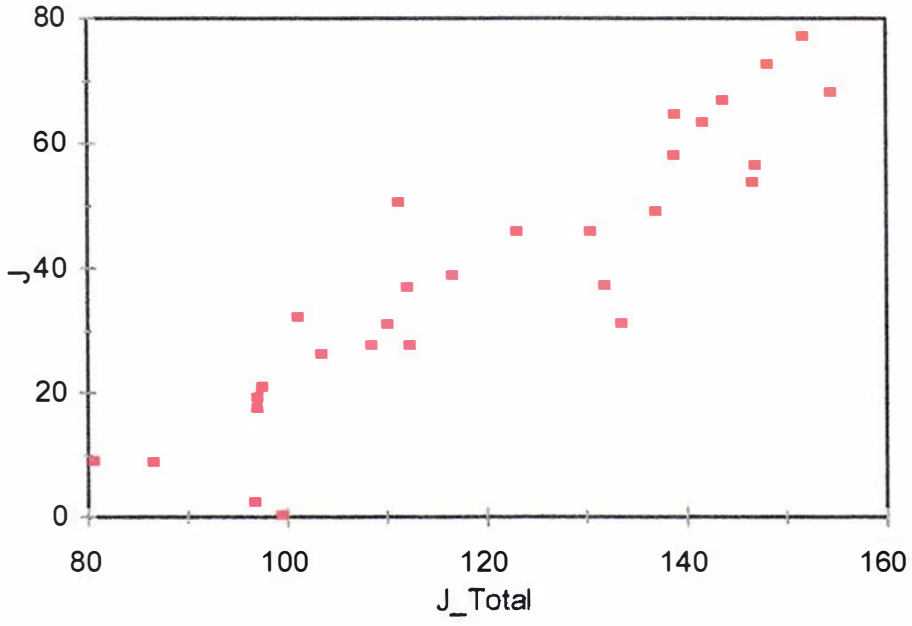

Figure IV.32 Relationship between partial flux of ethanol and total flux, Experiment III. *J*: flux in $g.m^{-2}.h^{-1}$; ■: raw data.

For *n*-propanol, the butanol isomers, and ethyl acetate, the partial flux was virtually independent of the total flux in Experiment III (Figures IV.33 to IV.35 an Figure IV.37). The poor fit with the linear model (Equation IV.7) was probably due the large uncertainty of the experimental data (Figures IV.27 to IV.31) and the slight improvement of the data fitting with the inclusion of the coupling terms (Equations IV.5 and IV.6) is not enough to show that coupling is a physically significant process (Table IV.19). However, in Figure IV.36, the correlation between the flux of *i*-amyl alcohol and the total flux is another evidence for the possibility of flux coupling.

Given that most minor organic components belong to the same chemical family and should therefore behave similarly towards ethanol or total flux coupling, it can be speculated that the influence of ethanol or total flux was stronger for *i*-amyl alcohol than for the other minor organic components because of *i*-amyl alcohol's higher content in the feed: 1% (w/w) for *i*-amyl alcohol compared to 0.1% to a few ppm for the other minor organic components. Therefore, the possibility of coupling influencing the partial flux of other organic components should not be dismissed if their feed concentration is higher than the range studied. Given the lack of similar studies, it is however not yet possible to provide guidelines on the concentration where the influence of coupling may become significant.

In conclusion, for the system under study, for *i*-amyl alcohol, it is recommended that the coupling model with total flux should be used for best accuracy. For all other components, the linear model based on the feed activity only described their partial fluxes satisfactorily.

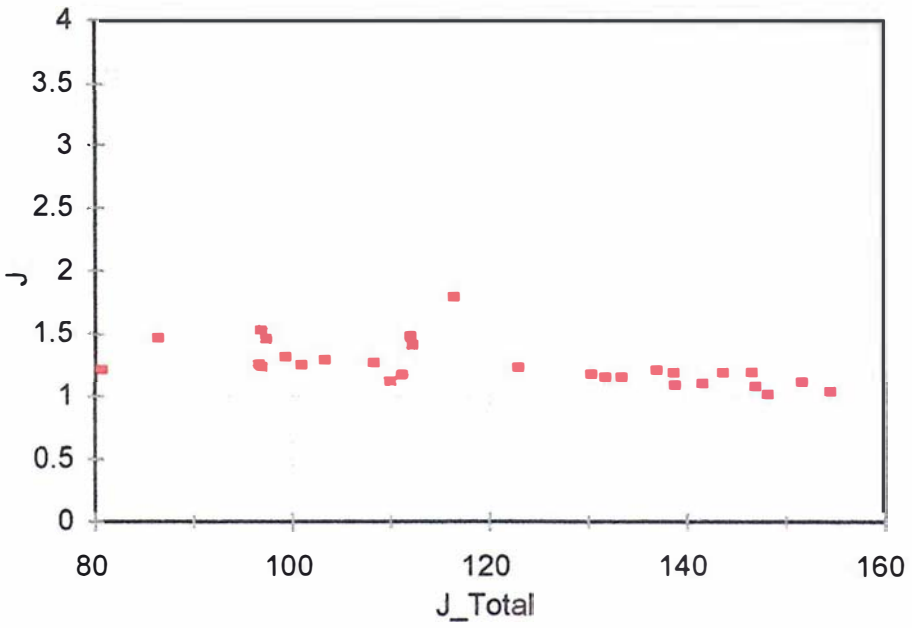

Figure IV.33 Relationship between partial flux of *n*-propanol and total flux, Experiment III. *J*: flux in $g.m^{-2}.h^{-1}$; ■: raw data.

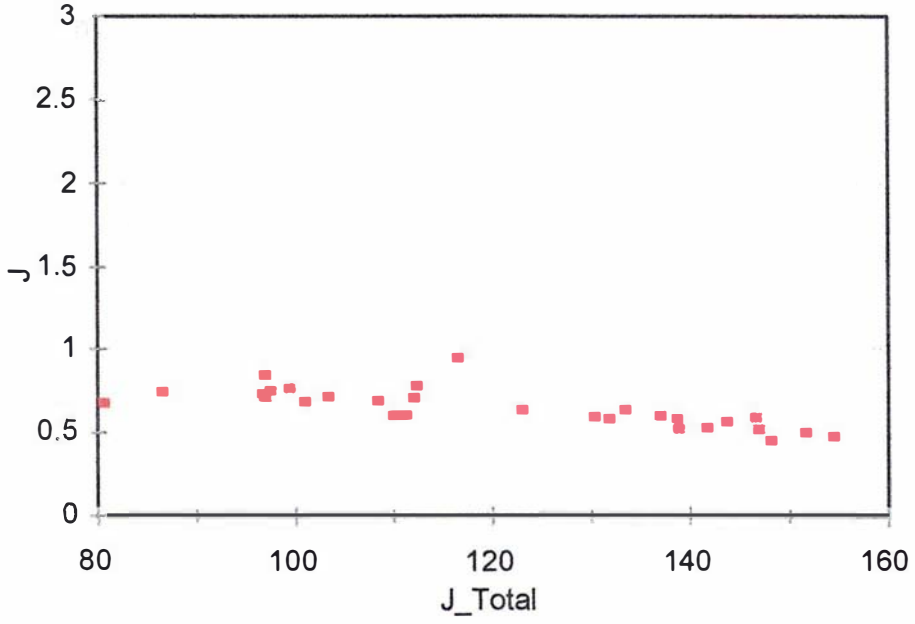

Figure IV.34 Relationship between partial flux of *i*-butanol and total flux, Experiment III. *J*: flux in $g.m^{-2}.h^{-1}$; ■: raw data.

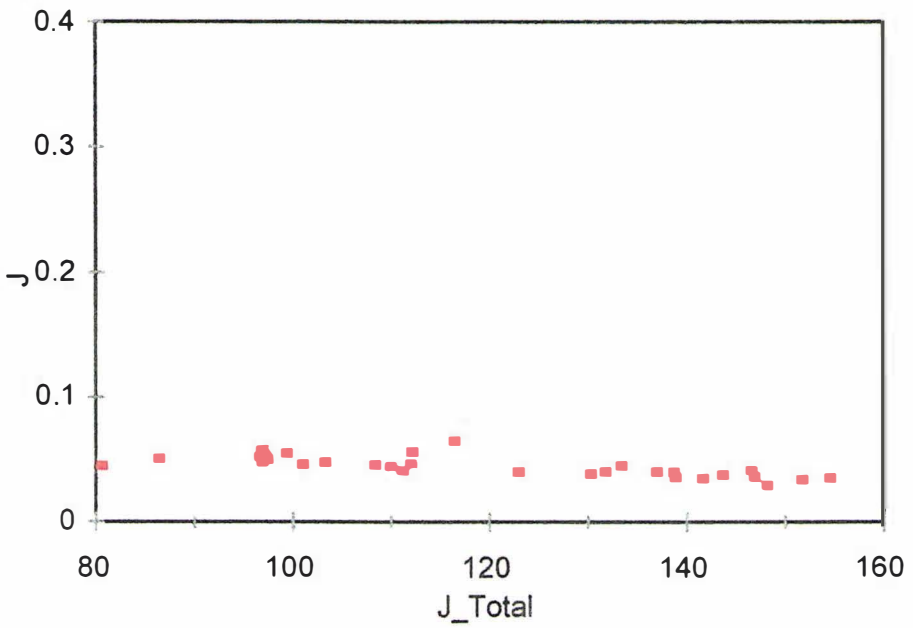

Figure IV.35 Relationship between partial flux of *n*-butanol and total flux, Experiment III. *J*: flux in $g.m^{-2}.h^{-1}$; ■: raw data.

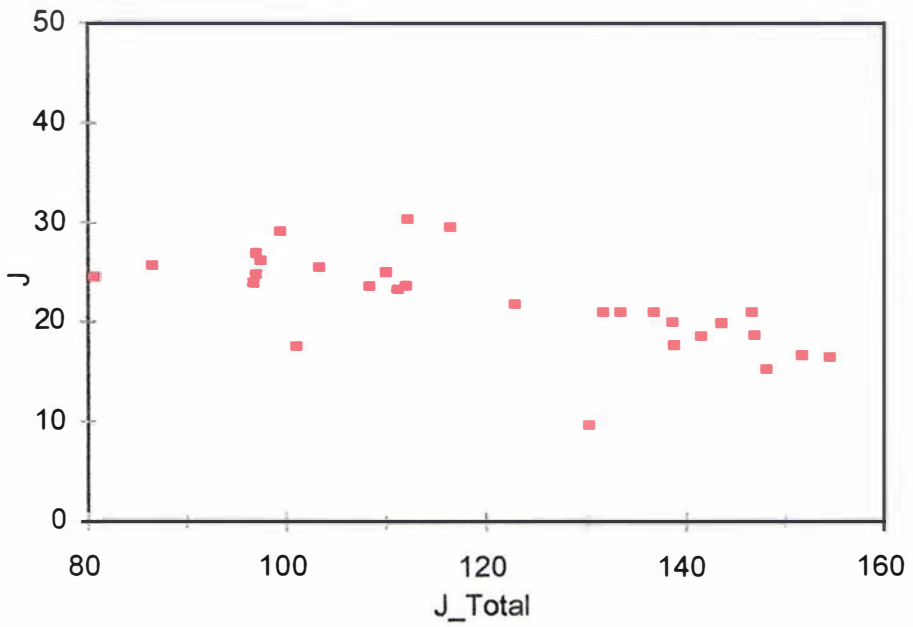

Figure IV.36 Relationship between partial flux of *i*-amyl alcohol and total flux, Experiment III. *J*: flux in $g.m^{-2}.h^{-1}$; ■: raw data.

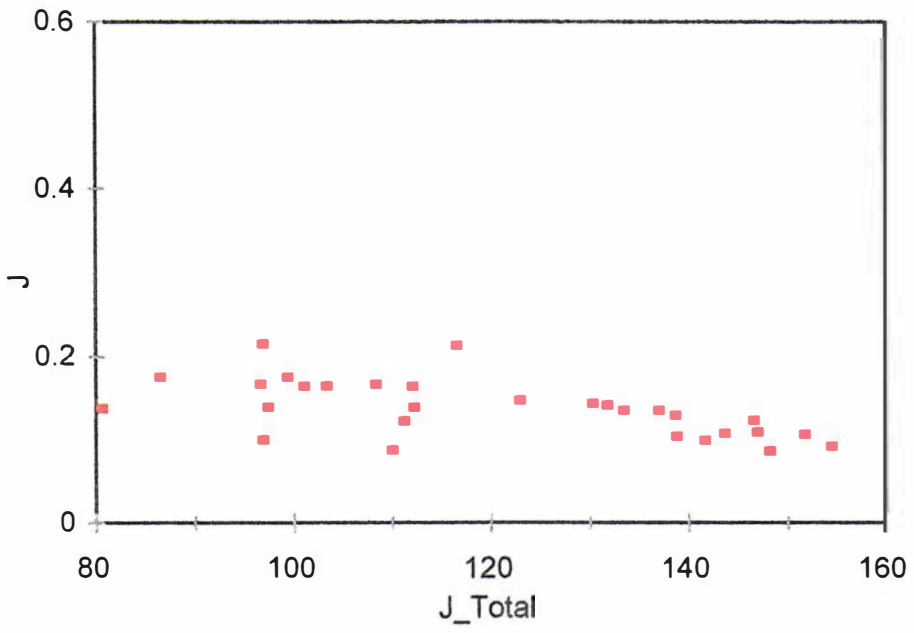

Figure IV.37 Relationship between partial flux of ethyl acetate and total flux, Experiment III. *J*: flux in $g.m^{-2}.h^{-1}$; ■: raw data.

IV.4 THE INFLUENCE OF TEMPERATURE ON FLUX

As the temperature dependency of sorption and diffusion can be expressed by an Arrhenius-type relationship (Mulder, 1991), so can the temperature dependency of the permeation rate:

$$J_i = J_{ref}\, e^{\left(-\frac{E_p}{RT}\right)} \qquad [IV.8]$$

where, J_{ref} pre-exponential factor, often flux at zero K, in $kg.m^{-2}.s^{-1}$;

E_p activation energy of pervaporation in $J.mol^{-1}$;

R universal gas constant in $J.mol^{-1}K^{-1}$;

T operating temperature in K.

Consequently, the activation energy of pervaporation (E_p) combines the energies of activation of diffusion and of sorption of the permeant in the membrane, but also the heat of vaporization of the species at the permeate side of the membrane (Feng & Huang, 1996). According to Feng & Huang (1996), in general, the activation energy for diffusion is positive, while, if sorption is exothermic, the activation energy of sorption is negative. Therefore, if sorption dominates, the membrane permeability coefficient should decrease with an increase in temperature. However, when the effect of temperature on the saturated vapour pressure is more significant than on sorption, an increase in temperature should still result in an increased flux.

IV.4.1 ANALYSIS OF EXPERIMENTAL RESULTS

The experimental data for GFT 1070 in Experiment II included not only variations in temperature, but also in feed activity. It was observed in Section IV.3 that there was a linear correlation between flux and feed concentration expressed as activity. Figure B.1 (Appendix B) shows that flux and temperature can be described by an Arrhenius type

relationship. Therefore, it was decided to use the data obtained at 60°C as reference and Equation IV.8 was modified to include the influence of both activity and temperature in the flux (Tarjus *et al*, 1996):

$$J_i = (J_{60} + P_{60} \ln (a_i))\, e^{\left[-\frac{E_p}{R} \left(\frac{1}{T} - \frac{1}{T_{60}} \right) \right]} \qquad [IV.9]$$

where, a_i activity of component *i* in the feed.

J_{60} flux of component *i* at 60°C;

P_{60} permeability of component *i* at 60°C;

T_{60} Temperature of component *i*.

Table IV.20 lists the parameters for Equation IV.9 fitted to all temperatures and concentrations studied with GFT 1070 in Experiment II.

Table IV.20 Parameters for Equation IV.9 relating both temperature and concentration with flux in Experiment II.

	J_{60}	P_{60}	E_p (J.mol^{-1})	r^2
ethanol	372±32	131± 32	44,890±6,177	0.77
ethyl acetate	15.7±0.54	1.96±0.11	10,991± 19,011	0.06
***n*-propanol**	52.3±1.7	8.79±0.43	39,431±8,295	0.69
***i*-butanol**	22±0.66	3.17±0.17	35,957±4,280	0.67
***n*-butanol**	2.18±0.05	0.23±0.007	36,868±5,628	0.54
***i*-amyl alcohol**	156±9.8	37.1±10	36,376±3,768	0.67

The values for the activation energy (E_p) are of the same order of magnitude to those presented by Karlsson (1994) for similar organic compounds permeating through GFT 1060 at temperatures between 6 and 35°C, and to the data compiled for organophilic and hydrophilic membranes by Feng & Huang (1996). For example, in the review by Feng & Huang (1996), an activation energy between 31 and 55 kJ.mol^{-1} for ethanol was reported.

Karlsson (1996) reported 47 and 51 kJ.mol^{-1} for *i*-butanol and *i*-amyl alcohol, respectively, for a flux vs. temperature curve based on a single concentration.

The relative concentration of each organic compound in the product was calculated as:

$$w_{i,rel} = \frac{J_i}{\sum_{j \neq i} J_j} \qquad [IV.10]$$

where, $w_{i,rel}$ relative concentration in w/w;

J flux of component *i* or *j*.

Figures IV.38 to IV.42 show the influence of the feed temperature on the distribution of the product concentration. Some changes in product composition were evident with a change in opereating temperarature, however, these changes did not follow any clear pattern.

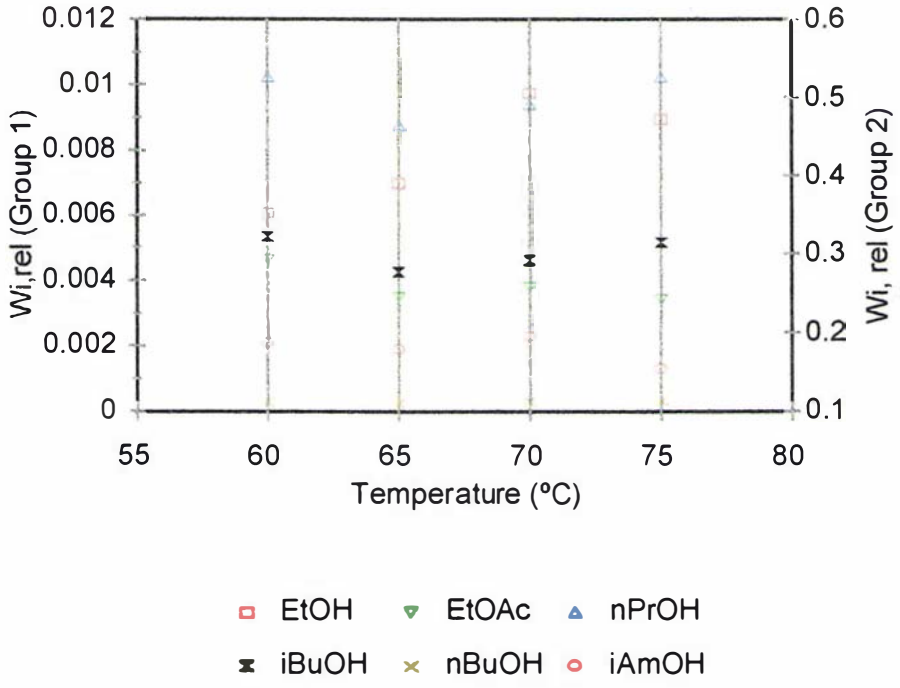

Figure IV.38 Plot of distribution of relative product concentration for an ethanol feed concentration of 5% (w/w) at varying temperatures. *Group 1:* nPrOH: *n*-propanol; iBuOH: *i*-butanol; nBuOH: *n*-butanol. *Group 2:* EtOH: ethanol; iAmOH: *i*-amyl alcohol.

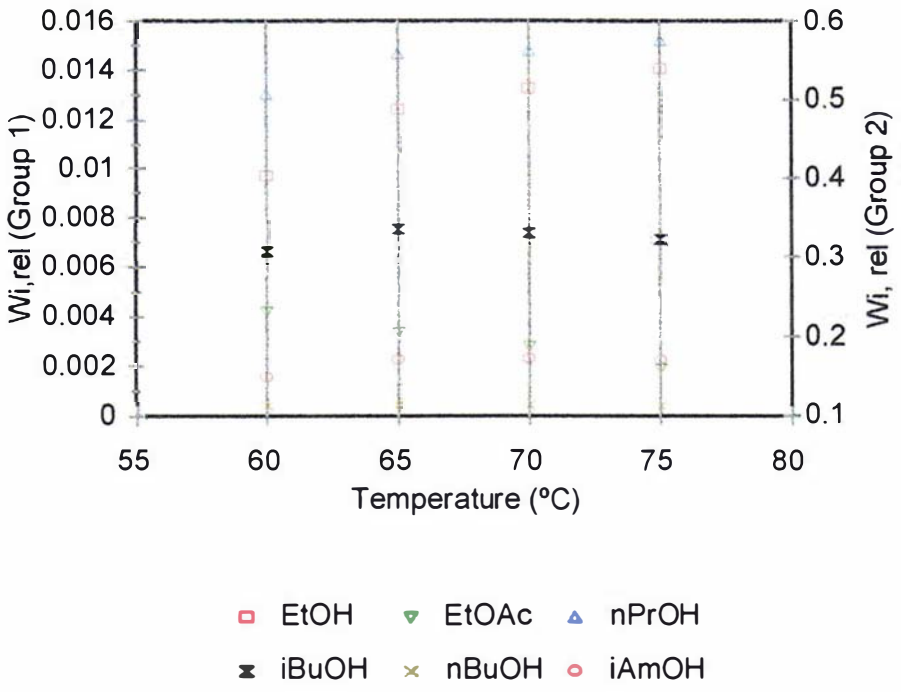

Figure IV.39 Plot of distribution of relative product concentration for an ethanol feed concentration of 7.5% (w/w) at varying temperatures.*Group 1:* nPrOH: *n*-propanol; iBuOH: *i*-butanol; nBuOH: *n*-butanol. *Group 2:* EtOH: ethanol; iAmOH: *i*-amyl alcohol.

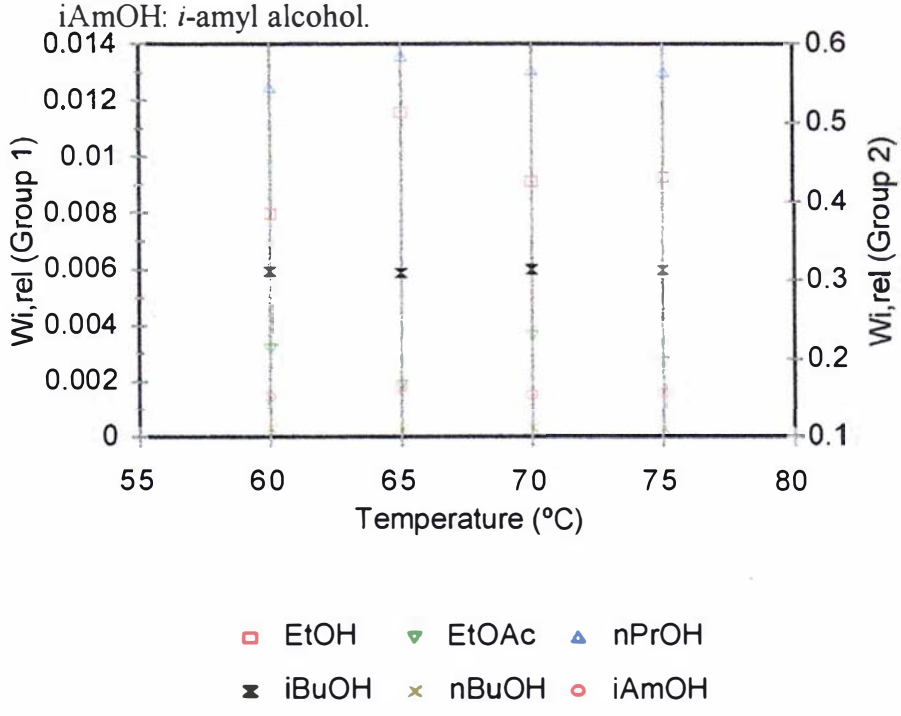

Figure IV.40 Plot of distribution of relative product concentration for an ethanol feed concentration of 10% (w/w) at varying temperatures.*Group 1:* nPrOH: *n*-propanol; iBuOH: *i*-butanol; nBuOH: *n*-butanol. *Group 2:* EtOH: ethanol; iAmOH: *i*-amyl alcohol.

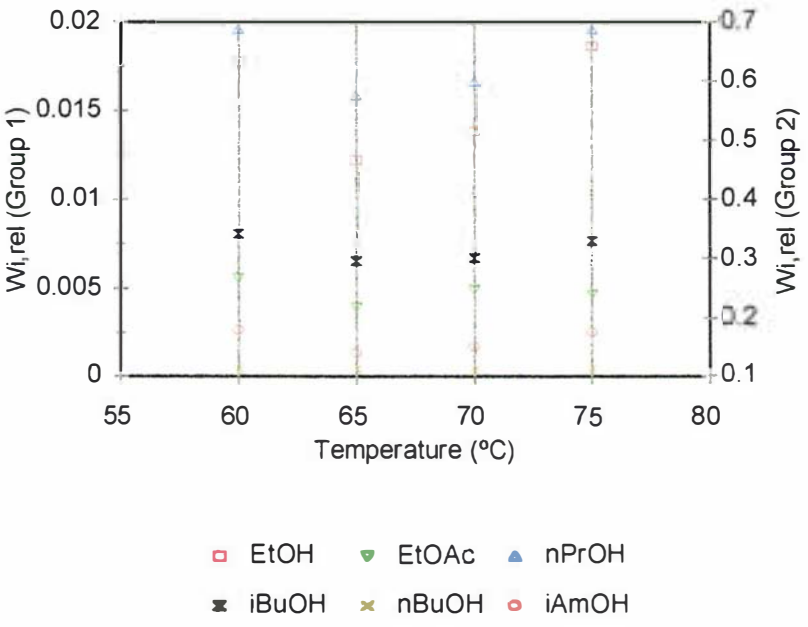

Figure IV.41 Plot of distribution of relative product concentration for an ethanol feed concentration of 15% (w/w) at varying temperatures.*Group 1:* nPrOH: *n*-propanol; iBuOH: *i*-butanol; nBuOH: *n*-butanol. *Group 2:* EtOH: ethanol; iAmOH: *i*-amyl alcohol.

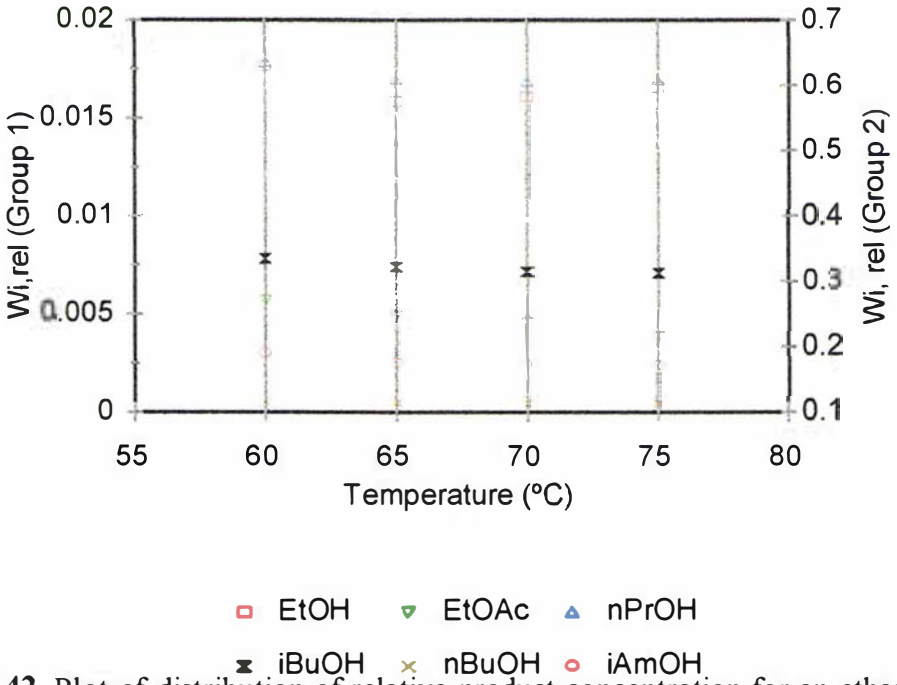

Figure IV.42 Plot of distribution of relative product concentration for an ethanol feed concentration of 20% (w/w) at varying temperatures.*Group 1:* nPrOH: *n*-propanol; iBuOH: *i*-butanol; nBuOH: *n*-butanol. *Group 2:* EtOH: ethanol; iAmOH: *i*-amyl alcohol.

Figures IV.43 to IV.45 show the influence of temperature on the enrichment factor. In general, except for ethyl acetate, there was no change in enrichment factor with a change in temperature. For ethyl acetate, an increase in temperature resulted in a decrease in the enrichment factor. The relevance of the enrichment factor in pervaporation will be discussed in detail in Section IV.7.

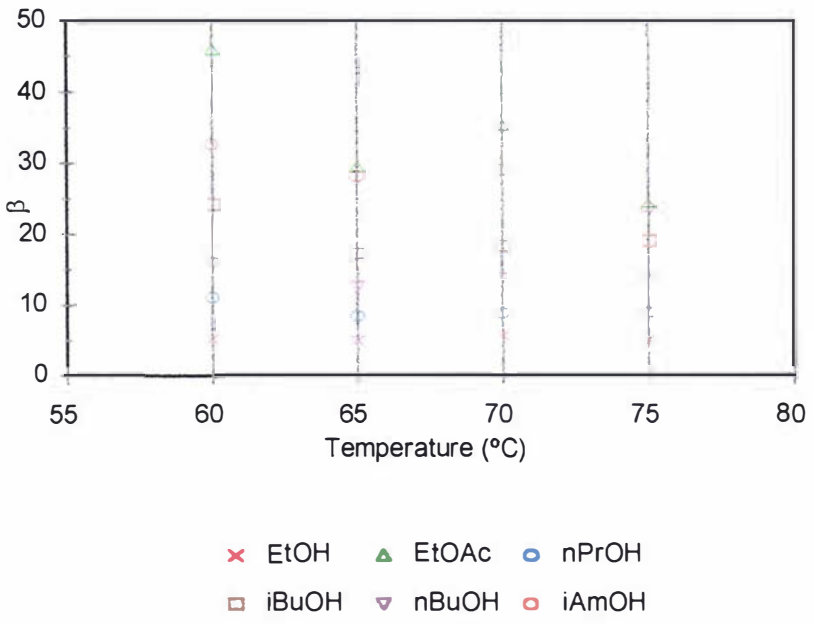

Figure IV.43 Plot of enrichment factor for an ethanol feed concentration of 5% (w/w) at varying temperatures. EtOH: ethanol; nPrOH: *n*-propanol; iBuOH: *i*-butanol; nBuOH: *n*-butanol; iAmOH: *i*-amyl alcohol; EtOAc: ethyl acetate.

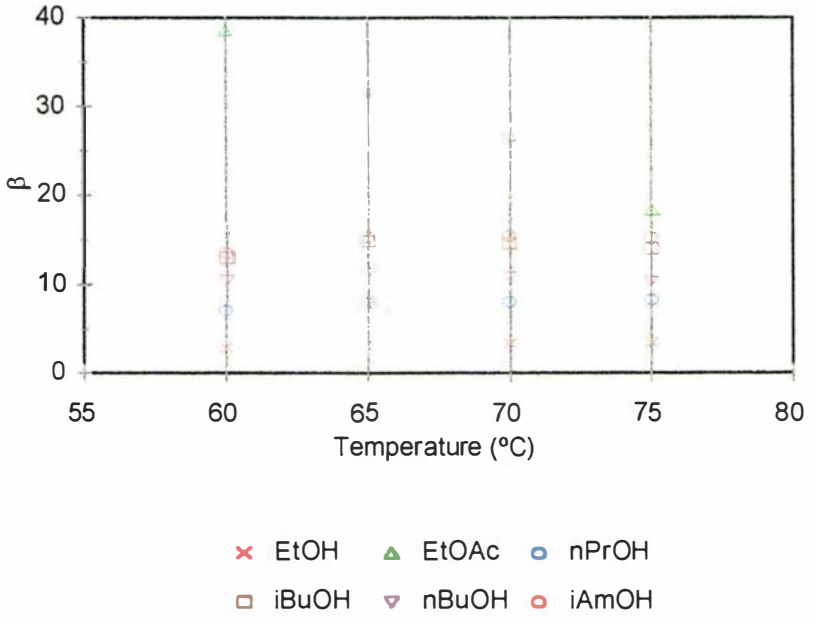

Figure IV.44 Plot of enrichment factor for an ethanol feed concentration of 10% (w/w) at varying temperatures. EtOH: ethanol; nPrOH: *n*-propanol; iBuOH: *i*-butanol; nBuOH: *n*-butanol; iAmOH: *i*-amyl alcohol; EtOAc: ethyl acetate.

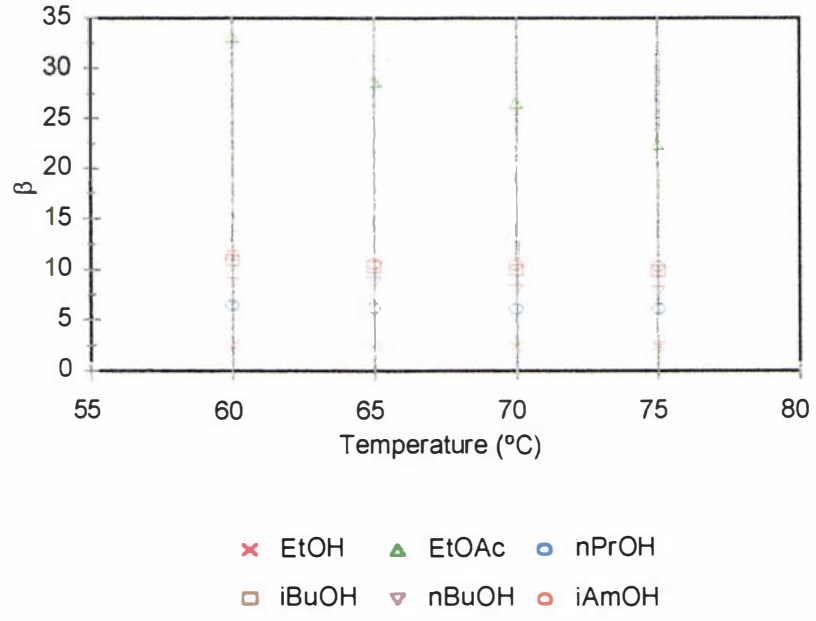

Figure IV.45 Plot of enrichment factor for an ethanol feed concentration of 15% (w/w) at varying temperatures. EtOH: ethanol; nPrOH: *n*-propanol; iBuOH: *i*-butanol; nBuOH: *n*-butanol; iAmOH: *i*-amyl alcohol; EtOAc: ethyl acetate.

IV.5 Comparison between membrane types

Three commercially available membranes were tested: GFT 1060, GFT 1070, and GKSS PEBA. In Experiment I, all three membranes were tested at 70°C with feed concentrations of 1%, 30%, and 90% (w/w) ethanol, and fusels concentration varying from a few ppm to approximately 1% (w/w). The ethanol concentration was used to identify each test, so, *low*, *medium*, and *high*, correspond to tests performed with an ethanol feed concentration of 1%, 30%, and 90% (w/w), respectively.

Figures IV.46 to IV.51 summarize the flux behaviour for all three membranes. The total flux followed the expected order, as given by the manufacturers' information sheet:

$$GFT\ 1060 \gg GFT\ 1070 \approx PEBA$$

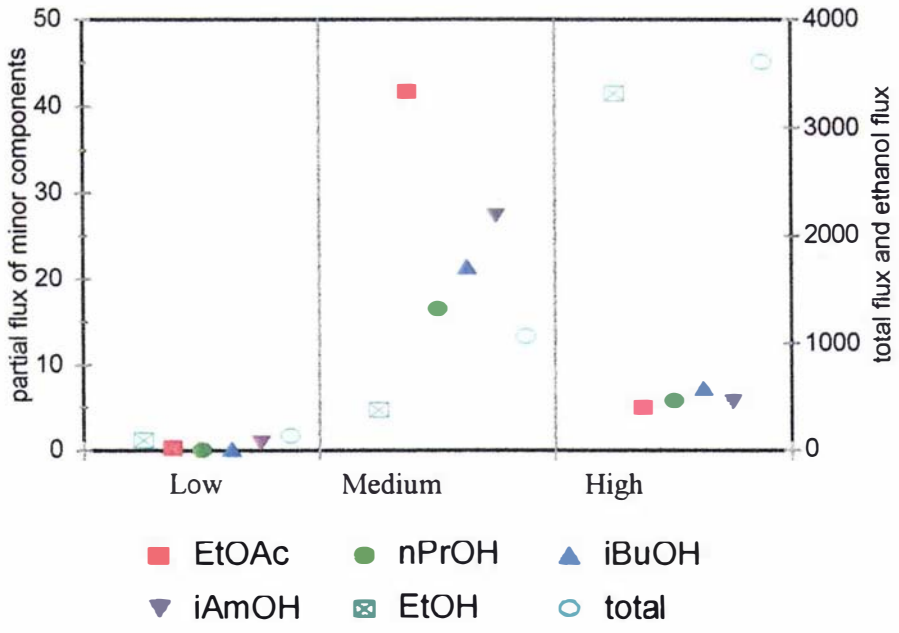

Figure IV.46 Effect of feed concentration on the total and partial fluxes ($g.m^{-2}.h^{-1}$) through PEBA (Experiment I). EtOAc: ethyl acetate; nPrOH: *n*-propanol; iBuOH: *i*-butanol; iAmOH: *i*-amyl alcohol; EtOH: ethanol.

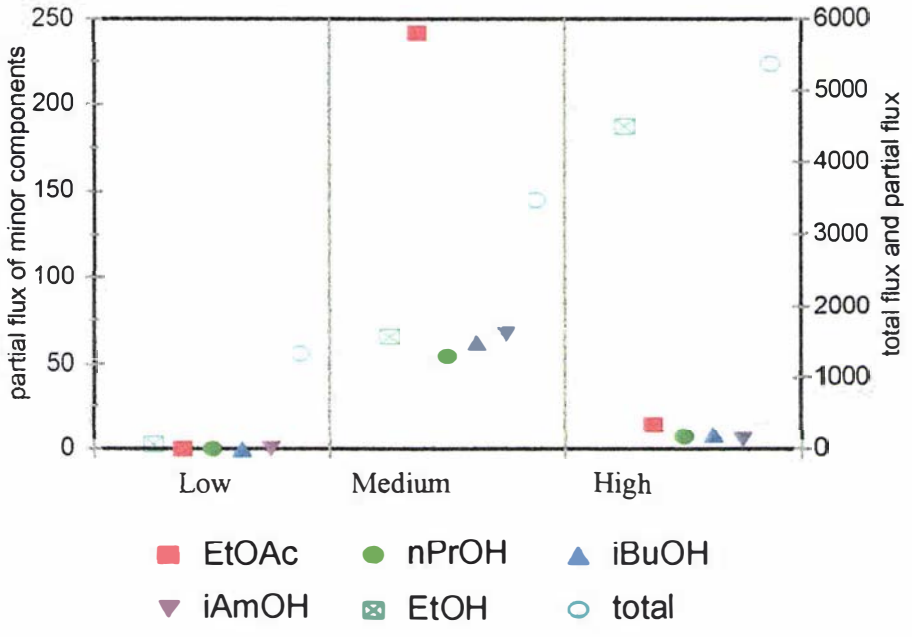

Figure IV.47 Effect of feed concentration on the total and partial fluxes ($g.m^{-2}.h^{-1}$) through GFT1070 (Experiment I). EtOAc: ethyl acetate; nPrOH: *n*-propanol; iBuOH: *i*-butanol; iAmOH: *i*-amyl alcohol; EtOH: ethanol.

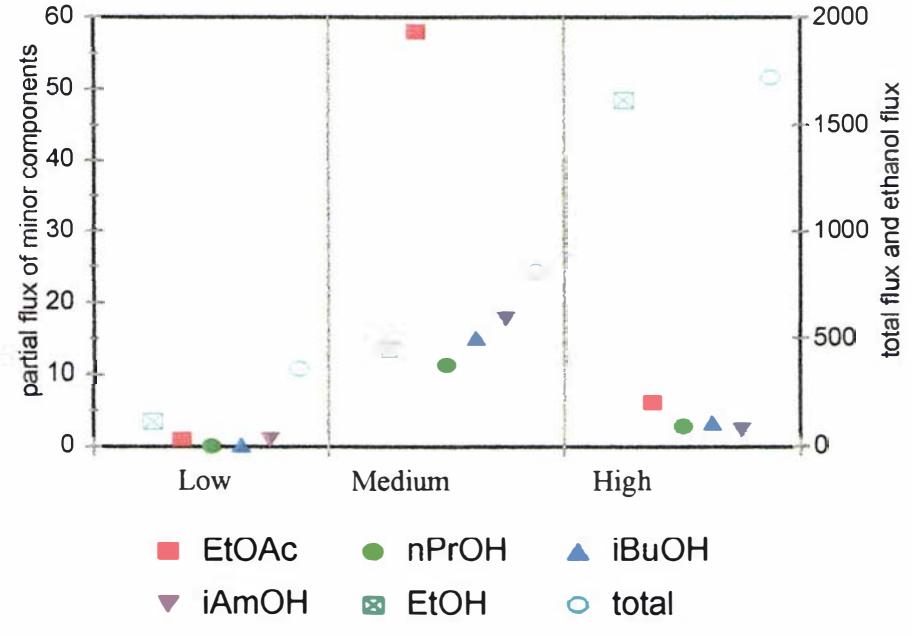

Figure IV.48 Effect of feed concentration on the total and partial fluxes ($g.m^{-2}.h^{-1}$) through GFT 1060 (Experiment I). EtOAc: ethyl acetate; nPrOH: *n*-propanol; iBuOH: *i*-butanol; iAmOH: *i*-amyl alcohol; EtOH: ethanol.

For the fusels' partial fluxes (Figures IV.49 to IV.51), with the exception of ethyl acetate, there was little difference between the three membranes. In general, the differences observed in the order of magnitude of the fusels partial fluxes among the three test runs, *low*, *medium*, and *high*, for all membranes, can be related to the differences in the fusels' feed concentration.

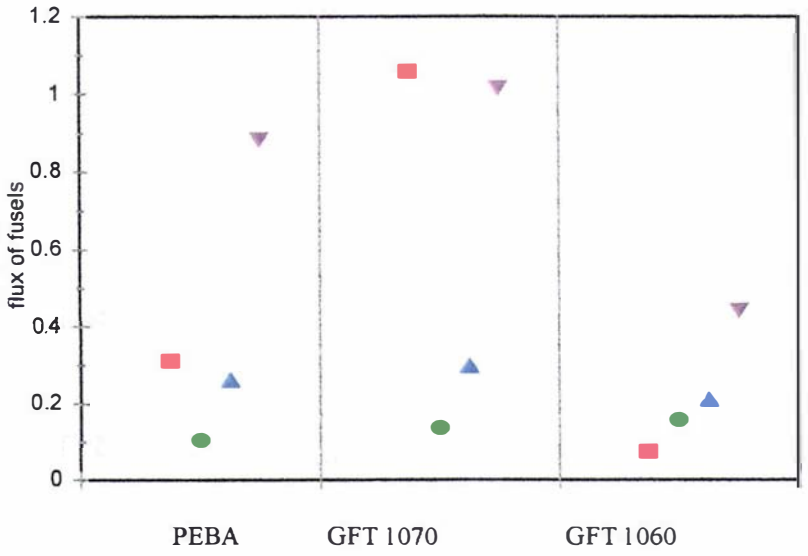

Figure IV.49 Effect of membrane type on the partial flux of fusels ($g.m^{-2}.h^{-1}$) when the feed solution contains approximately 1% (w/w) ethanol. ■: ethyl acetate; ●: *n*-propanol; ▲: *i*-butanol; ▼: *i*-amyl alcohol.

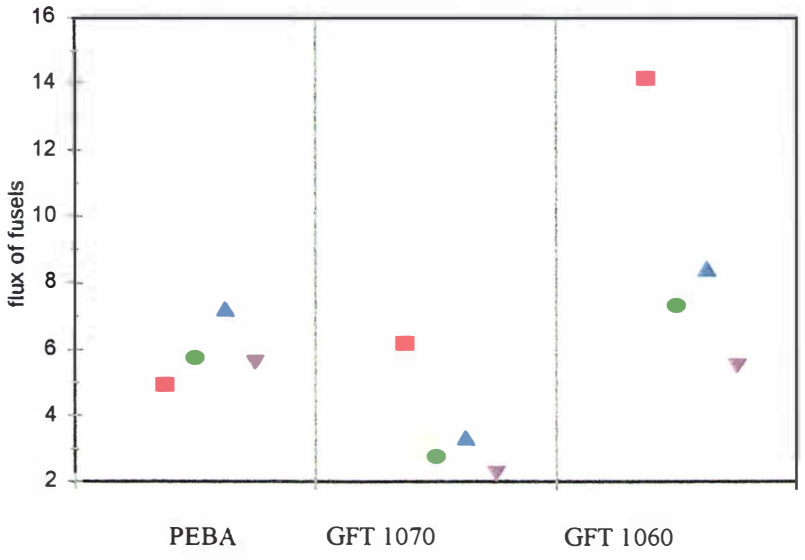

Figure IV.50 Effect of membrane type on the partial flux of fusels ($g.m^{-2}.h^{-1}$) when the feed solution contains approximately 30% (w/w) ethanol. ■: ethyl acetate; ●: *n*-propanol; ▲: *i*-butanol; ▼: *i*-amyl alcohol.

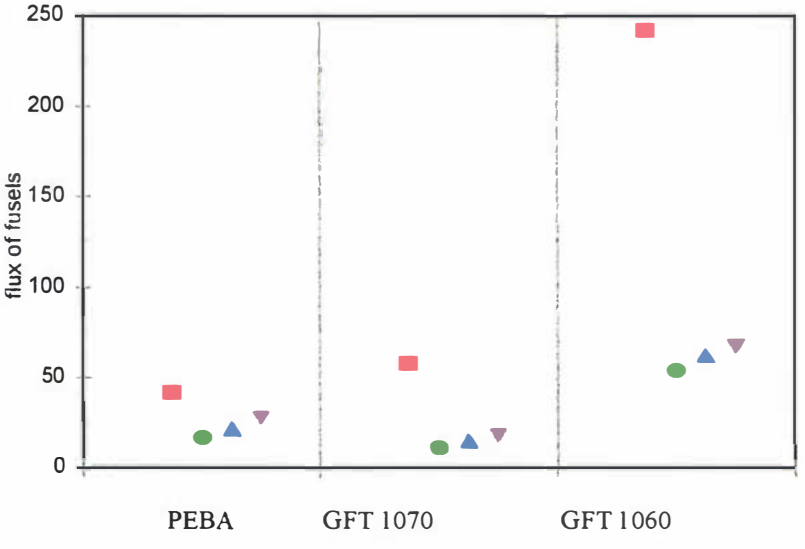

Figure IV.51 Effect of membrane type on the partial flux of fusels ($g.m^{-2}.h^{-1}$) when the feed solution contains approximately 90% (w/w) ethanol. ■: ethyl acetate; ●: *n*-propanol; ▲: *i*-butanol; ▼: *i*-amyl alcohol.

Figures IV.52 to IV.54 show the effect of membrane type and feed concentration on the enrichment factor of pervaporation. For each figure, the raw data appears in the following left to right order: ethanol, ethyl acetate, *n*-propanol, *i*-butanol, *i*-amyl alcohol. In general, the lower the concentration of organic components in the feed, the higher the enrichment factor. Again, there was no significant difference between the membranes studied.

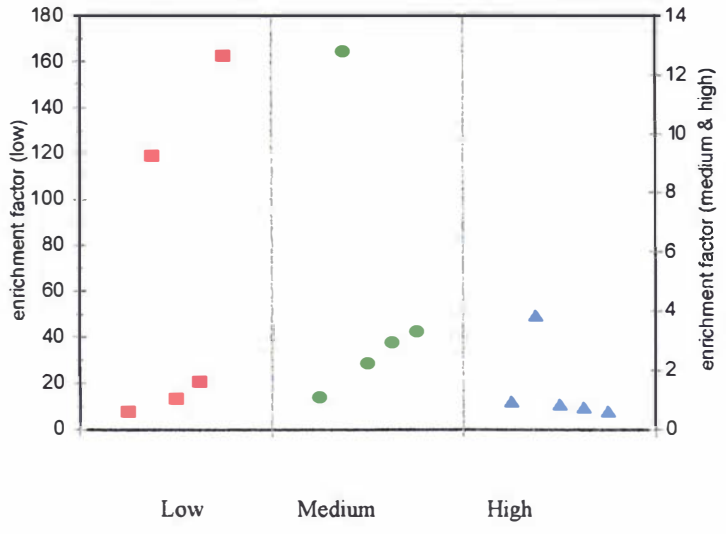

Figure IV.52 Effect of membrane type and feed concentration on enrichment factor (PEBA, Experiment I). From left to right: ethanol, ethyl acetate, *n*-propanol, *i*-butanol, *i*-amyl alcohol.

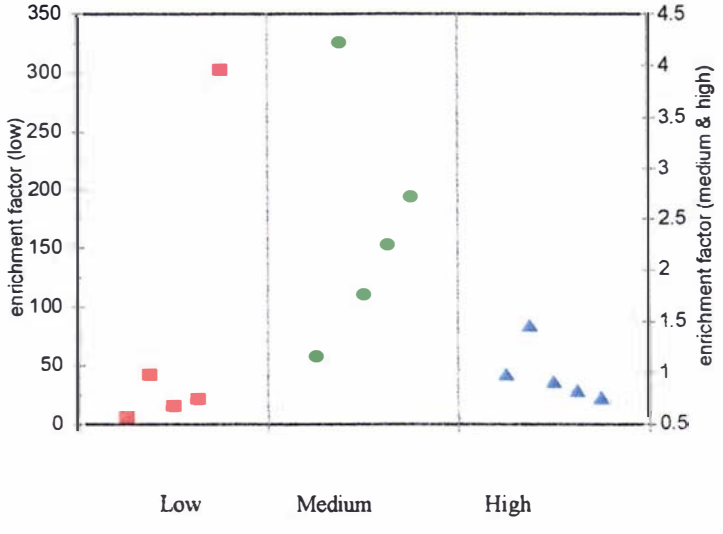

Figure IV.53 Effect of membrane type and feed concentration on enrichment factor (GFT 1070, Experiment I). From left to right: ethanol, ethyl acetate, *n*-propanol, *i*-butanol, *i*-amyl alcohol.

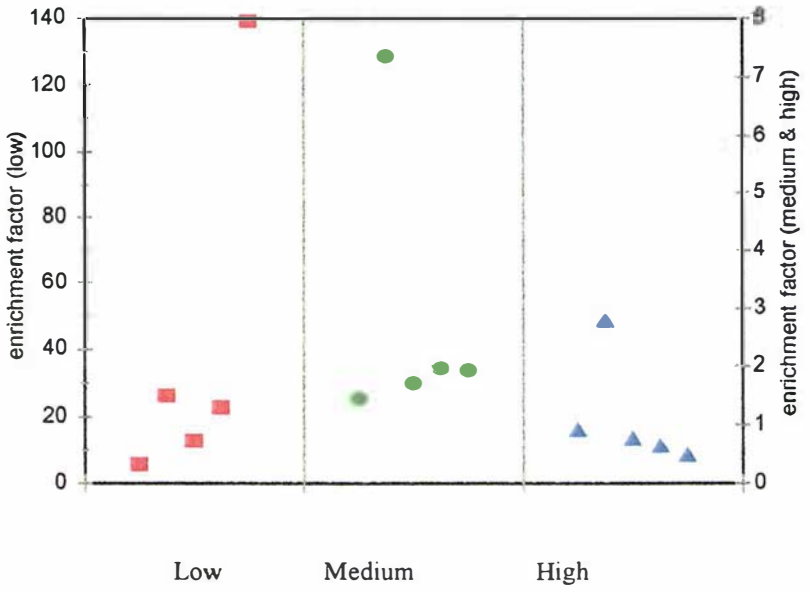

Figure IV.54 Effect of membrane type and feed concentration on enrichment factor (GFT 1060, Experiment I). From left to right: ethanol, ethyl acetate, *n*-propanol, *i*-butanol, *i*-amyl alcohol.

IV.6 Comparison between pervaporation and Evaporation

Figures IV.55 to IV.57 show the ratio of the enrichment factor of pervaporation to that for evaporation for ethanol, ethyl acetate, and each fusel in the feed mixture, *n*-propanol, *i*-butanol, *i*-amyl alcohol, in left to right order.

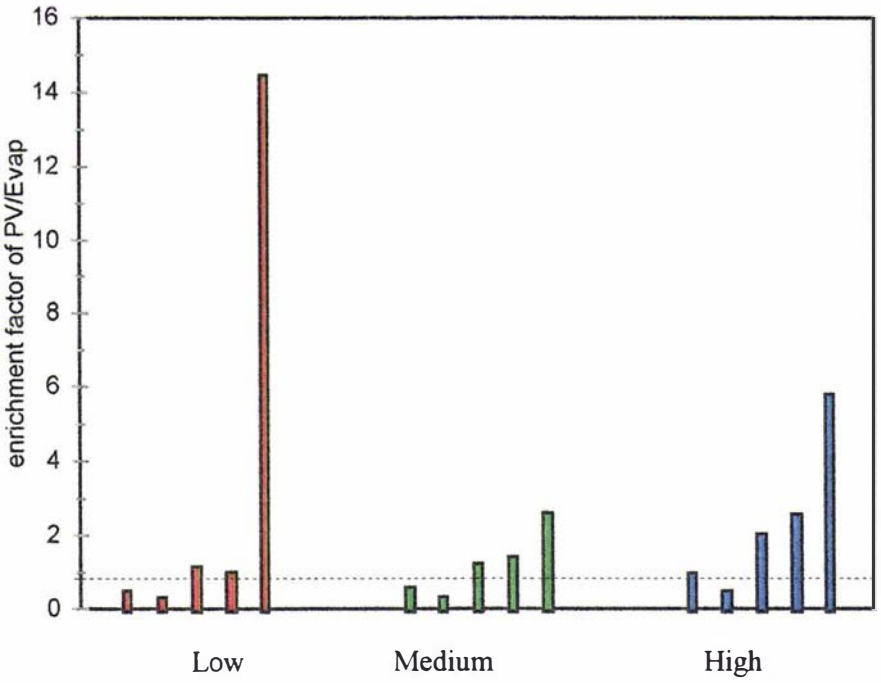

Figure IV.55 Ratio of pervaporation enrichment ratio (PV) to evaporation enrichment ratio (D) for the PEBA membrane in Experiment I. From left to right: ethanol, ethyl acetate, *n*-propanol, *i*-butanol, *i*-amyl alcohol.

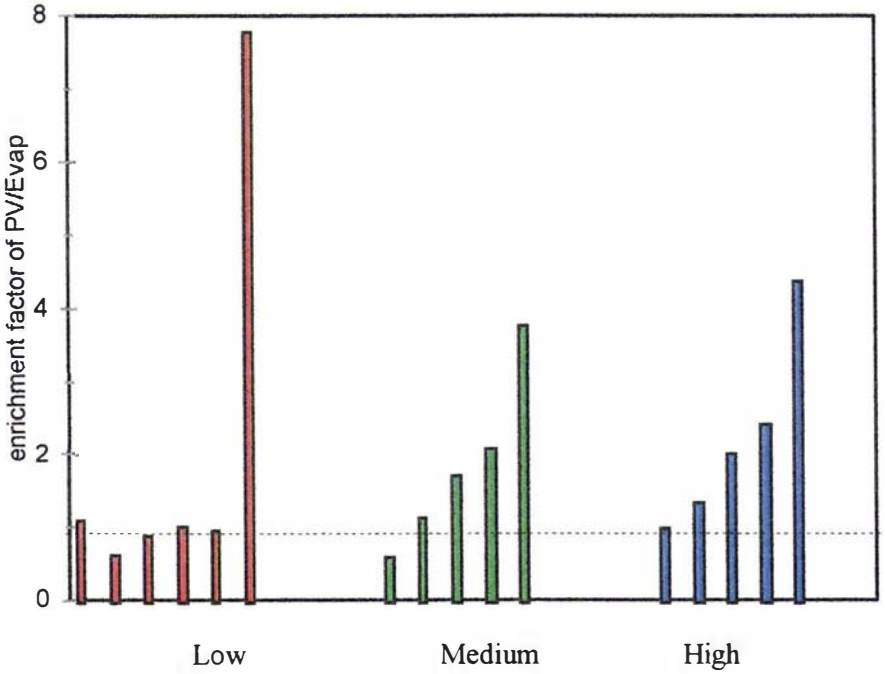

Figure IV.56 Ratio of pervaporation enrichment ratio (PV) to evaporation enrichment ratio (D) for the GFT 1070 membrane in Experiment I. From left to right: ethanol, ethyl acetate, *n*-propanol, *i*-butanol, *i*-amyl alcohol.

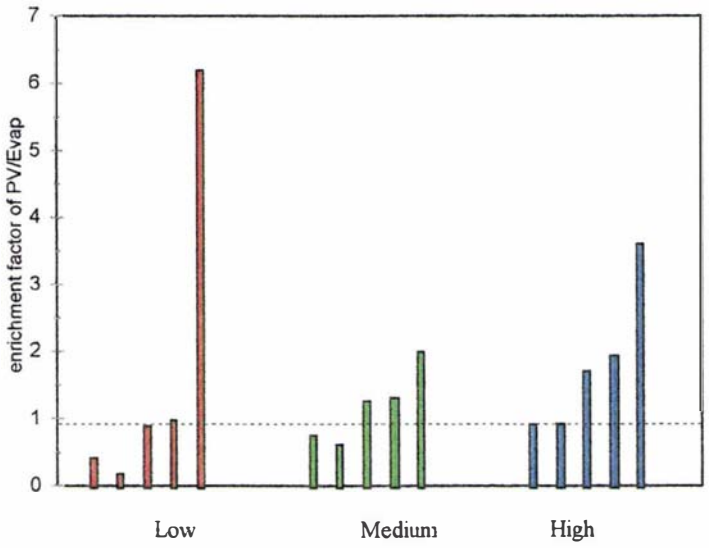

Figure IV.57 Ratio of pervaporation enrichment ratio (PV) to evaporation enrichment ratio (D) for the GFT 1060 membrane in Experiment I. From left to right: ethanol, ethyl acetate, *n*-propanol, *i*-butanol, *i*-amyl alcohol.

In Experiment I, for all membranes and feed concentrations studied, the enrichment ratio of pervaporation was generally less than to two theoretical distillation stages. In some cases, the enrichment obtained with pervaporation was lower than that expected for a single stage distillation (evaporation). It would be advantageous if only ethanol had an enrichment factor for pervaporation that was lower than its enrichment for evaporation, for this could enhance the separation between ethanol and fusels. However, ethyl acetate also had a lower enrichment with pervaporation than with evaporation.

Furthermore, apart from *i*-amyl alcohol, pervaporation did not seem to improve the differentiation between the fusels. That is, though the organic components permeate preferentially through the membranes, the separation between ethanol-water and the fusels was not improved by the use of pervaporation in comparison to evaporation, except for *i*-amyl alcohol. For *i*-amyl alcohol, when the total fusel's concentration is *low*, the enrichment achieved with pervaporation is six to fourteen times higher than what could be achieved with a single stage evaporation, whereas for all other components there was little difference between evaporation and pervaporation. Consequently, pervaporation with hydrophobic membranes was not expected to have a significant impact in the purification process at NZDCL.

IV.7 ENRICHMENT FACTOR

IV.7.1 DEVELOPMENT OF A NEW RELATIONSHIP FOR ENRICHMENT FACTOR

IV.7.1.1 INTRODUCTION

According to the solution-diffusion model (Section II.3.2.3), pervaporation is governed by the interaction between the dense membrane polymeric material and the penetrating molecules. It follows that sorption is a function of the chemical affinity between polymer and permeant, and transport of the permeant molecules through the polymer matrix is a function of the solute size and the mobility of the polymer chains. Ultimately, these interactions, together with the driving force, determine the component fluxes and concentration of the components in the product.

The choice of polymer material is critical to the success of the separation. As organophilic separation is still an emerging application of pervaporation, guidelines for membrane material selection are crude, application data bases are virtually nonexistent, and predictive models are still poorly developed. When considering pervaporation for a novel application, the safest route is to test extensively each and every polymer that might be effective in the desired separation and can reasonably be expected to be manufactured into suitable membranes. A considerable number of new membranes are under development or have been proposed for development. In Chapter VII some of the polymers used for membrane manufacture will be reviewed.

Initially, flux and selectivity are the two key parameters which should be used for comparison and selection of membrane materials. In this study, selectivity was quantified by the enrichment factor.

In general, the enrichment factor (β) is defined as the ratio of the mass or molar fraction

of each component in two distinct phases. In pervaporation, for each component of the feed mixture, β is the ratio of the mass fraction in the product over the mass fraction in the feed:

$$\beta_i^{PV} = \frac{w_i^p}{w_i^f} \qquad [IV.11]$$

where, for each component i, β^{PV} enrichment factor for overall separation;

w^p mass fraction in the product;

w^f mass fraction in the feed.

As will be discussed in Chapter V, for hydrophobic membranes it was noticed that the overall enrichment factor of pervaporation was usually determined by preferential sorption (Mulder & Smolders, 1986; Hauser *et al.*, 1989; Mulder & Smolders, 1991; Bartels-Caspers *et al.*, 1992; Ruckenstein & Sun, 1995; Zhang & Drioli, 1995). In view of this observation, Jonquières, Favre, Heintz and their respective co-workers have investigated methods for either predicting or correlating the sorption properties of polymeric materials with basic physical-chemical properties of the membrane material and the feed solution. Ultimately, they aimed at correlating those results with overall pervaporation performance (Ennecking *et al.*, 1993; Favre *et al.*, 1993; Heintz & Stephan, 1994a; Jonquières *et al.*, 1996; Jonquières & Fane, 1997).

So far, only solutions with components of broadly similar molecular structure have been tested. The work of Ennecking, Favre, Heintz, and respective co-workers was considered in Chapter II and will be further discussed in Chapter V. Overall, it was concluded that the Flory-Huggins equation was not appropriate to predict sorption of poor solvents (alcohols) in PDMS membranes and that the UNIQUAC equation showed good agreement between experimental and predicted values for the solutions tested. Jonquières and co-workers (Jonquières *et al.*, 1996; Jonquières & Fane, 1997) observed that for certain membranes, (polyurethaneimides and PDMS) the alcohol fluxes of binary or ternary aqueous solutions could be correlated with solubility parameters. This work was restricted to butanol isomers in either water or water-acetone mixtures because of the relevance of these components

in the acetone-butanol-ethanol fermentation process, and to alcohols (methanol, ethanol, and propanol isomers) in ether. It can be inferred that, because the size of the molecules in this study were broadly similar, the influence of diffusion in pervaporation would be small and could thus be neglected.

However, given the inverse relationship between molecular size and diffusivity, it can be postulated that for multicomponent solutions of varying molecular size, the enrichment factor of the larger molecules will be overestimated if only sorption parameters are used.

Assuming that only sorption and diffusion are responsible for the separation, Figure IV.58 represents the mass distribution of a component across the pervaporation membrane. For each preferentially sorbed component, w^f is its concentration in the feed, $^m w$ is its concentration at the membrane interface in equilibrium with the feed, and the product composition, w^p, differs from that at the feed side of the membrane interface to the extent that there are different rates of diffusion for the components.

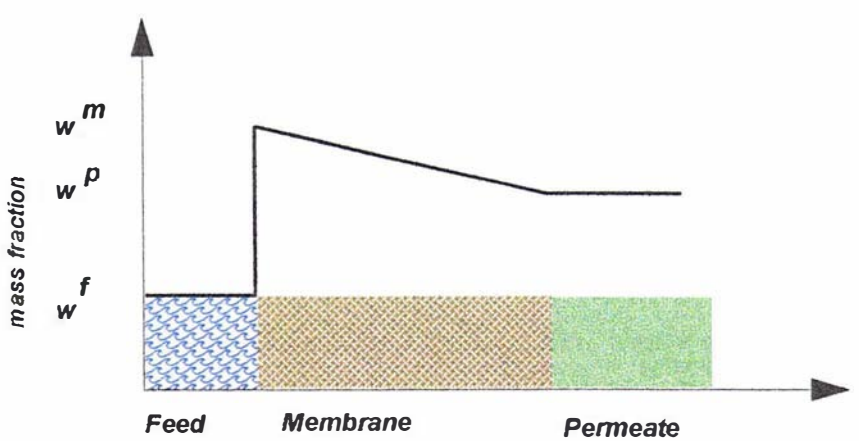

Figure IV.58 Representation of the mass fraction distribution during pervaporation.

Thus, Equation IV.11 can be extended:

$$\beta_i^{PV} = \frac{w_i^p}{w_i^m} \frac{w_i^m}{w_i^f} \qquad [IV.12]$$

By analogy with Equation IV.11 and in light of the mechanism suggested above, the first term on the right hand side of Equation IV.12 may be defined as the enrichment factor due to diffusion and the second term, the enrichment factor due to sorption. Equation IV.12 then becomes:

$$\beta_i^{PV} = \beta_i^S \beta_i^D \qquad [IV.13]$$

where, for each component i, β^S enrichment factor for sorption;
β^D enrichment factor for diffusion.

IV.7.1.2 Enrichment factor for sorption

In sorption, it is generally assumed that equilibrium exists at the feed-membrane interface and therefore, the chemical potentials of each component in both phases are equal. For liquids and fluids dissolved in membranes, this can be simplified to equal phase activities:

$$a_i^f = a_i^m \qquad [IV.14]$$

where, for each component i, a^f activity in the feed;
a^m activity in the membrane interface.

Given that the same reference conditions are used for both phases, Equation IV.14 can be expressed as:

$$x_i^f \gamma_i^f = x_i^m \gamma_i^m \qquad [IV.15]$$

where, for each component i, x^f mol fraction in the feed;

x^m	mol fraction in the membrane interface;
γ^f	activity coefficient in the feed;
γ^m	activity coefficient in the membrane interface.

Hence, the enrichment factor of sorption may be calculated from:

$$\beta_i^S = \frac{w_i^m}{w_i^f} = k \frac{x_i^m}{x_i^f} = k_i \frac{\gamma_i^f}{\gamma_i^m} \qquad [IV.16]$$

where, k_i ratio of molar and mass fraction for component *i*.

There has been little success in developing a universal methodology for estimating the composition or the activity coefficient of solvents dissolved in dense polymers. On the other hand, it is often straightforward to estimate the activity coefficient of a liquid solution. Reid *et al.* (1986) introduced and discussed the main methods available for the estimation of the activity coefficient of a liquid solution and Gmehling *et al.*, (1977) presented a collection of experimental data and fitted parameters.

IV.7.1.3 Enrichment factor for diffusion

Diffusion fluxes are molecular movements that result from driving forces, such as pressure gradients, temperature gradients, external force fields, and concentration gradients (Reid *et al.*, 1986). In pervaporation, the driving force is a concentration gradient and flux is proportional to a difference in concentration between the membrane faces:

$$J_i = - D_i \frac{\partial c_i}{\partial z} = - D_i \rho \frac{\partial w_i}{\partial z} \qquad [IV.17]$$

where, for each component i, J component flux in $g.m^{-2}.h^{-1}$;

D diffusion coefficient, diffusivity, or proportionality constant between flux and driving force in $m^2.h^{-1}$;

c concentration in $g.m^{-3}$;

z membrane thickness in m;

w mass fraction;

ρ density of mixture in $g.m^{-3}$.

For a membrane of thickness z, with vacuum at the permeate side and at steady state:

$$J_T \, w_i^p = D_i \, \rho \, \frac{(w_i^m - 0)}{z} \qquad \text{[IV.18]}$$

where, J_T total flux in $g.m^{-2}.h^{-1}$.

Combining Equations IV.12, IV.13, and IV.18:

$$\beta_i^D = \frac{w_i^p}{w_i^m} = \frac{\rho}{z \, J_T} D_i \qquad \text{[IV.19]}$$

For liquids permeating through dense polymers, there is no fully developed theoretical methodology for predicting the diffusion coefficient. It is generally accepted that the semi-empirical free volume theory (Section II.3.2.5) applies and diffusion is then described as a function of molecular spacing in the polymer matrix, solute velocity and volume, and free volume in the polymer. In general, the larger the solute molecule, the lower the diffusivity. Diffusivity also decreases with a decrease in the mobility of the polymer molecules, so the presence of zeolites and the use of cross-linking will lower the total flux. In general, the effect of the presence of zeolites in the enrichment factor depends on its affinity for the

different components of the feed mixture. This is evident in the work of te Hennepe *et al* (1987), who studied the effect of zeolites in the permeation of water/ethanol and water/propanol mixtures. They suggested that the strong interaction between the zeolites and alcohols had a greater effect on the permeation of water than on the permeation of organic compounds: "by exclusion of water from the pore system water has to permeate around the zeolite particles, leading to a lower water flux and a higher selectivity [towards the alcohol]" (te Hennepe *et al*, 1987).

IV.7.1.4 ENRICHMENT FACTOR FOR PERVAPORATION

Given the difficulty in predicting diffusivity and sorption of small molecules (as penetrants) in dense polymers, empirical and semi-empirical methods were employed in this study to correlate enrichment factors. By substituting Equations IV.16 and IV.19 into Equation IV.13, the enrichment factor of pervaporation may be described as a function of the activity coefficient and the molecular size of each component of the feed mixture:

$$\beta_i^{PV} = K_i \gamma_i^f D_i \qquad \text{[IV.20]}$$

where, D_i diffusion coefficient, which is a function of molecular size; [D_i = *f(molecular size)*].

$$D_i = f(V_i) = K_i' \frac{1}{V_i} \qquad \text{[IV.21]}$$

$$\beta_i^{PV} = K_i'' \gamma_i^f \frac{1}{V_i} \qquad \text{[IV.22]}$$

$$K_i'' = k_i \frac{\rho}{z J_T \gamma_i^m} \qquad \text{[IV.23]}$$

where, K_i'' coefficient of proportionality, which is a function of the polymer type, structure, and volume fraction, and of the composition of the solvent at the membrane interphase;

V_i molecular volume.

Equation IV.20 relates the overall enrichment factor of pervaporation to parameters that are easily available for every solution and that would be relevant in the sorption and diffusion behaviour of the penetrant molecules, i.e., the activity coefficient and molecular size of the feed components. However, the coefficient of proportionality must be fitted experimentally, as it depends on the nature and composition of the feed solution, and on the polymer used.

Néel *et al.* (1985) also suggested that there is a relationship between selectivity, in this case the separation factor α, and the sorption and diffusion coefficients of components A and B of a binary mixture:

$$\alpha = \frac{S_A D_A}{S_B D_B} \qquad [IV.24]$$

where, S sorption coefficient, defined as c_i^m/c_i^f;

D diffusivity in $m^2.h^{-1}$.

However, Equation IV.24 is only valid for binary solutions when both the sorption and diffusion coefficients are not concentration-dependent. In contrast, Equation IV.20 can be applied to multiple component solutions and includes any non-idealities present in either the sorption or diffusion coefficients as discussed in Section IV.7.2.

IV.7.2 Analysis of experimental results

All experiments were conducted following the procedure outlined in Section IV.2.

To fit the data from Experiment II to Equation IV.20, the influence of molecular size on diffusivity was represented by the van der Waals volume of each solvent (Equation IV.25).

$$\beta_i^{PV} = K_i'' \frac{\gamma_i^f}{V_i} \qquad [IV.25]$$

where, V_i van der Waals volume in $m^3.kg^{-1}$.

The van der Waals volume was either calculated using the procedure described by Bondii (1964) or retrieved from the ChemSep® (CACHE Corporation) library. Good fits could also be obtained using the molecular weight or a measure of radius of the molecule. In contrast to the van der Waals volume, the molecular weight does not differentiate amongst isomers. The use of a measure of radius requires it to be elevated to the third power and there is therefore no difference between using either radius or volume to represent the influence of molecular size in Equation IV.25. Coefficients (K_i'') were generated for all alcohols of the feed mixture.

In Table IV.21 the coefficients of proportionality (K_i'') and relevant statistics for each membrane tested are listed. Although the coefficient of proportionality K_i'' is a function of the polymer type, structure, and volume fraction, and composition of the solvent at the membrane interface, the model proposes that the net outcome of these complex factors is such that the relationship between the dependent and independent variables can be represented by a linear relationship. For GFT 1070, GFT1060, and PEBA membranes, the model represented the raw data with a correlation coefficient r^2 greater than 0.82, which indicates that there is a strong linear correlation between the activity coefficient of the feed, the van der Waals volume of each alcohol (independent variables), and the overall enrichment factor of pervaporation (dependent variable). A statistical test of the hypothesis that $K = 0$ also confirmed with 99.9% confidence that there is a linear association between enrichment and activity coefficient. Figures IV.59 to IV.61 show the raw data and fitted lines for each membrane. The external, blue, dashed lines define the 95% limit of confidence for the slope of the fitted line.

Table IV.21 Coefficient of proportionality (K'') and statistics for GFT 1070, GFT 1060, and PEBA.

Membrane Type	K''	r^2	number of observations
GFT 1070	1.93	0.82	255
GFT 1060	1.50	0.89	25
PEBA	1.77	0.86	25

Blume *et al.* (1990) reported a pervaporation enrichment factors between 2 and 10 for ethanol, methanol, and propanols permeating through PDMS membranes, and between 50 and 150 for ethyl acetate. As shown in Figures IV.59 to IV.61, for ethanol and *n*-propanol the results from Blume and co-workers are in clear agreement with the data obtained in this study. However, in the present study, the enrichment factor for ethyl acetate was never higher than 55.

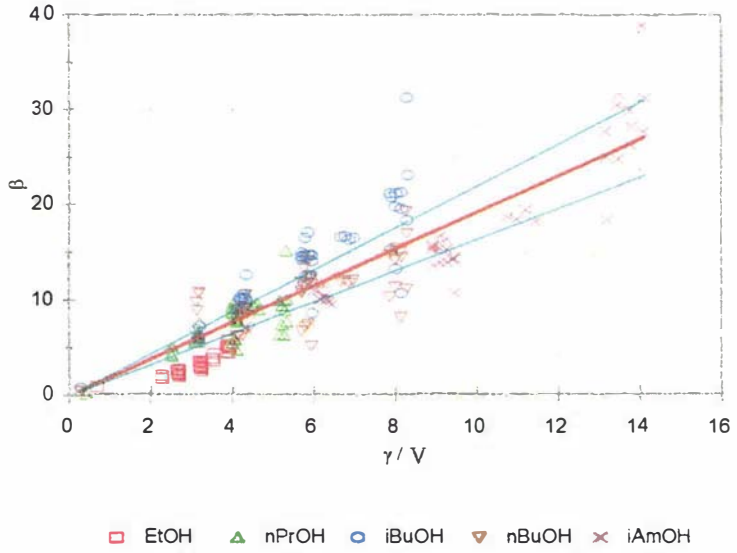

Figure IV.59 Relationship between overall enrichment factor (β^{PV}), van der Waals volume (V), and activity coefficient (γ) for alcohols in a mixture with water and ethyl acetate permeating through GFT 1070 (Experiment II). EtOH: ethanol; nPrOH: *n*-propanol; iBuOH: *i*-butanol; nBuOH: *n*-butanol; iAmOH: *i*-amyl alcohol.

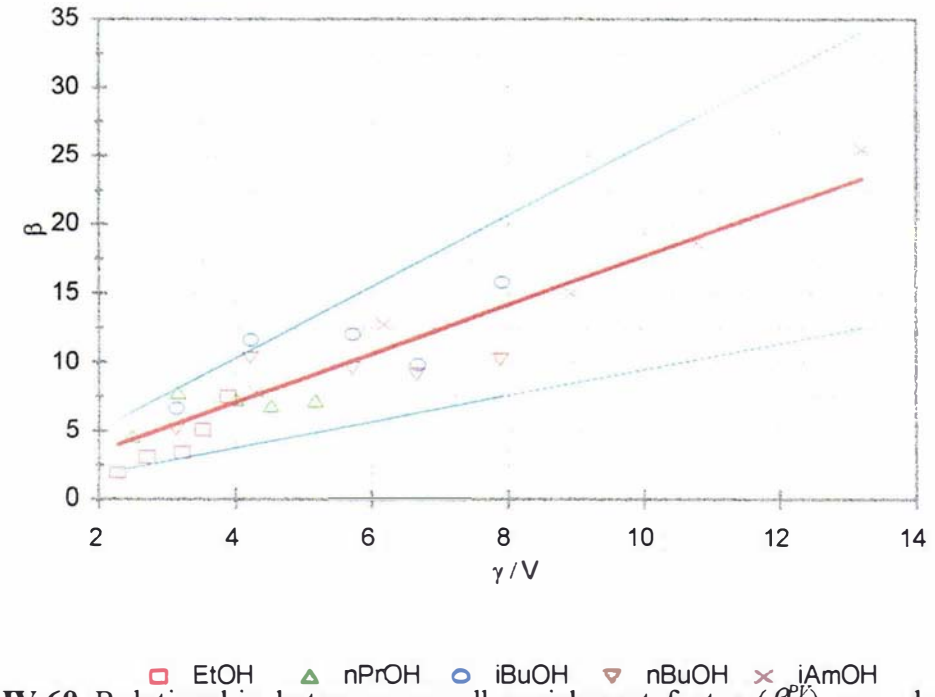

Figure IV.60 Relationship between overall enrichment factor (β^{PV}), van der Waals volume (V), and activity coefficient (γ) for alcohols in a mixture with water and ethyl acetate permeating through GFT 1060 (Experiment II). EtOH: ethanol; nPrOH: *n*-propanol; iBuOH: *i*-butanol; nBuOH: *n*-butanol; iAmOH: *i*-amyl alcohol.

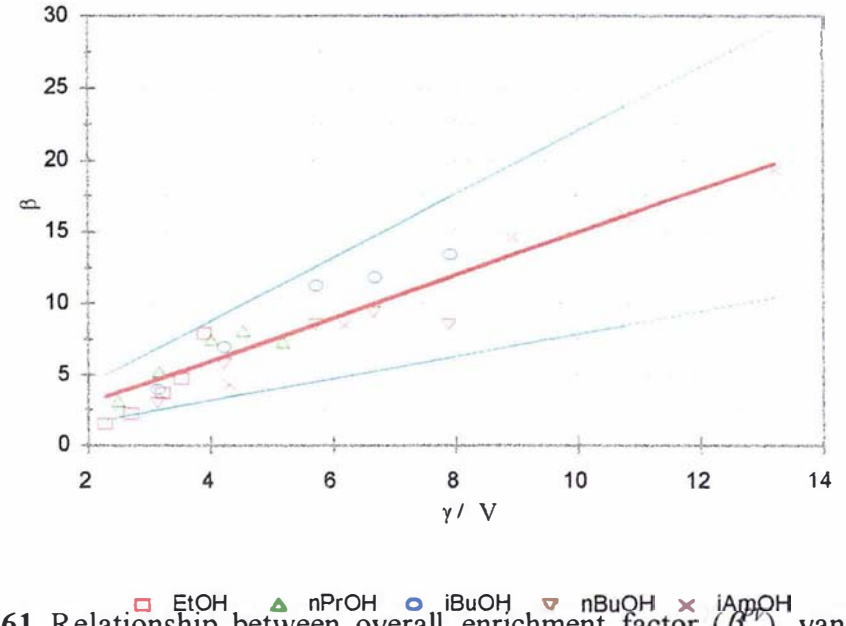

Figure IV.61 Relationship between overall enrichment factor (β^{PV}), van der Waals volume (V), and activity coefficient (γ) for alcohols in a mixture with water and ethyl acetate permeating through PEBA Experiment II). EtOH: ethanol; nPrOH: *n*-propanol; iBuOH: *i*-butanol; nBuOH: *n*-butanol; iAmOH: *i*-amyl alcohol.

Figures IV.62 to IV.64 show the raw data from Experiments I and III and the best fit model obtained from the Experiment II data only for GFT 1070, GFT 1060, and PEBA, respectively. The external, blue, dashed lines define the 95% limit of confidence for the slope of the fitted line. Although Experiments I and III were conducted at different operation conditions than that of Experiment II, the model still provides a good description of this data.

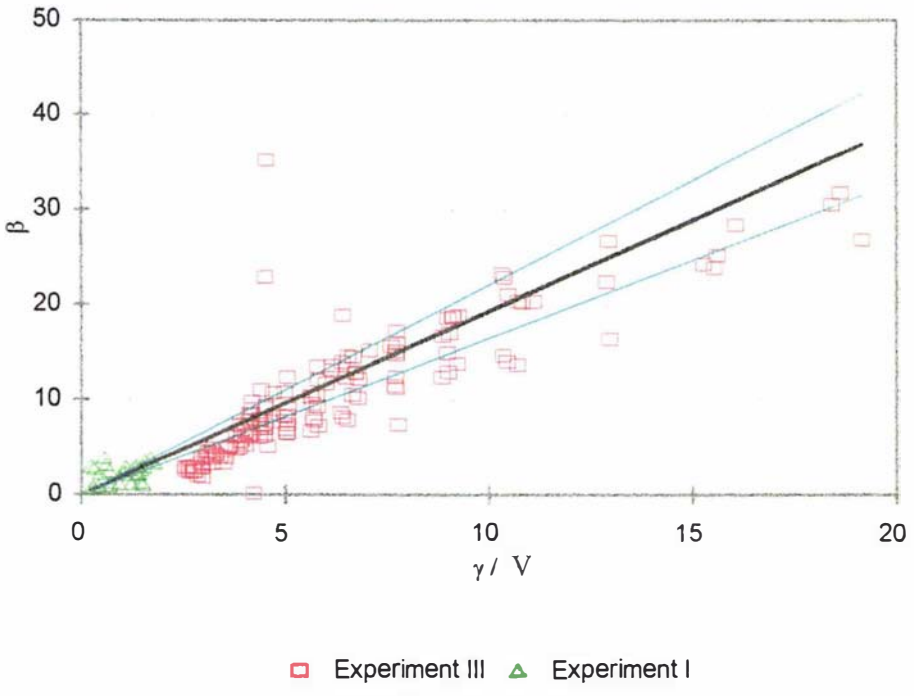

Figure IV.62 Relationship between overall enrichment factor (β^{PV}), van der Waals volume (V), and activity coefficient (γ) for alcohols in a mixture with water and ethyl acetate permeating through GFT 1070 (Experiments I and III).

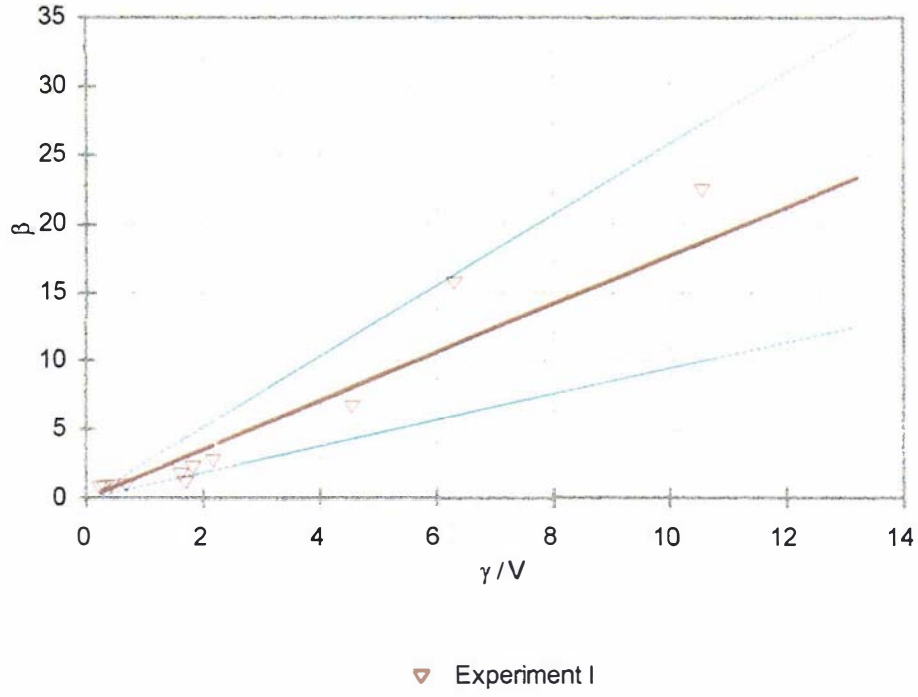

Figure IV.63 Relationship between overall enrichment factor (β^{PV}), van der Waals volume (V), and activity coefficient (γ) for alcohols in a mixture with water and ethyl acetate permeating through GFT 1060 (Experiment I).

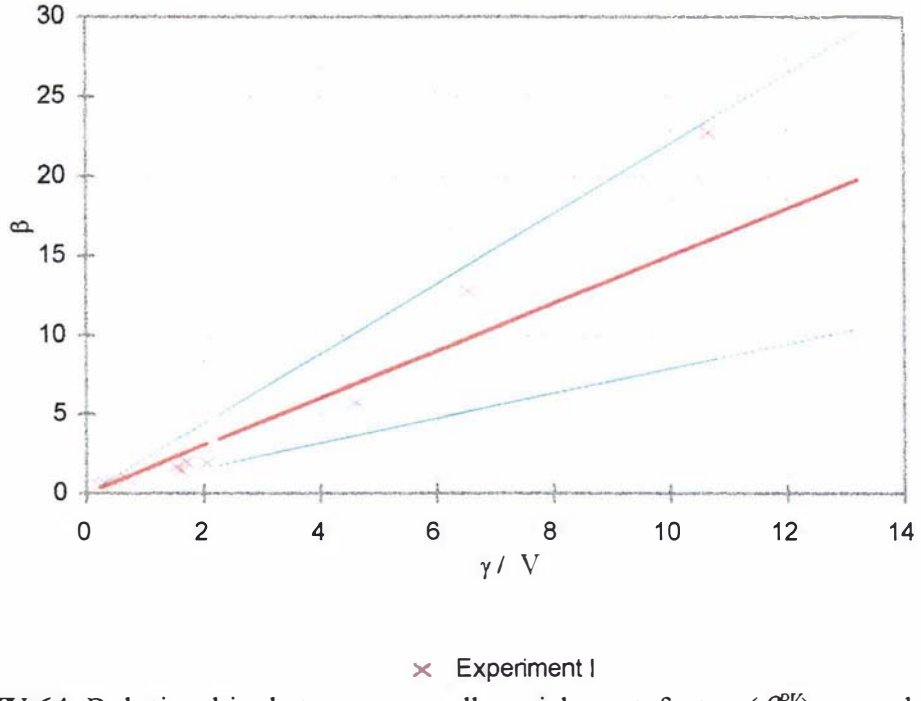

Figure IV.64 Relationship between overall enrichment factor (β^{PV}), van der Waals volume (V), and activity coefficient (γ) for alcohols in a mixture with water and ethyl acetate permeating through PEBA (Experiment I).

The ethyl acetate enrichment factor was not well described by the same model as the alcohols. Analysis of the data from Karlsson (1996) for alcohols and aldehydes confirms the applicability of the model but also suggests that different chemical families align at different areas in the plot. That is, the value of the coefficient of proportionality K_i'' might also depend on the chemical family (Figure IV.65). As ethyl acetate was the only ester used in the present study and its activity did not vary across a wide range, it was not possible to investigate how the ester family would behave in the presence of alcohols or to estimate a value for its coefficient of proportionality K.

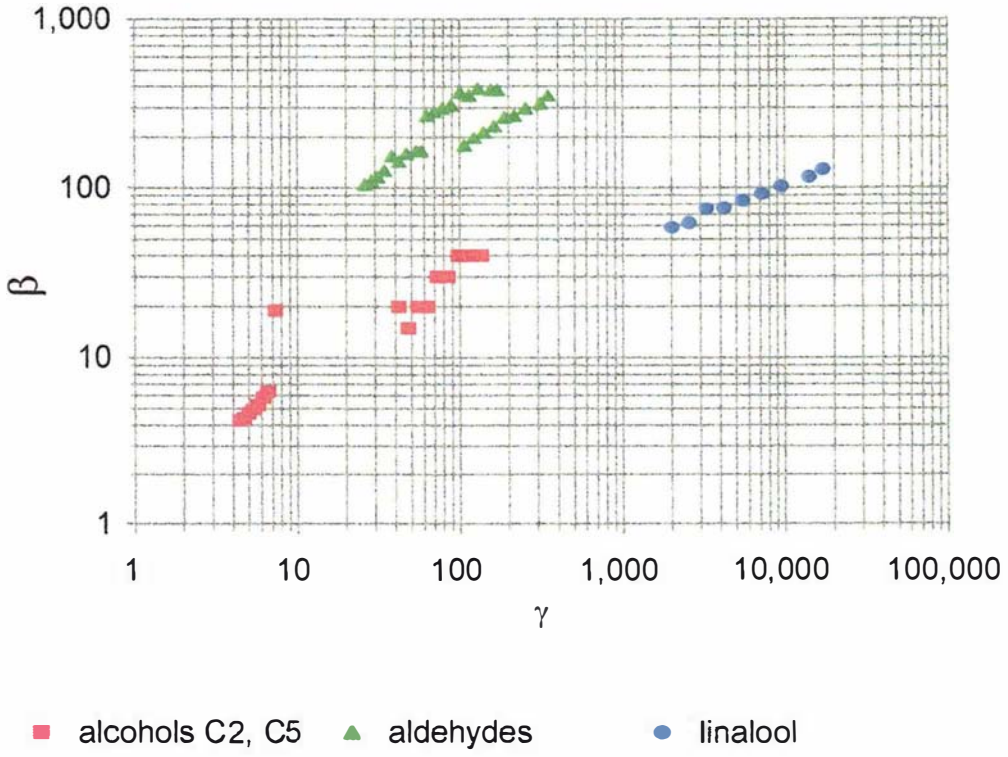

Figure IV.65 Relationship between enrichment factor (β) and activity coefficient (γ) for alcohols and aldehydes in an aqueous solution permeating through GFT 1060 at 20°C (calculated from Karlsson, 1996).

A closer look at the data from Karlsson (1996) for alcohols showed that the coefficient of proportionality K_i'' for linalool clearly differed from that of ethanol and 1-pentene-3-ol (Figure IV.66). For the former the coefficient of proportionality K_i'' was 0.00047 (r^2 = 0.97), whereas for the latter, the coefficient of proportionality K_i'' was 0.0203 (r^2 = 0.76). The lower the coefficient of proportionality K_i'', the lower the enrichment factor. For

linalool, if a common coefficient of proportionality K_i'' for all alcohols was used, the enrichment factor would be grossly overestimated. This result serves two purposes:

- based on the behaviour of ethanol and 1-pentene-3-ol, it confirms that Equation IV.25 describes adequately the behaviour of the pervaporation enrichment factor based on data from the feed solution, even when other phenomena such as concentration polarization occurs. Given the low concentrations that Karlsson (1996) selected for his study, concentration polarization was inherent in the behaviour of this sample and its occurrence was confirmed and modelled by Karlsson (1996).
- based on the behaviour of linalool, it highlights the importance of taking into account the influence of molecular size in the calculation of the overall pervaporation enrichment factor as suggested in Equation IV.25.

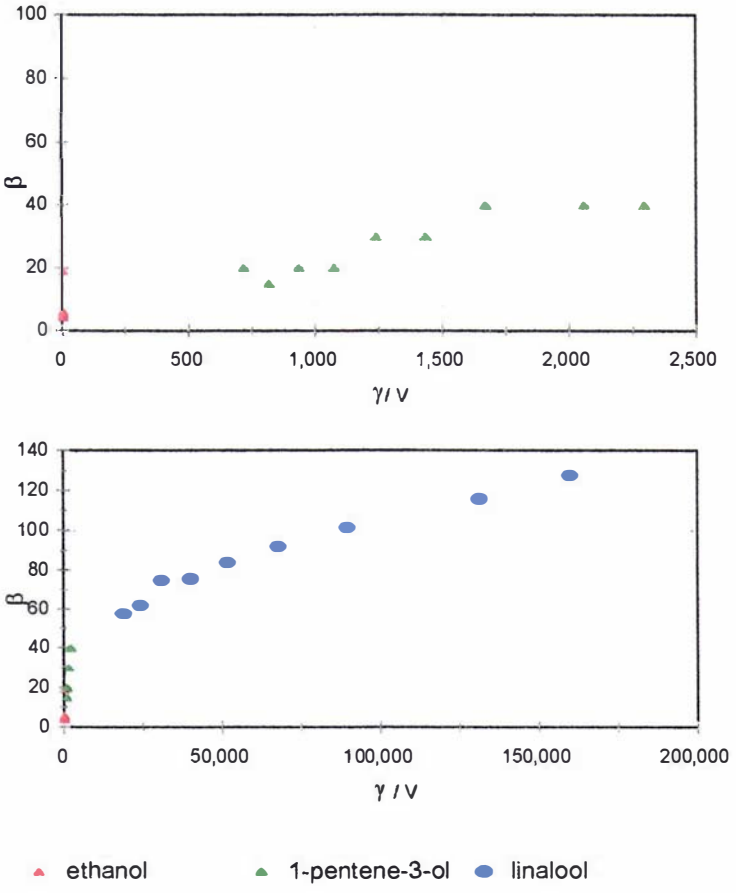

Figure IV.66 Detail of relationship between enrichment factor (β), van der Waals volume (V) and activity coefficient (γ) for alcohols (calculated from Karlsson, 1996).

In view of the behaviour of linalool, it might be inferred that over a certain molecular size, the separation is dominated by diffusion. Therefore, the contribution of molecular size to the separation is larger than that predicted by Equation IV.25. This could be described by incorporating an additional term in Equation IV.25.

$$\beta_i^{PV} = K^{\alpha_1} \frac{\gamma_i^f}{V_i} + \alpha_2 \qquad [IV.26]$$

The format of Equation IV.26 was chosen arbitrarily, other options such as the addition of an extra term to the denominator or elevating the volume to a power might also correct the predictions when larger molecules are present. As shown in Figure IV.67, for $K = 0.0203$ for all components, for ethanol and 1- pentene-3-ol Equation IV.26 reduces to Equation IV.25 with $\alpha_1 = 1$ and $\alpha_2 = 0$. However, for linalool, the suggested values for the fitted parameters in Equation IV.26 were $\alpha_1 = 1.97$; $\alpha_2 = 57.9$ kg.m^{-3}.

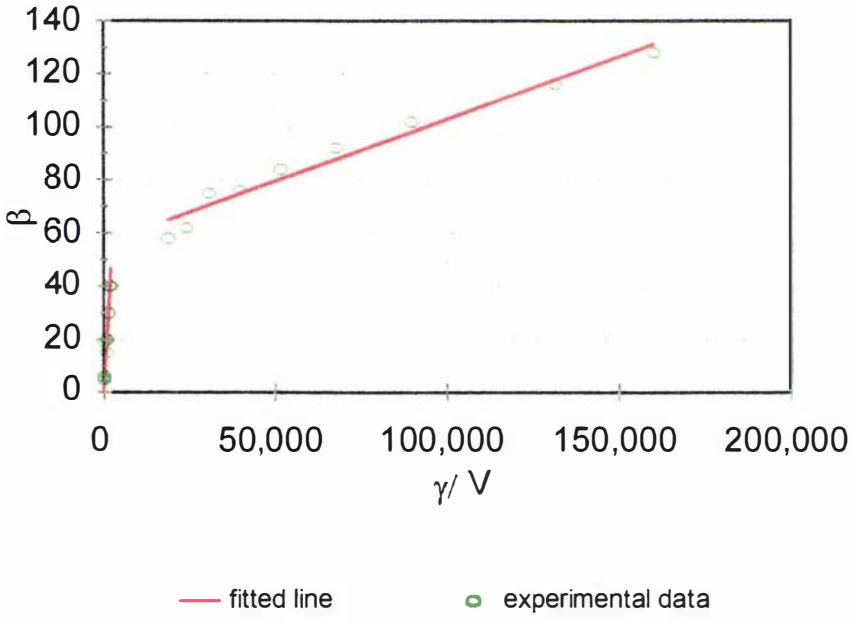

Figure IV.67 Fitting of experimental data on the overall enrichment factor (β^{PV}), the van der Waals volume (V), and the activity coefficient (γ) for alcohols from the work of Karlsson (1996).

The van de Waals volumes were calculated following the procedure reported by Bondi (1964). The values obtained for ethanol, 1-pentene-3-ol, and linalool were 0.03, 0.05, and 0.11 $m^3.kg^{-1}$, respectively. The van der Waal volume of ethanol as reported in the data base of ChemSep® is also 0.03 $m^3.kg^{-1}$. Equation IV.26 requires three fitted parameters instead of only one as in Equation IV.25. However, for the smaller molecules, namely ethanol and 1-pentene-3-ol, Equation IV.26 reduces to Equation IV.25. The favoured approach would be to describe parameters α_1 and α_2 as a continuous function of molecular size. However, this would only be possible when more experimental data on a continuous homologous series becomes available.

Equations IV.25 and IV.26 open new opportunities in the study of pervaporation for the prediction of the selectivity of membranes prior to experimental work. These equations are useful in the analysis of two common situations:

- in the comparison of the behaviour of the pervaporation of identical feed solutions permeating through different membranes under identical process conditions;

- in the evaluation of the enrichment factors of each component of the feed mixture permeating through the same membrane under identical process conditions.

Therefore, the effects of changes in feed composition due to upstream process changes could be readily evaluated and it would then be easier to determine a course of action for the downstream process.

The coefficient of proportionality K'' must be known if different membrane types are to be compared. However, assuming that the conditions for which Equations IV.25 and IV.26 were developed apply and provided that the flux characteristics of each membrane relative to one another (high or low flux) are known, it is already possible to estimate the order of magnitude of the K values for each membrane. For example, the GFT 1060 membrane is described as a high flux membrane, whereas the GFT 1070 is a low flux membrane. According to the data summarized in Table IV.21: $K''_{GFT\ 1060} < K''_{GFT\ 1070}$, as would be

expected from the definition of K given in Equation IV.23. Therefore, for each component of identical mixtures in the presence of either membrane, it is expected that the membrane with the lowest flux would present the highest selectivity. This relationship between flux and selectivity is well known in pervaporation (Mulder, 1991).

On the other hand, Equation IV.25 also enables the enrichment factor of each component of a feed mixture permeating through the same membrane under identical process conditions to be evaluated. In general, the higher the activity coefficient or the lower the molecular size of a component in the feed mixture, the higher its enrichment factor. Since molecular size (van der Waals volume) and feed activity coefficients are easily calculated, it is possible to use this methodoly to estimate the rank of the enrichment factors of even the most complex mixtures.

Jonquières & Fane (1997) proposed the use of a polarity parameter, $E_T(30)$, to assess the pervaporation performance of solvents. It was noted that the polarity parameter $E_T(30)$ and the activity coefficient of the solvent at infinite dilution are strongly correlated. However, Jonquières & Fane (1997) justified the use of the polarity parameter $E_T(30)$ over the activity coefficient at infinite dilution based on the greater accuracy of calculating the polarity parameter of binary solutions. Compared to the methodology proposed by Jonquières & Fane (1997), the use of the activity coefficient in Equation IV.25 has the advantage of including the influence of feed concentration, temperature, and any non-idealities due to the presence of other components. Furthermore, only limited pure component and binary solution data are easily available on the polarity parameter $E_T(30)$, while the activity coefficient of any component can be readily calculated provided that its molecular structure and the composition of the feed mixture are known. Additionally, Equation IV.25 relates the performance of pervaporation not only to the thermodynamic properties of the feed mixture, but also to the molecular size of the feed components. In doing so, Equation IV.25 accounts for both the effects of sorption and diffusion on the separation ability of pervaporation.

IV.7.3 SUMMARY

It was shown that it is possible to describe the enrichment factor of pervaporation of complex, multicomponent mixtures for each membrane type as a simple, linear function of feed properties, viz the molecular size of each component and the activity coefficient. A new equation was developed where it was assumed that both sorption and diffusion contributed to the separation. Experimental data collected during this study was well described by the new equation. This equation also described the experimental data adequately when concentration polarization occurred, such as for ethanol and 1-pentene-3-ol in the work of Karlsson (1996). However, for very large species, such as linalool, diffusion might become the dominant process and an extra, fitted parameter was arbitrarily added to the new equation in order to describe the behaviour of all alcohols in the mixture.

From the data of Karlsson (1996), it might also be suggested that for each chemical species in a mixture (alcohols, esters, aldehydes, etc) a different coefficient of proportionality K'' is required to describe the behaviour of their enrichment factor. This would explain why it was not possible to fit the data for ethyl acetate with the same parameters developed for the alcohols.

To date, there are too few reports with sufficient data to enable wider investigation of the utility or the limitations of the model proposed. It is still necessary to conduct a detailed evaluation of the effects of molecular weight on the overall enrichment factor of pervaporation and to explore the differences in the behaviour of distinct chemical families, if the model is to have a more generic application. Furthermore, while the relevance of these two parameters was identified in this study, the influence of other parameters, such as the free volume of the polymer or the ability of the chemicals present in the feed mixture to associate, cannot easily be discarded without further investigation.

In summary, for the systems studied, the new equations, Equations IV.22 and IV.23, enable the comparison of pervaporation behaviour for identical feed solutions permeating through different membranes under identical process conditions and the ranking of the enrichment

factors of each component of the feed mixture permeating through the same membrane under identical process conditions before experiments are performed.

IV.8 Conclusions

The main objective of this chapter was to investigate the influence of operation parameters on pervaporation performance.

The use of concentrated feed solutions led to the investigation of the effect of coupling with ethanol or the total flux on the partial flux of the minor organic components. For all minor components, except *i*-amyl alcohol, the partial flux was satisfactorily described as a function of the feed activity alone, as suggested by the solution-diffusion model. For *i*-amyl alcohol, flux was better described as a function of the feed activity as well as of coupling with either the ethanol partial flux or with the total flux. Given that the total flux through the membrane was highly correlated to the ethanol flux, it was not possible to differentiate between the effect of either ethanol or total flux in the flux of *i*-amyl alcohol.

It was confirmed that the influence of temperature on the flux through the membrane followed an Arrhenius-type model. In general, there was no significant influence of temperature on the distribution of the product concentrations or on the enrichment factor, except for ethyl acetate, for which the enrichment factor decreased with an increase in temperature. Overall, the higher the temperature, the higher the flux through the membrane and the lower the membrane area required for a given feed rate. The limit to the feed temperature is given by process requirements, energy expenditure to heat the feed, and the ability of the membrane material to withstand the working temperature.

The three membranes investigated had similar enrichment factors and did not improve the separation achieved by evaporation significantly.

Enrichment factor was shown to be a function of sorption, diffusion, and chemical family. For the system studied, the enrichment factor of alcohols could be calculated by a new, semi-empirical equation that related enrichment factor to the molecular structure of the permeants and feed conditions. If this relationship can be extended to other systems, it has the potential to be used as a pre-screening tool for the selection of membranes provided that the feed conditions are known.

Chapter V

SORPTION EXPERIMENTS

In Section IV.7 it was shown that the relationship between the thermodynamic properties and molecular structure of the feed mixture could be correlated with the overall enrichment factor of sorption. An empirical model was developed and shown to be applicable for the solvents tested. However, its wider use depends on further studies in order to test the limits and general applicability of the model. As reported in Chapters II and IV, it has been observed that the enrichment factor for sorption is often similar to the overall enrichment factor of pervaporation when organophilic membranes are employed. In this light, the main objectives for this chapter were to investigate the feasibility of using sorption experiments as a preliminary screening test for the selection of appropriate pervaporation membranes and, if possible, to predict the likely performance of a membrane by developing a model of the sorption of multicomponent solutions into the membrane material from the concentration of the feed solution. A detailed discussion on the mechanisms and equations applicable to sorption of solvents in polymers can be found in Section II.3.2.4.

V.1 INTRODUCTION

As discussed in detail in Chapter II, transport of liquid mixtures through dense polymeric membranes during pervaporation is usually described by a solution-diffusion model comprising three main steps: sorption of the feed mixture into the membrane, diffusion of the sorbed fluid through the membrane, and desorption of the permeate on the downstream side of the membrane.

For organophilic membranes, Spitzen *et al.* (1987) have pointed out that while diffusion is the rate-determining step, separation of the liquid mixture is usually determined by preferential sorption of the component in the polymer, i.e., the overall enrichment factor for pervaporation follows the sorption behaviour (Mulder & Smolders, 1986; Hauser *et al.*, 1989; Mulder & Smolders, 1991; Bartels-Caspers *et al.*, 1992; Ruckenstein & Sun, 1995;

Zhang & Drioli, 1995). Effectively, sorption determines the fluid concentration inside the membrane which then establishes the driving force for transport. Diffusion of each component of a liquid mixture through a membrane is influenced by molecular size. In the Stokes-Einstein equation, diffusion is described as inversely proportional to the radius of the molecule - the larger the molecule the lower the diffusivity (Watson & Payne, 1990). In the model developed for the overall pervaporation enrichment factor in the previous section, both the influence of sorption and of molecular size were adequately reflected by the activity coefficient and Van der Waals volume, respectively.

Consequently, two scenarios are possible:

- in the pervaporation of components of vastly different molecular size, diffusion not only determines the flow rate through the membrane, but it should also strongly influence the separation ability of the membrane. In an environment where the difference in size between the permeating species is large, it would be possible that the smaller molecules, and therefore faster permeating species, could also have the higher overall enrichment factor, even if the membrane preferentially sorbed the larger molecule.

- in the pervaporation of components of broadly similar molecular size, the enrichment factor should follow the trend set by sorption. For systems that have such behaviour, prediction of the sorption enrichment factor could be used to assess the appropriateness of the membrane material to separate the components, thus providing a simple tool for pre-selection of the membrane type and its applicability for a given use.

The work discussed in this chapter is based on the postulate that the second scenario is applicable to the pervaporation of aqueous mixtures of alcohols and esters using hydrophobic membrane. Sample availability menat that the analysis was restricted to the PEBA membrane.

As discussed in Section II.3.2.4, the Flory-Huggins equation is considered inadequate to predict sorption of polar compounds in polymers (Favre *et al.*, 1993), but good results were reported with the UNIQUAC equation in the presence of polar compounds (Heintz & Stephan, 1994a). It was therefore decided to use the UNIQUAC equation to attempt the prediction of sorption in PEBA membranes. If the molecular structure of the polymer is known, the UNIFAC equation can also be used to examine the experimental fitting of the membrane-binary interaction parameters obtained for UNIQUAC. Unfortunately, the required structural information for the PEBA membrane material was of proprietary nature and was not available.

In order to calculate the mass fraction of the solvent inside the polymer material, it was assumed that the external solvent solution was in equilibrium with the membrane interface, therefore the component activities in both phases were the same (Equation V.1). Both for the fitting of binary interaction parameters between the membrane and solvent, and for multicomponent predictions, the UNIQUAC equation set (Equations V.2 to V.8), as modified by Ennecking *et al.* (1993), was used. All other parameters were extracted from the vapour-liquid equilibrium literature (Gmehling *et al*, 1977; Prausnitz *et al.*, 1986).

$$a_i = a_i' \qquad [V.1]$$

$$\ln a_i = \ln\Phi_i + \frac{z}{2} q_i \ln\frac{\Theta_i}{\Phi_i} + l_i - \sum_{j=1}^{n} \Phi_j \frac{r_i}{r_j} l_j - q_i' \ln\sum_{j=1}^{n} \Theta_j' \tau_{ji} + q_i' - q_i' \sum_{j=1}^{n} \frac{\Theta_j' \tau_{ij}}{\sum_{k=1}^{n} \Theta_k' \tau_{kj}} \qquad [V.2]$$

$$\ln a_i' = \ln\Phi_i + \frac{z}{2} q_i \ln\frac{\Theta_i}{\Phi_i} + l_i - \sum_{j\neq M}^{n} \Phi_j \frac{r_i}{r_j} l_j - q_i' \ln\sum_{j=1}^{M} \Theta_j' \tau_{ji} + q_i' - q_i' \sum_{j=1}^{M} \frac{\Theta_j' \tau_{ij}}{\sum_{k=1}^{M} \Theta_k' \tau_{kj}} - r_i \Phi_M \left(\frac{z}{2} \left(1 - \frac{q_M}{r_M} \right) - 1 \right) \qquad [V.3]$$

where:

$$l_i = \frac{z}{2}(r_i - q_i) - (r_i - 1) \qquad [V.4]$$

$$\Phi_i = \frac{w_i/\rho_i}{\sum_{j=1}^{n} w_j/\rho_j} \qquad [V.5]$$

$$\Theta_i = \frac{\Phi_i(q_i/r_i)}{\sum_{j=1}^{n} \Phi_j(q_j/r_j)} \qquad [V.6]$$

$$\Theta_i^* = \frac{\Phi_i(q_i^*/r_i)}{\sum_{j=1}^{n} \Phi_j(q_j^*/r_j)} \qquad [V.7]$$

$$\tau_{ij} = e^{-\frac{a_{ij}}{RT}} \qquad [V.8]$$

where, a_i thermodynamic activity of a component i in a multicomponent solution consisting of n components;

a_i^* thermodynamic activity of a component i inside a polymer;

a_{ij} UNIQUAC iteraction parameter ($J.mol^{-1}$)

r_i, q_i dimensionless parameters for the relative molecular size and surface of component i related to the size and surface of a CH_2 segment in polyethylene, respectively;

r_M, q_M dimensionless parameters for the relative molecular size and surface of the membrane material related to the size and surface of a CH_2 segment in polyethylene, respectively;

R universal constant of gases in $J.mol^{-1}.K^{-1}$;

T temperature in K;

z coordination number assumed to be 10;

ρ density in $kg.m^{-3}$;

τ_{ij} binary interaction parameter.

The experimental work was divided into four parts:

- Sorption of pure components into PEBA beads at temperatures ranging from 20 to 55 °C. This was done to evaluate the affinity of the membrane material for each component separately, to evaluate the time required for the beads to reach equilibrium, to assess the quantity of solvent sorbed into the membrane and use this information in planing multicomponent tests, and to generate interaction parameters necessary for prediction of sorption with UNIQUAC.

- Sorption of binary solvent solutions into PEBA beads for generation of the UNIQUAC interaction parameters.

- Sorption of multicomponent solvent solutions into PEBA beads for comparison of experimental enrichment factors with predicted values from UNIQUAC.

- Pervaporation of multicomponent solvent solutions through PEBA membranes for comparison of overall enrichment factors with those obtained from sorption experiments.

V.2 SORPTION EXPERIMENTS

V.2.1 BACKGROUND TO EXPERIMENTAL PROCEDURE

In studies of sorption, experiments with gaseous systems were traditionally preferred due to the ease of measuring the gain of weight of a polymer sample during the experimental procedures (Felder & Huvard, 1980). Heintz *et al.* (1991) used vapour data to extrapolate the solubility at a saturated state for PVA in contact with aqueous mixtures of methanol, ethanol, and *i*-propanol. Unfortunately, the solubility of saturated liquids in polymers was found to be higher than the solubility of the correspondent equilibrium saturated vapour, due to a higher affinity of the liquid phase to the polymer. This difference in affinity

resulted in higher swelling of the polymer exposed to the liquid phase in comparison to the polymer exposed to the vapour phase. Therefore, the study of solubility of liquids in polymers should not be extrapolated from vapour-phase data without regard for difference in the behaviour of the polymer in the presence of liquid or vapour phases (Hauser *et al.*, 1989b).

Hauser *et al.* (1989c) developed a series of methodologies for the experimental study of sorption of liquids in polymers. These procedures consisted of immersing the polymer in the solvent mixture, until equilibrium was reached, i.e., until the weight of the polymer no longer changed with time. The concentration of the solution inside the polymer was then measured by near infrared spectrometry (IR), desorption followed by gas chromatography analysis (GC), or measurement of the density of the solvent solution before and after the experiment had taken place. The IR methodology was applied for polymers that did not absorb sufficient solvent to be analysed by GC, while the measurement of density applied only for binary solutions. All the methodologies developed had an estimated error of about 8 to 10%.

In view of these previous studies, it was decided to conduct all sorption experiments in the presence of a liquid phase. The weight of beads used for each test was carefully selected so that there would be enough solvent extracted from the beads to be analysed by GC. The GC analysis procedure was outlined in Section IV.2.2.

V.2.2 Sorption experiment with pure solvents

V.2.2.1 Materials and methods

In this work, sorption experiments were conducted with poly-ether-*block*-amide (PEBA) beads containing UV stabiliser (PEBAX 4033, Elf-Atochem Pty, Ltd.). The beads were used without further treatment. All solvents used were of analytical grade (AR) and were not purified further. The water used was treated by a Milli-Q system (Millipore Corp.).

Duran flasks with a capacity of 5 ml were used. Each flask received approximately 1 g of PEBA beads and 2 to 3 ml of pure solvent (water, ethanol, ethyl acetate, *n*-propanol, *i*-butanol, or *i*-amyl alcohol). Duplicates were prepared. The flasks were kept in a water bath (Julabo Labortechnik GmbH) at constant temperature. Every second day, the beads were taken from the flask, quickly dried with tissue paper, weighed, and returned to the flask. Solvent was added to the flask in order to keep a constant level throughout the experiment. This procedure was repeated until the weight of the beads did not increase by more than 0.1% from their previous weight, which indicated that equilibrium was reached. The overall increase in weight of the beads was then recorded. Hauser *et al.* (1989c) found that uncontrolled losses of solvent by evaporation during this procedure were usually smaller than 1% of the absorbed solvent.

For one set of beads the experiment started at 20°C. After the weight was constant, the temperature of the bath was increased by 5°C and the whole procedure was repeated. The experiment was carried out from 20°C to 55°C. The upper temperature limit was imposed by the behaviour of the flasks; at temperatures of 60°C and higher the flasks could not be effectively sealed and within a week the caps were damaged by the combined effect of temperature and concentrated solvent vapour. A second set of beads was started at 40°C and the experiment was carried out in a similar manner until the temperature of the bath was 55°C. The reason each set of beads commenced at a different temperature was to partially investigate whether the previous history of the polymer would affect the results.

V.2.2.2 Results and discussion

Tables V.1 and V.2 show the results of the first and second set of experiments, respectively. The reproducibility of the experiment at a given temperature (> 40°C) was within approximately 15% for water and organic solvents, and for ethyl acetate, within 20% (Table V.3). The reproducibility was calculated as the percentage difference between duplicates for each set of experiments. The higher variation observed for ethyl acetate was possibly due to its higher volatility.

The variation in the reproducibility of the sorption results was not considered significant for the temperature range studied (20 to 55°C) regardless of the starting temperature. However, when working with broader temperature ranges, it would still be advisable to investigate whether the temperature history influences the sorption results.

Table V.1 Mass fraction of solvent in PEBA pellets after equilibrium with pure solventfor the first set of experiments. T: temperature in °C; EtOH: ethanol; nPrOH: *n*-propanol; iBuOH: *i*-butanol; iAmOH: *i*-amyl alcohol; EtOAc: ethyl acetate.

T	Water	EtOH	nPrOH	iBuOH	iAmOH	EtOAc
20	0.017	0.23	0.34	0.32	0.29	0.26
25	0.016	0.23	0.36	0.34	0.31	0.26
30	0.019	0.25	0.39	0.39	0.33	0.28
35	0.022	0.28	0.43	0.44	0.38	0.30
40	0.022	0.30	0.44	0.46	0.41	0.30
45	0.022	0.32	0.47	0.48	0.44	0.36
50	0.024	0.35	0.50	0.52	0.47	0.37
55	0.024	0.38	0.53	0.58	0.54	0.37

Table V.2 Mass fraction of solvent in PEBA pellets after equilibrium for the second set of experiments. T: temperature in °C; EtOH: ethanol; nPrOH: *n*-propanol; iBuOH: *i*-butanol; iAmOH: *i*-amyl alcohol; EtOAc: ethyl acetate.

T	Water	EtOH	nPrOH	iBuOH	iAmOH	EtOAc
40	0.021	0.29	0.41	0.45	0.39	0.29
45	0.021	0.29	0.46	0.51	0.46	0.31
50	0.021	0.35	0.51	0.55	0.50	0.31
55	0.021	0.38	0.55	0.61	0.55	0.33

Table V.3 Difference in mass fraction between first and second set of experiments based on duplicated measurements within each set. T: temperature in °C; EtOH: ethanol; nPrOH: *n*-propanol; iBuOH: *i*-butanol; iAmOH: *i*-amyl alcohol; EtOAc: ethyl acetate.

T	Water	EtOH	nPrOH	iBuOH	iAmOH	EtOAc
40	4%	1%	8%	2%	3%	5%
45	4%	11%	3%	-6%	-4%	16%
50	16%	0.03%	-2%	-6%	-5%	20%
55	13%	-1%	-2%	-5%	-2%	12%

For each solvent, the relationship between the quantity of solvent sorbed and the temperature was adequately described by an Arrhenius-type equation (Figure V.1) and the fitted coefficients are listed in Table V.4. The fitted values of the activation energy of sorption of ethanol are slightly less than the data compiled for organic and hydrophilic membranes by Feng & Huang (1996), who reported values between 680 and 1200 $kJ.g^{-1}$ (15 and 26 $kJ.mol^{-1}$) for experiments over a temperature range between 20 and 75°C. For ethyl acetate, *i*-butanol, and *i*-amyl alcohol, the fitted values of the activation energy are of the same order of magnitude but considerably lower than those presented by Karlsson (1995) for GFT 1060 of 35, 47 and 51 $kJ.mol^{-1}$, respectively. These correspond to the values reported in Table V.4 of 9, 13 and 14 $kJ.mol^{-1}$. These discrepancies are probably due to differences in concentration of the external solution, which also has a large influence in the amount of solvent sorbed by the membrane. While in this experiment pure solvents were used, in the experiments reported by Karlsson (1995) and Feng & Huang (1996), the solvent concentration was generally of a few ppm.

Table V.4 Arrhenius-type equation coefficients for pure solvents in PEBA.

Equation: $$S = S_o \, e^{\left(\frac{E_a}{RT}\right)}$$

S: mass fraction of solvent in PEBA; S_o: constant; E_a: activation energy ($J.mol^{-1}$); R: universal constant of gases in $kJ.mol^{-1}K^{-1}$; T: temperature in K; EtOH: ethanol; nPrOH: *n*-propanol; iBuOH: *i*-butanol; iAmOH: *i*-amyl alcohol; EtOAc: ethyl acetate.

	Water	EtOH	nPrOH	iBuOH	iAmOH	EtOAc
S_o	0.77	33	22	74	89	12
E_a	9,352	12,205	10,171	13,272	14,023	9,482
r^2	0.86	0.98	0.99	0.98	0.99	0.93

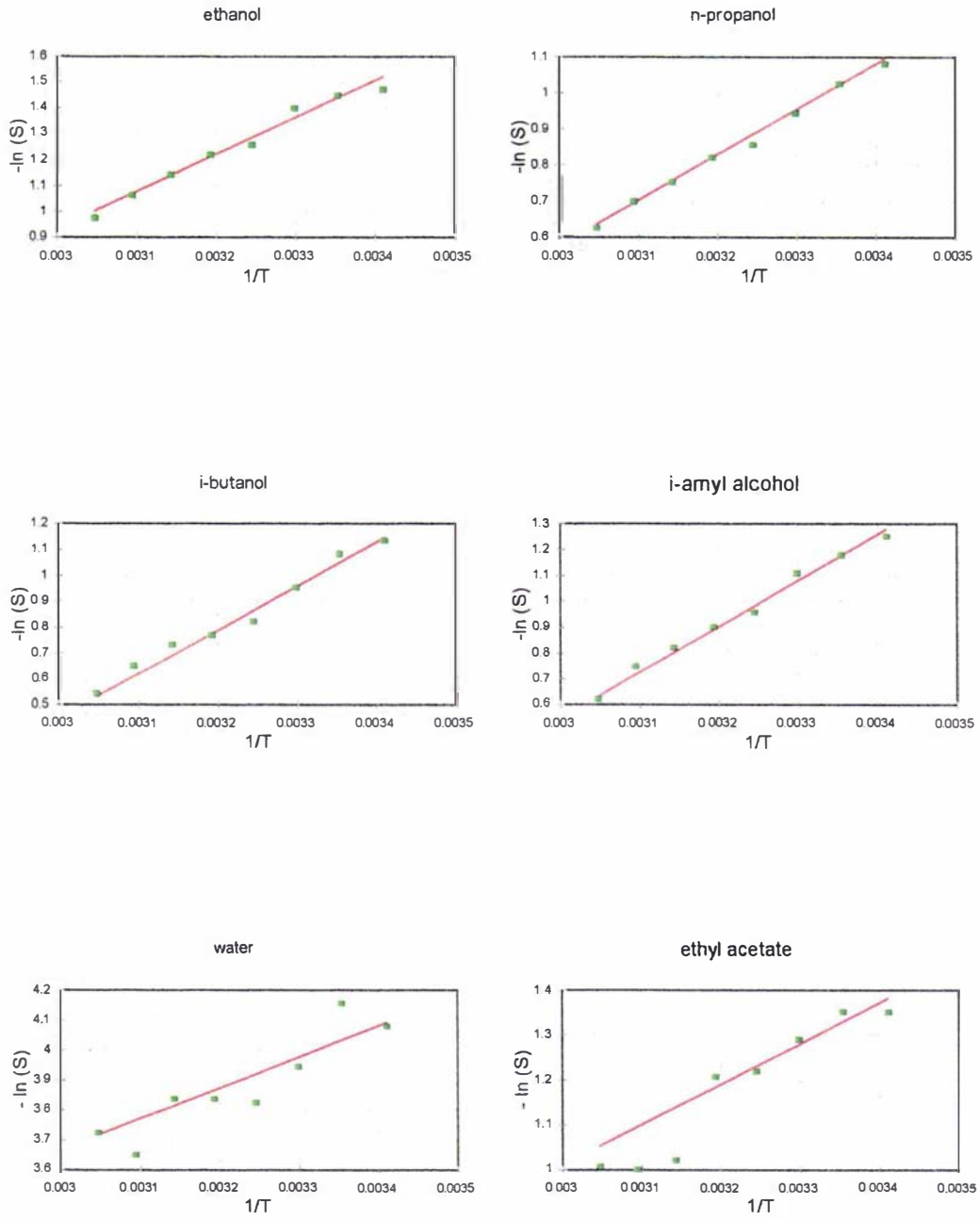

Figure V.1 Plot of experimental values and best fit Arrhenius equation for sorption of pure solvents in PEBA membranes from 20 to 55°C.
■ experimental points; — fitted line.

Table V.5 shows that, with the Arrhenius-type equation, the error between the predicted and the experimental values did not exceed 5% for all organic solvents except ethyl acetate and for water, for both of which the error was as high as 13%.

Table V.5 Percentage difference between experimental and predicted sorption values generated with the Arrhenius-type equation defined in Table V.4. T: temperature in °C; EtOH: ethanol; nPrOH: *n*-propanol; iBuOH: *i*-butanol; iAmOH: *i*-amyl alcohol; EtOAc: ethyl acetate.

T	Water	EtOH	nPrOH	iBuOH	iAmOH	EtOAc
20	-1%	-5%	-1.5%	-1%	-3%	-3%
25	13%	0.9%	0.2%	3%	0.02%	2%
30	-3%	4%	-0.9%	-0.3%	3%	1%
35	-9%	-3%	-3%	-4%	-2%	-1%
40	-3%	0.7%	-0.03%	-0.7%	1%	2%
45	2%	0.1%	-0.4%	4%	2%	-11%
50	-5%	-0.8%	0.4%	4%	3%	-9%
55	0.6%	-3%	-1%	1%	-1%	-5%

note: pencentage difference = (experimental value - predicted value)/ experimental value * 100

From the increase in weight of the PEBA beads in the presence of each solvent, it would be expected that *n*-propanol, *i*-butanol and *i*-amyl alcohol would be the easiest solvents to remove from a multicomponent, aqueous solution followed by ethyl acetate and ethanol. The quantity of water sorbed by the beads (about 20 $mg.g^{-1}$ of dry polymer material) was comparable to that reported by Böddeker *et al.* (1990) and negligible when compared to the solvent uptake (between 300 and 1400 $mg.g^{-1}$ of dry polymer material), which confirmed the hydrophobicity of the membrane. However, the lower values of the activation energy (Table V.4) indicate, as discussed in Section II.3.2.4, that ethyl acetate and water should permeate preferentially at higher temperatures. Since the affinity of the membrane material for water is minimal in comparison to its affinity for organic solvents, it was not expected that the lower activation energy alone would reverse this trend or that a considerable enrichment of water in the permeate would be expected.

In the sorption experiment with pure solvents, ethyl acetate had a slightly lower affinity for the membrane than the higher alcohols, but, because its activation energy was much lower than that for the alcohols, these two influences together could result in an enrichment of ethyl acetate through pervaporation higher than that predicted from the sorption experiments with pure components alone. This analysis is confirmed by the results presented in Section V.3.

The results of the sorption experiments with pure solvents were used, together with the results of the sorption experiments with binary solutions presented in the next section, to generate the binary iteration parameters for the UNIQUAC equation. Attempts to generate these parameters from pure solvent experiments with liquid solutions alone were not successful, possibly because the experimental data did not include the influence of interactions between components. An example of the complexity of the phenomena under investigation was given by Mulder *et al.* (1983). In a study of the sorption and permeation behaviour of water and ethanol using polysulfone (Psf), a hydrophobic polymer, it was found impossible to extend the behaviour of pure components to binary solutions. Water alone did not permeate through PSf, but in the presence of ethanol it became the preferential permeant.

V.2.3 SORPTION EXPERIMENT WITH MULTICOMPONENT SOLUTIONS

This experiment comprised two parts: sorption of binary solutions for generation of PEBA -solvent interaction parameters and sorption of multicomponent solutions into PEBA beads for comparison of experimental enrichment factors with predicted values. Pervaporation experiments with multicomponent solutions through PEBA membranes at the same temperature and similar feed concentration as the sorption experiments were also conducted in order to compare enrichment factors of sorption and pervaporation (Section V.3).

V.2.3.1 SORPTION OF BINARY SOLUTIONS

V.2.3.1.1 MATERIALS AND METHODS

Sorption experiments were conducted with poly-ether-*block*-amide (PEBA) beads containing UV stabiliser (PEBAX 4033, Elf-Atochem Pty, Ltd.). The beads were used without further treatment. The solvents used were of analytical grade (AR) and were not purified further. The water used was treated by a Milli-Q system (Millipore Corp.).

Binary solutions of solvents were prepared as specified in Table V.6. The solvents were paired to avoid partial miscibility at any concentration being studied. A known amount of PEBA beads was immersed in each solution in Duran flasks (100 and 250 ml). The flasks were sealed and kept in an oven (Contherm series 5) at 50°C. Based on results of the previous experiment with pure solvents, the quantity of PEBA beads introduced in each flask was chosen so that approximately 2 to 4 ml of solvent solution could be extracted from the beads. Triplicates were prepared.

Table V.6 Experiment design for determining sorption from binary solutions. *m:* approximate mass of PEBA beads in each flask in g; *v:* approximate volume of solution in each flask in ml; EtOH: ethanol; nPrOH: *n*-propanol; iBuOH: *i*-butanol; iAmOH: *i*-amyl alcohol; EtOAc: ethyl acetate.

Pair of solvents	volume ratio	*m*	*v*
EtOH : water	1:99	40	250
	10:90	40	250
	20:80	40	250
	40:60	40	250
nPrOH : iBuOH	1:99	5	100
	10:90	5	100
	90:10	5	100
	99:1	5	100
iAmOH : EtOAc	1:99	5	100
	10:90	5	100
	90:10	5	100
	99:1	5	100

The beads were kept in the oven for a minimum of four weeks to guarantee that equilibrium was reached. This length of time was chosen based on equilibrium times of the previous experiment with pure solvents. After four weeks, the beads were taken from the solution, quickly blotted using paper tissue, transferred to pre-weighed, pre-dried, sealable flasks, weighed, and attached to an extraction system (Figure V.2). The remaining solution in the original flask was analysed by gas chromatography. Solutions containing ethyl acetate and *i*-amyl alcohol needed to be diluted with ethanol (up to 50%) to improve reproducibility of the GC analysis. It was observed that the amount of sample dispensed by the auto-sampler when only ethyl acetate and *i*-amyl alcohol were present in the solution was not reproducible.

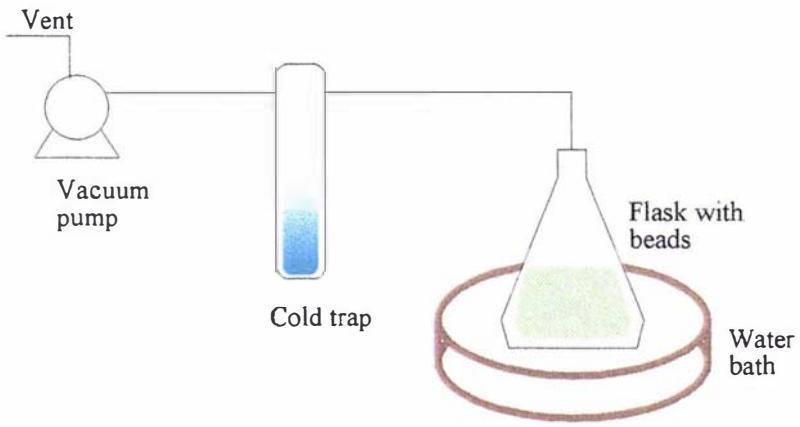

Figure V.2 Schematic diagram of the extraction system.

In the extraction system, the flask was placed in a water bath and the whole system was evacuated for 24 h. The extracted solution was collected in a cold trap, cooled to -196 °C by liquid nitrogen, weighed and analysed by gas chromatography. The difference between the weight of the beads immediately before and after extraction provided a second measurement of the weight of the extracted solution.

V.2.3.1.2 RESULTS

The beads were extracted until their weight was approximately the same as before the sorption experiment. It was observed during the experiment that some polymer material dissolved in the external solvent solution, and a slight loss in the weight of beads was observed. The averaged difference between the weight of the beads before and after the sorption experiment was -0.89% for water/ethanol, -2.22% for *i*-amyl alcohol/ethyl acetate, and -4.23% for *n*-propanol/*i*-butanol. The higher loss in weight of the beads in the *n*-propanol/*i*-butanol solution was probably due to butanol being able to solubilize PEBA as indicated by Böddeker *et al.* (1990).

Although triplicates of each set of solutions were prepared, slight deviations in the weight of the beads inside the flasks and some minor leakage of vapours during experiments, resulted in external solutions that were not identical.However, the results of Favre *et al.* (1993) and Ruckenstein & Sun (1995) suggest that it is reasonable to expect a reproducibility between 2 and 15%. Reproducibility was not evaluated in this trial as the possibility of random, uncontrolled loss of solvent by vapour leakage from the Duran flasks could not be ruled out. Consequently, each result was used individually in generating the UNIQUAC binary interaction parameters.

Tables V.7 and V.8 list in the same order the measured composition of the solution in equilibrium with the PEBA beads and the solution extracted from the PEBA beads at 50°C, respectively. The UNIQUAC binary interaction parameters between each solvent and the PEBA beads (Table V.9) were estimated from these results using a Newton-Raphson algorithm with MatLab® (Mathworks, USA). The predictions of sorption of multicomponent solutions by PEBA using the UNIQUAC equations were calculated using the optimization function *fmins* of MatLab® , which employs the simplex search method of Nelder and Mead. It was assumed that $(q/r)_M = 2/3$ (Prausnitz *et al.*, 1986).

Table V.7 Concentration of external solutions in equilibrium with PEBA beads at 50°C in mass fraction. All tests listed individually.

ethanol	water	*i*-propanol	*i*-butanol	ethyl acetate	*i*-amyl alcohol
1	0	1	0	1	0
1	0	1	0	1	0
0	1	0	1	0	1
0	1	0	1	0	1
0.90	0.10	0.99	0.01	0.01	0.99
0.79	0.21	0.99	0.01	0.01	0.99
0.93	0.07	0.99	0.01	0.01	0.99
0.68	0.32	0.02	0.98	0.11	0.89
0.78	0.22	0.01	0.99	0.11	0.89
0.81	0.19	0.01	0.99	0.11	0.89
0.10	0.90	0.89	0.11	0.89	0.11
0.13	0.87	0.90	0.10	0.90	0.10
0.12	0.88	0.89	0.11	0.89	0.11
0.01	0.99	0.11	0.89	0.99	0.01
0.01	0.99	0.00	1.00	0.97	0.03
0.01	0.99			0.99	0.01

Table V.8 Mass fraction of solvents inside PEBA beads at 50°C. All tests listed individually. EtOH: ethanol; nPrOH: *n*-propanol; iBuOH: *i*-butanol; iAmOH: *i*-amyl alcohol; EtOAc: ethyl acetate; M: PEBA beads.

EtOH	water	M	nPrOH	iBuOH	M	EtOAc	iAmOH	M
0.35	0	0.65	0.51	0	0.50	0.31	0	0.69
0.35	0	0.65	0.50	0	0.50	0.37	0	0.63
0	0.02	0.98	0	0.55	0.45	0	0.50	0.50
0	0.03	0.97	0	0.52	0.48	0	0.47	0.53
0.31	0.04	0.65	0.53	0.01	0.47	0.00	0.54	0.46
0.26	0.07	0.67	0.51	0.01	0.48	0.01	0.57	0.42
0.34	0.04	0.63	0.51	0.01	0.48	0.01	0.48	0.51
0.10	0.04	0.86	0.01	0.53	0.45	0.06	0.47	0.47
0.11	0.01	0.87	0.01	0.52	0.47	0.05	0.45	0.50
0.11	0.02	0.87	0.01	0.55	0.44	0.05	0.46	0.48
0.01	0.06	0.93	0.44	0.05	0.51	0.28	0.06	0.67
0.02	0.06	0.92	0.45	0.05	0.51	0.31	0.04	0.65
0.02	0.05	0.93	0.48	0.05	0.47	0.31	0.04	0.65
0.00	0.06	0.94	0.05	0.45	0.49	0.28	0.03	0.69
0.00	0.06	0.94	0.00	0.58	0.42	0.26	0.04	0.69
0.00	0.06	0.94				0.31	0.00	0.69

Table V.9 Interaction parameters for UNIQUAC equation from fitting of experimental data and from Gmehling *et al.* (1977). *r*, *q*, *q**: dimensionless parameters for the relative molecular size and surface of each component related to the size and surface of a CH_2 segment in polyethylene; ρ: density ($kg.m^{-3}$); a_{ij}: UNIQUAC iteration parameter ($J.mol^{-1}$); EtOH: ethanol; nPrOH: *n*-propanol; iBuOH: *i*-butanol; iAmOH: *i*-amyl alcohol; EtOAc: ethyl acetate; M: PEBA beads. $(q/r)_M = 2/3$ (Prausnitz *et al.*, 1986).

	iAmOH	EtOAc	iBuOH	nPrOH	EtOH	water	M
r	4.5979	3.4786	3.4535	2.7799	2.1055	0.9200	
q	4.2040	3.1160	3.0480	2.5120	1.9720	1.4000	
q^*	1.15	3.1160	0.88	0.89	0.92	1.4000	
ρ	812.0	902.0	805.76	803.6	785.1	1000.0	1010.0

a_{ij}	iAmOH	EtOAc	iBuOH	nPrOH	EtOH	water	M
iAmOH	1.0000	48.0007	-155.0435	255.1797	-18.3336	-223.7897	59.9881
EtOAc	112.7077	1.0000	178.9328	257.0573	-823.2360	757.5853	113.9535
iBuOH	155.1437	14.2012	1.0000	518.7489	451.1680	3357.972	21.9942
nPrOH	-210.9129	-144.8524	-323.0754	1.0000	71.7593	143.6749	26.2939
EtOH	82.3751	-62.7027	-319.0997	-35.2815	1.0000	50.8846	95.1778
water	819.6231	151.6420	853.9001	337.0647	232.0091	1.0000	86.3523
M	-20.4320	37.2329	41.1884	64.2133	104.8386	112.6323	1.000

V.2.3.2 Sorption experiment with multicomponent solutions

V.2.3.2.1 Materials and methods

The experiment was conducted according to the procedure outlined in Section V.2.3.1.1, except that each solution prepared contained all six components (water, ethanol, *n*-propanol, *i*-butanol, *i*-amyl alcohol, ethyl acetate). Each flask contained approximately 10 g of PEBA beads and 250 ml of solution. Eight solutions were prepared to cover a concentration range of approximately 0.5% to 40% (w/w) for ethanol and up to 2% (w/w) for organic solvents. The composition of the mixtures was analysed by GC (Section IV.2.2).

V.2.3.2.2 Results and discussion

Table V.10 summarizes the concentration of each solution in equilibrium with the beads. Table V.11 summarizes the concentration of the solutions extracted from the beads. The difference in weight of the beads before and after the experiment was on average -0.17%.. This result again confirmed that all the sorbed solution was extracted from the beads.

Figure V.3, shows the sorption isoterms for four fusels into the PEBA and curve fits using Henry Law. The correlation coefficients are greater than 0.8 for ethyl acetate and *n*-propanol, but less than 0.5 for *i*-butanol and *i*-amylalcohol. However, Henry law is of limited value since it is not valid outside the range studied. In view of this limitation, it was decided to investigate a semi-empirical model (UNIQUAC) for predicting sorption behaviour.

Table V.10 Mass fraction of solvent in multicomponent external solution in equilibrium with PEBA beads. EtOH: ethanol; nPrOH: *n*-propanol; iBuOH: *i*-butanol; iAmOH: *i*-amyl alcohol; EtOAc: ethyl acetate.

	iAmOH	EtOAc	iBuOH	nPrOH	EtOH	water
1st set	0.007	0.0056	0.0098	0.011	0.10	0.87
2nd set	0.0075	0.0059	0.010	0.012	0.12	0.85
3rd set	0.0068	0.0054	0.0094	0.010	0.10	0.87
4th set	0.0001	0.0011	0.0009	0.0078	0.07	0.92
5th set	0.0027	0.0027	0.004	0.008	0.03	0.96
6th set	0.0045	0.0003	0.0014	0.0016	0.01	0.99
7th set	0.0001	0.0021	0.004	0.0093	0.09	0.89
8th set	0.0003	0.0021	0.0015	0.013	0.03	0.95
9th set	0.0001	0.0036	0.0049	0.0079	0.36	0.62

Table V.11 Mass fraction of solvent in multicomponent solution extracted from PEBA beads. EtOH: ethanol; nPrOH: *n*-propanol; iBuOH: *i*-butanol; iAmOH: *i*-amyl alcohol; EtOAc: ethyl acetate; M: PEBA beads.

	iAmOH	EtOAc	iBuOH	nPrOH	EtOH	water	M
1st set	0.015	0.0042	0.0089	0.0044	0.017	0.08	0.87
2nd set	0.013	0.0037	0.0073	0.0037	0.019	0.08	0.87
3rd set	0.013	0.0031	0.0072	0.0034	0.020	0.08	0.87
4th set	0.011	0.0002	0.0032	0.0007	0.0003	0.06	0.93
5th set	0.0015	0.0022	0.0033	0.0029	0.0071	0.06	0.92
6th set	0.0010	0.0004	0.0008	0.0013	0.012	0.06	0.93
7th set	0.0097	0.0015	0.0038	0.0029	0.0004	0.06	0.92
8th set	0.0049	0.0016	0.0067	0.0015	0.0015	0.06	0.92
9th set	0.065	0.0026	0.0032	0.0030	0.0003	0.02	0.91

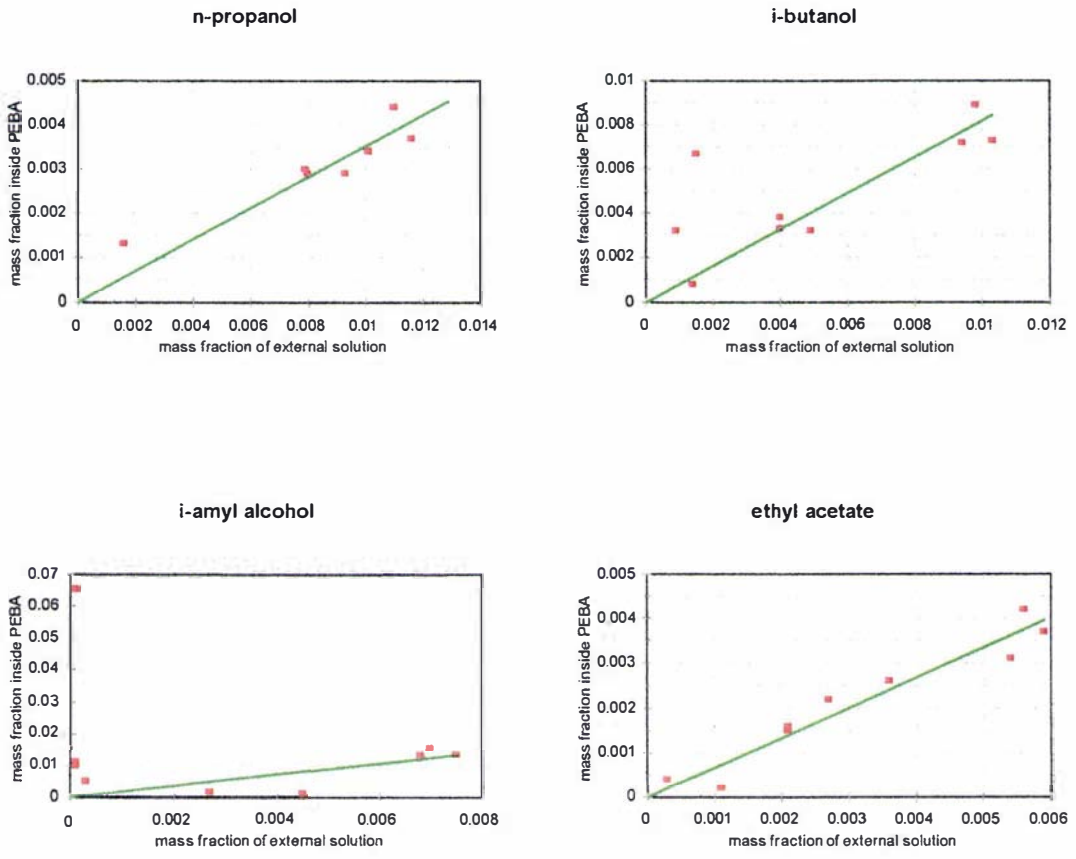

Figure V.3 Isotherm of fusels from a multicomponent mixture in equilibrium with PEBA beads at 50°C. ■ experimental data; – fitted line (Henry's Law).

Figure V.4 depicts both the experimentally determined concentration of solvents within the beads and those concentrations predicted with UNIQUAC. Although the predicted points generally appear close to the experimental points, the differences were consistently less than 5% only for the total amount of solvent inside the PEBA beads (as indicated in column M, Table V.12). For water, errors in prediction were within 15%, with the exception of set 9, and for organic materials they were as high as 381%, although commonly within 30 to 130%. Solution set nine gave results for water and total solvent which differed markedly from those for the other eight sets. No clear reasons for this were identified. This set contained a lower amount of water and a higher amount of organic

compounds than the other sets, but this alone does not explain the results as the binary parameters were estimated from data for similar solvent concentrations. Alternatively it could be that UNIQUAC is simply not suitable for the prediction of the sorption behaviour of such a complex system.

It was noticed during the experiments that small amounts of the PEBA beads (up to 5% depending on the solvent mixture) would dissolve in the solvent solution. This may account for some of the errors observed because the calculation of UNIQUAC solvent-membrane interaction parameters assumes that no membrane material exists in the external solution.

Table V.12 Difference between predicted values with UNIQUAC and experimental data for the sorption of aqueous, multicomponent solutions of alcohols and esters. EtOH: ethanol; nPrOH: *n*-propanol; iBuOH: *i*-butanol; iAmOH: *i*-amyl alcohol; EtOAc: ethyl acetate; M: PEBA beads.

	iAmOH	**EtOAc**	**iBuOH**	**nPrOH**	**EtOH**	**water**	**M**
1st set	-47%	76%	60%	23%	127%	-15%	-1.3%
2nd set	-84%	146%	101%	132%	130%	-13%	-2.5%
3rd set	-85%	100%	110%	97%	97%	-17%	-1.0%
4th set	89%	50%	84%	-43%	-67%	6%	-1.7%
5th set	-7%	18%	48%	-31%	-86%	-5%	0.9%
6th set	-60%	0%	-12%	-54%	-86%	0.7%	1.2%
7th set	179%	67%	292%	-34%	-175%	9%	-3.6%
8th set	59%	119%	246%	-293%	-153%	0.2%	-1.6%
9th set	31%	54%	381%	77%	133%	383%	-10.3%

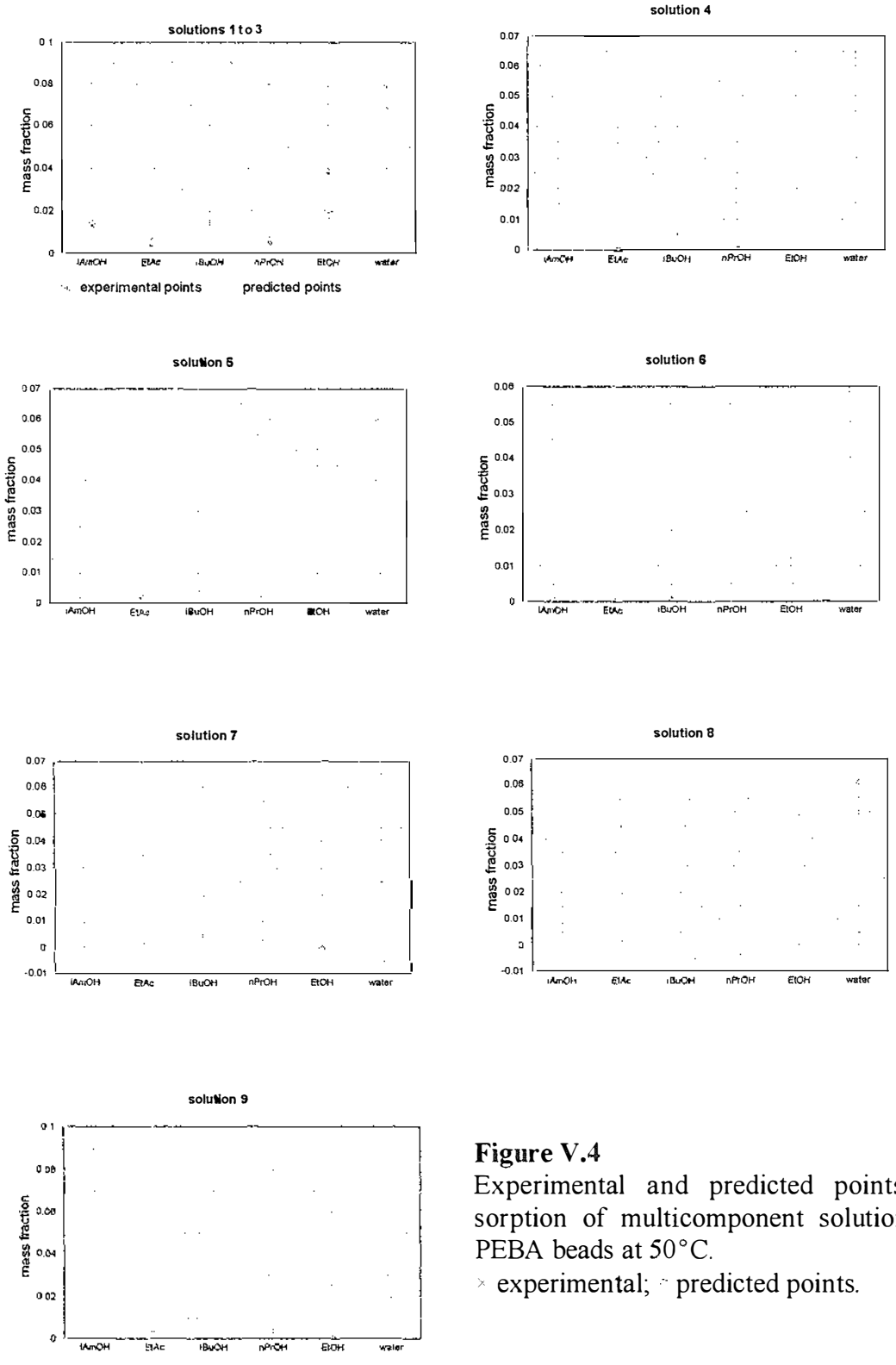

Figure V.4
Experimental and predicted points for sorption of multicomponent solutions in PEBA beads at 50°C.
× experimental; ◦ predicted points.

Using a larger number of solvent-solvent combinations to estimate the binary interaction parameters could improve the prediction of the sorption data. As the sorption isotherms in Figure V.5 show, the binary solutions were not fully representative of the behaviour of fusel oils and ethyl acetate in the multicomponent solution. Since in the binary solution both components had similar affinities for the membrane material, preferential sorption was not observed. In light of this data, it would probably have been better to pair each organic solvent with water, so that preferential sorption would occur. This option would increase the number of pairs under study from 3 to 5 and all flasks would need to contain at least 40 g of PEBA beads. At the time the experiment was performed, insufficient beads were available to pursue this option.

The plot of the *i*-amyl alcohol isotherm (Figure V.5) also shows a large scatter of the experimental data. It is possible that working with polymer slabs instead of beads would decrease the scatter because less time is required for handling the membrane material and the surface area to be blotted is reduced.

Overall, the extent to which the predictions can be improved is unclear. Most of the studies reported in the literature failed to state the error between predicted and experimental data (Ennecking *et al.*, 1993; 1996; Heintz & Stephan, 1994a) and, to date, little work has been performed with sorption of multicomponent solutions.

The first immediate issue to resolve is whether the membrane material, in bead or slab form, should be treated with vacuum, solvents, or temperature prior to commencing a test. It seems relevant to try to minimize the loss of membrane material to the external solution and to equalize the initial conditions. Furthermore, only by standardising experimental procedures, will it be possible to fairly compare results from different laboratories.

Development in this area is still slow since, to date, the mechanisms of sorption and solubility are little understood and a universal molecular theory has yet to be developed. The common approach is to either use one of the semi-empirical equations developed for vapour-liquid equilibrium (Ennecking *et al.*, 1993; 1996), or to search for parameters that

show relevance in the description of the phenomenon under study (Jonquières *et al.*, 1996). In general, the problems encountered with predicting sorption of solvents into polymers are similar to those of ternary liquid-liquid equilibrium (LLE) predictions using binary information for UNIQUAC. According to Sørensen & Arlt (1980), research to improve quantitative predictions is ongoing and to date no significant breakthrough has been reported. In this context, it is reasonable to expect that the predictions of sorption of multicomponent solutions in PEBA membranes using UNIQUAC can only be considered qualitatively at this stage.

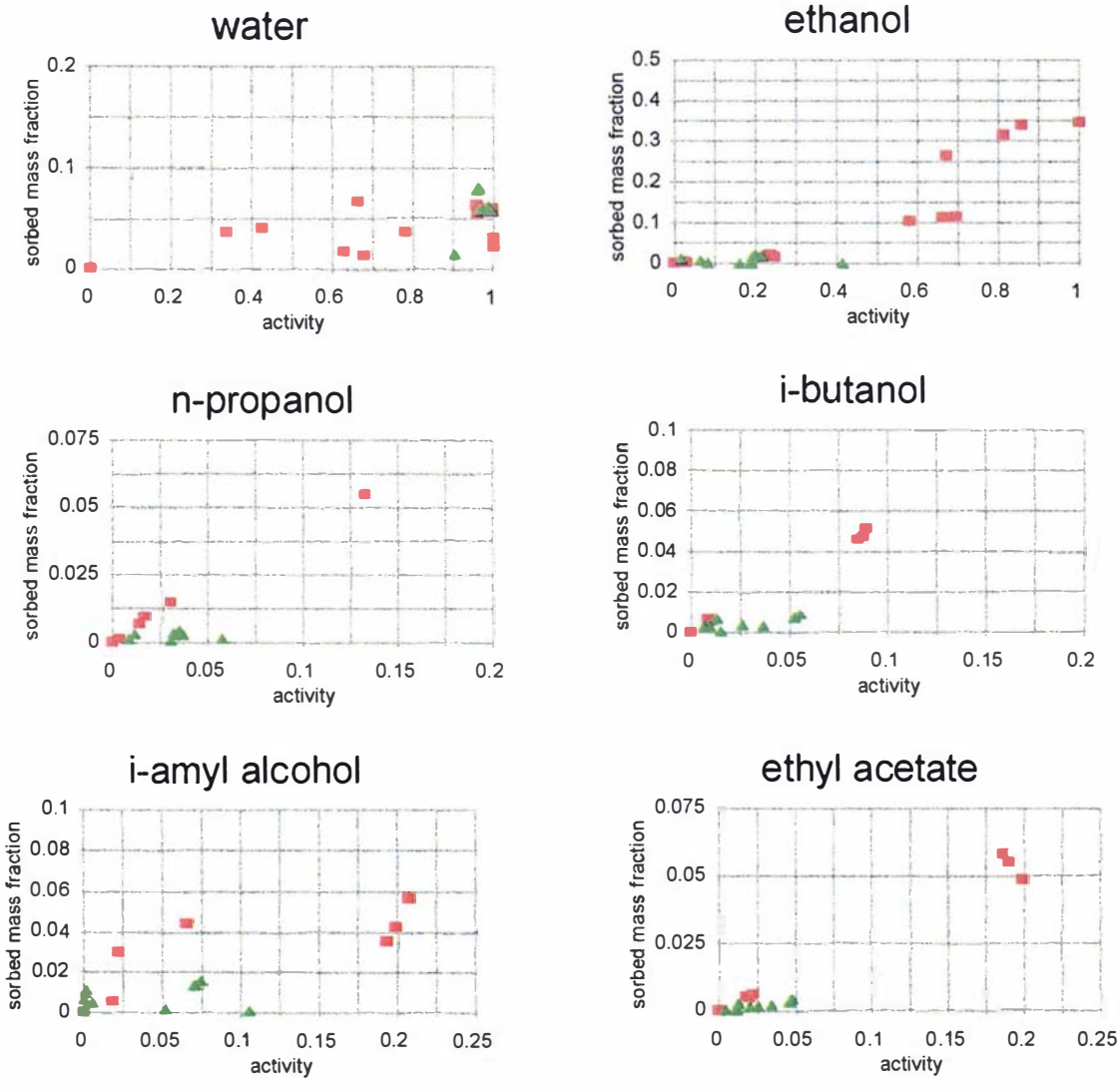

Figure V.5 Comparison between binary and multicomponent isotherms at 50°C. ■ binary solution; ▲ multicomponent solution.

V.3 PERVAPORATION EXPERIMENTS

V.3.1 MATERIALS AND METHODS

Pervaporation experiments were conducted according to the procedure described in Section IV.2.1.2. The feed tank was kept at constant temperature and pressure (approximately 70°C and 1 bar, respectively) in order to provide a temperature of 50°C at the pervaporation cell. PEBA membranes (GKSS, Geestacht, Germany) were used throughout the experiment. Table V.13 lists the feed compositions pervaporated.

Table V.13 Mass fraction of feed streams used for pervaporation trials. EtOH: ethanol; nPrOH: *n*-propanol; iBuOH: *i*-butanol; iAmOH: *i*-amyl alcohol; EtOAc: ethyl acetate.

Trial	EtOH	EtOAc	nPrOH	iBuOH	iAmOH	water
1	0.07	0.0018	0.0036	0.0027	0.0046	0.91
2	0.12	0.0041	0.0079	0.0050	0.0082	0.85
3	0.13	0.0057	0.011	0.0069	0.015	0.83
4	0.18	0.0061	0.010	0.0064	0.018	0.78
5	0.17	0.0056	0.0094	0.0058	0.017	0.80

V.3.2. RESULTS AND DISCUSSION

In Figure V.6 the enrichment factors measured for pervaporation through PEBA membranes are compared to the enrichment factors predicted for the multicomponent sorption into the beads. Given that the size of the molecules under study was broadly similar, ie. their molecular weights varied between 46 to 88 $kg.kmol^{-1}$ and their van der Waals volumes varied between 0.03 and 0.06 $m^3.kmol$, it was to be expected that pervaporation and sorption enrichment factors would follow similar patterns. The data in Figure V.6 confirmed this expectation. It is therefore worthwhile to investigate means of predicting sorption enrichment factors so that they can be used as a tool in the pre-screening of membranes.

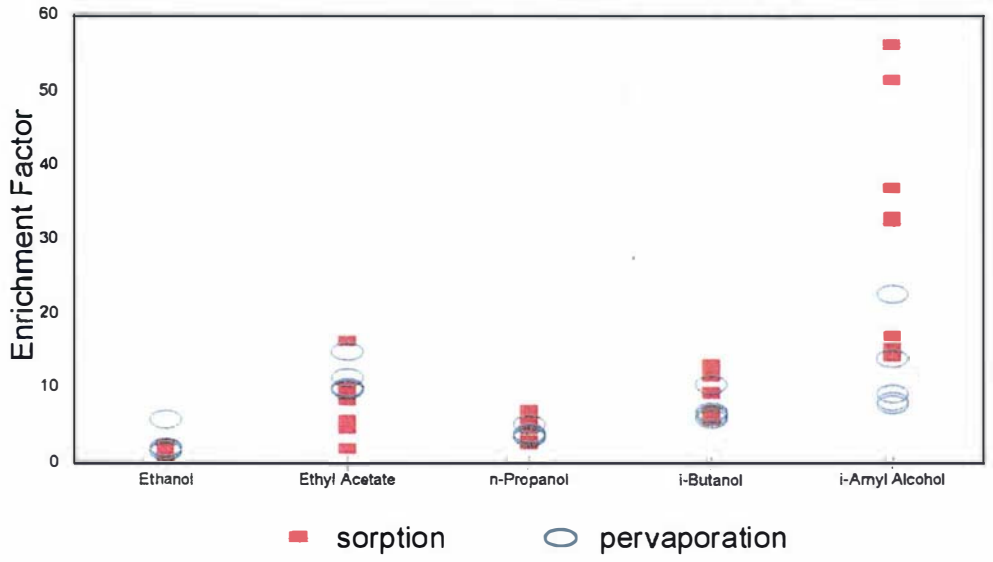

Figure V.6 Comparison of the ranges of experimental enrichment factors obtained for sorption into PEBA beads and pervaporation through PEBA membranes.

In Section V.2 the analysis of sorption experiments using pure components at varying temperatures indicated that the higher alcohols (C_3 to C_5) and ethyl acetate would have the highest enrichment factor. This analysis was confirmed in Figure V.6. For ethyl acetate, the activation energy was the predominant influence in pervaporation and multicomponent sorption, which explained why the overall enrichment factor of ethyl acetate in absolute values was as high as that for the fusels even though its affinity for the membrane as a pure component was similar to that of ethanol.

The ratio between the average enrichment factor of pervaporation and sorption of each organic species of the multicomponent solution are plotted in Figure V.7. Clearly, the ratio of actual (pervaporation) to predicted (sorption) enrichment factor decreased with increasing molecular weight, probably reflecting the reduction in diffusivity with increasing molecular size. A similar trend was evident in Figure V.6 although it was only for *i*-amyl alcohol that the enrichment factor for pervaporation was significantly greater compared to the sorption enrichment factor. A correction function to account for diffusion effects could thus be employed to improve the prediction of pervaporation performance in this case.

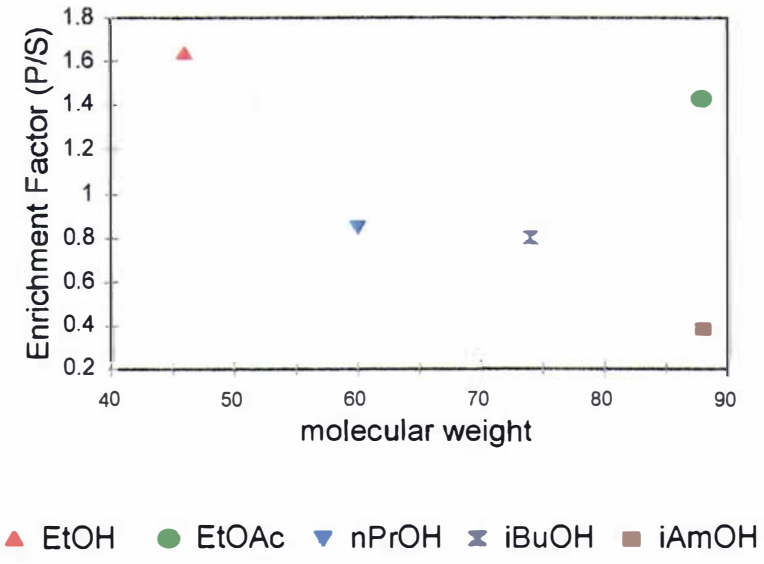

Figure V.7 Relationship between the ratio of the average enrichment factor for pervaporation and sorption, and the molecular weight of organic components. EtOH: ethanol; nPrOH: *n*-propanol; iBuOH: *i*-butanol; iAmOH: *i*-amyl alcohol; EtOAc: ethyl acetate.

For ethyl acetate there was little difference between the pervaporation enrichment factor and the sorption enrichment factor and molecular weight did not seeme to be a relevant factor (molecular weight of ethyl acetate and of *i*-amyl alcohol = 88). In this study, the components under investigation were restricted to alcohols and ethyl acetate. According to Wiley (1997), a plot of sorption versus molecular weight of all solvents studied so far, showed that alcohols behave differently from other substances, possibly because they have a tendency to aggregate by forming hydrogen bonds. In consequence, their behaviour was similar to components of higher molecular weight, ethanol in particular, showed a tendency to forming dimers. This theory is partially confirmed in Figure V.7, where it can be observed that although the molecular weight of ethanol is approximately half of the molecular weight of ethyl acetate, both show similar behaviour in relation to the ratio of pervaporation over sorption enrichment factor in the multicomponent mixture. Therefore, in order to develop a general equation for the prediction of the enrichment factor of pervaporation from sorption, a factor to account for the tendency of the solvent to associate by hydrogen or other bonding should be included.

From the above discussion it becomes clear that although the separation ability of a membrane might be determined by sorption, the accuracy of predicting the behaviour of pervaporation using sorption data might decrease greatly when there is a broad distribution of the molecular weight of the components in the feed and when the solvents have a tendency to aggregate via hydrogen bonds or other interactions. However, these limitations do not reduce the value of using sorption as a pre-screening methodology, specially if simple, reliable equations that predict the behaviour of sorption starting from basic properties of the feed solution and membrane material become available.

The study of sorption is also important in understanding the mechanisms of pervaporation. It is often impossible to obtain direct information on the behaviour of diffusion and there is no universal theory that allows the calculation of diffusivity of solvents through dense polymers. The shortcomings of the currently available correlations for the prediction of the equilibrium
between multicomponent phases are well known` amongst physical-chemists. In general, the equations are inaccurate or fail to differentiate between isomers. Structural information concerning branching, atom connections, shape and size of the molecule are being quantified and used in correlations that promise to be more accurate than the current ones in the prediction of equilibrium data (Kier & Hall, 1976). If a reliable equation to predict sorption becomes available, it would be possible to separate the contribution of sorption from the overall pervaporation process, and then to isolate the contribution of diffusion. With this information it becomes feasible to evaluate which parameters influence diffusion.

V.4 Conclusions

In pervaporation, the separation of the liquid mixture is largely considered to be primarily determined by preferential sorption (Spitzen *et al.*, 1987). In this work, for all organic species studied except *i*-amyl alcohol, the sorption enrichment factor had a similar value to the pervaporation enrichment factor. For *i*-amyl alcohol the enrichment factor for

pervaporation was likely to be overestimated when sorption alone was considered. The behaviour of *i*-amyl alcohol highlighted one of the limitations of using sorption data to predict pervaporation enrichment factor: depending on the distribution of the molecular sizes of the feed mixture, it is likely that the influence of diffusion in the separation ability of the membrane cannot be ignored. Also, when comparing the behaviour of ethanol and ethyl acetate, it becomes clear that a general equation to predict the enrichment factor of sorption will need to account for interactions between molecules in the mixture.

In this study it was also found that experiments with pure components at varying temperatures give valuable information on the behaviour of multicomponent solutions during pervaporation, through analysing the combined effects of the variation of the activation energy and the affinity of the membrane material for the pure component.

Although Henry's law gives a satisfactory description of the sorption of fusels into PEBA beads for the concentration range studied, it cannot be use for predictions. It was thus necessary to assess the ability of semi-empirical equations (UNIQUAC), traditionally used for vapour-liquid equilibrium, to predict the sorption of solvents into dense membranes as there is not yet a theory that fully explains this phenomenon. Furthermore, it had already been shown that the Flory-Huggins equation was considered inadequate for the system under study (Favre *et al.*, 1993).

Use of the UNIQUAC equation was not particularly successful in the prediction of sorption. Although the general sorption trends were predicted, the absolute values were not particularly accurate. Before suggesting modifications to the equations available, it is necessary to evaluate whether improvement in the prediction could be achieved by introducing a pre-treatment step to equalize the membrane material, by using membrane slabs instead of beads to decrease the time spent in blotting the material, and by improving the match between the sorption behaviour of the ternary systems (membrane - solvent 1 - solvent 2) used for generation of the UNIQUAC interaction parameters for each solvent and the membrane material, and the sorption behaviour of the multicomponent solution under study.

As already mentioned, sorption largely determines the separation ability of pervaporation of organic components of broadly similar molecular sizes through hydrophobic membranes. However, the importance of developing a reliable equation for the prediction of sorption is not limited to its use as a pre-screening tool for the selection of membranes. Given the difficulties in separating experimentally the effects of sorption and diffusion during pervaporation, the study of the effect of diffusion on pervaporation depends largely on how well sorption can be predicted.

Chapter VI

DISCUSSION: FUNDAMENTALS

Assuming that the solution-diffusion mechanism explains solvent transport during pervaporation, it will only be possible to predict the separation ability of pervaporation from elementary physico-chemical data once all the parameters that influence transport have been identified and systematically evaluated. In the mean time, relationships that link molecular structure to the physico-chemical properties of polymers and solvents would be most useful in providing information that would also allow the development of polymers tailored for specific separations.

To date, most research groups have focussed on studying properties of the separation obtained with pervaporation using feed solutions of industrial interest. Although this approach has certainly given pervaporation an early and somewhat fast entry into a few industrial applications, its shortcomings include:

- The development of new applications for pervaporation lacks comprehensive guidelines, therefore most of the work has to be done from scratch.

- In general the applicability and limitations of pervaporation are little known, and many process designers may be reluctant to consider pervaporation as an option to traditional separation technologies.

- The development of new membranes is largely left to trial-and-error, and, as mentioned in the Literature Reviews (Chapters II and VII), the growth in the use of pervaporation depends to a great extent on the properties of the membranes available.

In summary, the lack of a systematic study of pervaporation could slow the development and use of pervaporation in the long run.

So far, there is general agreement that the temperature influence on pervaporation flux can be described by an Arrhenius-like relationship. Consequently, it is often advantageous to work at the highest possible temperature that the membrane material and the process will allow whenever it is important to either increase flux or reduce membrane area. However, the influence of temperature on the selectivity of the membrane towards individual species has yet to be investigated to the same extent.

Attempts to describe the solution-diffusion model from physical-chemical and structural properties of the system are often hindered by:

- the lack of comprehensive theories of solution and diffusion of solvents into dense polymers;

- the incomplete identification of all the relevant parameters that influence transport through the membrane.

The lack of comprehensive theories of solution and diffusion of solvents into dense polymers results in the widespread use of empirical or semi-empirical equations to describe the behaviour of the system under study. In this case, the equations developed can only be applied with confidence to experimental conditions similar to those for which they were developed.

As long as the influence of all relevant parameters is not identified and systematically studied, it will not be possible to develop the universal relationships required to improve the understanding of pervaporation. In this study, a few parameters were identified, that advance or confirm the observations of previous studies. In particular, these pervaporation experiments have shown that there is a linear relationship between the logarithm of the activity of each component of the feed mixture studied and their partial fluxes. However, there is still limited understanding of flow coupling and what physical-chemical properties of the feed mixture could be used to indicate its presence and order or magnitude.

The pervaporation experiments reported in this study have also shown that the enrichment factor of alcohols could be related to their activity coefficient and van der Waals volume and that overall pervaporation enrichment factors could be predicted by sorption enrichment factors. However, a few questions are still unanswered. Firstly, a systematic approach is needed to better evaluate in greater detail the influence of the molecular size of the solvent on the separation ability of the membrane. In this same line, it is relevant to define what is the cut-off molecular size for the polymers available and how it can be best established (large solvents may not be transported through pervaporation membranes if their molecular size is greater than the polymer free volume). In view of the difference in behaviour of an ester and an alcohol of the same molecular weight, it becomes imperative to investigate how the interaction among solvents inside the polymer or between membrane and solvent influences transport. This should include the influence of polymer type, presence of zeolites and other particles, and manufacture technique.

A similar approach needs to be applied to sorption studies. There is to date no universally accepted theory, testing procedure, or material pre-conditioning guideline. Furthermore, since many research groups have used either laboratory manufactured membrane slabs or membrane raw material in the form of beads for testing the behaviour of sorption, it is unknown how well these results relate to the equivalent commercial product. The study of sorption is also further limited because most of the information on the composition and structure of the polymers used are of proprietary nature. There is however much to be gained from manufactures co-operating in basic studies, which could benefit all in providing information to assist in the design and optimization of improved systems and products.

Part Two

APPLICATIONS

Chapter VII

LITERATURE REVIEW: APPLICATIONS

VII.1 ETHANOL PRODUCTION

During the past fifty years, ethanol acquired economic value as a fuel, a solvent, a substrate in chemical synthesis, and in the fortification of neutral spirits (gin and vodka). In general, the production of fermentation (or non-synthetic) ethanol consists of two steps: ethanolic fermentation of a sugar-rich solution, followed by concentration and purification of the ethanol by distillation. The usual substrates are sugar-cane syrup, starch from various grains (corn, rice, oats, rye, etc), and lactose from whey.

In New Zealand, all industrial and potable ethanol required for the domestic market is produced from deproteinated whey by fermentation. The technology was established in 1980 when the first distillery was commissioned by the New Zealand Co-operative Dairy Co. Ltd. at Reporoa (Mawson, 1987) and as of 1994 there were three major distilleries (Table VII.1) producing over 17 Ml of absolute ethanol per annum (Mawson, 1994).

Table VII.1 Production sites of whey ethanol in New Zealand (Mawson, 1987).

Distillery	**Reporoa**	**Tirau**	**Edgecumbe**
Date commissioned	1980	1981	1982
Substrates processed	Deproteinated lactic whey	Deproteinated lactic whey	Sulfuric acid whey permeate Maize
Grades of alcohol produced	Industrial 95% (v/v) 99.5+% (v/v) Potable 96.5% (v/v)	Industrial 95% (v/v)	Industrial 99.5+% (v/v) Potable 96.5% (v/v)

Whey, the fluid obtained by separating coagulum from milk, is a dilute, aqueous solution of lactose (approx. 5% w/w), proteins (approx. 0.8% w/w), and ash (approx. 1% w/w) (Reesen, 1978; Short, 1978). Until recently whey was treated as a waste product because of its low quantity of total solids, but tougher waste disposal legislation forced the industry to seek alternative uses for whey (Zadow, 1984). Whey proteins make an attractive product for the food industry, particularly in the form of whey protein concentrate (WPC), because of their high nutritional and functional value. The deproteinized whey which results from the production of WPC contains mainly lactose, which can be purified by crystallisation and used in the food industry for flavour enhancement, protein stabilization, controlled browning, or rearranged into lactulose (Short, 1978). From demineralized whey, the lactose can be fermented into methane, lactic acid, or ethanol (Short, 1978).

The product from whey fermentation is an approximately 2.5% (v/v), dilute mixture of ethanol and fermentation by-products. A mixture of higher alcohols and esters, known as fusel oils, constitutes the main by-product and is present in a concentration of less than one percent of total ethanol produced. The composition and concentration of the fusel oils vary depending on the substrate, the microorganisms used, and the fermentation conditions. Drucker (1981) presented a summary of the typical compositions of fusel oils for the most common fermentation conditions. Fusel oils impart an aroma which is generally desirable in the beverage industry (wine, brandy, whisky), but not in the production of ethanol for industrial purposes or for neutral spirits production (gin, vodka).

Distillation, the next step in the production of alcohol, must remove most of these by-products and raise the ethanol content to the required specification. In general, the purification and concentration of ethanol to very near its azeotropic point can be achieved with three columns (Figure VII.1) and the energy for distillation is provided by direct steam injection. In the first column the beer is concentrated to 90% (v/v) ethanol and it is possible to remove from this column a side stream rich in fusel oils. In the second column, the ethanol-rich stream is refined by extractive distillation: the ethanol-rich feed is diluted to allow for the separation of the fusel oils, which concentrate at the top of the column and are removed from the reflux drum. The bottom product of the extractive distillation

column, a dilute (8-10 % v/v), purified ethanol stream, is brought to the final concentration of 96.5% (v/v) ethanol in the third column.

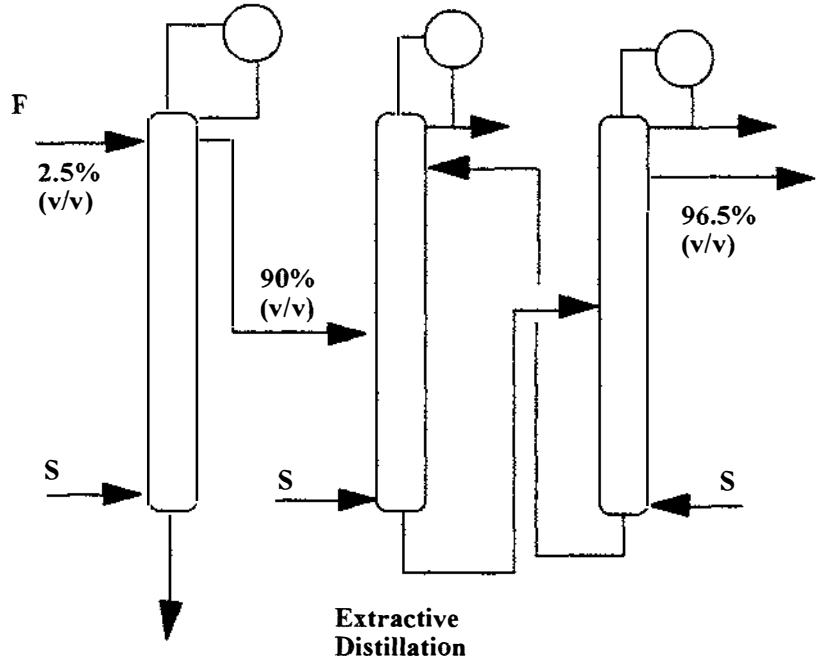

Figure VII.1 Schematic drawing of an ethanol purification plant.
F: feed stream; S: steam stream.

Due to its low lactose content, the fermentation of whey results in a beer containing 2.5% (v/v) ethanol. According to Maiorella *et al.* (1984), distillation costs increase significantly if the concentration of the fermentation broth fed to the column is below 6% but no further savings are realized in increasing the concentration over 9%. In order to increase the ethanol concentration of the fermentation broth, pre-concentration of whey by reverse-osmosis or evaporation is an established procedure (Mawson, 1987). Another option under study is continuous fermentation with ethanol removal by pervaporation (Mulder *et al.*, 1983; Younaian *et al.*, 1990; Shabtai & Mandel, 1993). Improvements in this process are still required to solve problems related to the concentration of salts in the fermentation broth (Shabtai & Mandel, 1993), fouling of the membrane (Younian *et al.*, 1990; Shabtai & Mandel, 1993) and increased consumption of electricity (Néel, 1990). Mulder *et al.* (1983) have suggested that an ultrafiltration unit installed before pervaporation could separate the solids from the fermentation broth and thus reduce the possibility of fouling

of the pervaporation membrane. The yeast cells would then be recycled to the fermentation vessel.

It has been estimated that steam consumption constitutes a quarter of the total production cost of whey ethanol (Mawson, 1987) and that, worldwide, distillation accounts for 15% of the total industrial energy usage (Fell, 1997). In general, traditional process changes aimed at reducing the energy input during distillation include tray retrofitting (Mix *et al.*, 1978), efficient use of insulation, introduction of heat recovery schemes and vapour recompression, and multi-effect pressure distillation (Mawson, 1987). It has also been suggested that energy savings and process simplification could be achieved by direct removal of ethanol from the fermentation broth with either selective membranes, extractive fermentation or flash fermentation, liquid extraction, adsorption or absorption with either water or ethanol selective materials, or carrier gas distillation (Douglas & Feinberg, 1983; Maiorella *et al.*, 1984).

In the removal of fusel oils, the wine industry uses a spinning cone column (SCC) that is supposed to have a higher efficiency in the mass transfer between the vapour and liquid phases than tray columns (Harders *et al.*, 1995). Whilst these wine flavours are similar to the composition of by-products from ethanolic fermentation of whey, detailed data on the separation ability of the SCC is not available in the public domain.

Larsson & Zacchi (1996) compared the concentration and purification step for the production of 94% (w/w) ethanol from a dilute glucose solution of approximately 5% (w/w) using distillation with heat integration, distillation with an absorption heat transformer, distillation with mechanical vapour recompression, phase separation with potassium carbonate, and extraction of ethanol from the fermentation broth with Aldol 85. It was concluded that distillation with heat integration was the most economical option.

Douglas & Feinberg (1983) reported on a series of Solar Energy Research Institute (SERI) sponsored developments (Table VII.2) for ethanol separation using non-distillation techniques. Their conclusions were based on the energy requirements for the production

of dehydrated ethanol (> 99.5% w/w) from a feed containing 10 to 15 % (w/w) ethanol. Solvent extraction with 2-ethyl hexanol (EHOH) and ISOPAR-L (a branched paraffinic refinery cut) were judged almost energy- and cost- competitive with the other systems under consideration, while grain adsorption systems were simple, inexpensive and economical over a wide range of plant sizes. Membrane systems were not adequate to concentrate 50% (w/w) ethanol to above 97% (w/w) ethanol. Although the SERI results on pilot plant and industrial size experiments are not available, the membrane(pervaporation)-distillation and molecular sieve-distillation hybrid systems that appeared to date have been adopted for the commercial production of anhydrous ethanol.

Table VII.2 Summary of energy costs for non-distillation systems in ethanol production (Douglas & Feinberg, 1983).

System	Concentration (w/w)	Energy Requirement (Btu/gal)	Note
Conventional distillation	10 - 99.9	27,000	
Vapour reuse distillation	10 - 99.9	18,000	
Diffusion/carrier gas distillation	10 - 85	9,900	did not achieve a concentration over 85% (w/w) ethanol during experiments
Solvent extraction	26 - 98 10 - 26	12,600 5,000	requires distillation to bring initial concentration to 26% (w/w) ethanol
Adsorption in grain	91 - 99.9 10 - 91	2 to 3,000 11,200	requires distillation to bring initial concentration to 91% (w/w) ethanol
Membrane dehydration	8 - 99.5	13,200	requires distillation to bring initial concentration to 91% (w/w) ethanol

K-Engineering (1993) reported on a molecular sieve-distillation hybrid process, where potassium aluminosilicate beads adsorbed water from a vapour stream containing a minimum of 95% v/v of ethanol. Although the process required an increase in the operation pressure from ambient to 2-4 bar (g.) in order to overcome the pressure drop and used vacuum to regenerate the molecular sieves, it used only a third of the energy necessary to dehydrate ethanol by extractive distillation with benzene. It is not clear

whether these figures included the energy to vaporize the feed. However, adsorbents that perform well with an ethanol liquid feed are also available (Teo & Ruthven, 1986).

According to Ballweg *et al.* (1982), membrane-distillation hybrid schemes compare favourably with internal heat recovery systems, multi-pressure columns and vapour recompression systems. The latter have the disadvantage of incurring higher investment and maintenance costs than membrane-distillation hybrid schemes, and of increasing the complexity of plant operation.

Until recently, production of ethanol at 99.5+% (v/v) by distillation required either addition and subsequent separation of a solvent or distillation under vacuum. Pervaporation was first used commercially as an option for dehydrating ethanol in 1982 when a plant was installed in Brazil by GFT (Ballweg *et al.*, 1982). In this process, pervaporation followed a distillation step to dehydrate ethanol past its azeotropic point and to concentrate the ethanol to its required (99.5+% v/v) specification.

Although pervaporation is characterized by low permeate fluxes, low condensation temperature, and requires the integration of heat exchangers and energy for reheating, dehydration beyond the azeotropic point has proved a niche market for pervaporation. In such azeotrope-breaking operations, a combination of pervaporation and distillation is often superior to either pervaporation or distillation alone (Rautenbach & Vier, 1995). Pearce (1990) suggested that hybrid process could be used for debottlenecking distillation and for improving the economics of producing anhydrous ethanol. It was shown that the production costs of 99% ethanol could be reduced by 30%, with a reduction of 60% in energy consumption, and the production costs of 99.9% ethanol could be reduced by 20% (a detailed discussion on the application of pervaporation in dehydration, costs, and energy usage follows in Section VII.2.2.1). As a consequence of the commercial success of this new process, by September 1994 up to 100 plants were installed in commercial companies, varying from pilot plants with 1 to 4 m^2 membranes to units of 2,000 m^2 (Shanley *et al.*, 1994).

VII.2 PERVAPORATION

VII.2.1 MEMBRANE MATERIAL

Although pervaporation has been known since 1917 and was extensively studied by Binning, Lee and co-workers in the early 1950s, it was the development of composite membranes in the 1980s that made it possible to commercialize the first pervaporation system (Wijmans *et al.*, 1994). Composite membranes consist of a porous layer with a thin, dense, coated layer on the top. Each layer is made of a different material. The porous support provides mechanical support and allows unrestricted flow of the vapour phase, while the top layer provides selectivity. The composite membranes have the same high fluxes characteristic of asymmetric membranes but are less fragile. With the development of plasma polymerization techniques, ultra thin, defect-free membranes can be prepared, further improving the performance of pervaporation membranes.

In general, the choice of materials for pervaporation is restricted by the separation to be performed. For dehydration, hydrophilic polymers, such as glassy polymers, have been used successfully. The type of functional group involved in the manufacture of the polymer and the degree of crystallinity dictates the physico-chemical properties of the membrane. Crystallinity has a great influence in pervaporation because solution and diffusion occur only in the amorphous phase. Crystallites prevent a high degree of swelling, which can permanently damage some membranes. Although polymers that have crystallites within their structure show lower permeability compared to the amorphous polymer, some have found wide spread use due to their higher selectivity (Koops & Smolders, 1991).Examples of polymers that present some degree of crystallinity are poly(vinyl alcohol) (PVA), nylon, poly(vinylidene fluoride) (PVF), poly(phenylene oxide) (PPO) and polyethylene (PE). Examples of amorphous polymers are cellulose acetate (CA), polysulfone (PF), polypropylene (PP), polystyrene (PS) and poly(vinyl chloride) (PVC). Hydrophilic polymers contain functional groups which are strong acceptors of proton-donating species such as water (Néel, 1991), furthermore, the high polarity of water increases the differentiation between organic and water molecules, thus improving the selectivity of the membranes.

Removal of organic fluids from water requires polymers that show hydrophobic characteristics. Elastomers have shown good selectivity towards organic fluids and high permeation fluxes. The absence of polar groups inside the flexible chains of elastomers enable them to absorb organic fluids in preference to water. Examples of elastomers used in pervaporation are poly(butadiene-acrilonitrile), and poly(dimethyl siloxane) (PDMS).

For organic-organic separations the choice of polymer to be used is not clear yet. So far the difference in polarity between the organic components of the fluid and the characteristics of the fluid to be separated dictate the choice between hydrophobic and hydrophilic membranes (Koops & Smolders, 1991).

An extensive review of polymers used for pervaporation can be found in Néel (1991). Table VII.3 summarizes the separations under study to date and the polymers tested.

VII.2.2 APPLICATIONS

When compared to traditional separation techniques, membrane processes have in general the advantages of using less energy, operating under minimal temperature changes, without the need of additives, operating continuously, not reacting with the stream to be separated and, because of their modular aspect, they are easy to install and to scale up (Cartwright, 1994). The mild operating conditions favour the application of pervaporation in the food and biotechnology industries where maintenance of product functionality and quality are critical. Pervaporation, in spite of all these advantages, had to wait until suitable membranes were developed to become commercially available. The current and potential applications of pervaporation can be classified under three major categories:

- ❖ solvent dehydration, which uses hydrophilic membranes;
- ❖ solvent recovery from aqueous streams, which uses hydrophobic membranes;
- ❖ organic-organic separations.

Table VII.3 Polymers for pervaporation (Zhang & Drioli, 1995).

Polymer	Application
Cellulose and derivatives	Extraction of water from aqueous solution of ethanol, separation of benzene/cyclohexane mixtures.
Chitosan	Extraction of water from an aqueous solution of ethanol.
Collagen	Extraction of water from an aqueous solution of alcohols and acetone.
Cuprophane	Extraction of water from an aqueous solution of ethanol.
Ion-exchange resins	Extraction of water from an aqueous solution of ethanol, pyridine.
LDPE	Separation of C_8 isomers.
NBR	Separation of benzene/n-heptane.
Nylon-4	Extraction of water from an aqueous solution of ethanol.
PA	Extraction of water from an aqueous solution of ethanol, acetic acid.
PA-co-PE	Separation of dichloroethane/trichloroethylene mixtures.
PAA	Extraction of water from an aqueous solution of ethanol, acetic acid.
PAN	Extraction of water from an aqueous solution of ethanol.
PAN-co-AA	Extraction of water from an aqueous solution of ethanol.
PB	Extraction of *n*-propanol, ethanol from an aqueous solution.
PC	Extraction of water from an aqueous solution of ethanol, acetic acid.
PDMS filled with silicate, molecular sieves, etc.	Extraction of alcohols from an aqueous solution, separation of butanol from butanol/oleyl alcohol mixture.
PEBA	Extraction of alcohols and phenol from and aqueous solution, recovery of natural aromas.
PI	Extraction of water from an aqueous solution of ethanol, acetic acid; separation of benzene/cyclohexane and acetone/cyclohexane mixtures.
Plasma polymerized fluorine-containing polymers	Extraction of ethanol from an aqueous solution.
Plasma polymerized PMA	Separation of organic/organic mixtures.
Polyion complexes	Extraction of water from an aqueous solution of ethanol.
Polysulfones	Extraction of water from an aqueous solution of ethanol, acetic acid.
POUA	Separation of benzene/*n*-hexane mixtures.
PP	Separation of xylene isomers.
PPO	Extraction of water from an aqueous solution of alcohols, separation of benzene/cyclohexane mixtures.
PTMS/PDMS composite	Extraction of ethanol from an aqueous solution.
PTMSP and derivatives	Extraction of ethanol from an aqueous solution.
PUR	Extraction of ethanol from an aqueous solution.
PVA	Extraction of water from an aqueous solution of alcohols, acetic acid, ethers, pyridine, etc.
PVC	Extraction of water from an aqueous solution of ethanol.
Silicone rubber (PDMS, etc)	Extraction of alcohols, ketones, hydrocarbons, halogenated hydrocarbons, amines, acetic acid, natural aromas, etc., from an aqueous solution.

AA: acrylic acid; LDPE: low density polyethylene; NBR: poly(butadiene-acrylonitrile); PA: polyamide; PAA: poly(acrylic acid); PAN: polyacrylonitrile; PB: polybutadiene; PC: polycarbonate; PDMS: polydimethylsiloxane; PE: polyester; PEBA polyetheramide-block-polymer; PI: polyimide; PMA: poly(methylacrilate); POUA: poly(oxiethylene urethane acrylate); PP: (polypropylene); PPO: poly(phenylene oxide); PTMSP: poly(trimethylsilylpropyne); PUR: polyurethane; PVA: poly(vinylalcohol); PVC: poly(vinylchloride).

Table VII.4 summarizes the applications of pervaporation and indicates the state-of-the-art for each. These are discussed in more detail in the following Section.

Table VII.4 Applications of pervaporation processes (modified from Zhang & Drioli, 1995).

Applications	State-of-the-art
Dehydration, azeotropes, close boiling point mixtures, pervaporation aided distillation:	
- Alcohols: MeOH, EtOH, PrOH, BuOH	Industrially realized
- Ketones: acetone, methyl ethyl ketone	Industrially realized
- Acids: acetic acid, chlorinated acetic acid, sulfuric acid, sulphonic acid, hydrochloric acid	Pilot test
- Amines: pyridine, cyclohexamine	Pilot test
Extraction of organic from aqueous solutions:	
- removal of toxic components: hydrocarbons, halogenated hydrocarbons, amines, phenols	Partially industrially realized
- recovery of natural aromas in agro-food industry	Pilot test
- recovery of trace components: perfumery	Pilot test
Organic mixtures:	
- Aliphatic/aromatic: benzene/hexane, benzene/ethanol, benzene/cyclohexane	Laboratory tested
- Isomers: butanols, C_8 isomers	Laboratory tested
- Halogenated HCs: dichloroethane/trichloroethylene	Laboratory tested
- Others: alcohol/esters, chlorohydrocarbons	Laboratory tested
Pervaporation aided chemical biochemical reactors:	
- esterification: ethyl acetate, butyl acetate	Laboratory tested, pilot tested
- continuous membrane fermenter separator: EtOH, MeOH, perfumery, and alcoholic beverage	Laboratory tested
- processing of vegetable/animal fats	Laboratory tested, pilot tested
- fine chemistry: synthesis of dimethylurea	Laboratory tested

VII.2.2.1 APPLICATIONS FOR HYDROPHILIC MEMBRANES

Solvent dehydration is the major application of pervaporation. From 1982 to 1993 GFT/Carbone Lorraine commissioned over 70 pervaporation plants for the dehydration of organic solvents (ethanol, *i*-propanol, ethyl acetate) and a payback time of only 12 months was reported for a typical plant (Le Carbone, 1993; Zhang & Drioli, 1995). The largest capacity plant installed in Bentheniville, France, processes 150,000 $l.h^{-1}$ of 99.95% (v/v)

ethanol through 2,400 m^2 of membrane. While GFT/Carbone Lorraine are the market leaders in this field, other companies that develop or install membrane modules include: Mitsui, Japan; Lurgi, Germany; Membrane Technology Research Inc., USA; British Petroleum, UK; Texaco, USA; and Air Products, USA (Baker, 1991).

Typical commercial processes operate with a feed temperature between 50 and 100°C. A permeate pressure lower than 20 mbar is achieved by using condensation temperatures from 30°C to -20°C, depending on the application. The PVA/PAN composite membrane developed by GFT is the only membrane to be employed commercially. The membrane selectivity (α) for concentrating ethanol from 90 to 99.9% lies between 50 and 2,000 for permeate fluxes below 4 $kg.m^{-2}.h^{-1}$ (Fleming & Slater, 1992c).

When compared to distillation, pervaporation is mainly suitable for concentrating ethanol feeds of 85% or higher (Matsuura, 1994). The energy requirements of distillation remain constant for feeds between 20 and 70% (Leeper, 1986). This gives distillation an advantage in economy of scale, and, therefore, the association of pervaporation with distillation for the production of anhydrous ethanol is considered the best option (Section VII.1). Matsuura (1994) calculated that a conventional distillation process consumes 4 to 6 kg $steam.kg^{-1}$ of ethanol produced. When associated with pervaporation, the steam consumption was reduced to 2.7 kg $steam.kg^{-1}$ of ethanol produced. Table VII.5 shows a comparison of the costs to produce 99.5% ethanol by pervaporation, distillation and adsorption with molecular sieves.

Table VII.5 Separation options for small scale ethanol/water system (Basis: 1,000 $l.day^{-1}$, 99.5% ethanol) (Baker, 1991).

	Pervaporation	**Distillation**	**Adsorption**
System cost	$ 75,000	$ 140,000	$ 90,000
Pumps	3 kW	2 kW	2 kW
Steam	45 $kg.h^{-1}$ @ 1.8 bar	70 $kg.h^{-1}$ @ 7.3 bar	90 $kg.h^{-1}$ @ 7.3 bar, 220°C
Entrainer		3 $l.day^{-1}$	

In another dehydration application, an experimental plant installed by Lurgi GmbH dehydrates ethanol from a fermentation broth as a pre-distillation step (Néel, 1991). This pervaporation, pre-concentration step has the potential to generate a distillation feed with a higher ethanol content than by reverse osmosis. Reverse osmosis is limited by the osmotic pressure and will only concentrate the ethanol water mixture to 13% ethanol (Leeper, 1986; Matsuura, 1994). By maximazing the ethanol feed-concentration for distillation, the new process scheme could potentially use less energy than distillation alone.

Hydrophilic membranes are also applied to enhance chemical reactions by shifting the equilibrium of the reaction through the removal of excess water. In 1993 the first pervaporation plant linked to a reactor was installed by Le Carbone Lorraine (Le Carbone, 1993) for an esterification process. The continuous removal of water from the reaction vessel allowed the full conversion of reactants.

In Brazil, *i*-amyl alcohols of 96 and 99% concentration are recovered from a side stream of the ethanol production plant by distillation. In the current process, the formation of azeotropes reduces the amount of *i*-amyl alcohol that can be recovered and hinders the fractionation of the side stream (Chamberlain *et al.*, 1994; 1995). According to Chamberlain *et al.* (1994), a preliminary extraction of water would allow multicomponent fractionation of the side stream. Chamberlain *et al.* (1995) employed pervaporation with PVA composite membrane to reduce the water content from 14% to 8%. Simulations of the distillation process showed that this reduction increased the recovery of *i*-amyl alcohol to 90% in the production of 99% grade product and allowed the return of the ethanol-rich top stream to the ethanol production plant.

While dehydration by pervaporation is an established separation technique, a study commissioned by the US Department of Energy showed that its competitiveness could be further increased by reducing the costs of modules and developing higher flux membranes (Baker, 1991).

VII.2.2.2 APPLICATIONS FOR ORGANOPHILIC MEMBRANES

The application of pervaporation for solvent recovery is linked to the continuing development of hydrophobic membranes. Few applications have been introduced to the industry and intensive research is continuing into the development of new membranes, understanding transport mechanism, and investigating new applications. Extensive reviews of the research carried out with hydrophobic membranes in the past twenty years were published by Leeper (1986), Böddeker & Bengtson (1991), Néel (1991), and Karlsson (1996).

The membranes commercially available were developed by Deutsche Carbone/GFT (PDMS membranes) and GKSS (PEBA membranes). A number of investigations of alternative organophilic membranes and comparisons with the performance of PDMS membranes have been carried out (Blume *et al.*, 1990; Böddeker *et al.*, 1990; Feng & Huang, 1992; Hickey *et al.*, 1992; Will & Lichtenthaler, 1992; Yoshikawa *et al.*, 1994) and new membranes are continually being developed. Alternative membranes from polymers, such as PEBA, PE, PB, PTMSP, PPO, polyurethaneimide, polyurethaneamide, etc., have improved the selectivity of the process, but these gains have usually been counterbalanced by a loss in flux (Böddeker & Bengtson, 1991, Doghieri *et al.*, 1993, Fadeev *et al.*, 1993, Tanihara *et al.*, 1994; Chen & Martin, 1995; Okushita *et al.*, 1995; Ruckenstein & Sun, 1995; Bac *et al.*, 1996; Jonquières *et al.*, 1996; Kujawski *et al.*, 1996; Liang & Ruckenstein, 1996; Ruckenstein & Liang, 1996; Uragami *et al.*, 1996; Schäfer *et al.*, 1997).

VII.2.2.2.1 SOLVENT REMOVAL

Böddeker *et al.* (1990) compared the performance of PDMS, polyurethane (PUR) and PEBA to separate isomeric butanols. The PDMS membrane provided the highest selectivity relative to water while the PEBA membrane gave the highest flux and the strongest discrimination amongst isomers. However, a comparison of the separation obtained with

pervaporation through PEBA, evaporation, RO, and adsorption in silicates showed no improvement in the selectivity of the process with the introduction of pervaporation.

Blume *et al.* (1990) compared the performance of PDMS with a polyolefin composite membrane in a spiral-wound module for the separation of ethanol and ethyl acetate from water. The polyolefin composite membrane presented extremely low fluxes - one tenth of the flux through the PDMS - which hindered its commercial application. The PDMS membrane showed a small selectivity for ethanol-water separations (β of 2 to 10) but very high selectivity for ethyl acetate-water separations (β of 50 to 150). Blume *et al.* (1990) observed that the order of enrichment on the PDMS membrane for ethanol and ethyl acetate followed the same order as the vapour pressure of the solvents in an aqueous solution.

Feng & Huang (1992) studied the separation of *i*-propanol from water through PDMS and silicone polycarbonate membranes. Silicone polycarbonate membranes were not as effective in the separation as PDMS. For the PDMS membrane, they observed that the water flux remained constant for all the concentrations studied (the *i*-propanol concentration in the feed ranged from 0 to 6% w/w). However, the presence of water, regardless of the feed concentration, enhanced the flow of *i*-propanol, suggesting the occurrence of coupling effects.

Hickey *et al.* (1992) compared the separation performance of ethanol, *n*-butanol and *t*-butanol from dilute aqueous mixtures using PDMS and poly (methoxy siloxane) (PMS). The objective of their work was to analyse the effects of process parameters on the performance of a pervaporation module associated with an acetone-butanol-ethanol (ABE) fermentation process. Because the separation of *n*-butanol had greater potential economic benefits than the separation of ethanol, their conclusions were based on the results from water-*n*-butanol separation. The PDMS membrane showed better performance than the PMS membrane for the removal of *n*-butanol and it was also observed that *n*-butanol permeated more readily than *t*-butanol in agreement with the results of Böddeker *et al.* (1990). As expected, experiments showed that an increase in the temperature of the feed

increased both the flux exponentially and the selectivity at lower *n*-butanol concentrations, whereas an increase in the permeate pressure decreased the flux.

Yoshikawa *et al.* (1994) investigated the separation of alcohols from water in binary mixtures through crosslinked polybutadiene (PB) membranes. This membrane was chosen because of its hydrophobic character and ease of modification. Nevertheless, the uncrosslinked PB showed no selectivity and the crosslinked membrane showed selectivity for *i*-propanol and *n*-propanol only at high solvent concentrations (> 85%). Although the membrane materials were of hydrophobic nature, sorption experiments showed that it incorporated more water than alcohols.

VII.2.2.2.2 WASTE TREATMENT

Application of pervaporation for solvent recovery can still be very competitive compared with established separation techniques when solvents are present in the water at very low concentration. This is particularly so for removal of volatile organic compounds (VOC). Compared to biological disposal techniques and incineration, pervaporation has the advantage of producing water at the required purity for disposal or recycle into the process while also allowing the recuperation of the solvent. Figure VII.2 shows a comparison of the costs to treat water by pervaporation, carbon adsorption, incineration, air stripping and biological techniques. Pervaporation is more cost effective than carbon adsorption and incineration over the concentration range of 0.1 to 3% solvent in the feed, and is able to treat solvents at a higher concentration than that recommended for air stripping and biological treatment. Pervaporation is twice as expensive as carbon adsorption when the feed stream solvent concentration is lower than approximately 0.01% and similarly more expensive than incineration when the feed stream solvent concentration is higher than 80%. Simmons *et al.* (1994) listed the pollutants that can be recovered from aqueous streams with the present technology. These included acetaldehyde, acetone, CFC, alcohols, and aromatic hydrocarbons; to this Böddeker & Bengtson (1991) added dioxanes, acids, and chlorinated hydrocarbons.

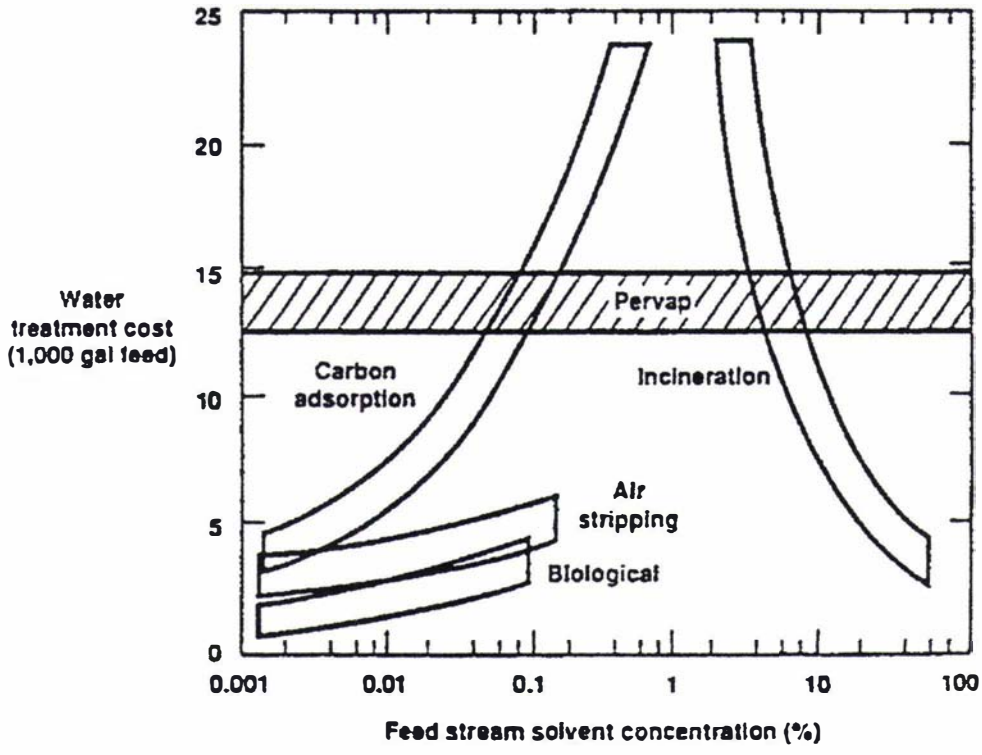

Figure VII.2 Comparison of the costs to treat water effluents by pervaporation, carbon adsorption, incineration, air stripping and biological techniques (Baker, 1991).

Matsuura (1994) cited the application of pervaporation in a di-isopropyl benzene plant to remove benzene from a 15,000 gal.day^{-1} water stream containing also cumene, chlorides, solids and aluminium. Le Carbone Lorraine (1993) has installed a pervaporation plant for the recovery of MEK from the printing ink drying plant used in the labelling of aluminium cans at the Cebal packaging industry in Froges, France. A module using PDMS membranes has also been commissioned by Le Carbone Lorraine for the reduction of dichloroethylene from 8,600 ppm to 5 ppm in the effluent of an industrial site.

Barber & Miller (1994) calculated that the removal of trichloroethylene (TCE) from ground water by pervaporation has a 70% lower operation cost than activated carbon units, but the capital investment was much higher. Pervaporation is however very competitive

in the removal of methyl ethyl ketone (MEK) and benzene from water when compared with steam stripping and chemical oxidation. When associated with other techniques, such as activated carbon adsorption, anaerobic biological treatment, steam stripping, or oxidation, pervaporation can yield a cleaner water stream than either operation alone (less than 1 ppb of organic solvent) with a 20% reduction in operation costs (Barber & Miller, 1994).

VII.2.2.2.3 THE BEVERAGE INDUSTRY

In the beverage industry, the application of pervaporation to the production of spirits and to the dealcoholization of wine and beer has been investigated by Moutounet *et al.* (1992), who reported that, because of low membrane permeability, pervaporation alone for the production of spirits from the ethanol fermentation is not productive enough. However, pervaporation offers the advantage of producing a spirit with higher quality residues, no copper, and a low furfural content.

Beaumelle *et al.* (1992), in a study of wine dealcoholization, compared the selectivity obtained with pervaporation through a PDMS membrane to that by evaporation for propanol and ethyl acetate in the presence of water, and in the presence of a mixture of water and ethanol. In all the cases, the vapour liquid equilibrium showed higher selectivity than pervaporation. In their analysis, those results were a consequence of concentration polarization due to the low Reynolds number of the feed flow and of low feed concentration of the preferentially permeating species.

Brüshke (1990) also studied the pervaporation of aroma compounds, such as high alcohols, acids, esters and aldehydes, present in a mixture of water and ethanol through PDMS membranes. The objective of this work was to produce a low alcohol beer. Three membranes were used: plain PDMS, zeolite-filled PDMS, and polyacetylene modified membranes. Polyacetylene modified membranes were considered too unstable for the application. A PDMS membrane without fillers did not show selectivity towards ethanol due to high swelling and lost its mechanical stability after a short period of use. With the

zeolite-filled PDMS membrane, a reduction of 50% in the ethanol content of the beer was possible without undue change in the aroma and taste. A reduction of 90% in the ethanol content of the beer removed all esters, 90% of the higher alcohols and 60% of the acids. Following pervaporation, fractionated condensation of the permeate made the recovery of an aroma fraction possible.

VII.2.2.3 OTHER APPLICATIONS: ORGANIC-ORGANIC SEPARATIONS

The study of organic separations by pervaporation is still in its early stages because of the relatively recent introduction of hydrophobic membranes. Most of the research effort has been directed to the development and selection of membranes for the various potential applications.

Organic-organic separations represent the sector with the largest opportunity for reducing energy and process costs if suitable pervaporation membranes can be developed. In the USA alone, 40% of the industrial energy costs are spent in fractionation of organic mixtures by distillation (Baker, 1991). So far, research in this area has succeeded in developing a process for the separation of methanol from methanol/MTBE/*i*-butane mixtures and methanol from dimethyl carbonate (DMC) (Ruston, 1990; Matsuura, 1994). Both DMC and MTBE blends are used as gasoline enhancers. In spite of the improvements in the economics of the MTBE production possible with pervaporation, difficulties in altering the distillation tower piping and the process conditions have hindered the possibility of retrofitting an existing plant with a membrane system (Ruston, 1990).

Wijmans *et al.* (1994) studied the integration of pervaporation into the synthesis processes of DMC. The objective was to separate the methanol from the non-aqueous organic mixture. Because of the similarity of methanol to water, hydrophilic membranes (PVA) were applied. A concentration of 95% methanol in the permeate was achieved and a study of the process indicated that the optimal configuration was characterized by a relatively small concentration difference between feed and retentate, with fixed feed flow rate and

installation of the pervaporation module at a point below and away from the azeotrope. The hybrid process (pervaporation-distillation) was superior to two-pressure distillation in the cases studied, with reductions of operating costs of 10-40% and almost identical capital costs. However, as the capital cost of pervaporation increases linearly with capacity, for economy of scale there is an advantage in using distillation. This characteristic emphasises the importance of reducing membrane/module costs.

Will & Lichtenthaler (1992) attempted to separate n-propanol from methanol and from methanol-water mixtures in the 0 to 100% range of concentration by pervaporation and vapour permeation using a hydrophilic PVA-PAN composite membrane. In vapour permeation the feed is in the vapour phase, but in all other aspects the process is similar to pervaporation. Pervaporation exhibited higher fluxes than vapour permeation, but the selectivity was not high enough for commercial application. On the other hand, vapour permeation experiments showed very high selectivities but fluxes were too low for commercial application.

VII.2.2.4 Advantages of hybrid processes

Wijmans *et al.* (1994) state that pervaporation is unlikely to be used alone. Rather, because of its low fluxes, pervaporation is most efficient when used in conjunction with distillation in a hybrid process. The main applications of pervaporation are in breaking an azeotrope and removal of a single component. When used to unload a distillation column, significant reductions in energy consumption and operation costs can be achieved together with an increase in throughput. Numerous options exist for the integration of pervaporation and distillation. The choice of a design depend on the product characteristics, process, and on the economic analysis.

According to Acharya & Stern (1990), distillation has problems associated with start up and control. Distillation is also a capital and energy intensive process. On the other hand, most membrane processes have problems associated with fouling, plasticization, and

rupture which cause changes in composition of the retentate and the permeate. They believe however that the disadvantages of both distillation and membrane processes can be alleviated by using a hybrid process design.

Moganti *et al.* (1994) and Stephan *et al.* (1995) have developed a methodology based on the minimum area of a McCabe and Thiele diagram and Smoker's equation method for the design of membrane-distillation hybrid process. The principle underlying this method is that optimal membrane placement reduces the number of trays required for a specific separation in the distillation column, thus reducing capital costs.

VII.2.2.5 Overview of membrane applications

Overall, the implementation of pervaporation in a process should be considered from the perspective of its being an auxiliary technique. Until membranes with both high selectivity and high flux become available, pervaporation is unlikely to replace traditional separation techniques.

The use of pervaporation with hydrophilic membranes for dehydration of solvents is a mature technology. It has found its niche in the breaking of azeotropic mixtures and in offering an option to processes where the use of high temperature is limited by product characteristics or process economics. In the competitive environment of today's industry, its range of applications might still be further enlarged by reducing membrane and module costs.

The use of pervaporation for solvent removal or organic-organic separations still awaits a technological breakthrough. The application of organophilic pervaporation for the removal of solvents from waste streams has had a timid start and requires an effort from the membrane manufacturing industry to either extend membrane life-expectancy or reduce membrane and module costs, if this technique is to compete fairly with the established techniques. In the food, beverage, and chemical industries, despite intense research in the development of new membranes, the low selectivity and mechanical

stability of the commercially available membranes have hindered the application of pervaporation in those applications considered so far.

In the applications to which pervaporation has so far been introduced, the overall process gained a reduction in energy consumption and an increase in the simplicity of its design. These advantages should assure the continuing interest in the development of pervaporation.

VII.2.3 MODULE DESIGN

VII.2.3.1 GENERATION OF THE DRIVING FORCE

As noted, the driving force in the pervaporation process results from a gradient in chemical potential across the membrane. The simplest way to generate this driving force is to use a vacuum pump to remove the permeate from the membrane cell. This mode of operation requires substantial vapour volumes to be pumped at large costs (Strathmann & McDonogh, 1993), but compared to all other operation modes it provides the highest fluxes.

In industrial plants the need to reduce costs has restricted the use of the vacuum pumps to the start up of the process and at short periods each hour for the removal of incondensable gases (Fleming & Slater, 1992d). The vacuum at the membrane cell is instead maintained by the temperature difference between the condenser and the permeate side of the membrane (Néel *et al.*, 1985; Colman *et al.*, 1990; Mulder, 1994). Néel *et al.* (1985) termed this type of operation thermopervaporation. They also stated that thermopervaporation generally achieved a lower transport rate than vacuum pervaporation because the residual downstream pressure was higher than in vacuum pervaporation. This mode of operation also had the disadvantage of incurring higher module costs (Franken *et al.*, 1990; Strathmann & McDonogh, 1993).

Another alternative is to use a sweep gas to remove the permeate. Strathmann & McDonogh (1993) and Wijmans *et al.* (1994) have pointed out that this operation mode is only viable if the permeating species has little value and is to be discarded without requiring condensation.

A third option is to use condensable vapour as a carrier gas. Besides lowering the partial pressure of the permeating components, it provides the enthalpy of evaporation by condensing at the membrane surface. This option had the disadvantage of requiring a further separation step when the permeating component is of economical interest (Rautenbach *et al.*, 1991).

VII.2.3.2 Module configuration

Plate and Frame

The plate and frame modules consist of flat sheet membranes which are assembled in many different designs. The major difficulty with these designs is the edge sealing of the membrane, but otherwise plate and frame modules are very robust, and it is technically easy to replace individual sheets, although labour intensive. The membrane can be cleaned physically if necessary making it useful for heavy fouling, high value product situations. (Howell, 1993).

Spiral wound modules

Spiral wound modules are one of the most popular configurations for commercial use. The major advantage of spiral wound modules is the large surface area per unit volume which reduces the number of modules required for a given membrane area, thus reducing costs. They are also robust and easy to link with other modules. (Howell, 1993).

Spiral wound modules comprise a membrane envelope with the open end sealed to a porous pipe. The envelope contains a thin spacer to keep the two sides apart and the separating surface is on the outside of the envelope. The envelope then is the coiled around

VII.3 DISTILLATION

The evaluation of hybrid pervaporation-distillation schemes require that the performance of both distillation and pervaporation be modelled as a function of feed concentration, temperature, and pressure. Distillation is a separation process in which a vapour and a liquid phase comprising components with different volatilities coexist. The more volatile compound(s) or the light fraction should be enriched in the vapour phase. To increase its purity, the vapour phase undergoes a series of condensations and vaporizations.

Continuous distillation is achieved in a column similar to the one schematically represented in Figure VII.3. On each plate, condensation and vaporization of the mixed phases occurs simultaneously. At the top of the column, the vapour phase, enriched with the light component, and the excess heat are withdrawn. At the bottom of the column, a reboiler (or direct steam injection) provides the necessary energy for the separation.

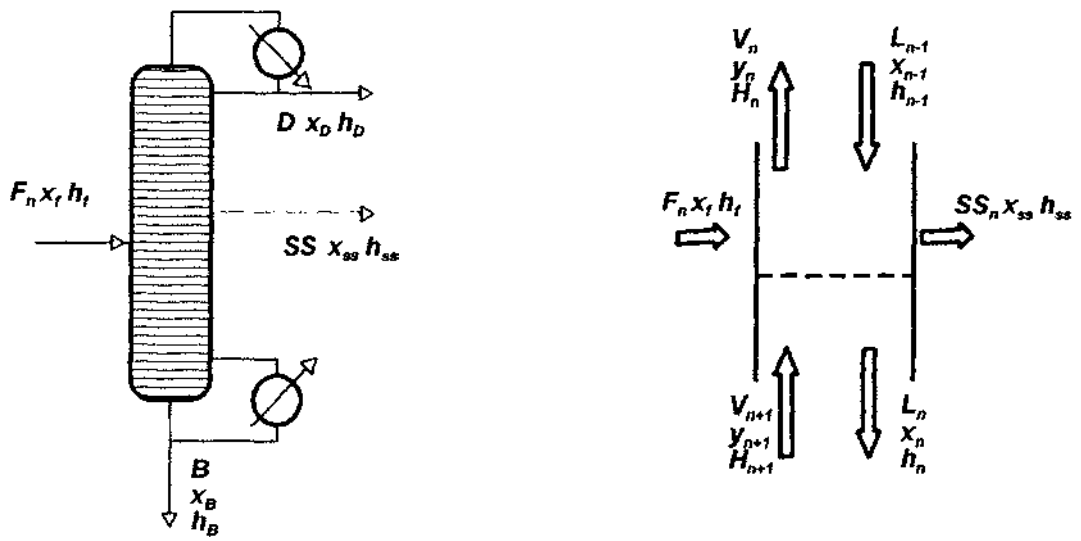

Figure VII.3 Schematic representation of a distillation column and of a theoretical plate.

The equations that describe continuous, steady-state distillation were published over a

the central pipe with the spacer incorporated to keep succeeding layers of the spiral apart. This tight spiral coil is placed in a tube. (Howell, 1993).

The disadvantages of the spiral configuration are the narrow flow channels which result and the potential blockage of the space-filling turbulence promoters when the wrong type of feed is used. As with any type of membrane system, achieving a proper seal may also prove a problem and the material used to seal the edges of the envelope can cause difficulty when in contact with solvents. (Howell, 1993).

Hollow fibre

Hollow fibre modules are easy to build, are robust, and enclose large membrane areas in small volumes. They also permit the use of turbulent or laminar flow patterns, but the fibres are fragile and may break causing reduction of selectivity. Their use is thus restricted to clean feeds. (Howell, 1993).

Tubular

Tubular membranes are similar to hollow fibre membranes but have a larger internal diameter (often 5mm). They are appropriate for turbulent flow operation and accept feeds with high content of particulates and high viscosities. (Howell, 1993).

Of the membrane module configurations available, the plate and frame, and the spiral wound were the first to be developed and remain the most widely used throughout the industry. However, the need to reduce membrane and module costs, and increase flux without losing selectivity is driving the research and development on hollow fiber modules for pervaporation. So far, no interest has been shown in tubular modules, as most pervaporation applications have a clean feed.

hundred years ago. They are based on the assumption that chemical and thermal equilibrium was reached in every stage. These equations consisted of total and component mass balances around a theoretical plate and an energy balance (Equations VII.1 to VII.7):

(1) Total mass balance and heat balance for the column:

$$F - D - B - SS = 0 \qquad \text{[VII.1]}$$

$$h_f F - h_D D - h_B B - h_{SS} SS = 0 \qquad \text{[VII.2]}$$

(2) Total and component mass balance for the *n*th theoretical plate:

$$F + V_{n+1} + L_{n-1} - V_n - L_n - SS_n = 0 \qquad \text{[VII.3]}$$

$$x_f^i F + y_{n+1}^i V_{n+1} + x_{n-1}^i L_{n-1} - y_n^i V_n - x_n^i (L_n + SS_n) = 0 \qquad \text{[VII.4]}$$

$$\sum_{i=1}^{m} x_n^i = 0, \quad \sum_{i=1}^{m} y_n^i = 0, \quad y_n = f(x_n, T_n, P_n) \qquad \text{[VII.5]}$$

(3) Total heat balance for the theoretical plate:

$$h_f F + H_{n+1} V_{n+1} + h_{n-1} L_{n-1} - H_n V_n - h_n (L_n + SS_n) = 0 \qquad \text{[VII.6]}$$

$$H_n = f(y_n, T, P), \quad h_n = f(x_n, T_n, P_n) \qquad \text{[VII.7]}$$

Where, for each stage n and a system with m components, F is the feed flow rate, D is the distillate flow rate, B is the bottoms flow rate, L is the liquid flow rate, V is the vapour flow rate, SS is the side stream flow rate, H and h are the enthalpy of the vapour and liquid, respectively, x is the liquid mol fraction, y is the vapour mol fraction, T is the

temperature and P is the pressure at each tray.

Despite their apparent simplicity and adequate description of the distillation process, only the development of computers made it possible to solve the above system of equations for multicomponent systems. Firstly, the large set of equations, many of them non-linear, and a large difference in magnitude of values of the variables made their direct solution difficult. Secondly, while the assumption of thermal equilibrium is valid if the temperatures of adjacent trays do not differ much, in practice chemical equilibrium is never achieved.

To solve the first problem, various mathematical methods were developed. The most significant contribution was that of Naphtali & Sandholm (1971), who developed a method based on the linearization of the distillation equations grouped by plate. With this arrangement, the partial derivatives needed by the Newton-Raphson method are easy to calculate and, if advantage is taken of the sparsity of the matrices, the amount of storage required is largely reduced. The procedure for the solution of distillation equations is iterative in nature and the method is very dependent on the initial values. Although Naphtali & Sandholm (1971) claimed that convergence is accelerated as the solution is approached, in its original format, the method does not always find the correct path to the solution of highly non-ideal systems (Powers *et al.*, 1988).

Many variations and small improvements were introduced to the algorithm developed by Naphtali and Sandholm (Holland, 1981; Cho & Joseph, 1983a, 1983b, 1984; Bhargava & Hlavacek, 1984; Kovach & Seider, 1987; Powers *et al.*, 1988; Huss & Westerberg, 1996a, 1996b). Of the methods available, two stand out as having particular utility: the homotopy-continuation and the collocation algorithm.

Homotopy is the transformation of a set of equations which is difficult to solve into a set whose solution is easily found by continuation from a given approximation (Bhargava & Hlavacek, 1984; Kovach & Seider, 1987). The method, as Bhargava & Hlavacek (1984) point out, involves a trade off between robustness and computation time. It is able to avoid

singularities of the Jacobian and to find multiple solutions in the homotopy path, but the computation time is higher than for the Newton-Raphson algorithm. Powers *et al.* (1988) described the solution of the linearized equations as the most time consuming task in the solution of the distillation problem, which they minimized by lumping a number of stages together. Simandl & Svrcek (1991) reduced the amount of time to solve a distillation column by updating the relative volatilities (K values) only at the end of a computation of all trays.

Collocation is based on the substitution of the Jacobian differential equations by an approximation, usually a polynomial. It is a common method for the numerical solution of differential equations and has the advantage of being less time consuming than homotopy, but the accuracy depends on the precision of the approximation.

To solve the second problem, the assumption of chemical equilibrium is in general discarded. The methods developed to deal with the non-ideality of the separation fall into three categories:

- ❖ equilibrium-stage models that do not explicitly incorporate stage efficiency;
- ❖ equilibrium-stage models that incorporate stage efficiency,
- ❖ non-equilibrium models.

In the first procedure, developed by Lewis (1922), the equilibrium equations are solved and the number of real stages is related to the number of equilibrium stages by a constant. This procedure is the most simple and fast to compute, it applies only to binary or nearly ideal systems and its accuracy depends on the experience of the user. It is generally applied in the design of columns when no information regarding the behaviour of the mixture is available.

In the second procedure, the difference between the equilibrium and the real separation is incorporated into the calculations at each plate by introducing a correction to the phase equilibrium equation. Of the numerous efficiency equations developed, the equations of Murphree (1925), Hausen (1953), and Holland (1981) have received the most attention.

As Seader (1989) points out, all three equations are based on the assumption that vapour and liquid streams entering or leaving a tray are of uniform concentration. The equations from Murphree and Holland owe their success to their ease of incorporation into computer algorithms, but the value of the efficiency must be back calculated from experimental data. The algorithm developed by Hausen is considered superior to the algorithm developed by Murphree because it eliminates the need for the vapour leaving a tray to be at its bubble point. The difficulty in back calculating efficiency values from experimental data and the increase in computer time to calculate the efficiency are disadvantages of this algorithm.

In recent years, a model based on mass and heat transfer equations rather than on efficiency correlations was developed (Krishnamurthy & Taylor, 1985a; 1985b; 1985c). Powers *et al.* (1988) point out that efficiency values estimated for a specific separation do not necessarily apply if operation parameters, such as mass flow rate and column pressure, are changed. Furthermore, in multicomponent systems the efficiencies are not uniform for all the components in the mixture. In fact, as Krishnamurthy & Taylor (1985c) have shown, for a ternary system containing water, acetone and methanol, the efficiency for each component at each tray may vary from $-\infty$ to $+\infty$. In a multicomponent system, the flow interactions between the mixture components may be so strong and complex that it can overwhelm the thermodynamic driving force in establishing the direction of the separation. In conclusion, for multicomponent systems the degree of separation is determined by thermodynamic equilibrium as well as by mass and energy transfer.

The schematic representation of a non-equilibrium model is shown in Figure VII.5. The mass and heat balance equations are solved for each phase separately, with mass and heat transfer equations added to the conservation equations. Equilibrium is assumed to occur only at the interface.

The model requires knowledge of the column geometry and the selection of appropriate transport-coefficient correlations. In comparison to the equilibrium model, it is in general more accurate and, if the appropriate transport-coefficient correlations are selected, it is

VII.4 PROCESS INTEGRATION

Distillation is a prime target for energy conservation, because it is an energy-intensive operation. Approaches to energy saving in distillation fall broadly into three categories (Linnhoff *et al.*, 1983; Humphrey & Seibert, 1992):

- ❖ augmenting distillation with advanced processes to form energy-efficient hybrid systems: vapour-recompression, multi-effect distillation, membranes, etc.;
- ❖ replacing distillation with energy saving alternatives: adsorption, membranes, liquid-liquid extraction, and other processes;
- ❖ achieving better integration of distillation with the overall process.

Process integration is an established discipline for planning, assessment and design of site-wide utility systems (Cleland, 1998). Process integration techniques aim at maximizing utility usage through optimization of the level of heat exchange between process-process or process-utility streams. Process integration techniques provide the necessary tools for integration of distillation and distillation hybrid schemes with the overall process and also target cost minimization by obtaining the optimal process design for the product specification. The techniques developed use either a combinatorial or a thermodynamic approach to solve the process integration problem.

Tioe (1990) reviewed the main combinatorial techniques used in process integration. In the combinatorial formulation, all possible stream matches were analysed. This type of solution required the use of complicated computer algorithms and large computation time, but did not necessarily guarantee that the optimum solution would be produced. Even when heuristics were used to assist the problem solution, difficulties arose from the large number of possible combinations.

A breakthrough was achieved when, in 1977, Nishida and co-workers presented an algorithm based on maximization of energy recovery, minimization of total heat transfer area, and minimization of total network cost (Tioe, 1990). Soon afterwards, process

sensitive to changes in operation parameters. On the other hand, it requires more computer time to be solved and still needs the development of more reliable correlations, as Taylor (1996) admits:

> "I start by quoting a very good friend of mine, Hans Wesselingh, who once wrote: *"Our knowledge of multicomponent mass transfer coefficients is improving, but this is a slow process. I still occasionally have to pray that my estimate of some coefficient will not be off by more than one order of magnitude."* "

Mass and heat balance equations for the vapour phase:

$$y^i_{Fv} F_v + y^i_{n+1} V_{n+1} - y^i_n SS_v - y^i_n V_n - N^i_n = 0$$

$$H_{Fv} F_v + H_{n+1} V_{n+1} - H_n SS_v - H_n V_n - E_n = 0$$

Mass and heat balance equations for the liquid phase:

$$x^i_{Fl} F_l + x^i_{n-1} L_{n-1} - x^i_n SS_l - x^i_n L_n + N^i_n = 0$$

$$h_{Fl} F_l + h_{n-1} L_{n-1} - h_n SS_l - h_n L_n + E_n = 0$$

Heat and mass transfer equations:

$$N^i_n = k^i_n (y^i_n - y^i_{nI})$$

$$E_n = h_n (T_n - T_{nI})$$

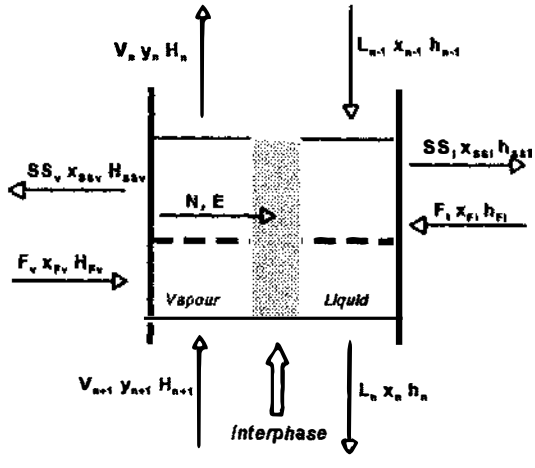

Figure VII.4 Schematic representation of the non-equilibrium stage model and main equations for steady state. Where, for each stage n, F is the feed flow rate, SS is the side stream flow rate, L is the liquid flow rate, V is the vapour flow rate, h and H stand for the enthalpy of liquid and vapour respectively, x is the mol fraction of species i in the liquid, y is the mol fraction of species i in the vapour, N is the mass transfer rate, E is the heat transfer rate, k is the mass transfer coefficient, h is the heat transfer coefficient, T is temperature and the subscripts v, l and I stand for vapour, liquid and interphase, respectively.

integration became a simpler task as Linnhoff and co-workers introduced the principles of heat and power thermodynamics (Linnhoff, 1993).

Pinch technology, as the new methodology was termed, was first developed as a tool for the definition of heat exchanger networks. Later, the methodology was "[...] extended to address systems including distillation, heat pumps, co-generation turbines, furnaces, etc. and to address non-energy objectives such as capital costs, operability, and emissions" (Linnhoff, 1993). From a design technique, "Pinch" developed into a process analysis tool and the methodology became better known as "Pinch Analysis".

Pinch analysis uses grid diagrams, composite curves, and the pinch to analyse any production process. Grid diagrams are schematic representations of the heat exchanger network. Composite curves represent the overall heat and mass balance of a process and allow the prediction of optimized hot and cold utility targets ahead of design, the understanding of driving forces for heat transfer, and the location of the heat recovery 'pinch' (Linnhoff *et al.*, 1995). Composite curves are built from the summation of all the heat released by hot streams (streams that need to be cooled) and all the heat required by cold streams (streams that need to be heated). The pinch is identified from the composite curves as the location where the hot and the cold composite curves have their closest approach and heat transfer is most constrained.

For distillation, a pinch is defined as the region where the operating conditions in the column most closely approach equilibrium (Ognisty, 1995). In the analysis of distillation columns, column composite curves are built from the heat exchanged on each stage at a particular temperature level. These curves were labelled column grand composite curves (CGCC). For these distillation columns, the pinch is located at the narrowest gap between the heat duty curve and the origin. The size of the gap represents the amount of excess heat associated with refluxing the column above the minimum. Changes in the column design and operation that bring the operation line closer to the equilibrium stage are reflected in the CGCC by a narrowing of the pinch. Details on the construction and analysis of the

CGCC, grid diagram and the composite curves are given in Linnhoff (1993) and Linnhoff *et al.* (1995).

Pinch analysis was commercialized early in its development. In New Zealand alone over twenty studies were carried out between 1982 and 1995, covering a broad range of industries, mainly in the meat, diary, brewing, fertilizer, food and pulp industries (Drew, 1995). In these studies, the energy savings identified typically ranged from 20 to 40% for industries that used predominantly fossil fuel and pay back times were estimated as approximately three years or less.

The early commercialisation of the technique lead to a number of commercial failures due to lack of know-how and incredibly large claims of design improvements (Linnhoff, 1993). Linnhoff (1993) admitted that " to this day, opinions remain divided. Morgan (M.W. Kellog) reports that Pinch Analysis significantly improves both the 'process design and the design process'. [Whereas] Steingmeyer (Monsanto) is concerned that Pinch Analysis may miss out on '... major opportunity for improvement...' ".

In consequence of its fast commercialisation, many studies on pinch analysis are not publicly available and the published literature deals mostly with guidelines. In general, when analysing distillation columns, it is recommended to start with the simplest alternative. Dhole & Linnhoff (1992) recommend the following sequence:

- reflux and pressure modifications. In distillation, the reboiler duty was identified by Humphrey & Seibert (1992) as the minimum energy required in the separation process and it is a direct consequence of the reflux ratio;
- feed pre-heating/cooling. Feed pre-heating will generally reduce the reboiler load, while cooling will reduce the condenser load;
- side condensing/reboiling. Side condensing/reboiling requires changes in the column piping and capital investment.

VII.5 SUMMARY

VII.5.1 PROJECT BACKGROUND

In New Zealand, industrial ethanol is produced by the fermentation of deproteinated whey. Besides ethanol, fermentation produces undesirable by-products such as higher alcohols (fusel oils), esters, and aldehydes. Purification and concentration of the fermented broth to product specification is accomplished by distillation. This increases the concentration of ethanol from approximately 2% (w/w) to 96.5% (v/v) or 99.9+% (v/v) and reduces the by-products concentration to the levels required by the client.

It is estimated that steam consumption for distillation constitutes a quarter of the total production cost of whey ethanol (Mawson, 1987) and that much of this energy, approximately 35%, is spent in the removal of impurities, such as fusel oils. Since the petroleum crisis of 1974, there has been greater awareness to the need of reducing the energy expenditure in the chemical industry. Various methods that reduce energy use in distillation have been developed. Adopted either in isolation or together, they include efficient use of insulation, introduction of heat recovery schemes, introduction of vapour recompression, multi-effect pressure distillation, selective removal of ethanol during fermentation, pre-concentration of whey by reverse-osmosis, molecular sieves, and membrane-hybrid schemes (Douglas & Feinberg, 1983; Maiorella *et al.*, 1984; Mawson, 1987; Mix *et al.*, 1978).

In the competitive environment of today's economy, continuous re-evaluation of process design and economics are justified in order to sustain and improve participation in the market. In light of such needs, the aim set for this project was to investigate alternative processes for the production of ethanol that could reduce the energy expenditure of distillation while maintaining or improving product quality. Of the listed options, membrane-hybrid schemes appeared to provide the best opportunity for reducing investment and maintenance costs, without increasing plant complexity. With membrane hybrid schemes, it is also possible to re-design the strategies for removal of the fusel oils

and thus reduce operation costs; and to add value to waste streams by extraction of additional products. Furthermore, the study of membrane-hybrid systems may extend the knowledge base and thus increase the ability of designers to address market opportunities, cf., production of flavour compounds.

VII.5.2 THE ROLE OF DISTILLATION MODELLING AND PINCH ANALYSIS

It was chosen to investigate the feasibility of pervaporation to selectively remove small aroma fractions from the ethanol-water mixture because in pervaporation separation is not limited by vapour-liquid equilibrium, the process might be carried out at lower temperatures, and as only the permeate is evaporated, there is a great potential for the reduction of energy requirements for separation when compared to distillation.

As pervaporation is generally used in association with distillation, a model of the distillation train is required for simulation of the combined processes. Distillation models consist of total and component mass balances around a theoretical plate and an energy balance. In general, chemical equilibrium is not achieved in the plates and a number of algorithms based on equilibrium stage-models that incorporate efficiency and non-equilibrium models have been developed. Equilibrium stage-models are easily incorporated in the calculation algorithms, but the efficiency values must be back calculated from experimental data and are generally applicable only for these operation conditions. Non-equilibrium models are based on mass and heat transfer equations that account for non-idealities in the interaction between components in a multi-component mixture.

Difficulties in the modelling and simulation of distillation arise from the large number of equations, some of them non-linear, that need to be solved simultaneously. With the advent of computers the solution of this system of equations became possible and mathematical methods are being continuously developed. However, the accurate solution of distillation for multicomponent mixtures remains a challenge given the limitations of the vapour

equilibrium data available, the limited understanding of the influence of flow regimes inside the column in the separation, and limitations of the existing mathematical methods.

In order to evaluate the current level of energy integration at NZDCL, to compare it with the alternative processes to be proposed, and to judge the advantages of these alternatives, use of process integration techniques is recommended. Process integration techniques developed to date fall broadly into two categories: combinatorial formulations and thermodynamic approaches. The latter has been developed recently and is the most attractive because of its application to a variety of processes. Of the thermodynamic approaches available, pinch analysis has been applied successfully in New Zealand, as elsewhewe, for the past ten years or more and guidelines for its application to distillation columns are available in Linnhoff *et al.* (1983), Linnhoff *et al.* (1994) and Ognisty (1995).

Chapter VIII

RESEARCH OBJECTIVES

The intensive use of energy by distillation provides serious motivation for studying opportunities for energy savings at NZDCL. In this light, the main objectives set for this part of the project were:

- to evaluate whether organophilic membranes developed for pervaporation provide an alternative and economical method for the purification and concentration of industrial ethanol;

- to carry out a pinch analysis of the production site in order to identify opportunities for energy savings.

Therefore, the specific aims of this research were:

- *to develop a simulation model of the distillation at NZDCL.*
  A model of the distillation at NZDCL was necessary to investigate the impact of changes in operation parameters on the product quality for the pinch analysis, to analyse the influence of pervaporation when associated with distillation, and to evaluate new process designs.

- *to acquire experimental data to verify the distillation model developed*, because published data on the composition profile of ethanol and fusel oils during distillation is scarce.

- *evaluate new process designs in terms of their energy usage.*
  Process integration techniques such as pinch analysis provide a systematic methodology to look at energy usage. Whilst process integration studies have been done at NZDCL, there was a need to update results and include new process designs generated from this study.

- *to model pervaporation of multicomponent mixtures.*

  In order to assess the impact of pervaporation in a hybrid process, a mathematical model of pervaporation is required. As the transport of multicomponent mixtures through pervaporation membranes is little understood, experiments needed to be designed to evaluate the influence of operation parameters such as membrane type, temperature, feed composition, feed flow rate and the occurrence of flow coupling or concentration polarization.

Chapter IX

DISTILLATION MODEL

IX.1 BACKGROUND

In Chapter VIII, Research Objectives, two tasks were set that required the simulation of distillation columns:

- to investigate the influence of introducing a pervaporation step on the operation of the distillation columns at the NZDCL;

- to investigate the impact of changes in distillation operating parameters on the product quality and energy usage as part of a pinch analysis.

Two commercial packages, HYSIM® v.2.1(Hyprotech Inc., Canada) and ChemSep® v.3.5 (Cache Corp., USA), were available. Preliminary analysis with each of the packages showed that HYSIM® had the advantage of dealing proficiently with complex arrangements of various distillation columns and heat exchangers simultaneously, but did not cope with the complex fusels-ethanol aqueous mixture: the more complex columns, BC and RC, converged when the only components were water and ethanol, but did not converge when fusels were added. ChemSep® had the advantage of being robust enough to deal with such complex mixtures, but its flowsheeting capability is limited and columns had to be calculated individually. The decision to use ChemSep® was based on two factors:

- technical support was readily available from Prof. R. Taylor of Clarkson University, USA;

- as the pervaporation unit used organophilic membranes to remove fusels from the ethanol-water mixture, it was considered more important to be able to converge columns dealing with complex mixtures than to have flowsheeting capability.

IX.2 MODEL CONSTRUCTION

Figures IX.1 and IX.2 are schematic representations of the existing columns at NZDCL. Given that ChemSep® has no flowsheeting ability, the way the BC columns were represented needed to be adapted (Figure IX.3). The modifications included:

- ❖ inclusion of a *pump around* from stage 38 to stage 40 to represent the bottoms stream from column BC2 that is fed straight into the top of BC1;
- ❖ inclusion of a heat loss on stage 39 to represent the partial condenser The heat load was calculated as the heat necessary to pre-heat the feed stream from approximately 45 to 68°C (Figure IX.2). The efficiency of stage 39 was set at 100% for every condition tested;
- ❖ the steam ejector was eliminated. The steam injected into the column included the steam recuperated through the ejector, which was calculated using a program developed with MatLab® (AppendixE), and the bottoms stream from BC (Figure IX.3) corresponded to the bottoms stream from BC1 before it entered the flash drum (Figure IX.2).

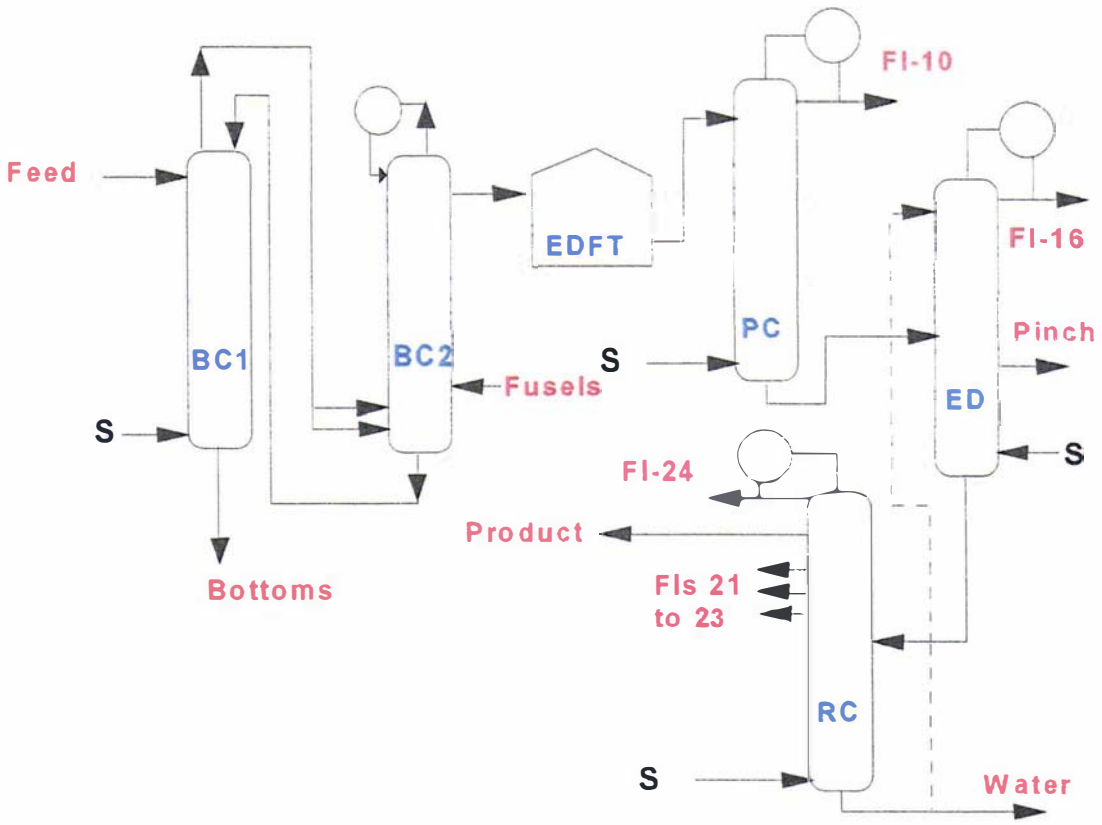

Figure IX.1 Schematic representation of the distillation columns at the NZDCL. ***S***: steam.

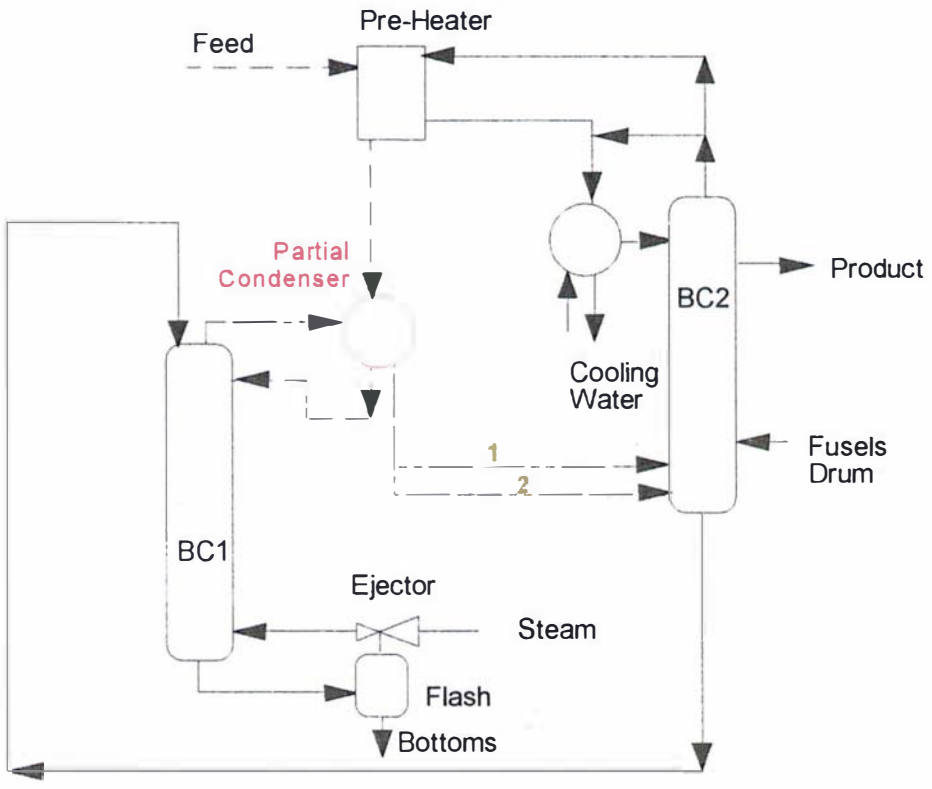

Figure IX.2 Detail of the BC columns and attached heat exchangers. 1: vapour phase feed stream to BC2; 2: liquid phase feed stream to BC2.

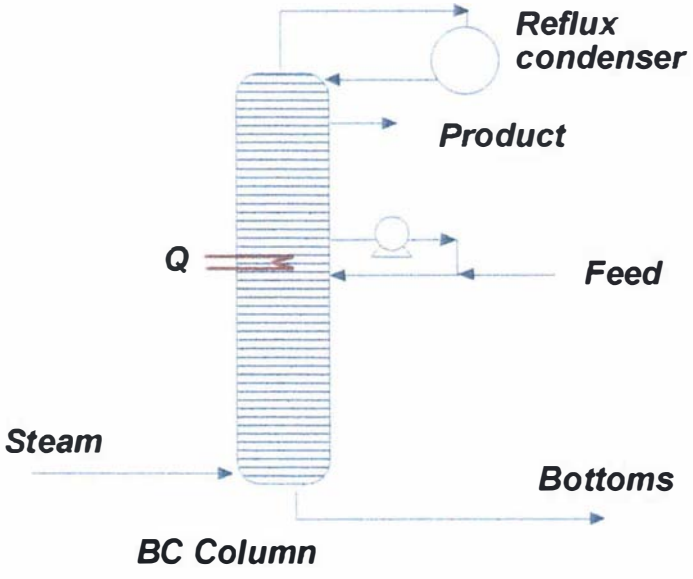

Figure IX.3 Schematic representation of columns BC1 and BC2 in ChemSep®. Q: heat load extracted from stage 39.

All distillation columns were built from the input menu of ChemSep® following the same specifications:

- ❖ components: water, ethanol, *i*-propanol, *n*-propanol, *i*-butanol, *n*-butanol, *i*-amyl alcohol, ethyl acetate;

- ❖ operation: refluxed absorber/stripper;
  condenser: total (liquid product);
  number of stages (Table IX.1): total number of trays + 1 (includes condenser);
  feed stages; side streams; pump around (Table IX.1);

- ❖ thermodynamic models: K-model: DECHEMA;
  Equation of State: ideal gas law;
  Activity coefficient: UNIFAC;
  Vapour pressure: Antoine;
  Enthalpy: excess;

- ❖ specifications: column pressure, heater/cooler; efficiency (Murphree); operation (Appendix A & E: program listings - **.sep*).

Table IX.1 Design and fitted parameters for BC, PC, ED and RC using ChemSep®.

	BC	PC	ED	RC
no. of trays[a]	28 + 38 + partial condenser	19*	56	67
feed stages	37, 40, 68	2, 20	16, 23, 57	47, 68
side streams	5	-	38	2, 32, 35, 45
pump around	38 to 40	-	-	-
efficiency[b]	0.04 to 0.1	1	0.015	0.5 - 1

[a] no. of trays does not include the reflux condenser; no. of stages includes the reflux condenser and was counted from top to bottom.
[B] fitted parameter

The algorithm generated the initial values for each stage automatically and solved all plates simultaneously using a Newton-Raphson iteration methodology. Convergence was achieved when the discrepancy between the component mass balances was lower than 0.0001 $mol.s^{-1}$ for all components.

Although it was chosen to use an equilibrium stage model, its accuracy can decrease when the operating conditions of the column being simulated are vastly different from the conditions for which the efficiencies were set. In addition, given the complex and strong interactions between the species under study, the equilibrium stage model may not consider all variables that influence separation. In light of these limitations, all results and accuracy limits presented in this study apply only to columns operating at similar conditions to those which were used to generate the model (Appendix A & E). However, general trends, such as the direction and magnitude of the change in the internal flow rates given a change in feed temperature, should still be applicable to other operating conditions.

An alternative to the equilibrium stage model would have been to use a non-equilibrium, rate-based model. A comparison of the RC column with ChemSep® using an equilibrium stage model and a non-equilibrium, rate-based model, showed no significant differences in the final results. Furthermore, not all information necessary to run the rate-based model was available for all columns. Therefore, this possibility was not investigated further.

IX.3 Model fitting

IX.3.1 Collection of distillation experimental data

The Murphree efficiency for each column in each model was fitted using experimental data collected at NZDCL (Table IX.1; Appendix E: program listings). Samples of feed, product, and selected side streams were taken from NZDCL at five distinct days spread throughout the production season of whey during the years of 1995 and 1996 (Appendix A). The samples were taken in triplicates, one per shift, and were collected at the beginning (11-Sep-95), middle (22-Nov-95; 05-Mar-96), and end (25-Apr-96) of the production season;

these were named sets 1 through 12 in chronological sequence. All samples were accompanied by information on feed and product flow rates, temperature, pressure, column operating parameters, tray position of input or output, and quantity of steam injected in each column. Samples taken between November 1995 and March 1996 represented full production. Figure IX.4 summarizes the sampling points selected.

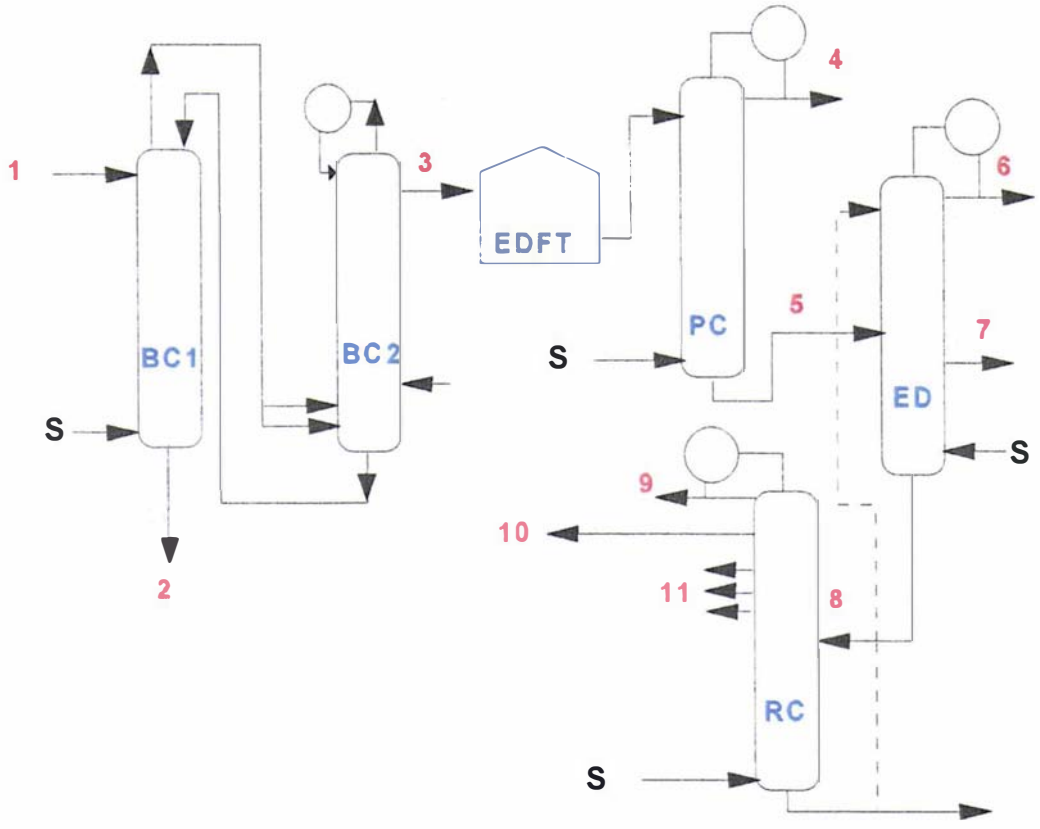

Figure IX.4 Sampling points at NZDCL. **1**: feed to BC1, tray 1; **2**: bottoms from BC1; **3**: product from BC2, tray 4; **4**: distillate from PC; **5**: bottoms from PC; **6**: distillate from ED; **7**: side stream from ED, tray 38; **8**: bottoms from ED; **9**: distillate from RC; **10**: product from RC, plate 2 ; **11**: side stream from RC, trays 32,35, and 45. **S**: steam.

In 1997, an extra set of samples from BC2 was collected between the 14th and 17th of October. The objectives were to observe whether any significant variation of the composition profile along the column occurred between cleaning operations during the operation cycle of 30 hours, and whether the composition profile along the column agreed with the composition profile simulated with ChemSep®. Figure IX.5 shows the sampling

points available on BC2. Trays 2, 9, 24 and 34 were sampled at a minimum interval of 3 hours for two consecutive days and trays 2, 9, 11, 24, 27, 29, 30, 31 and 34 were sampled on the 17th of October within a two hour interval.

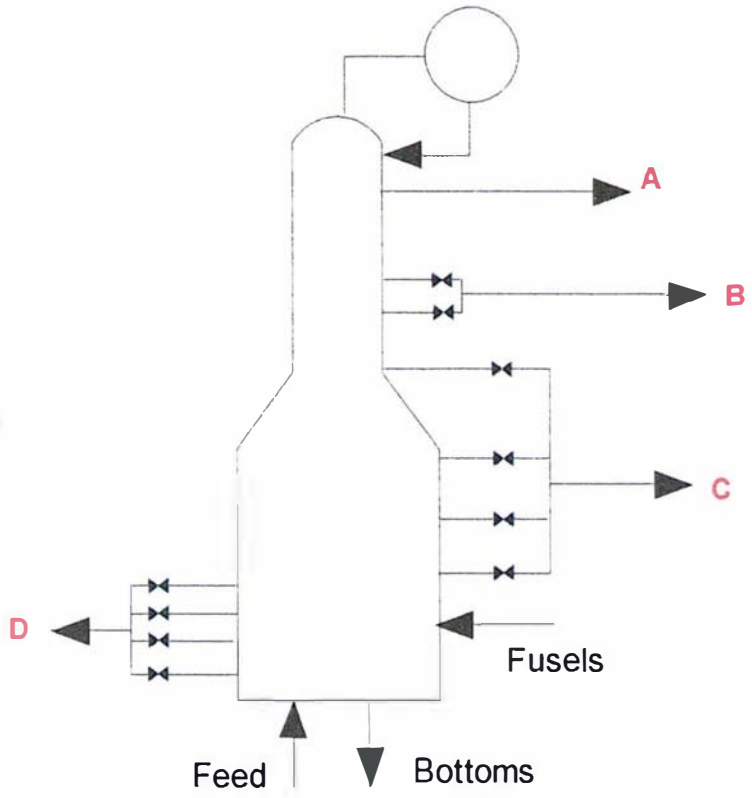

Figure IX.5 Sampling points at BC2. A: product stream, trays 2 or 4; B: trays 9 and 11; C: trays 24, 27, 29 and 30; D: trays 31, 33, 34 and 36.

In September and November 1995 the samples were collected straight from the sampling points into glass bottles and posted to Massey University, Palmerston North Campus. From 1996 onwards the sampling device shown in Figure IX.6 was employed to reduce uncertainty due to flashing. The device was screwed to the end of the sampling points and the samples were collected from the distillation column by first allowing the fluid to flow through the device for a couple of minutes, then the bottom valve was closed. When enough time to fill the device had elapsed, the top valve was closed. The device was

removed from the sampling point, cooled under running water, and, when it reached ambient temperature, the contents were transferred to a glass bottle and sealed.

At Massey University, the samples were analysed by gas chromatography following the methodology described in Section IV.2.2. The results are in Appendix A.

Figure IX.6 Stainless steel sampling device for distillation columns at NZDCL. A1: top valve; A2: bottom valve; B: inlet enlargement for screwing to sampling point at NZDCL; C: outlet. Total volume capacity: approximately 500 ml.

IX.3.2 FITTING OF EXPERIMENTAL DATA

The only data that needed fitting was the Murphree efficiency of columns BC, ED and RC and the number of theoretical trays of column PC. These fitted data were summarized in Table IX.1 and details of the column operating parameters can be found in the Appendix E. In general, no single set of plate efficiencies described adequately all the samples collected, so efficiencies were set case by case.

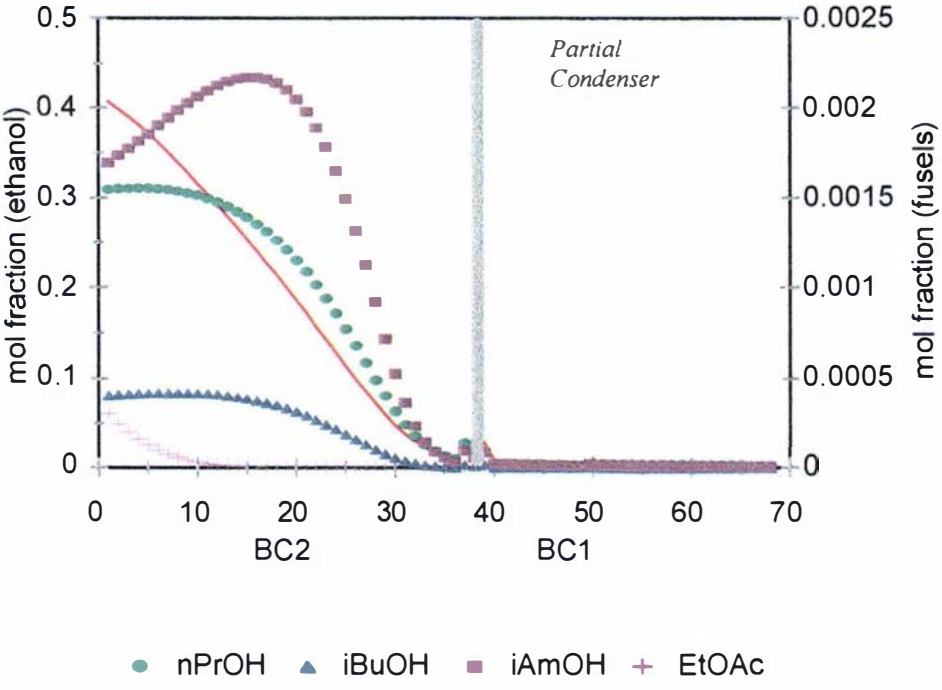

Figure IX.7 Calculated concentration profile for the BC column with ChemSep®; set 1 from 11-Sep-95. EtOH: ethanol; nPrOH: *n*-propanol; iBuOH: *i*-butanol; iAmOH: *i*-amyl alcohol; EtOAc: ethyl acetate. Fitted stage efficiency is 0.04, for stage 39 it is 1.

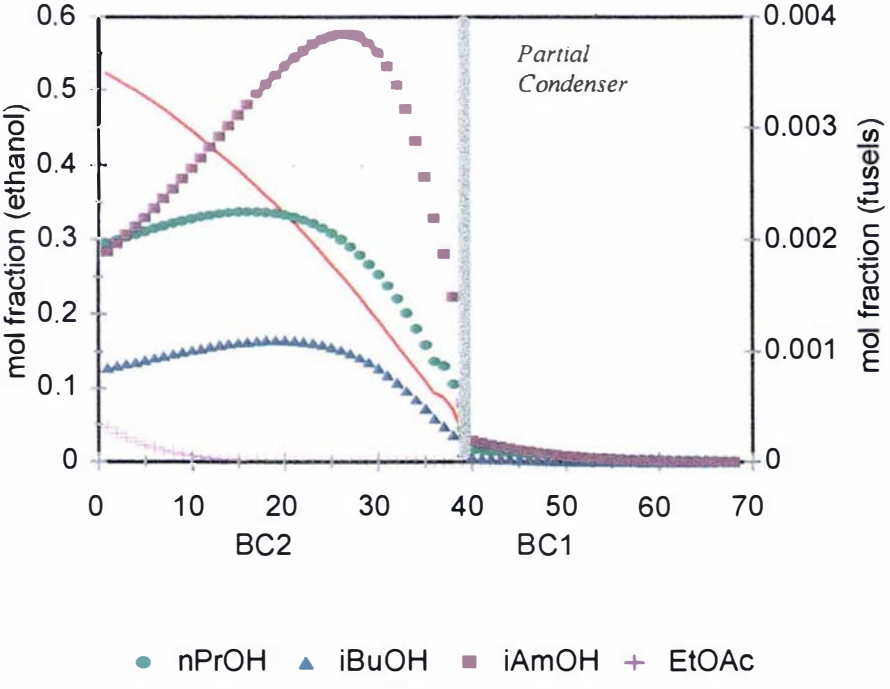

Figure IX.8 Calculated concentration profile for the BC column with ChemSep®; set 2 from 11-Sep-95.EtOH: ethanol; nPrOH: *n*-propanol; iBuOH: *i*-butanol; iAmOH: *i*-amyl alcohol; EtOAc: ethyl acetate.Fitted stage efficiency is 0.05, for stage 39 it is 1.

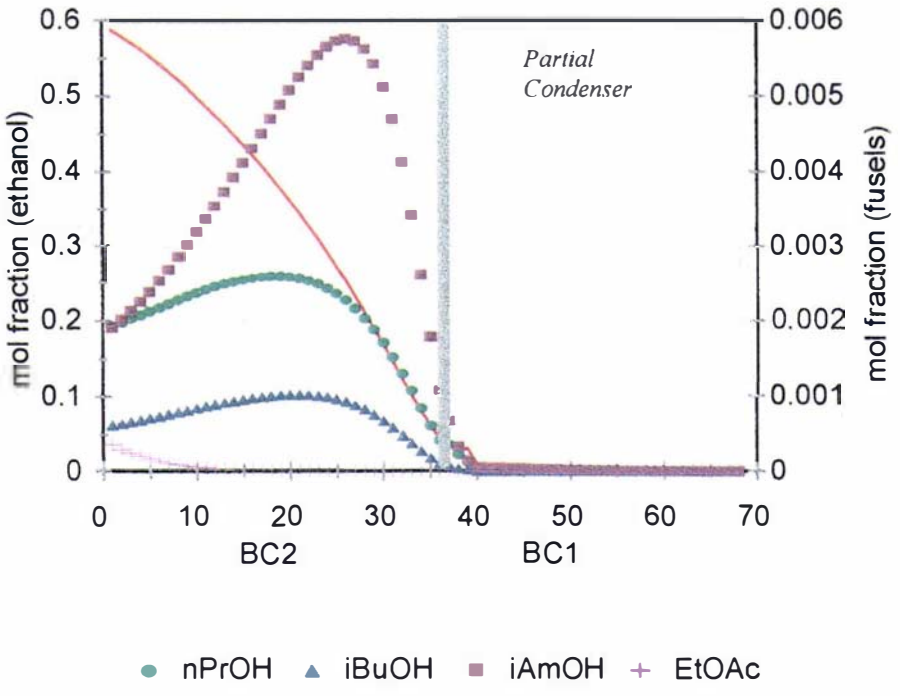

Figure IX.9 Calculated concentration profile for the BC column with ChemSep®; set 3 from 11-Sep-95. EtOH: ethanol; nPrOH: *n*-propanol; iBuOH: *i*-butanol; iAmOH: *i*-amyl alcohol; EtOAc: ethyl acetate.Fitted stage efficiency is 0.07, for stage 39 it is 1.

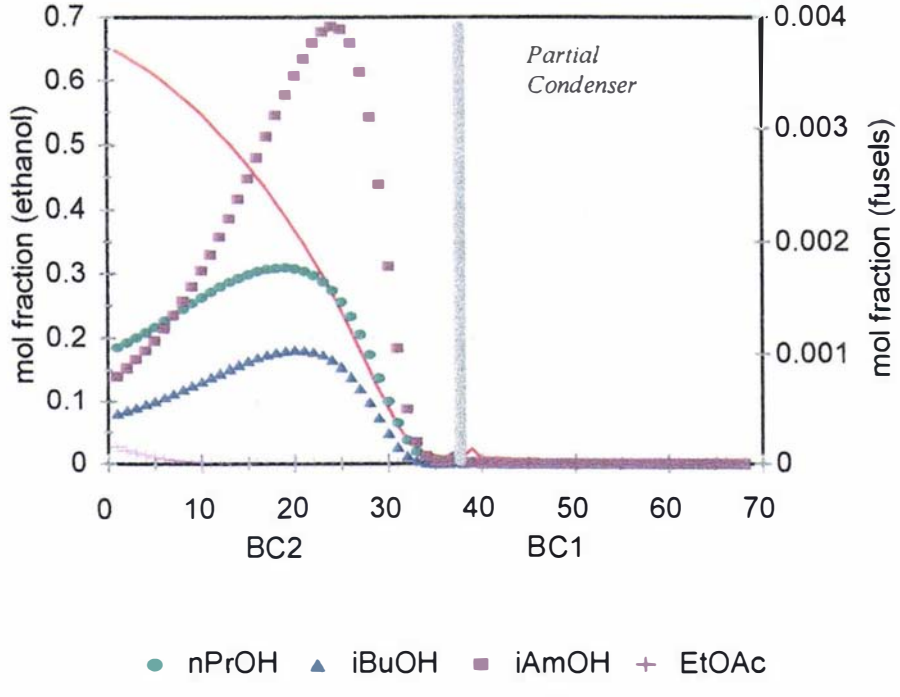

Figure IX.10 Calculated concentration profile for the BC column with ChemSep®; set 2 from 22-Nov-95. EtOH: ethanol; nPrOH: *n*-propanol; iBuOH: *i*-butanol; iAmOH: *i*-amyl alcohol; EtOAc: ethyl acetate.Fitted stage efficiency is 0.1, for stage 39 it is 1.

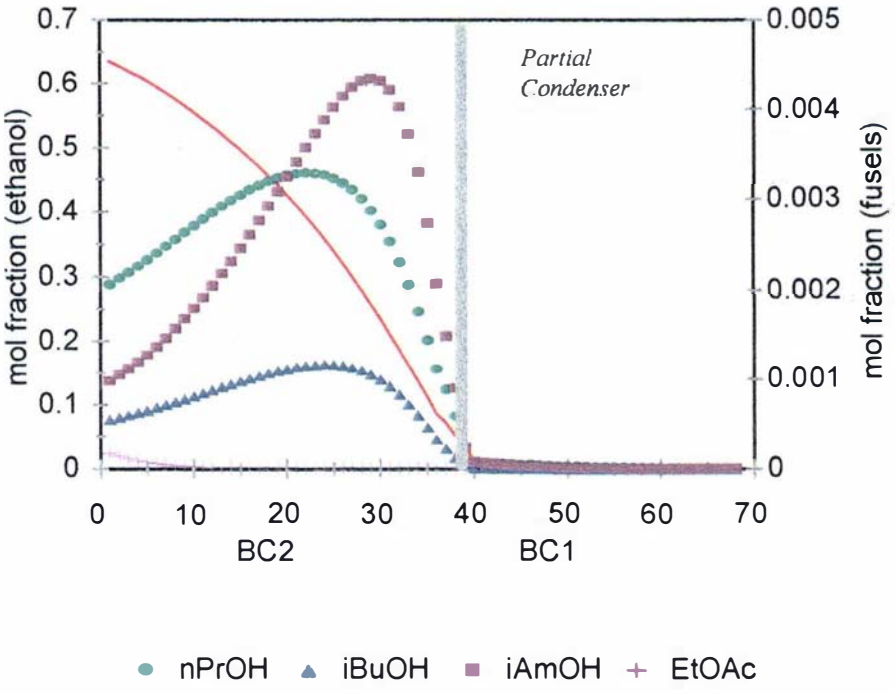

Figure IX.11 Calculated concentration profile for the BC column with ChemSep®; set 3 from 22-Nov-95. EtOH: ethanol; nPrOH: *n*-propanol; iBuOH: *i*-butanol; iAmOH: *i*-amyl alcohol; EtOAc: ethyl acetate.Fitted stage efficiency is 0.08, for stage 39 it is 1.

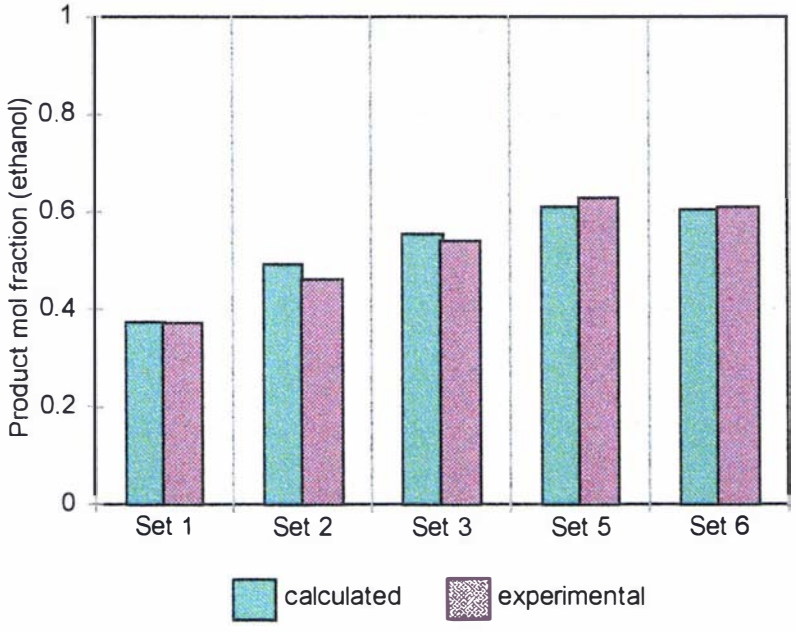

Figure IX.12 Comparison between calculated and experimental product mol fraction for ethanol leaving the BC column for sets 1 to 6.

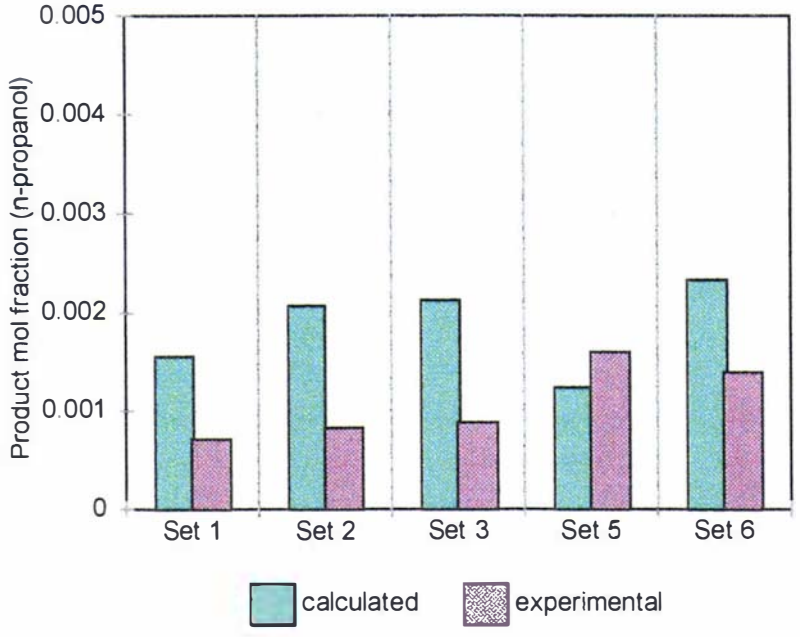

Figure IX.13 Comparison between calculated and experimental product mol fraction for *n*-propanol leaving the BC column for sets 1 to 6.

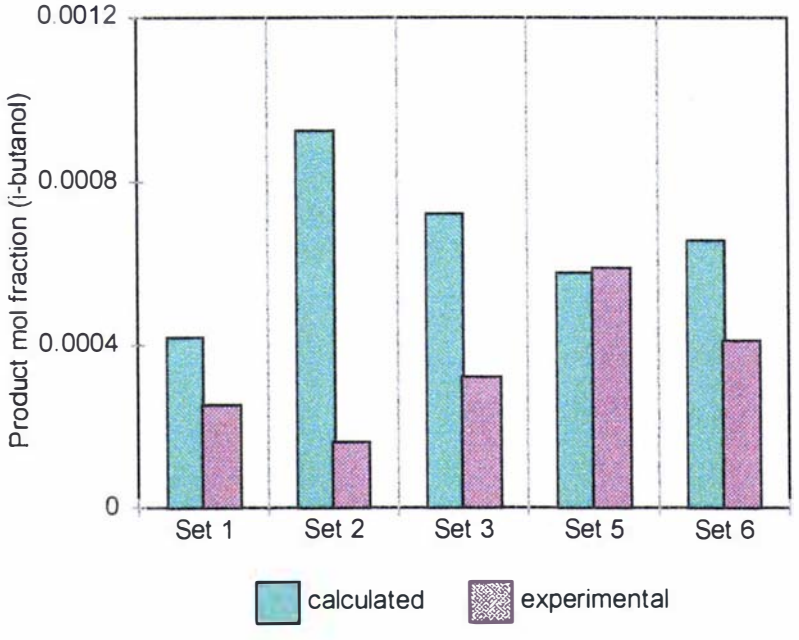

Figure IX.14 Comparison between calculated and experimental product mol fraction for *i*-butanol leaving the BC column for sets 1 to 6.

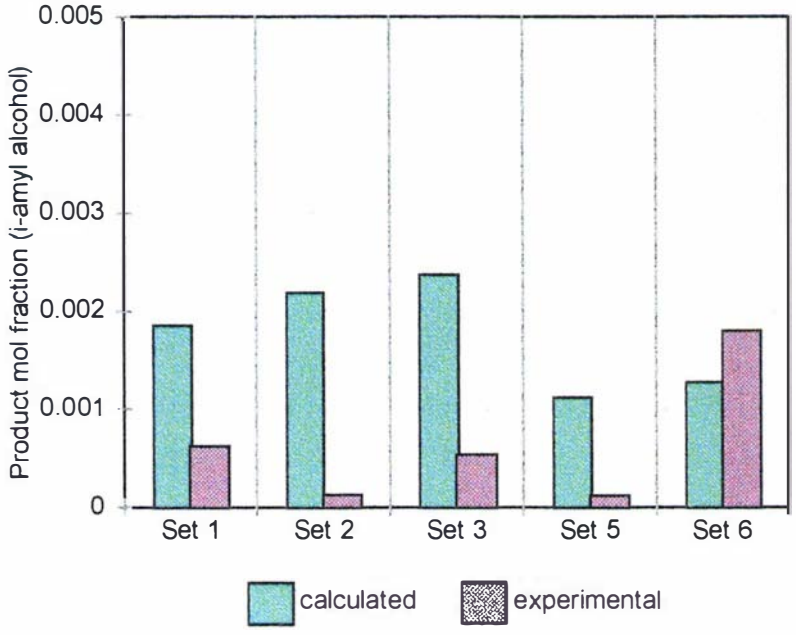

Figure IX.15 Comparison between calculated and experimental product mol fraction for *i*-amyl alcohol leaving the BC column for sets 1 to 6.

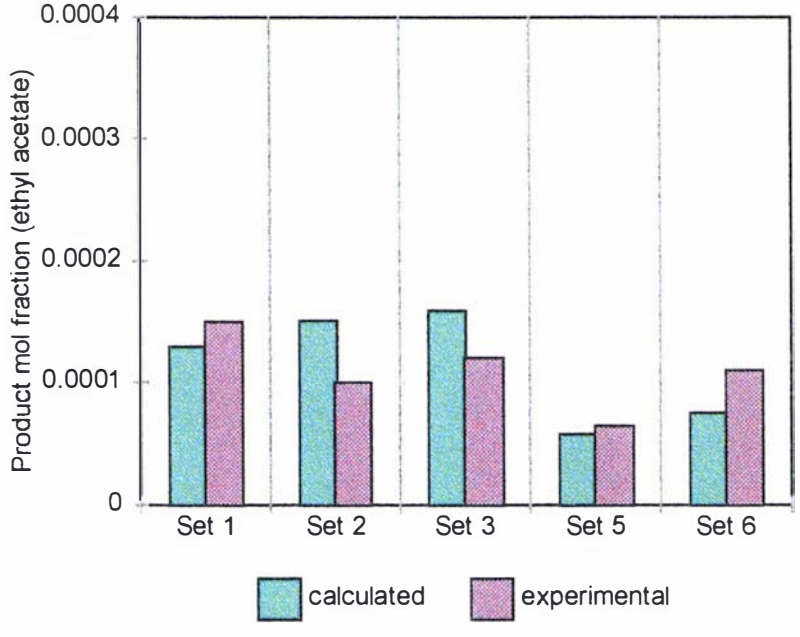

Figure IX.16 Comparison between calculated and experimental product mol fraction for ethyl acetate leaving the BC column for sets 1 to 6.

Figures IX.7 to IX.11 show the calculated concentration profiles for BC column, and Figures IX.12 to IX.16 highlight the difference between the experimental and calculated data. The accuracy of the calculated profiles is discussed in Section IX.4.2. In general, there is good agreement between the calculated and experimental values of the concentration of ethanol in the product stream of BC2. However, the concentration of fusels is often overestimated

For PC, ED, and RC columns (Appendix C), ChemSep® greatly underestimated the quantity of fusels being eliminated from the system through the distillate and side streams. For the ED column, the concentration of each of the fusel components in the distillate stream were underestimated by up to 100%. However, the ethanol concentration was within 15% of the experimental value in all but one case. For the bottoms stream of the ED column, the ethanol concentration differed from the experimental data by up to 60% and the *i*-amyl alcohol concentration differed from the experimental data by up to 100%. For the RC column, the concentration of fusels in each side stream was in general underestimated by approximately 100%, though in some cases it would be overestimated by up to 4000%. In all cases analysed, the final product stream contained ethanol at the azeotropic concentration, water, and traces of fusels, as would be expected.

IX.4 MODEL TESTING AND DISCUSSION

Since ChemSep® is a commercial program, other then to check its results against the experimental data available, against literature guidelines, and against a program developed with MatLab®, it was not tested any further. It was assumed that the program had been already fully verified prior to commercialization. The tests that were performed aimed at verifying the ability of the equilibrium and thermodynamic models to accurately predict the concentration profile along the BC columns, and its consistency in dealing with trace components.

To verify the program's ability to generate accurate concentration profiles:

- ❖ it was compared with published data from Pyke (1965) on the concentration profile of ethanol, fusels, and esters along a distillation column;

- ❖ it was tested against experimental data collected from the sampling points of the BC2 column at the NZDCL.

IX.4.1 COMPARISON OF CHEMSEP® WITH ETHANOL-FUSELS EQUILIBRIUM DATA PUBLISHED BY PYKE

Figure IX.17 shows the concentration profile of fusels in the presence of ethanol and water published by Pyke (1965). It must be noted that Pyke (1965) failed to state whether the data published was obtained from column samples or from mathematical simulations. The concentration profiles of each fusels reaches a maximum when the ethanol concentration is between approximately 25 and 55% (w/w), which corresponds to approximately 10 to 35% (mol). This result agrees with the profiles presented on Figures IX.7 through IX.11, where the fusels concentration reaches a maximum when the concentration of ethanol is between 20 and 40% (mol).

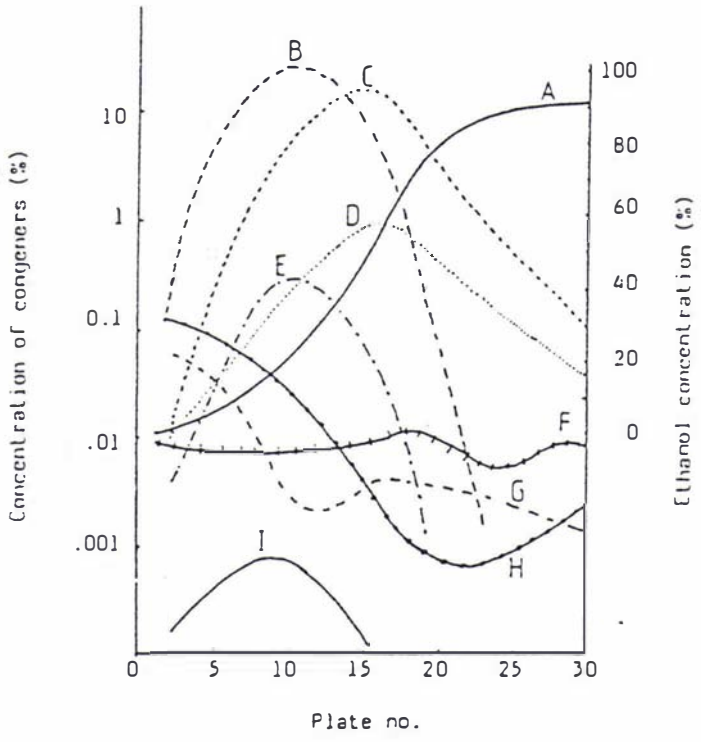

Figure IX.17 Changes in vapour concentration in a rectifier. A: ethanol, B: amyl alcohol; C: *i*-butanol; D: *n*-propanol; E: *n*-butanol (Pyke, 1965).

IX.4.2 TEST OF CHEMSEP® AGAINST COLLECTED DATA AT BC2

Figures IX.18 and IX.19 show the composition profile of ethanol, *n*-propanol, *i*-butanol, and *i*-amyl alcohol along the BC2 column on the 17th of October, 1997 between 12:00 and 14:00. Compared to the profile calculated for BC2, as shown in Figures IX.20 through IX.23, the following characteristics must be noted:

- the ethanol concentration profiles for both the calculated and sampled data were similar;

- in the simulation, the fusels concentration reached a maximum peak half way through the BC2 column and decreased in concentration along the column as the ethanol concentration increased. This behaviour agrees with that presented by Pyke (1965). The samples taken from BC2 showed a markedly different behaviour. The fusels had two concentration peaks instead of one, both near the product outlet at the top of the column, and both at a higher ethanol concentration than indicated by the literature (Pyke, 1965) and the samples taken from ED and RC (Appendix C).

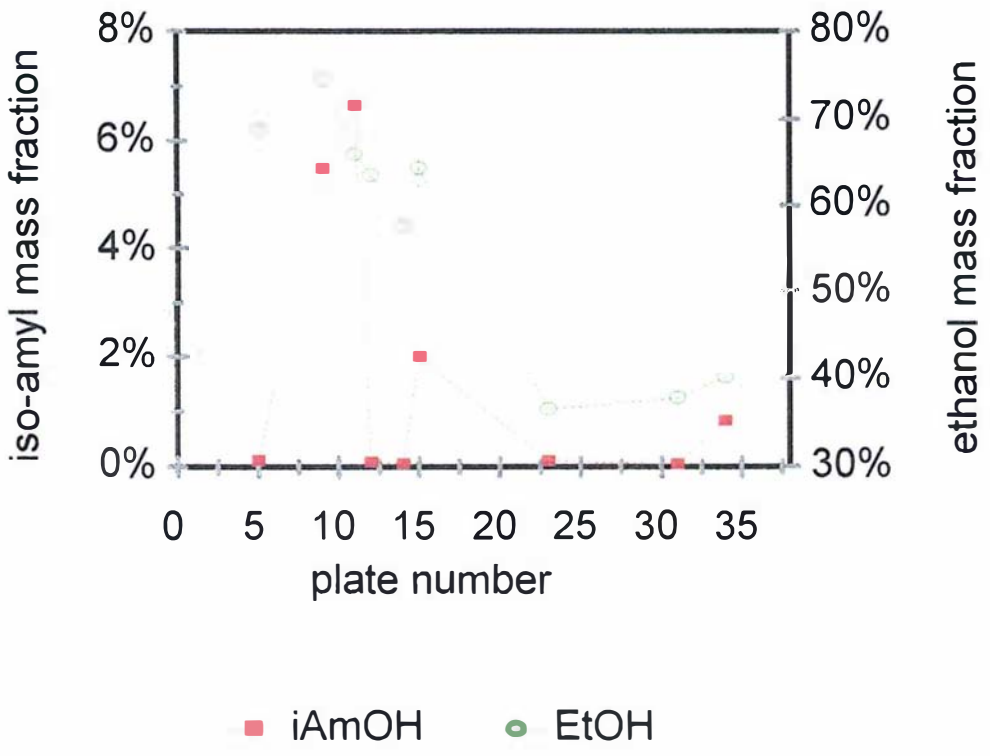

Figure IX.18 Composition profile of ethanol (EtOH) and *i*-amyl alcohol (iAmOH) along the BC2 column as on the 17th of October, 1997 between 12:00 and 14:00.

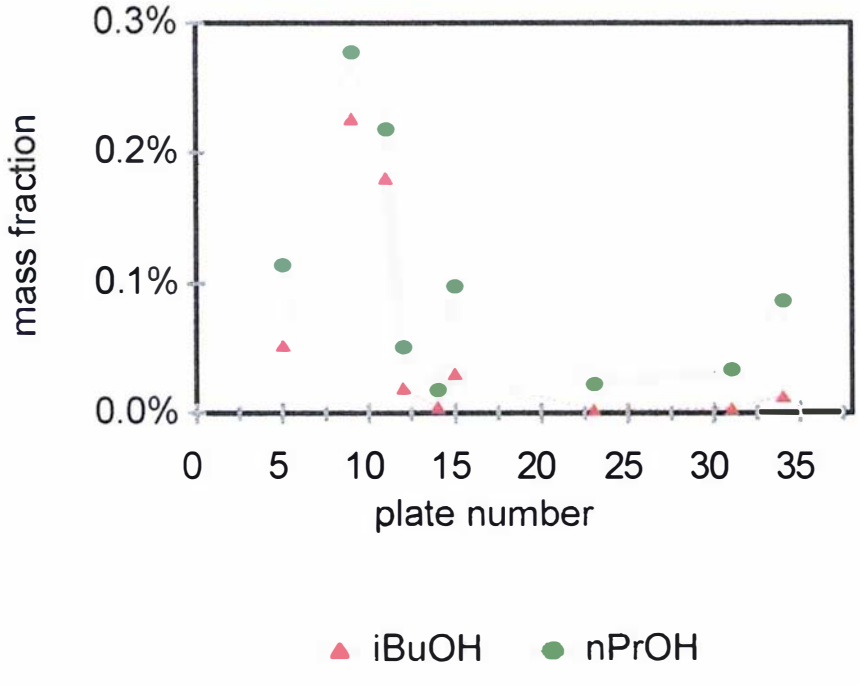

Figure IX.19 Composition profile of *n*-propanol (nPrOH) and *i*-butanol (iBuOH) along the BC2 column as on the 17th of October, 1997 between 12:00 and 14:00.

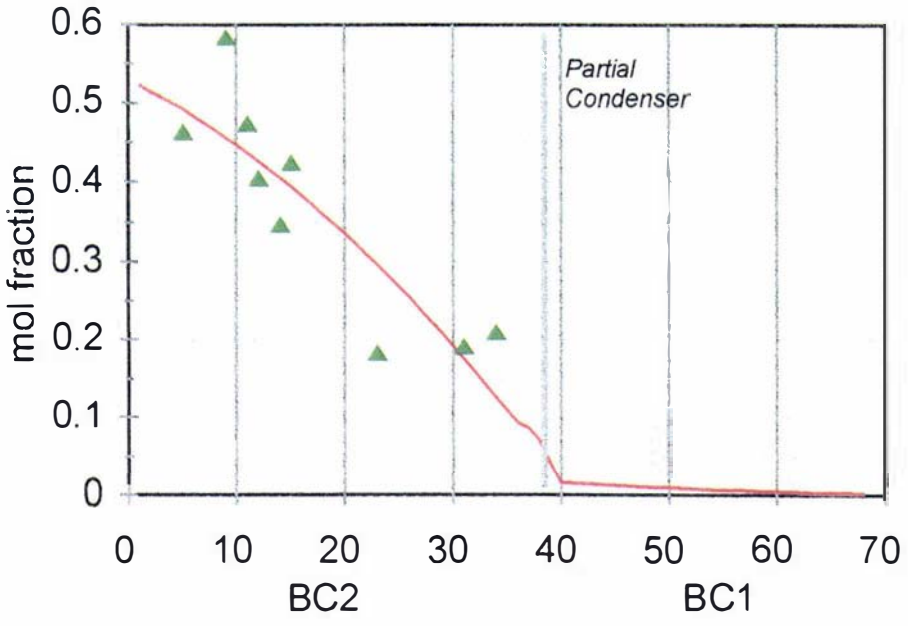

Figure IX.20 Comparison between calculated and sampled composition profile of ethanol along the BC2 column as on the 17th of October, 1997 between 12:00 and 14:00.

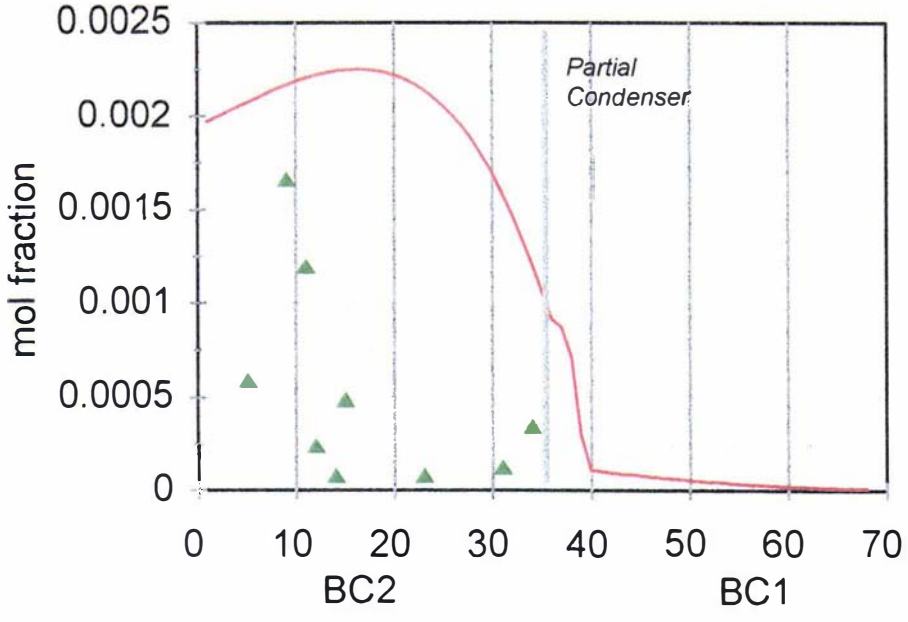

Figure IX.21 Comparison between calculated and sampled composition profile of *n*-propanol along the BC2 column as on the 17th of October, 1997 between 12:00 and 14:00.

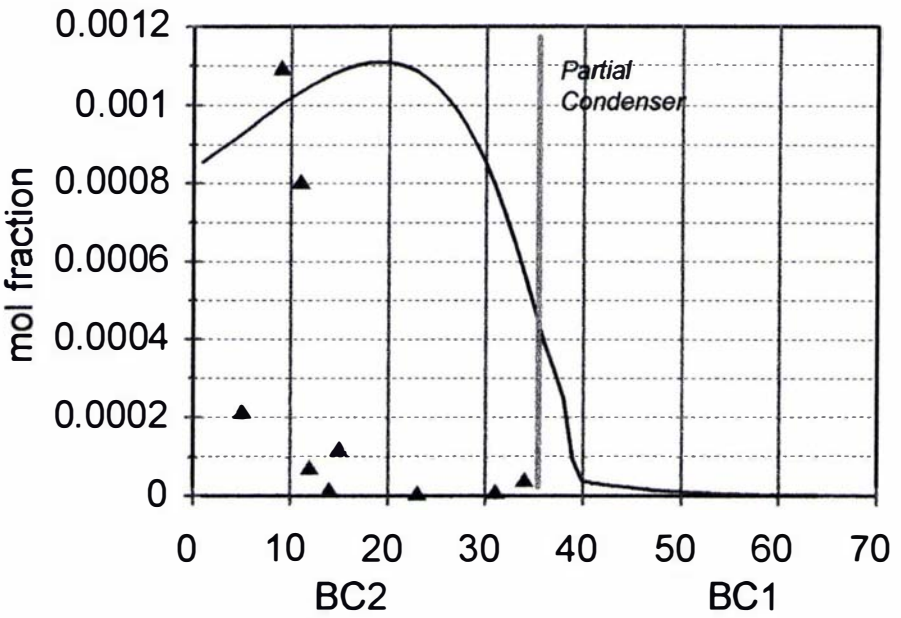

Figure IX.22 Comparison between calculated and sampled composition profile of *i*-butanol along the BC2 column as on the 17th of October, 1997 between 12:00 and 14:00.

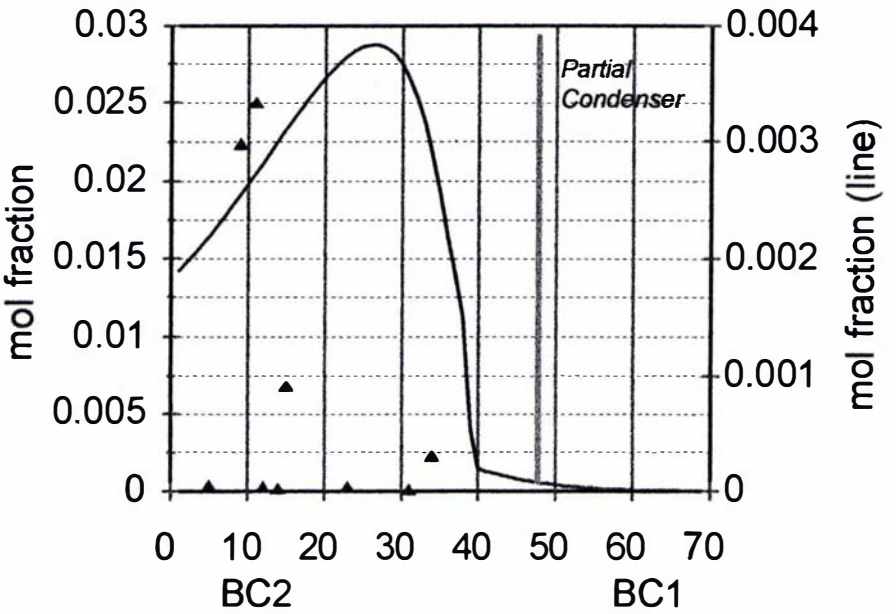

Figure IX.23 Comparison between calculated and sampled composition profile of *i*-amyl alcohol along the BC2 column as on the 17th of October, 1997 between 12:00 and 14:00.

Since no research on distillation was performed during this study, it is only possible to speculate on the causes of the behaviour presented by BC2.

The column operates at twice the design feed flow rate. One immediate consequence of this increase was the elimination of the BC2 side stream (around trays 30-35) to the decanter. This side stream was previously used to reduce the concentration of fusels in the column and this operation was eliminated because the bottom trays no longer held a liquid level. On sampling the column, it was observed that the two lower sampling points expelled a mixture of vapour and liquid instead of a liquid stream. It is possible that the lack of liquid level at the bottom of the column resulted in a reduction of the surface contact between the liquid and vapour phases, thus reducing the mass transfer at the lower half of the column and shifting most of the separation to the top half of the column.

As the fusels are no longer being removed from the column through a side stream as the original design recommended, they accumulate inside the column and are expelled at regular intervals through the nearest outlet - the product side stream. A consequence is that the column may never reach steady state during the operating time of 30 hours between clean ups, but has a cyclical behaviour. Figures IX.24 and IX.25 indicate that this hypothesis may have some foundation.

Figure IX.24 shows the variation of the concentration of ethanol and fusels at the BC2 product during a 32 hour period and Figure IX.25 shows the variation of the concentration of ethanol and fusels on plate 9 during the same time frame. An increase in the *i*-amyl alcohol concentration at the product stream was observed at hour 5 and was followed by a decrease in the *i*-amyl alcohol concentration on plate 9. Though this behaviour seemed to occur only once during this time frame, it indicates that fusels are possibly being expelled from the column in the product stream at regular intervals.

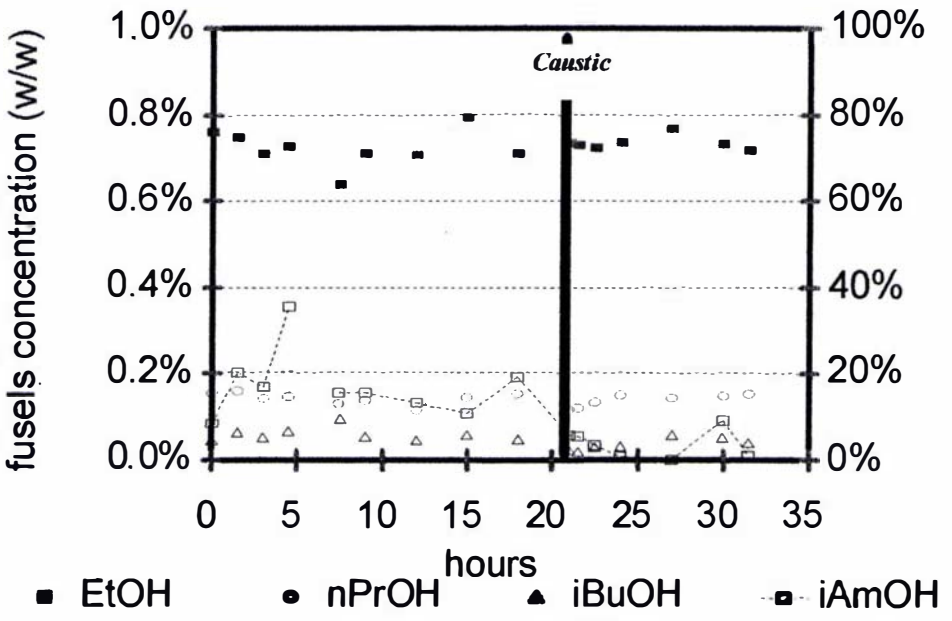

Figure IX.24 Variation of the concentration of ethanol and fusels at the BC2 product stream on between the 15th and 16th of October, 1997. EtOH: ethanol; iAmOH: *i*-amyl alcohol; iBuOH: *i*-butanol; nPrOH: *n*-propanol. The line marked caustic indicates the time that the column was shut for caustic cleaning.

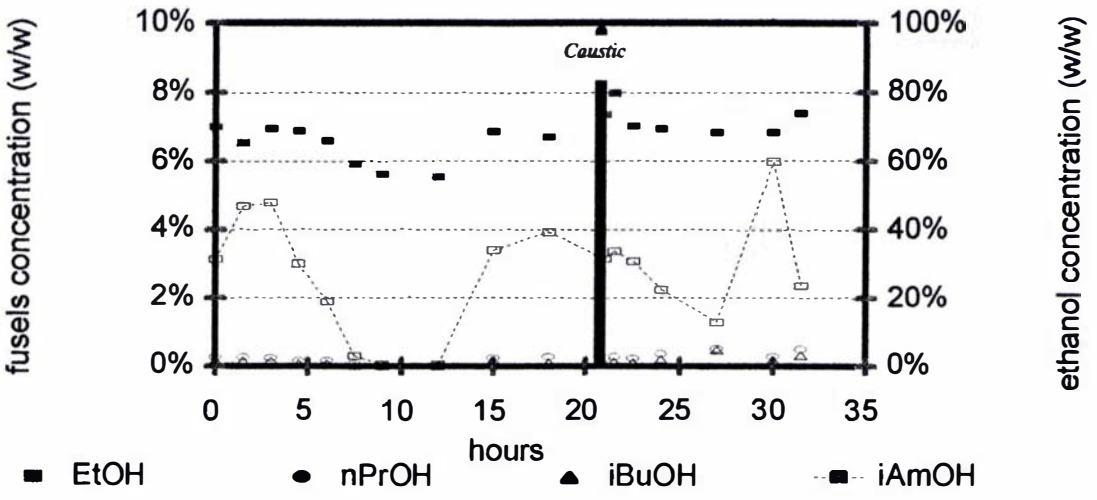

Figure IX.25 Variation of the concentration of ethanol and fusels from plate 9 at BC2 on between the 15th and 16th of October, 1997. EtOH: ethanol; iAmOH: *i*-amyl alcohol; iBuOH: *i*-butanol; nPrOH: *n*-propanol. The line marked caustic indicates the time that the column was shut for caustic cleaning.

The cyclic behaviour of column BC2 invalidates any attempt to simulate it with a steady state program. The consequence of the discrepancy between the simulation results of BC2 and its real profile and the impossibility of conducting tests on site mean that all results on the effects of pervaporation on distillation (Chapter XI) and on the effects of changing operation parameters (Chapter X) should be considered with care. In general, the trends observed in the simulations should be reliable though absolute results might be quite different from reality.

IX.4.3 Test of ChemSep® against a MatLab® program

Both ChemSep® and MatLab® were used to generate the composition profile of a fictitious column for water, ethanol, and *i*-butanol (Appendix E). The column had no reboiler or condenser: the liquid feed stream entered at the top of the column and steam was injected at the bottom. The objective of this test was to verify the ability of both programs to deal with trace components. Table IX.2 lists the concentrations of each component at the liquid phase calculated with both ChemSep® and MatLab®.

Between stages 14 and 20, the profile given by MatLab® was consistent with the equilibrium correlation, the concentrations of ethanol and *i*-butanol decreased down the column at a steady rate, furthermore, the K-value (ratio of vapour over liquid concentration) for ethanol and *i*-butanol was constant along the column, at 14 and 29, respectively. On the other hand, ChemSep® showed a discontinuity between stages 16 and 17 for *i*-butanol and between stages 18 and 19 for ethanol. There are no apparent reasons for such discontinuity as no feed or side streams were assigned near these stages. According to Taylor (1996) the column was oversized and the output values are so low that differences between them are meaningless.

Table IX.2 MatLab® and ChemSep® liquid concentration profile for a fictitious column distilling water, ethanol, and *i*-butanol. Discontinuity in Chemsep® data is noted in blue (see text).

	MatLab®			ChemSep®		
stages	**water**	**ethanol**	***i*-butanol**	**water**	**ethanol**	***i*-butanol**
1	0.957	4.08e-02	2.04e-03	0.997	0.002889	7.574E-05
2	0.995	5.25e-03	1.39e-04	0.9996	0.0003914	5.285E-06
3	0.999	6.38e-04	8.75e-06	0.9999	5.254E-05	3.645E-07
4	1	7.70e-05	5.47e-07	1	7.045E-06	2.51E-08
5	1	9.29e-06	3.41e-08	1	9.443E-07	1.728E-09
6	1	1.12e-06	2.13e-09	1	1.266E-07	1.19E-10
7	1	1.35e-07	1.33e-10	1	1.697E-08	8.193E-12
8	1	1.63e-08	8.27e-12	1	2.274E-09	5.641E-13
9	1	1.96e-09	5.15e-13	1	3.049E-10	3.883E-14
10	1	2.36e-10	3.21e-14	1	4.087E-11	2.674E-15
11	1	2.85e-11	2.00e-15	1	5.478E-12	1.841E-16
12	1	3.44e-12	1.25e-16	1	7.343E-13	1.268E-17
13	1	4.14e-13	7.79e-18	1	9.843E-14	8.779E-19
14	1	4.99e-14	4.86e-19	1	1.319E-14	6.544E-20
15	1	6.02e-15	3.03e-20	1	1.769E-15	9.499E-21
16	1	*7.25e-16*	*1.89e-21*	1	*2.372E-16*	*5.441E-24*
17	1	*8.74e-17*	*1.18e-22*	1	*3.19E-17*	*7.451E-12*
18	1	*1.05e-17*	*7.35e-24*	1	*4.381E-18*	*7.451E-12*
19	1	*1.25e-18*	*4.57e-25*	1	*1.49E-10*	*7.451E-12*
20	1	*1.37e-19*	*2.70e-26*	1	*1.49E-10*	*7.451E-12*

IX.5 Conclusions

The distillation columns at the NZDCL were simulated with a commercial package, ChemSep®, that had achieved convergence for large, complex distillation schemes. Of the available calculation modes, it was chosen to use Murphree stage efficiencies. Experimental data collected at NZDCL were used in fitting of the column stage efficiencies as well as in testing the reliability of the simulations. Variations in the Murphree efficiency at varying column operating conditions confirmed that, whenever stage efficiencies are used, the results obtained are only applicable for columns operating at similar conditions.

Overall, there was good agreement between the calculated and experimental concentration profiles of ethanol. Although the program results showed good agreement with the concentration profile of fusels presented in the literature (Pyke, 1965), it generally underestimated the quantity of fusels being eliminated from the system through the distillate and side streams of PC, ED, and RC. It was postulated that the cyclical behaviour of the BC column and the occurrence of flow regimes that interfered in the column's separation ability invalidated any attempt to simulate it with a program that was developed for steady state conditions and that relied solely on thermodynamic relationships to explain separation.

Given these limitations, the use of the ChemSep® program in evaluating the effect of changes in operation parameters and the introduction of a pervaporation step to the distillation scheme is limited to the following conditions:

- For pervaporation with organophilic membranes, if the simulation data is used in selecting a membrane area, the tendency of ChemSep® to underestimate the concentration of fusels will lead to the selection of a unit with a separation area which is smaller than what would be required to perform the job on site. However, the program can be reliably used to compare the performance of distillation alone versus pervaporation-aided distillation, since the aim of this exercise is to evaluate whether pervaporation would be able to reduce the concentration of fusels to such an extent as to fully eliminate the need for the ED column. In case the simulation indicates that pervaporation can successfully eliminate the ED column, it would also be imperative to examine the effect of pervaporation on situations where the concentration of fusels is at least twice as high as that originally estimated with ChemSep®. This can be easily accomplished by simulation.
- In evaluating the effects of changes in the operating parameters on distillation, apart from verifying the changes in energy usage, the secondary objective is to estimate relative changes in internal flow rates and product concentration. For the BC column, given that it already operates at twice its design flow rate, any indication of an increase in the internal vapour flow rate is likely to imply in a further decrease of the contact time between the two phases in BC2, thus impairing its separation ability. In this case it would be appropriate to question the quality of the distillate predicted under such conditions.

Keeping these limitations in mind, the program is certainly adequate for the task proposed.

Chapter X

PINCH ANALYSIS

X.1 INTRODUCTION

The objective was to analyse the present degree of process integration at the NZDCL and to seek opportunities for further energy savings arising from modifications to the existing process or from optimization of the heat exchanger network. The analysis was performed from a heat and mass balance for the site, which comprises the fermentation and distillation operations, and the total amount of water and steam consumed by NZDCL, plus the main operations at the neighbouring Bay Milk site, using a pinch analysis program (Hero®). A brief description of the principles involved in pinch analysis was given in Section VII.4.

X.2 PROCESS DESCRIPTION

Figures X.1 and X.2 show a simplified process diagram of the present fermentation and distillation operations at NZDCL, respectively. Both the fermentation and the distillation processes operate 24 hours daily for 43 weeks of the year. Fermentation is a batch process and there are six fermenters in total. Distillation operates continuously, however, due to the precipitation of calcium salts on BC1, this column must be cleaned at least every 30 hours. Besides the BC columns, the fermenters and the RO plant are also cleaned periodically using excess water (not recovered) from the RC column.

The whey from Bay Milk is first concentrated in the reverse osmosis (RO) plant, pasteurised using indirect heat from the bottoms stream of BC, and then fermented. The resulting fermented beer is concentrated on the boiling columns (BC1 and BC2). Removal of fusel oils and concentration to the required level of ethanol content (95% v/v) is achieved by the purification (PC), extraction (ED) and rectifying (RC) columns (Chapter

VII). Heat to perform the separation is provided by steam purchased from the Bay Milk site.

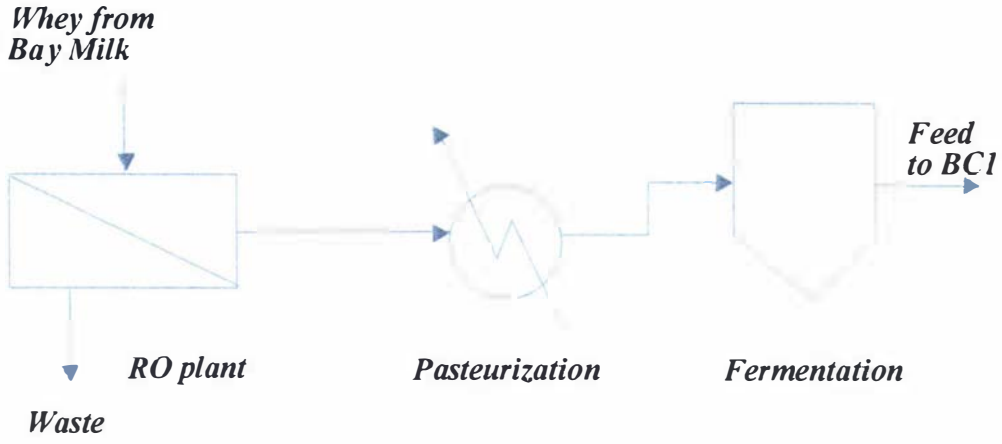

Figure X.1 Simplified process diagram of the fermentation operation at NZDCL.

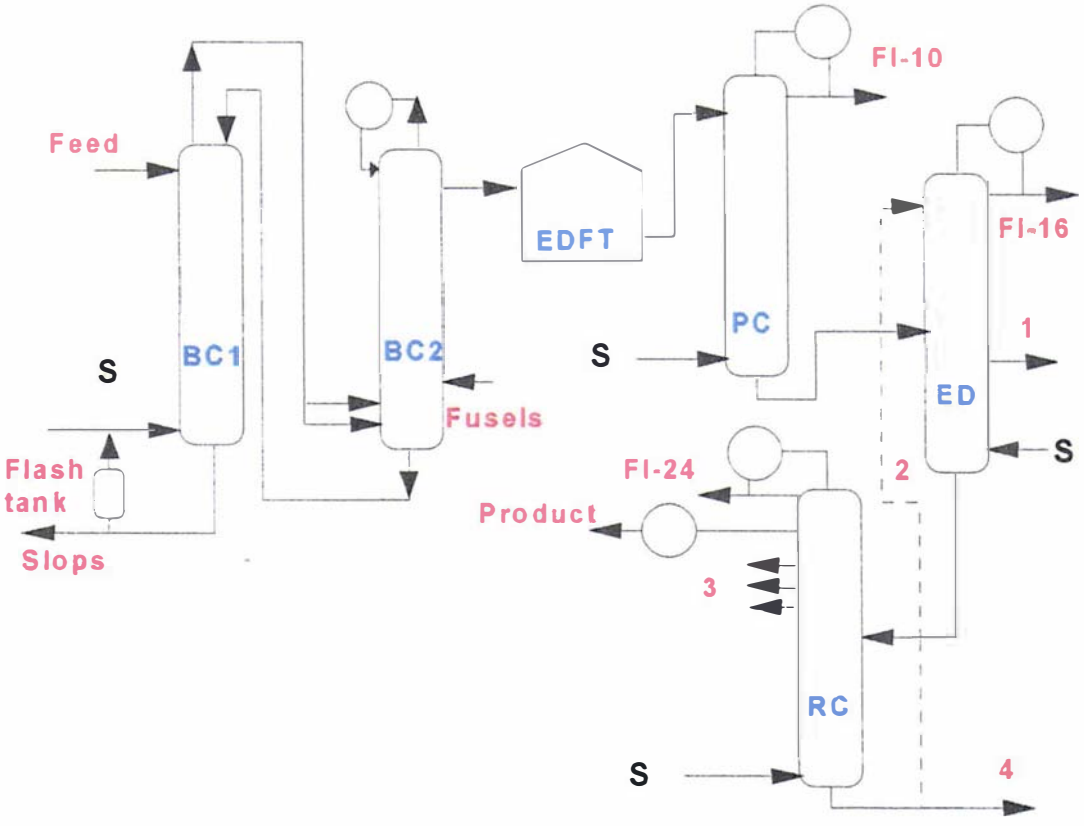

Figure X.2 Simplified process diagram of the distillation operation at NZDCL. **1**: side stream from ED; **2**: water to ED; **3**: side-streams from RC (*FI-21, FI-22, FI-23)*; **4**: excess water from RC; **S**: steam.

X.3 Mass and Heat Balance

The overall mass balance for the NZDCL is summarized in Table X.1. The values used in the overall mass balance of NZDCL were obtained from the operation workers and represented typical values during the whey season (August 1994 through May 1995). The total steam required by NZDCL was included in the mass balance. Prices of cooling water and steam were based on the values for the first half of 1995. Minor waste streams were not included in the calculations, so there is a slight difference in the overall mass balance. The amount of steam used in the fermentation site was neglected since it is very small in comparison to the amount used in the distillation.

Table X.1 Overall mass balance for the NZDCL distillation site. The data were based on operation 24 hours a day, 7 days a week, 43 weeks a year.

Stream (Figure X.2)	Flow In ($kg.h^{-1}$)	Flow Out ($kg.h^{-1}$)	ethanol (mol fraction)	Cost (NZ$/year)
steam	7,500		0	1,428,727
cooling water (whole site)	232,000	232,000	0	50,310
feed - BC1	44,500		0.02 (w/w)	
slops		48,000	0	
product - BC2		900	0.75	
Feed - PC	1,200		0.75	
FI-10		10	0.79	
FI-16		30	0.31	
water from RC		9,800	0	
water to ED	6,800		0	
FI-24		30	0.88	
product - RC		1,000	0.88	
Total*	60,000	59,770		

* excluding cooling water.

The mass balance data for the Bay Milk sites were available from the report by Watson (1993), but cannot be reproduced here for reasons of confidentiality. This report only considered the ultrafiltration (UF) and anhydrous milk fat (AMF) operations at Bay Milk.

From the overall mass balance it can be seen that steam is a major cost. Steam is used in the distillation site both as a source of energy and as an aid in the separation of fusels from the ethanol/water mixture. The energy entering the distillation system with the steam must largely exit through the condenser load. Therefore, the amount of cooling water used in the site is essentially proportional to the amount of steam necessary for the separation. Existing heat recovery is limited to the steam flashing of the BC1 slops stream back into BC1, heat recovery from the BC1 slops stream for the pasteurization of incoming whey, use of the excess water from the RC column for cleaning the RO plant and the fermenters, and feed pre-heating using the heads of the BC1 and BC2 columns.

For the pinch analysis, flows and concentrations of intermediate distillation streams that are heated or cooled were required. The values of concentration and mass flow rate, given in Table X.2, were obtained by using Hysim® to simulate the process. In this simulation, only water and ethanol were considered. This simplification was considered acceptable as ethanol and water were by far the main components of the feed stream (over 99.9% of the total feed stream) and the main objective of this exercise was to generate data on flow rate and energy content of intermediate streams rather than to consider separation of fusels.

Table X.2 Intermediate NZDCL stream values estimated from a Hysim® simulation.

Stream	Flow ($kg.h^{-1}$)	ethanol (mol fraction)
Head BC1	4,100	0.14
Head BC2	3,400	0.80
Reflux PC	400	0.79
Reflux ED	2,100	0.31
Reflux RC	3,000	0.88

Table X.3 gives an overall heat balance for the NZDCL distillation site, excluding cooling water. The difference in the heat balance corresponds to the load recovered by the cooling water.

Table X.3 Overall mass and heat balances for the distillation site at NZDCL. Reference temperature 0°C.

	Stream	Flow rate ($kg.h^{-1}$)	c_p ($kJ.kg^{-1}.K^{-1}$)	T (°C)	Energy ($MJ.h^{-1}$)
Inlet	**Steam**	7,500	2,700	207	20,160
	Feed to BC1	44,500	4	34	6,230
Outlet	**Product**	1,000	3	36	108
	Excess RC water	3,000	4	110	1,320
	Slops	48,000	4	95	18,240
Difference		0			6,722

Table X.4 shows the distribution of cooling water usage for the whole NZDCL site. The amount of cooling water used in the distillation site was estimated from the overall heat balance, assuming that the water enters the site at 15°C and leaves at either 45°C for the distillation site or at 30°C for the fermentation site. On the distillation site, cooling water is used in the column condensers and for cooling the final product. The total amount of cooling water used in the fermentation site was calculated as the difference between the total amount of water entering the plant (Table X.1) and the total amount of water used in distillation. On the fermentation site, water is used for maintaining the temperature of the fermenters at 35°C and for cooling the whey after pasteurization. Since the pasteurization heat balance was well known, the amount of water used for cooling the fermenters was calculated as the difference between the total and the amount used in pasteurization (Table X.4).

Table X.4 Distribution of cooling water usage in the NZDCL site. The water enters at 15°C and leaves at approximately 45°C (distillation) or 35°C (fermentation).

	Flow rate ($kg.h^{-1}$)			Energy ($MJ.h^{-1}$)
Total cooling water	232,000			
Distillation site	56,000			6,722
Fermentation site	176,000	**fermenters (all)**	93,975	7,500
		pasteurization	82,328	6,586

Heating needs at the fermentation site include general cleaning as well as pasteurization. A recirculating, closed water circuit, heated by the bottoms of BC1 (slops), is used for pasteurization of the whey. Of the total water recovered on the rectifying column, some is returned to the extraction column, and the excess (about 3 $tonnes.h^{-1}$) is used on the fermentation site for cleaning. This water is stored at 80°C and about half is used for cleaning the fermenters. If the temperature of the water becomes lower than 70°C, then extra heating is accomplished by steam injection because the minimum temperature required is 65°C. The other half of the excess water is cooled to 45°C and used for cleaning the RO membranes. The amount of steam used in the fermentation site was neglected since it is very small in comparison to the amount used in the distillation.

Table X.5 summarizes all the NZDCL streams required for the pinch analysis, including information on their required temperature variation. The total heating needs of the distillation train were defined from the steam injection requirements for each column. It was assumed that heat yielded by steam equals its latent heat of condensation only. The total column heat requirement is distributed approximately 64.5% for the BC columns, 2.5% for the PC column, 14.5% for the ED column, and 18.5% for the RC column.

Table X.5 Summary of existing utilities and hot and cold streams at NZDCL.

Site Location	Stream	no.	Heat capacity flow rate* ($MJ.K^{-1}.h^{-1}$)	T_{in} (°C)	T_{out} (°C)	
Utility	**steam**		20,160	207	207	U
	cooling water (fermentation)		375.9	15	35	U
	cooling water (pasteurization)		329.3	15	35	U
	cooling water (distillation)		224	15	45	U
Fermentation	**beer at fermentation**	**(1)**	7,500	35	34	H
	cleaning of RO	**(2)**	6	15	45	C
	cleaning of fermenters	**(3)**	6	15	65	C
	beer to pasteurization	**(4)**	178	48	72	C
	beer after pasteurization	**(5)**	178	72	35	H
Distillation	**column heating**	**(6)**	20,160	207	208	C
	beer to distillation	**(7)**	178	34	68	C
	slops	**(8)**	192	95	15	H
	product BC2	**(9)**	3	79	53	H
	excess water (RO cleaning)	**(10)**	6	110	15	H
	excess water (fermenter cleaning)	**(11)**	6	110	15	H
	product RC	**(12)**	3	80	36	H
	head BC1	**(13)**	4,094	110	109	H
	head BC2	**(14)**	1,958	79	78	H
	head BC2 (water cooling)	**(15)**	1,117	79	78	H
	reflux PC	**(16)**	380	80	79	H
	reflux ED	**(17)**	1,995	89	88	H
	reflux RC	**(18)**	2,850	79	78	H

H: hot stream, requires cooling; C: cold stream, requires heating; U: utilities.

* heat capacity flow rate is the product of mass flow rate and specific heat capacity.

X.4 Pinch analysis

Two pinch analyses were performed. The first looked at the overall NZDCL site and evaluated how well integrated the process streams are assuming that the distillation train could not be altered. As part of this study, the possibility of process integration between the NZDCL and Bay Milk sites was investigated. The second analysis considered changes in the distillation scheme. The two changes considered were an increase in the temperature of the feed to BC1, and the use of heat pumping.

X.4.1 Pinch analysis of the NZDCL and Bay Milk sites

The composite curves of the NZDCL and Bay Milk sites individually, and for both sites combined were constructed using the Hero® software using the observed minimum temperature approach for heat exchange of 23°C for NZDCL streams, 10°C for Bay Milk streams and 10°C for the combined analysis (Figures X.3 to X.5). Details of the process streams used in this analysis are given in Table X.5, and for the Bay Milk site in Watson (1993). The hot and cold utility targets determined from the composite curves are summarized in Table X.6.

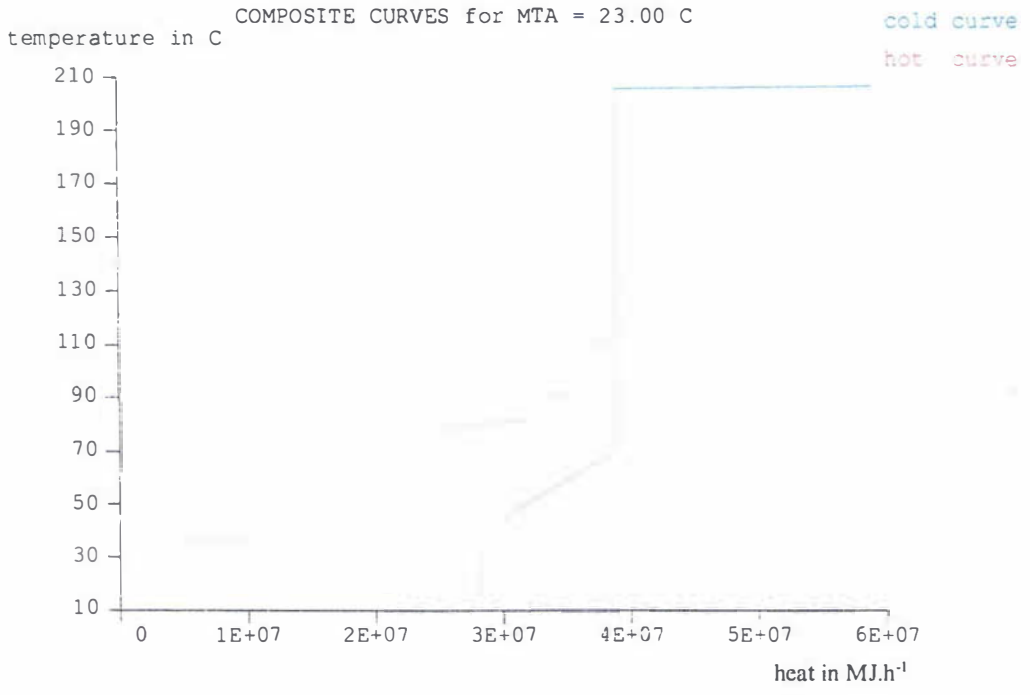

Figure X.3 Composite curves for the NZDCL site alone.

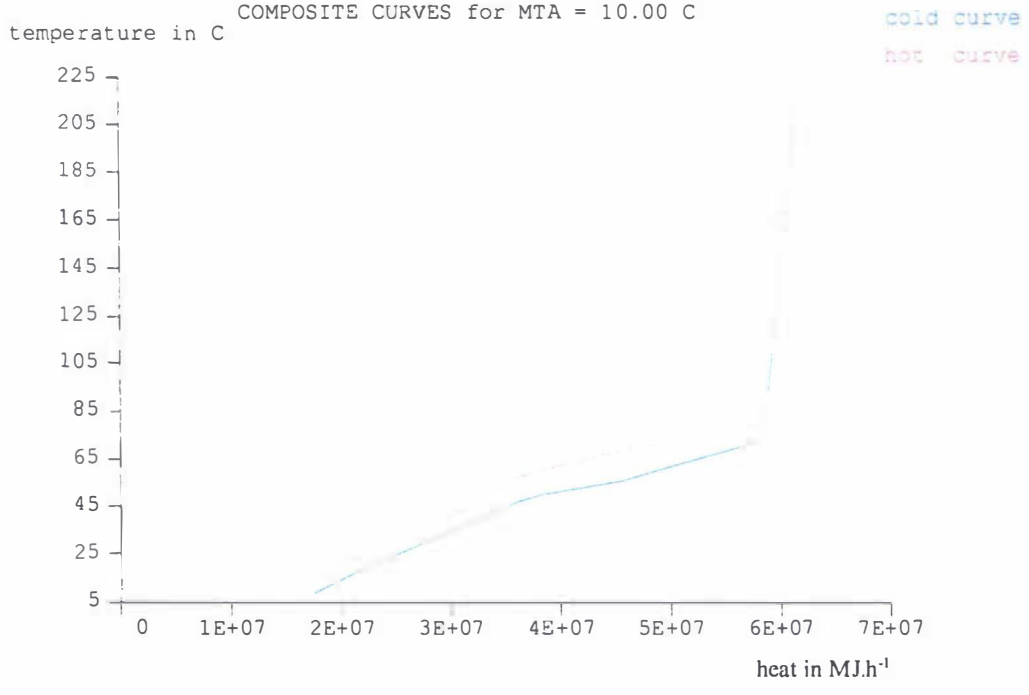

Figure X.4 Composite curves for the Bay Milk site alone.

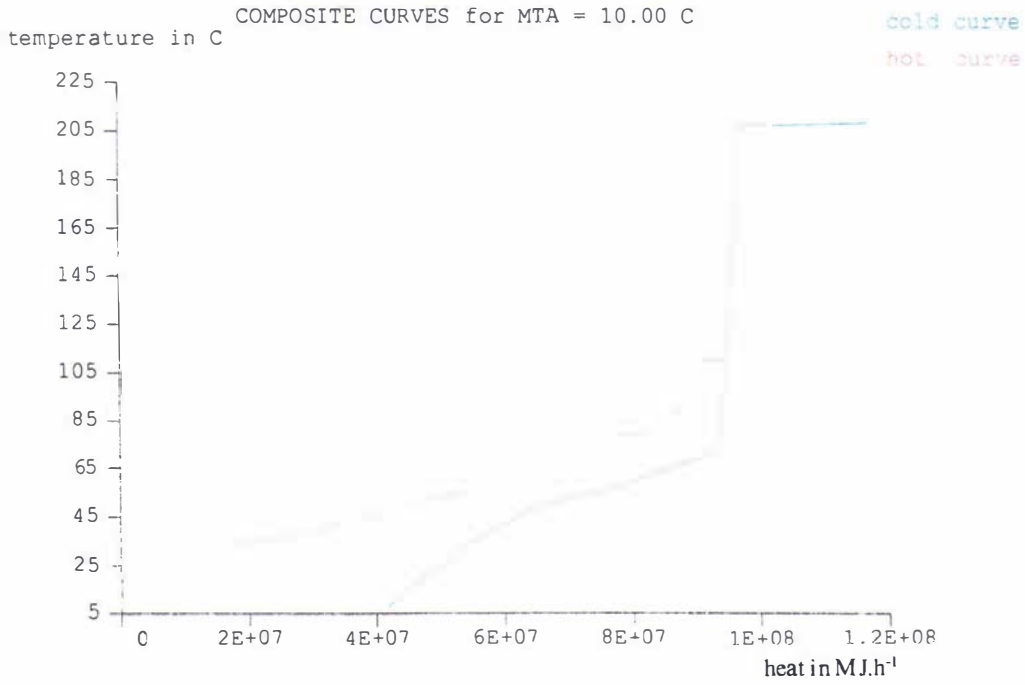

Figure X.5 Composite curves for the combined analysis of the Bay Milk and NZDCL sites.

Table X.6 Summary of hot and cold utility targets for the NZDCL and Bay Milk sites.

Site	MTA (°C)	Pinch temperature (°C)	Cooling Target ($MJ.h^{-1}$)	Heating Target ($MJ.h^{-1}$)
Current NZDCL utilities use			20,808	20,160
Target for NZDCL alone	23	110-87	32,564	20,160
Target for Bay Milk alone	10	60-50	17,187	10,298
Target for NZDCL and BM from separate analysis			49,751	30,458
Target for BM and NZDCL from combined analysis	10	110-100	41,910	22,795
Difference in combined targets			7,841	7,663
Target for NZDCL with feed pre-heated to 90°C	17	95-78	28,648	15,860

MTA: minimum temperature approach; NZDCL: New Zealand Distillery Co. Ltd.; BM: Bay Milk.

As expected, the hot utility target for NZDCL alone equalled the amount of steam presently being used. The minimum cold utility target was greater than the current cold utility usage by approximately 11,750 $MJ.h^{-1}$. The extra cooling is currently provided by losses to the ambient, particularly from discharge of slops to waste treatment well above 15°C and heat losses from the RC excess water from 110°C to 65 or 45°C.

Figure X.6 depicts the present heat exchanger network (HEN) at NZDCL. According to the rules of pinch analysis, to meet the minimum targets, heat should not be exchanged across the pinch, except with the use of a heat pump. The existing network meets these requirements. Although is seems that stream pairs 10 - 3 and 11 - 2 violate the minimum temperature approach, these streams are in fact the same and so the *"heat recovery"* can occur with zero temperature difference. In the analysis, they were kept separate so the possibility of their use for heat recovery in other areas would not be missed. The HEN also shows stream 8 (slops) being discharged at 73°C. In reality, it is discharged to waste treatment at about 40°C indicating that substantial heat losses occur within the NZDCL site. The ambient coolings of streams 8 to 11 are shown explicitly.

With the present distillation train operation there is an excess of waste heat on the NZDCL site so all heating requirements other than the steam heating of the distillation column can be provided by heat exchange with hot streams, with an approach temperature of 23°C or greater. Note that the true minimum temperature approach is smaller than 23°C because the indirect heat recovery using the closed water circuit between the slops and the beer to be pasteurized has two separate heat exchanging steps, but has been represented here as a single, direct heat exchanger. The minimum temperature aproach for each of the heat exchangers in the closed loop is therefore about 10-12°C. For the NZDCL site alone, the utility targets would not reduce if a smaller minimum temperature approach was used.

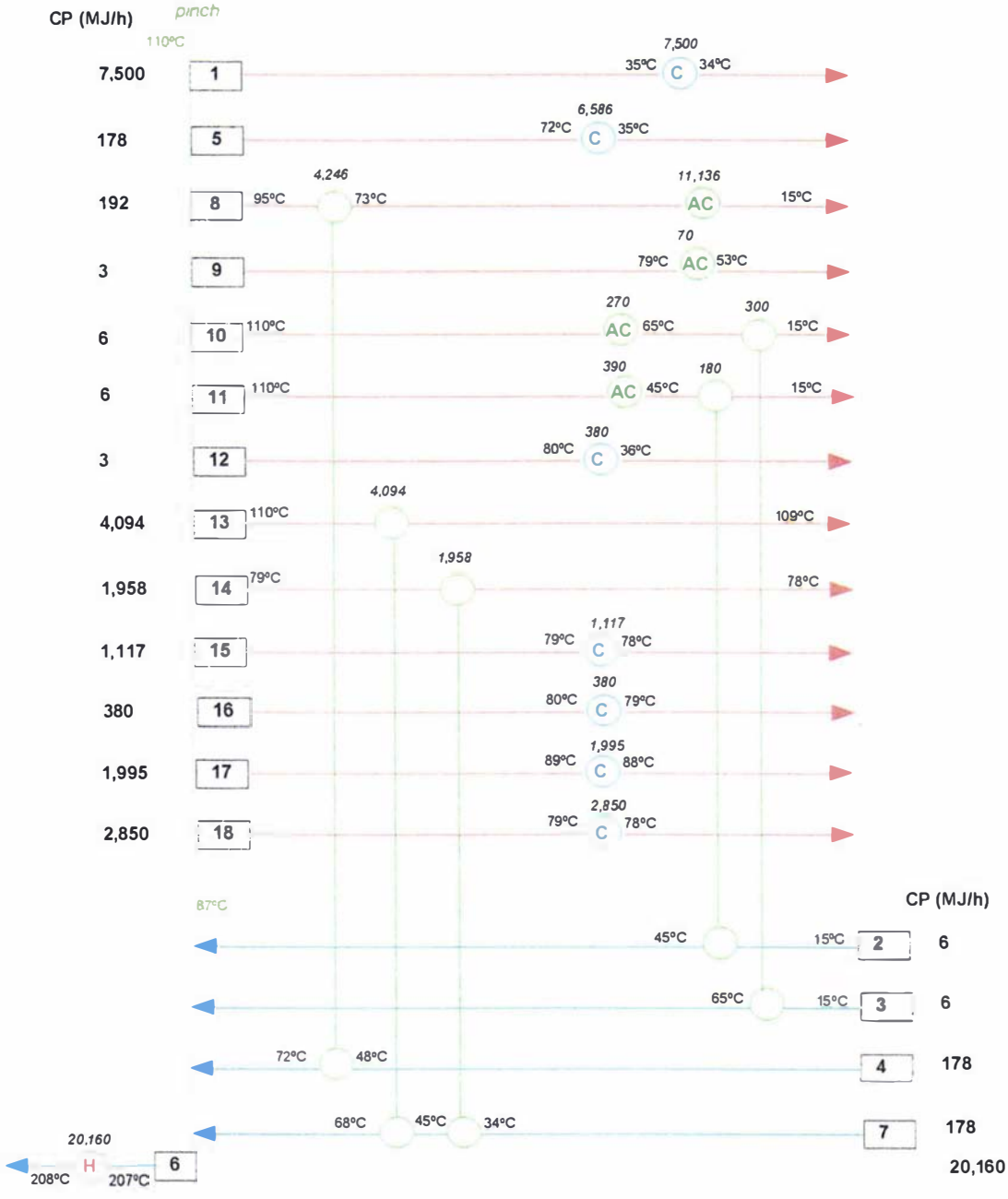

Figure X.6 Present heat exchanger network of the NZDCL site. H: hot utility requirement; C: cold utility requirement; AC: ambient cooling.

Table X.6 indicates that there is considerable opportunity for integration between Bay Milk and NZDCL sites. Such integration could save up to 7,663 $MJ.h^{-1}$ hot utility and 7,841 $MJ.h^{-1}$ cold utility. In general, the excess heat from NZDCL can be used at the Bay Milk site. The combined pinch is 110-100°C so no NZDCL hot streams exist above the pinch. Therefore, any inter-site heat recovery involving NZDCL streams can only occur below the pinch where the objective is to heat cold streams up to the pinch temperature. As none of the NZDCL cold streams require heating to the pinch temperature, any critical heat recovery must involve Bay Milk cold streams. As a first stage to assessing the potential for inter-site heat recovery, the NZDCL hot streams that could be exported were identified. Most of the hot streams are part of the distillation train which makes them difficult to export, so these were not considered further (streams 12 to 18). Of the remaining streams, only streams 5 and 8 represent significant heat loads. Therefore, the extent of practical interchange was assessed by choosing the HEN to heat the NZDCL cold streams using NZDCL hot streams; so that streams 5 and 8 could be exported at the maximum possible temperature. Such a HEN is given in Figure X.7.

In Figure X.7, the existing use of excess water (steams 10 and 11) for heating streams 2 and 3 is retained, rather than using hot streams 15 and 16 for the water heating, because it is a direct re-use and the heat flows are small. There is a small amount of heat available from the excess water before this re-use that could be exported to Bay Milk. Similarly, use of streams 13 and 14 to heat stream 7 is retained, because neither could be exported to Bay Milk, so there is no advantage in changing the existing arrangement. Hence, the main option to change the NZDCL heat recovery to maximize export to Bay Milk is to change the heating of stream 4.

Streams 17 and 18 can provide all the stream 4 heating through a indirect, recirculating, closed water circuit, with a 17°C temperature approach, thereby leaving the full heat content of streams 5 and 8 for export. An alternative would be to heat stream 4 regeneratively with stream 5. This is shown in Figure X.7a. The first option would allow greater export from the NZDCL because streams 17 and 18 are part of the distillation train so, if they are not used to heat stream 4, they can still not be used off-site. However, the

location of stream 5 at the same site as stream 4 is a significant advantage to the heat exchange between these streams and there is no need for indirect heating via a closed water circuit.

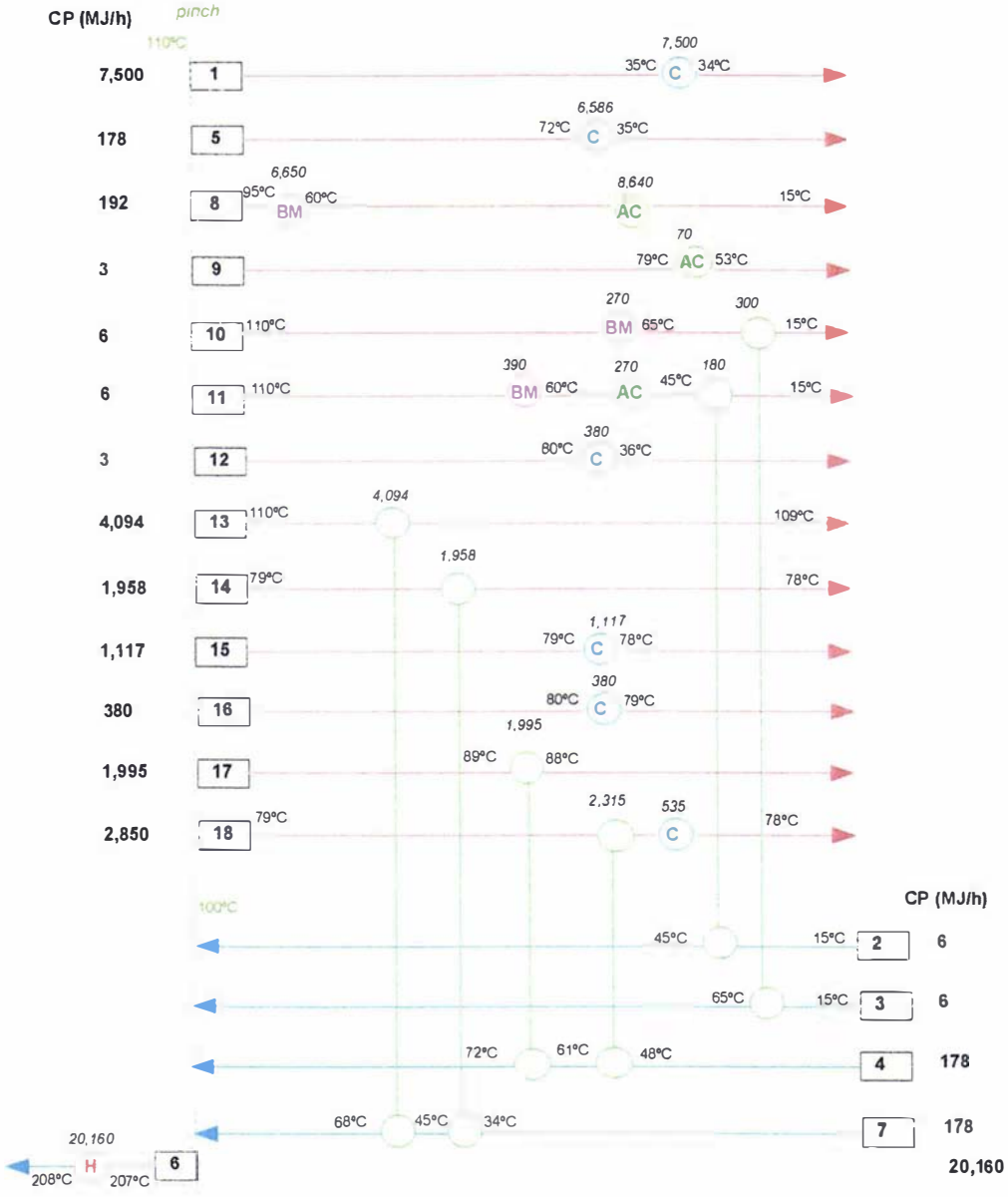

Figure X.7 Heat exchanger network for the NZDCL site including the possibility of exporting hot streams to Bay Milk (BM). H: heating requirement; C: cooling requirement; AC: ambient cooling.

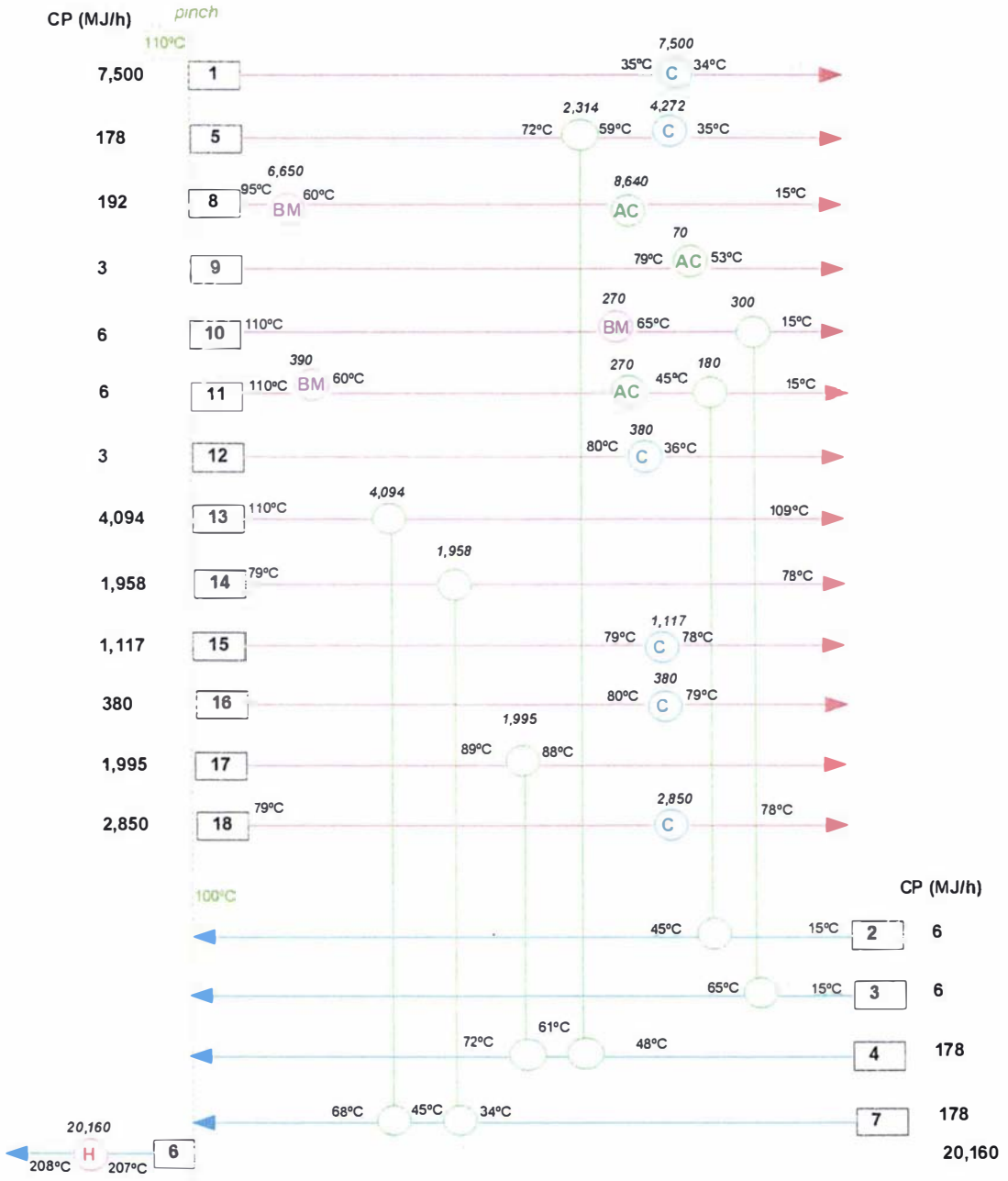

Figure X.7a Alternative heat exchanger network for the NZDCL site including the possibility of exporting hot streams to Bay Milk (BM). H: heating requirement; C: cooling requirement; AC: ambient cooling.

By adding streams 5 and 8 to a pinch analysis for Bay Milk only it can be shown that they can only be usefully cooled to about 60°C on the Bay Milk site (the pinch temperature for the Bay Milk site changes from 60°C to 73.2°C when these streams are added). This equates to 6,650 $MJ.h^{-1}$ which corresponds to 87% of the inter site heat recovery. As shown in Figure X.7, this heat can be fully provided by stream 8, therefore, there is no advantage in exporting stream 5. Similarly, export of streams 10 and 11 to cool them to 65°C and 60°C respectively could provide a further 7% of inter site heat recovery. Hence, although only a few streams were promptly available for inter-site heat recovery, most of the benefits can be achieved. At the NZDCL site, the only change from the existing heat recovery is the use of the ED and RC reflux streams to heat the beer for pasteurization. This can be accomplished by using a recirculating, closed water circuit heated by these streams similarly to that currently used between streams 8 and 4, or, alternatively, to use stream 5 for the partial heating of stream 4 in a regenerative heat exchanger.

A consequence of exporting some of the "slops" (stream 8) heat is that the energy to heat the beer for pasteurization (stream 4) would be available at a lower temperature. This would require larger heat exchangers than presently used and would add considerable complexity to the distillation plant as shown in Figures X.7 and X.7a. This aside, greater use of the slops by Bay Milk is possible but would not benefit the NZDCL site. Therefore, the full HEN on the Bay Milk site was not determined. If steam is used, this heat recovery of 6,650 $MJ.h^{-1}$ has the potential to save approximately NZ$ 1,250,000 per annum at the Bay Milk. Therefore this scheme deserves greater investigation.

X.4.2 Feed pre-heating

At the moment, feed enters the BC1 at 68°C but its bubble point is about 100°C, so there may be benefits if it is pre-heated further. Essentially, instead of the feed pre-heat being accomplished by some of the steam injected into the column, it might be possible to pre-heat it by using heat recovery. An increase in the feed temperature to the distillation column (BC1) was evaluated from the point of view of operation of the distillation column.

A simulation of the column showed that if the feed was pre-heated to 90°C then the total quantity of steam required to be injected into the BC columns would decrease by about 1,600 kg.h^{-1} of steam (25%) or about NZ$ 304,800 per annum, thus reducing the total column heating requirement from 20,160 MJ.h^{-1} to 15,860 MJ.h^{-1}. The new data for streams 6 and 7 for this situation are given in Table X.7.

Pinch analysis showed that if the feed is heated to 90°C rather than 68°C, it is possible to provide all the extra heat to the feed stream by heat recovery using other process streams if the minimum temperature approach (MTA) is reduced to 17°C or less. The new utility targets are given in Table X.7. The overall hot utility target decreases from 20,160 MJ.h^{-1} to 15,860 MJ.h^{-1}. The cold utility target also decreases from 32,030 MJ.h^{-1} to 28,114 MJ.h^{-1}. The pinch temperature is still 110 to 93°C but there is a near pinch at 95 to 78°C. A modified HEN that achieves this extra feed pre-heating is given in Figure X.8.

Table X.7 Summary of utilities and hot and cold streams at NZDCL when the feed is pre-heated to 90°C.

Site Location	Stream	Stream Number	Heat capacity flow rate* (MJ.K^{-1}.h^{-1})	T_{in} (°C)	T_{out} (°C)	
Distillation	**column heating**	(6)	15,860	207	208	C
	beer to distillation	(7)	178	34	90	C

H: hot stream, requires cooling; C: cold stream, requires heating; U: utilities.
* heat capacity flow rate is the product of mass flow rate and specific heat capacity.

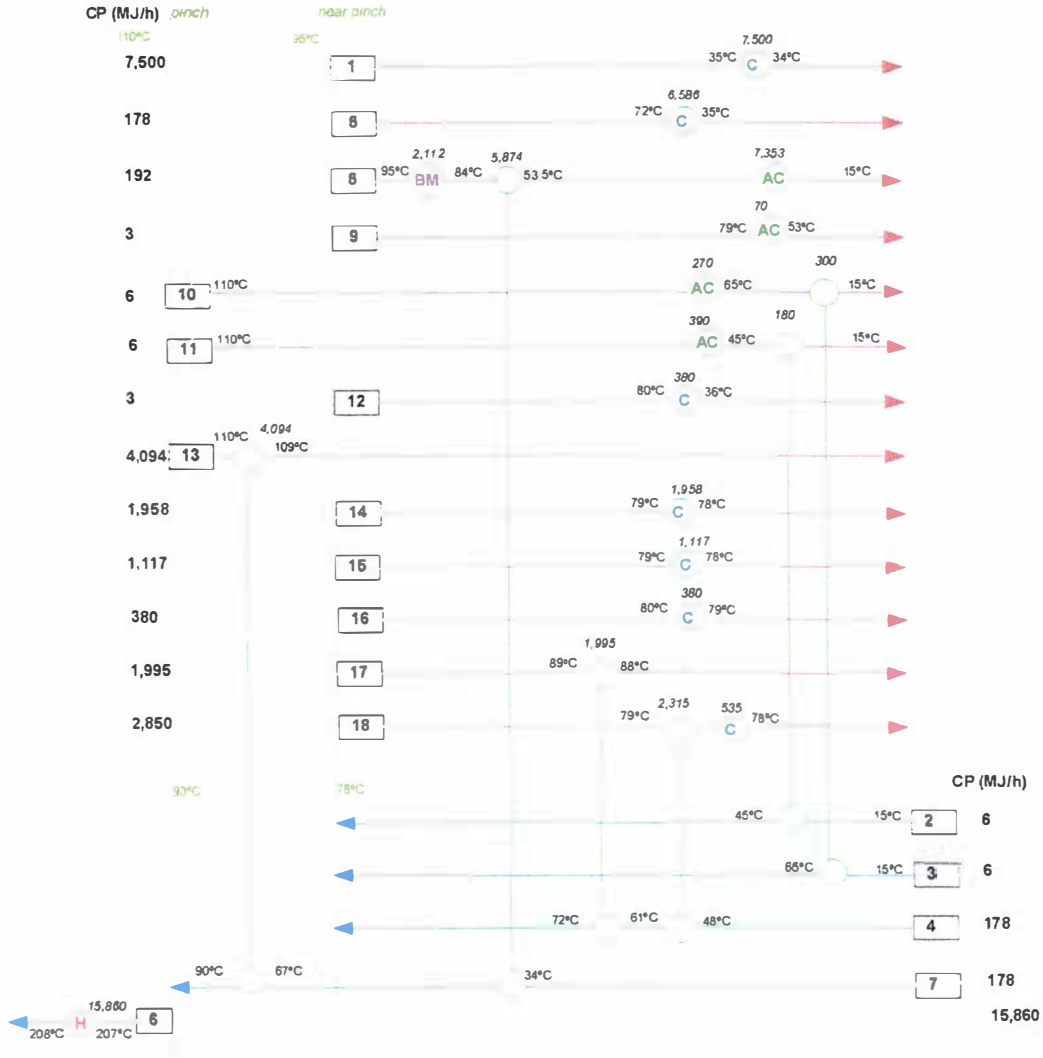

Figure X.8 Heat exchanger network of the NZDCL for a feed temperature of 90°C, steam supplied at 207°C, and MTA of 17°C.

Such a change may also influence the BC1 operation, so a full simulation of the impact of extra feed pre-heating was analysed using ChemSep®. In the calculation of the effects of the change in feed temperature, the extra energy added to the feed stream was removed from the distillation system by decreasing the amount of steam usage accordingly. The ChemSep® simulation showed that there was a reduction in the internal vapour flow rate in BC1 by approximately 25% and an approximately 10% increase in the internal vapour flow rate of BC2. The ethanol concentration of the product stream did not change significantly, but the fusel content of the product stream might increase by up to one order of magnitude, which is highly undesirable. Because BC1 and BC2 are currently operating far above design capacity and BC2 is operating well below design efficiency, it would not be advisable to further increase the vapour flow rate of column BC2, as it would further reduce the contact between phases, thus reducing its efficiency. Hence, the extra pre-heating may not be viable. If revamping or replacing columns BC1 and BC2 to accommodate the increased internal flow rates was undertaken, the increase in feed temperature should be accompanied by removal of the fusels fraction at a side stream in BC2 at the position the fusels concentrate in order to reduce their concentration in the product stream.

As shown in Figure X.8, the revised HEN requires the extra energy for increasing the feed temperature to be provided by stream 8, and would require the use of larger heat exchangers for pasteurization, as the temperature differential between the bottoms and the stream to be pasteurized would decrease from 23 to about 17°C. As in Section X.4.1 the ED and RC reflux streams could be used to heat the beer for pasteurization, which can be accomplished by using a closed water circuit heated by these streams. Alternatively, stream 5 could also be used to provide part of the heat required by stream 4 as shown in Figure X.7a. Overall, the HEN is a reasonably straight forward extension of the existing one, so a fuller economic analysis is justified. The savings in steam equate to about NZ$ 305,000 per annum. However, if pre-heat to 90°C is used, then the potential to export heat to Bay Milk is reduced from 6,650 $MJ.h^{-1}$ to approximately 2,100 $MJ.h^{-1}$, as shown in Figure X.8.

X.4.3 The introduction of heat pumps

Figure X.9 shows the grand composite curve for the NZDCL site alone for a MTA of 23 °C. At present the temperature difference between residual distillation cooling and heating requirements are too large for a heat pump to operate efficiently. If the heat to the distillation columns can be provided at 120°C rather than at 207°C and the minimum temperature approach is reduced to 5°C, then use of heat pumping may become feasible (Figures X.10). The heat pump could use water as the working fluid and would recover heat at about 72°C. It would reject it to the process at about 120°C. If the steam produced by the heat pump was to be injected into the column as at present, rather than via a reboiler, then the temperature lift would be reduced to 47°C and the efficiency of the heat pump would be maximized.

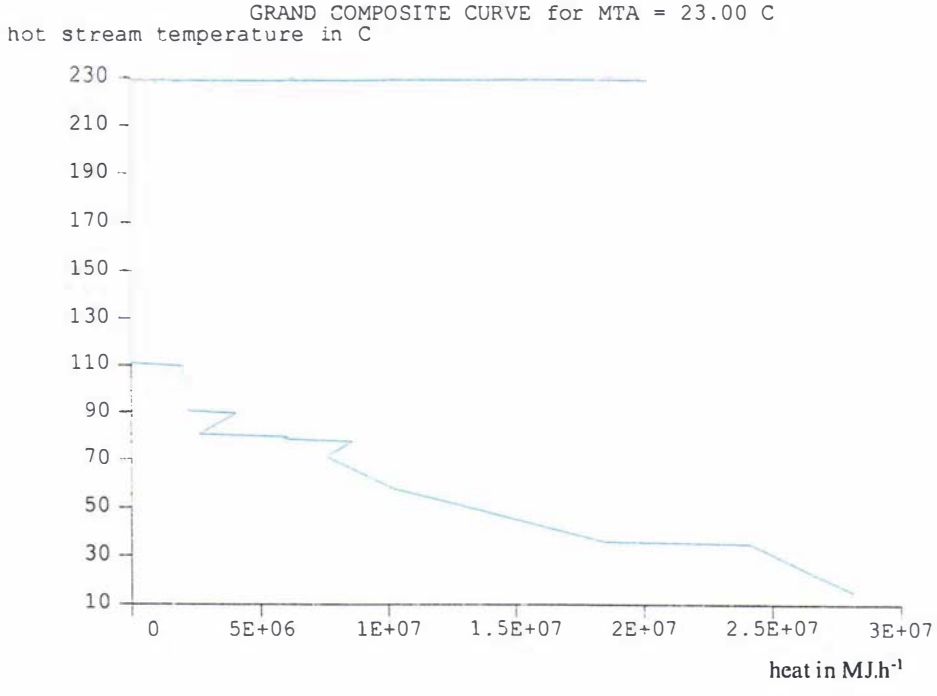

Figure X.9 Grand composite curves for the NZDCL site when steam is injected at 207°C, the BC1 feed temperature is 68°C and the MTA is 23°C.

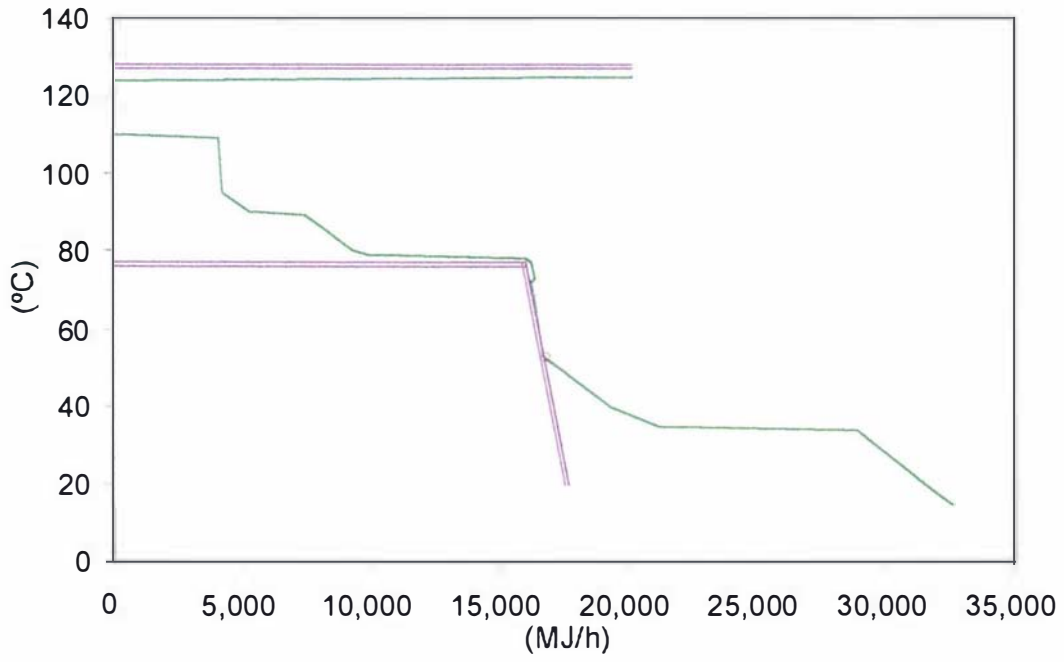

Figure X.10 Grand composite curves for the NZDCL site when steam is injected at 120°C, the BC1 feed temperature is 68°C and the MTA is 5°C showing placement of a heat pump.

Figure X.10 shows a possible scheme using an MVR heat pump to provide steam injection at 120°C. This new scheme has a potential to provide up to about 6,910 $kg.h^{-1}$ of steam (18,570 $MJ.h^{-1}$). In Figure X.11, a HEN that provides approximately 6,570 $kg.h^{-1}$ of stream through heat pumping is proposed, this amount of steam corresponds to approximately 95% of the potential identified in Figure X.10.

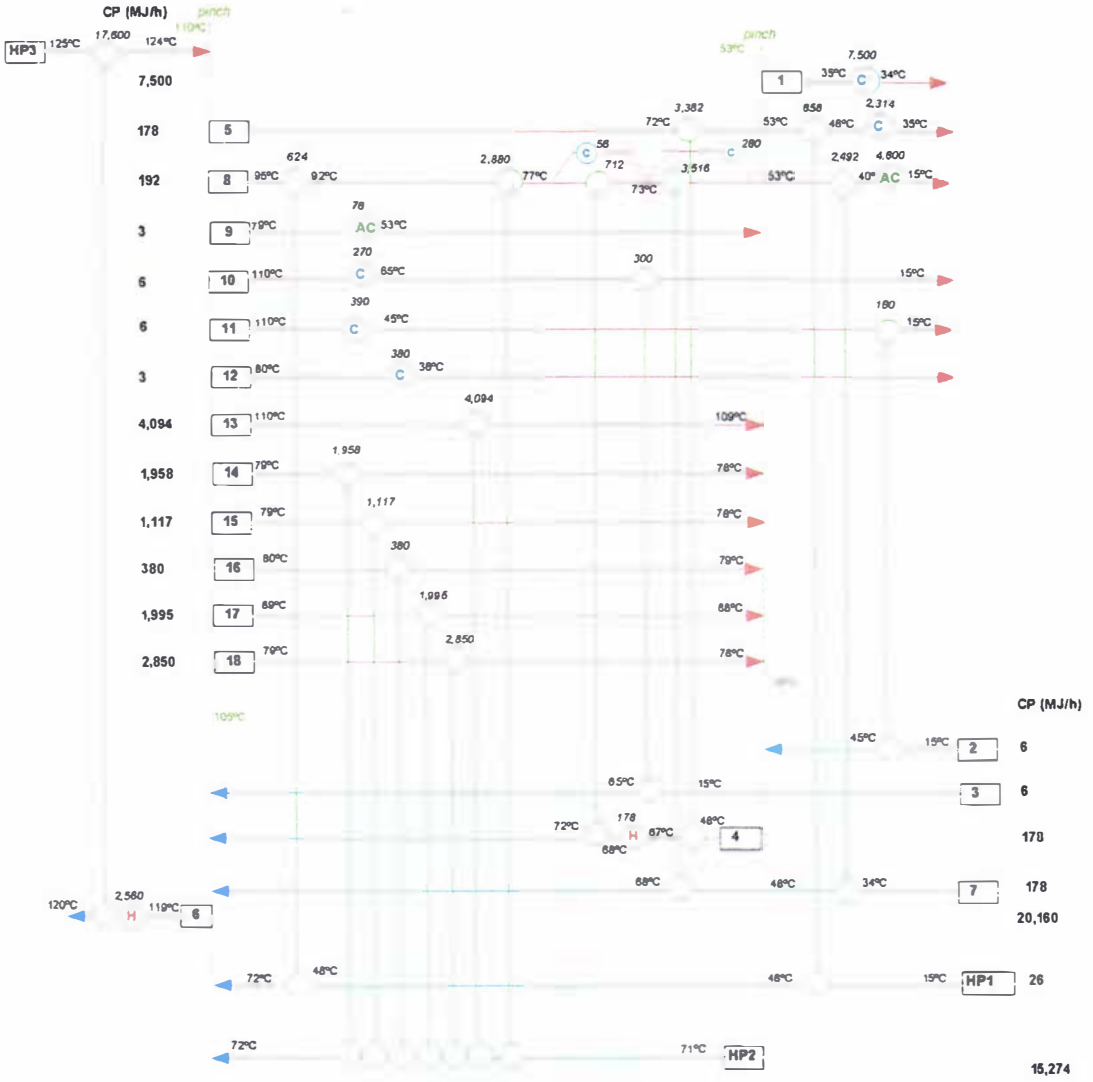

Figure X.11 New proposed HEN for the NZDCL with an MVR heat pumping for partial generation of steam.

In this proposed scheme, about 930 $kg.h^{-1}$ of steam must still be purchased. The rest of the steam is raised from water at 15°C (streams HP1 and HP2).The heating of streams 2 and 3 remains the same as in the existing HEN (Figure X.6). The pasteurization of the incoming whey (stream 4) could be accomplished by streams 5, 8, and small amount of purchased heating. The feed pre-heating (stream 7) can be fully provided by stream 8. In Figure X.11, two heat exchangers are used to represent this heat recovery. This is necessary to avoid violating the pinch analysis principles, however, in practice only one heat exchanger would be required on site. The excess heat from streams 5 and 8 could be used to raise the water temperature from 15 to 72°C (stream HP1) and stream 8 would also be used for some vapourisation of the steam (stream HP2). The heat from the reflux streams of columns PC, ED, RC, BC2 and the BC1 head (streams 13 to 18) are all required to provide the necessary heat to vapourize the pre-heated water stream (stream HP2). The temperature lift could be provided by an MVR heat pump (stream HP3). However, with a temperature lift of 47°C and an estimated coefficient of performance (COP_m) of approximately 7.2, the compressor economics must be assessed with care. A previous study carried out by Fieldes (1990) showed that the modifications required for the introduction of an MVR unit into the BC1-BC2 columns only would result in a pay-back time of approximately eight years, whereas for the increase in feed temperature alone, only six months are required. Figure X.12 shows the HEN in a flowsheet form.

In order to accomodate the MVR heat pumps, the following changes are also necessary:

- the pasteurization of the incoming whey would need to be accomplished by heat recovery with streams 5 and 8, but at a lower MTA than at present, and would thus require a higher number of heat exchangers and a larger overall heat exchange area;

- the feed pre-heating to 68°C would no longer be possible by heat recovery from streams 13 and 14, as these streams must be used for steam generation or their use would violate the pinch principles (the heat transfer from stream 14 to stream 7 crosses the pinch);

- since the vapourization of the water stream would be performed mostly by the reflux streams,vacuum condensers would be required for streams 13 to 18.

It would also become impossible to export any heat to the Bay Milk site and it would not be worthwhile to further pre-heat the feed to BC1.

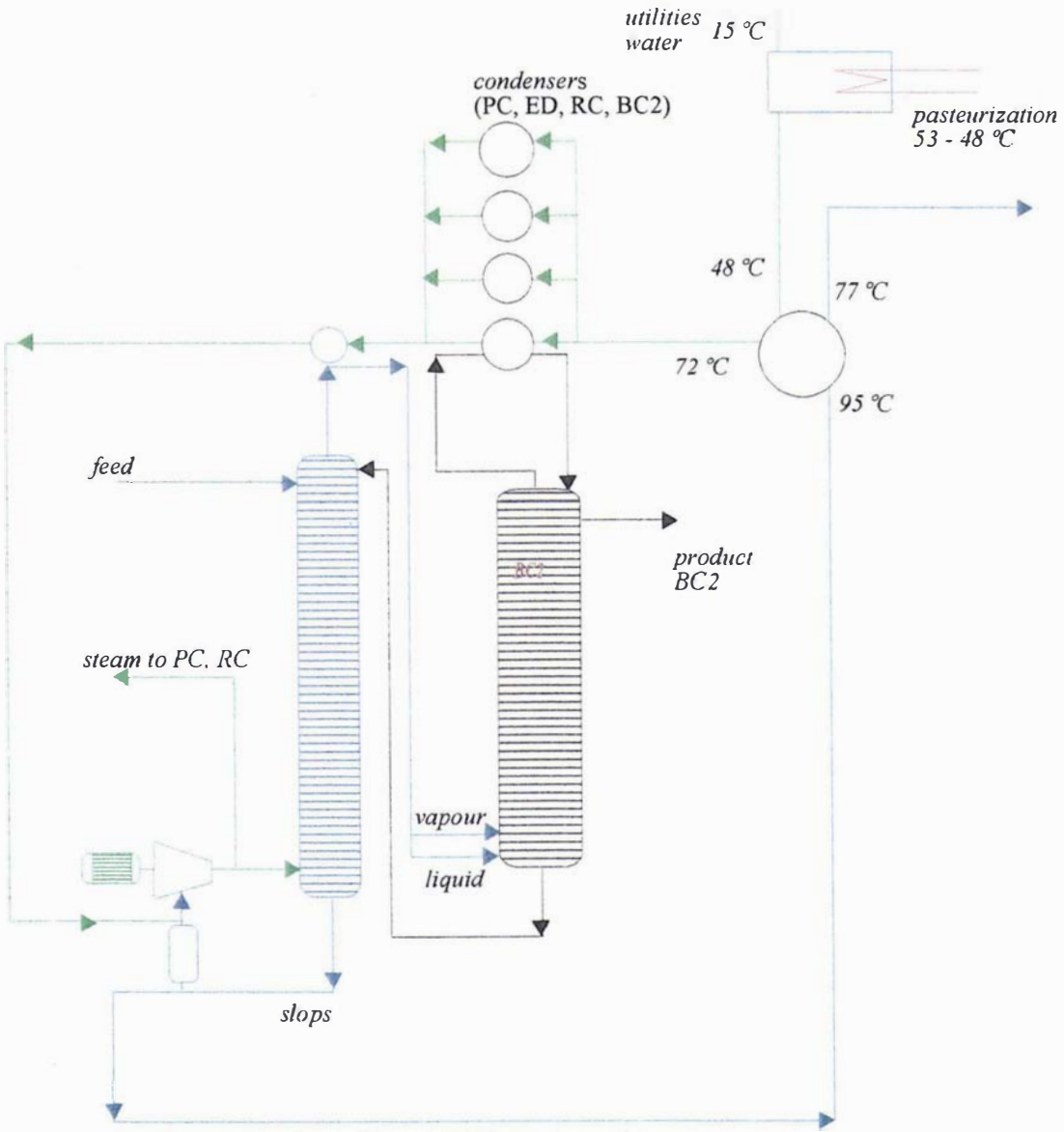

Figure X.12 Flow diagram for the BC columns when steam is partially generated by an MVR heat pump.

In general, the introduction of the MVR would significantly increase the complexity of the NZDCL. However, it could provide the steam requirements of all columns except for the ED column (Figure X.12). This would result in savings of approximately NZ$ 1,250,000 per annum in the purchase of steam. The feed pre-heating and integration with Bay Milk appear to offer greater cost reduction with greatly reduced complexity and capital cost.

X.5 Conclusions

The mass and heat balances show that steam for the distillation train is a major production cost and the pinch analysis indicated that the maximum amount of heat recovery was presently being used by NZDCL. Significant practical opportunities for further heat integration exist in combination with the Bay Milk site (NZ$1,250,000 per year), patently by exporting the slops stream and by tightening the heat recovey regimes.

Other process changes such as an increase in the feed temperature and use of heat pumps could also reduce the amount of steam necessary to produce ethanol. For example, increasing the feed temperature to 90°C has a potential to reduce the steam usage by 1,600 $kg.h^{-1}$ (about NZ$ 304,800 per year), but will require some modification of the HEN. Also, this change may adversely increase the fusel content in the BC2 product and the internal vapour flow rate of BC2. The use of a MVR heat pump could reduce the need for purchased steam by approximately 6,910 $kg.h^{-1}$ of steam (about NZ$ 1,316,000 per year), but would have significant capital cost. With the heat pump option, further pre-heating of the feed to the distillation columns and less heat export to Bay Milk is viable. Either option would require more detailed investigation on the impact of increased internal flow rates in the operation of BC1-BC2 and on the pay-back time for the modifications required.

Overall, the options studied offer considerable cost savings protential, and it is recommended that their economic feasibility is studied further.

Chapter XI

PERVAPORATION-AIDED DISTILLATION

XI.1 INTRODUCTION

Given that the enrichment factors of pervaporation with hydrophobic membranes at elevated ethanol concentrations did not differ significantly from the enrichment factors of evaporation, it is unlikely that the addition of a pervaporation unit to the purification process at NZDCL will give any significant improvement in the separation performance of distillation. The simulations run for this chapter had therefore the following objectives:

- ❖ verify and confirm the above hypothesis;
- ❖ investigate the effect of the module positioning in the membrane area requirements;
- ❖ investigate any other viable alternatives for pervaporation-aided distillation.

XI.2 PERVAPORATION-AIDED DISTILLATION USING ORGANOPHILIC MEMBRANES.

Using the equations derived in previous sections, the influence of a pervaporation module fitted with GFT 1070 was tested in the following positions (Figure XI.1):

- ❖ at the feed stream to BC1 - *Position I*;
- ❖ at the pinch of BC2; i.e., at the position where fusels tend to accumulate - *Position II*;
- ❖ at the product stream of BC2 - *Position III*;
- ❖ at the product stream of BC2 after it was diluted to an ethanol concentration of 10% (mol) - *Position IV*.

The distillation simulation program was built as described in Chapter IX and the membrane area was kept as a variable. As approximately 2% of the total ethanol fed into the system is lost through FI-10 and FI-16, the waste streams of PC and ED, the limit to the

membrane area used at each point was set so that permeation would result in a maximum 2% loss of the total ethanol fed into the membrane module

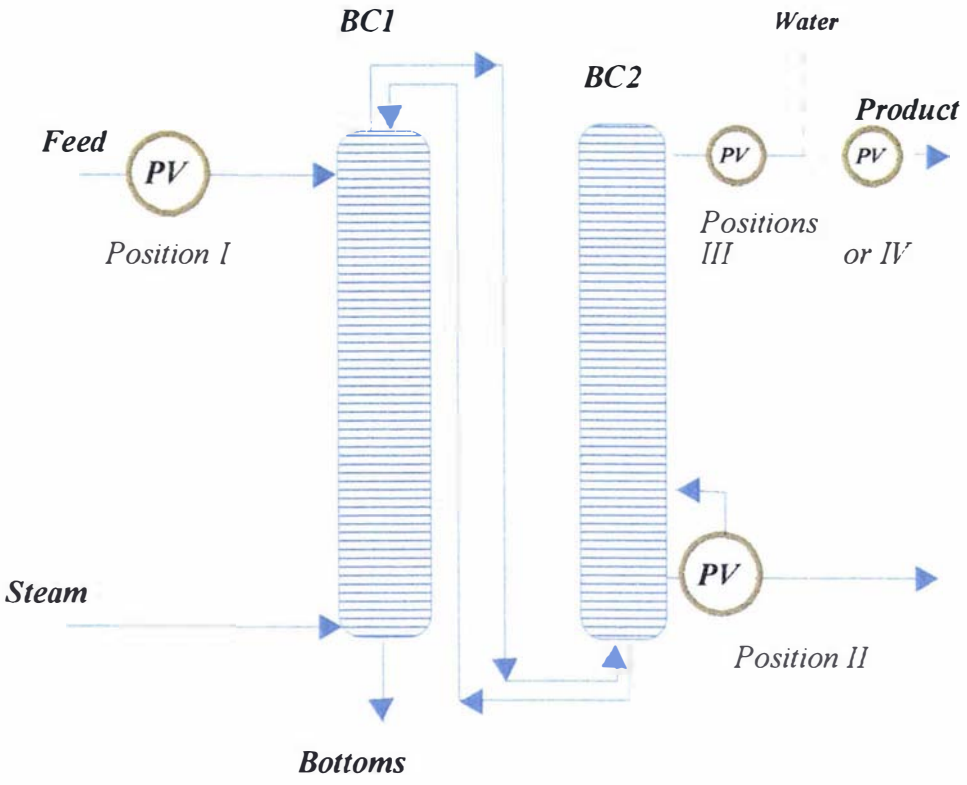

Figure XI.1 Schematic representation of the positioning of a pervaporation (*PV*) module coupled to BC1-BC2.

Table XI.1 Membrane area requirement for a module at various positions on BC1-BC2.

	Membrane Area (m^2)
Position I	1210
Position II	125
Position III	20
Position IV	120

Tables XI.1 and XI.2 list the total membrane area and the product partial flow rates resulting from each simulation. As expected, the final products did not change significantly because of the poor enrichment factors obtained with the membranes. From an economical point of view, the addition of the membrane step adds significant cost due to capital cost of the membrane area and the pumping volume. The lower the feed concentration, the higher the membrane area required and the higher the volume to be pumped through the membrane module.

Table XI.2 Comparison between products of BC1-BC2 with and without a pervaporation module. All values as partial flow rates in $kmol.h^{-1}$. EtOH: ethanol; nPrOH: *n*-propanol; iBuOH: *i*-butanol; nBuOH: *n*-butanol; iAmOH: *i*-amyl alcohol; EtOAc: ethyl acetate.

	EtOH	**nPrOH**	**iBuOH**	**iAmOH**	**EtOAc**
No membrane	24.5	0.05	0.023	4.5e-2	2.4e-3
Position I	24	0.048	0.022	4.4e-2	1.8e-3
Position II	23.5	0.046	0.021	3.9e-2	2.3e-3
Position III	24	0.048	0.022	4.3e-2	1.8e-3
Position IV	24	0.048	0.022	4.3e-2	1.8e-3

During the pervaporation runs with GFT 1070, it was observed that, when the feed concentration was between 5 and 7.5% (w/w) ethanol, the product would split into two phases if its temperature was kept at around 5 °C. Table XI.3 presents the analysis of one such run. The top layer consisted of approximately one third of the total collection. Although separation seems possible, because the fusels split between the two phases was close to 50%, there would be no significant gain in the removal of fusels by removal of the top layer followed by a return of the bottom layer to the products stream.

Table XI.3 Feed and product percentage concentration (w/w) of a pervaporation run with GFT 1070 at 75°C. EtOH: ethanol; nPrOH: *n*-propanol; iBuOH: *i*-butanol; nBuOH: *n*-butanol; iAmOH: *i*-amyl alcohol; EtOAc: ethyl acetate.

		water	EtOH	nPrOH	iBuOH	nBuOH	iAmOH	EtOAc
Feed		94%	5%	0.09%	0.02%	0.002%	0.48%	0.01%
Product	**Top**	66%	16%	1.62%	0.85%	0.06%	16%	0.54%
	Bottom	57%	33%	0.86%	0.31%	0.02%	9%	0.22%
Enrichment	**Top**	0.60	3	18	43	35	33	95
Factor	**Bottom**	0.69	7	9	16	10	19	40
Split	**Top**	0.37	0.19	0.48	0.58	0.63	0.47	0.55
	Bottom	0.63	0.81	0.52	0.42	0.37	0.53	0.45

Although this study concentrated on the analysis of the separation achieved by permeation through the membrane, it is also possible to increase the enrichment factor of the overall separation by fractionated condensation of the permeant. It was suggested by Brüschke (1990) that, in the elimination of ethanol from wine, the aroma fraction (similar to the fusels) could be fully recovered from the permeate by fractionated condensation. In Brüschke's study, it was implied that all ethanol would be removed from the feed stream. Given the large membrane area used for removal of just 2% of the total ethanol in the feed stream (Table XI.1), to fully remove the organic fraction would render the process uneconomical. It seemed thus more appropriate to first concentrate the feed stream with BC1-BC2, then remove the water fraction by pervaporation with hydrophilic membranes, as the membranes developed for this application have high enrichment factors and satisfactory fluxes, and finally fractionate the organic components to recover ethanol with the appropriate purity. This investigation will be fully described in Section XI.3

XI.3 PERVAPORATION-AIDED DISTILLATION WITH HYDROPHILIC MEMBRANES

The separation of fusel oils from ethanol is complicated by the formation of azeotropes in the presence of water and Tarjus *et al.* (1996) devised a novel process to these compounds from a light oil waste stream of Copersucar, Brazil's leading producer of ethanol (Table XI.4). In order to achieve the separation of fusel oils, first the waste stream was dehydrated by pervaporation. Using simulations run on Aspen Plus®, it was shown that only two small distillation columns were then necessary to recover ethanol at +99% (w/w) and to separate *i*-amyl alcohol from a fraction of *n*-propanol and butanols. Therefore, besides the recovery of ethanol, this new process generated two valuable products, *i*-amyl alcohol and a mixture of *n*-propanol and butanols, which, as natural products, can be sold for premium prices to the fragrance and food industries (Chamberlain *et al.*, 1995).

Table XI.4 Typical composition of a light oil waste stream from Copersucar (Tarjus *et al.*, 1996).

	mass fraction (%)
ethanol	40.27
***n*-propanol**	1.85
***i*-butanol**	14.9
***n*-butanol**	0.25
***i*-amyl alcohol**	4.93
water	37.8

Although pervaporation is often employed in the dehydration of binary streams containing no more than 15% (w/w) of water, experimental work was successful in reducing the water content of the complex aqueous mixture of ethanol and fusel oils shown in Table XI.4 from 37.8 % (w/w) to 0.5% (w/w) using GFT 1000 membranes (Tarjus *et al.*, 1996).

Furthermore, for a feed of 2,000 $kg.h^{-1}$ it was estimated that 1,300 m^2 of membrane was necessary.

At industrial scale, a similar approach is being used by Bend Research Inc. (Ray *et al.*, 1997) to recover acetone from an aqueous mixture containing four other solvents (methyl ketone, toluene, ethanol, and methanol) for the paint industry. First, water (9% w/w) is removed by pervaporation, then recovery of the acetone is accomplished by distillation.

The use of pervaporation to dehydrate complex mixtures that can then be easily separated by traditional techniques created an opportunity to re-evaluate the ethanol production path at NZDCL as outlined in Chapter VII. A new process is suggested in Figure XI.2, in which the first three columns are retained without modification.

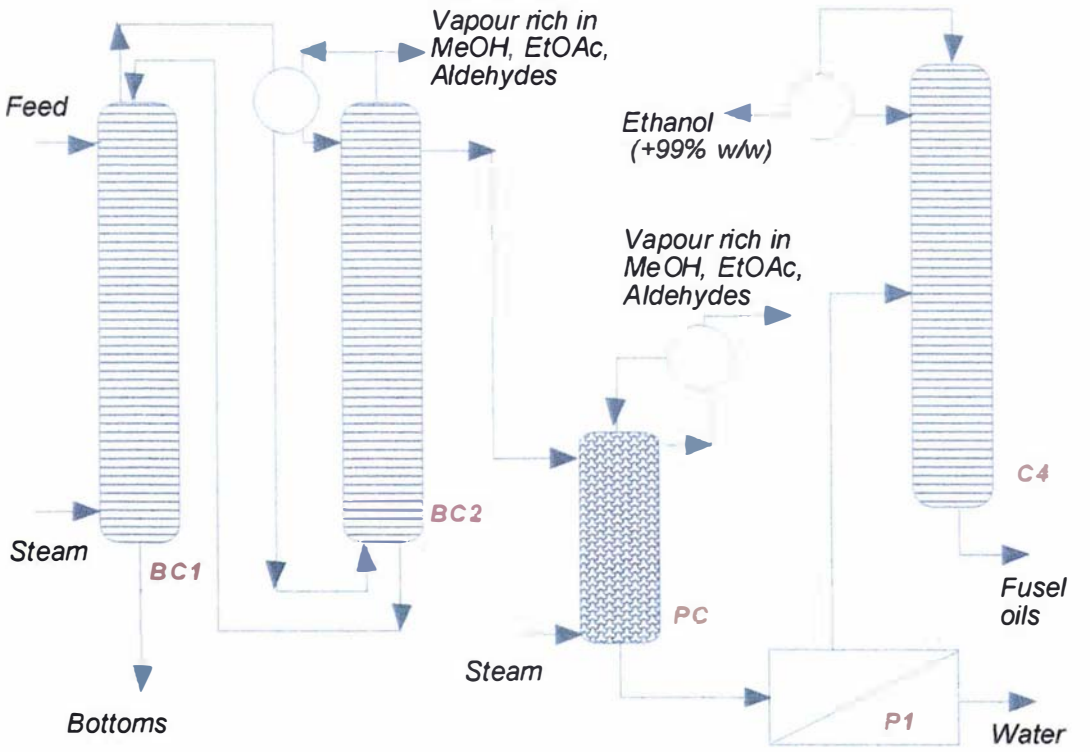

Figure XI.2 New ethanol production scheme. MeOH: methanol; EtOAc: ethyl acetate; BC1: distillation column 1; BC2: distillation column 2; PC: distillation column 3; C4: distillation column 4; P1: pervaporation unit.

In this proposed new scheme, the BC and PC columns continue to be responsible for the reduction of the water content and removal of light fractions, such as methanol, aldehydes and ethyl acetate. The bottom stream from the purifying column *(PC)* would contain ethanol, water (between 30 and 50% w/w), and a small amount of fusel oils (Appendix - Disk 1: *samples.wpd*). This stream would be dehydrated by pervaporation, followed by distillation to remove the fusel oils and produce +99% (w/w) ethanol. The permeate stream, containing mostly water, can be returned to BC1 if its ethanol concentration is sufficiently high to economically justify the recycle. In general an ethanol concentration between 5 and 30% (w/w) in the permeate stream is expected during the life time of a membrane.

Optionally:

- Further reduction of the fusels content can be accomplished by extraction of a side stream rich in fusel oils from the lower half of BC2. This scheme was once used at the NZDCL, to provide partial removal of the fusels fraction but did not eliminate the need of further separation in the ED and RC columns. Therefore, it would not eliminate the need for column C4 in the new proposed scheme, but it would reduce the volume of fusels separated with this column, which could allow for a smaller column, or help ensure that quality standards of the final product are maintained.

- It is possible to dehydrate a 95% (w/w) ethanol stream produced by BC2 when its operation is optimized, followed by distillation or selective extraction to eliminate methanol, ethyl acetate, and higher alcohols. In the case of distillation, the separation of methanol and ethyl acetate requires a stripping column such as PC to follow the dehydration step and can not be accomplished co-currently with the elimination of the higher alcohols. This scheme would therefore differ from the currently proposed scheme only by the change in placement of the PC column.

- Changes in the biological route of fermentation that could substantially reduce the production of methanol and ethyl acetate could be investigated. A study by van Winden (1997) showed that the production of fusel oils during lactose fermentation is influenced by the concentration of nitrogen in the medium. It would be interesting to investigate what other fermentation conditions would affect the production of fusel oils as well as ethyl acetate and methanol. Temperature and yeast strain are two well-known factors influencing by-product formation. The study of fermentation was not within the scope of this thesis.

- Dehydration can be also accomplished by traditional separation techniques such as adsorption by molecular sieving. A comparison of such techniques should include capital and operation costs, analysis of ethanol lost to waste in each process, availability of the energy source required by the process, and energy consumption. Once more, such study was not within the scope of this thesis.

In order to evaluate the feasibility of the scheme presented in Figure XI.2, the following experiments and simulations were carried out:

- dehydration of a model solution using a laboratory scale pervaporation unit and use of NZDCL data (Appendix A) to estimate the required size of the industrial pervaporation unit;

- dehydration of the product stream from BC2 using an industrial pervaporation unit already installed at NZDCL for the production of anhydrous ethanol;

- recovery of ethanol from the dehydrated stream using the distillation pilot plant at the Department of Process and Environmental Technology at Massey University;

- modelling of the new distillation unit, C4, using Hysim® and ChemSep®.

XI.3.1 MATERIALS AND METHODS

Laboratory-scale pervaporation unit

The pervaporation unit described in Chapter IV, Experiment II, was fitted with GFT 1000, a composite (PVA/PAN) hydrophilic membrane. All tests were conducted at 65°C, with a feed flow rate of approximately 34 $l.h^{-1}$. Table XI.5 lists the concentrations studied. These were based on the concentration achieved at the product stream of BC2 and on the assumption that if BC2 were optimised, it would be able to produce a stream with ethanol and water at their azeotropic concentrations. The product was analysed by GC for its alcohol content according to the procedure described in Section IV.2.2.

Table XI.5 Pervaporation feed concentration in w/w. EtOH: ethanol; iPrOH: *i*-propanol; EtOAc: ethyl acetate; nPrOH: *n*-propanol; iBuOH: *i*-butanol; nBuOH: *n*-butanol; iAmOH: *i*-amyl alcohol.

	1st. Set	2nd. Set	3rd. Set
water	8.7%	5.5%	4.2%
EtOH	82.5%	87.6%	88.4%
iPrOH	<0.01%	<0.01%	<0.01%
EtOAc	0.18%	0.07%	0.07%
nPrOH	1.4%	1.1%	1.2%
iBuOH	0.40%	0.26%	0.28%
nBuOH	0.02%	0.02%	0.02%
iAmOH	6.8%	5.5%	5.9%

Distillation pilot-plant

A pilot plant scale distillation column was used. This has a two metre high enrichment section and is packed with glass cylinders of approximately 0.7 cm of diameter and 1 cm of length. The HETP of the enriching section was calculated for a water-ethanol feed of

46.8 $l.h^{-1}$ containing approximately 14% w/w ethanol, a steam injection of approximately 10 $kg.h^{-1}$ and a reflux ratio of approximately 3. The HETP was 0.5 m at the enriching section, which corresponds to four theoretical plates. The original design of the column was modified to include a reboiler instead of steam injection. The dehydrated ethanol and fusel oil feed mixture was produced at the NZDCL by pervaporating the product from BC2. No special care was taken to remove methanol and ethyl acetate prior to distillation. The feed concentration and operation parameters are listed in Table XI.6 All concentrations were measured by GC (Section IV.2.2).

Table XI.6 Feed concentration and operation parameters for pilot-scale distillation of dehydrated mixture of ethanol and fusel oils. EtOH: ethanol; iPrOH: *i*-propanol; EtOAc: ethyl acetate; nPrOH: *n*-propanol; iBuOH: *i*-butanol; nBuOH: *n*-butanol; iAmOH: *i*-amyl alcohol; nd: not detected.

Feed (w/w)		Operation Parameters		
water	nd	**Feed**		
EtOH	99.24%	**temperature**	(°C)	25
iPrOH	<0.01%	**flow**	($l.h^{-1}$)	16.8
EtOAc	0.03%			
nPrOH	0.23%	**Reflux flow**	($l.h^{-1}$)	10.8 - 22.8
iBuOH	0.12%	**Steam to reboiler**	($kg.h^{-1}$)	15
nBuOH	nd			
iAmOH	0.38%			

XI.3.2 Results and discussion

XI.3.2.1 Pervaporation experiments

Table XI.7 summarizes the permeate concentration obtained with pervaporation of the feed mixtures given in Table XI.5. Water permeated preferentially resulting in a water concentration of 99.8% (w/w) in the permeate. With the set up used, the ethanol

concentration in the permeate was on average 0.23% (w/w). From the data collected at NZDCL, the expected ethanol concentration in the permeate, when the membranes are new, is around 5% (w/w) and Tarjus *et al.* (1996) reported a permeate water concentration of minimum 95% (w/w). The difference between the result obtained with the laboratory apparatus and on industrial equipment was probably due to the higher vacuum achieved at the permeate side of the membrane, lack of membrane defects, or better seal obtained with the laboratory scale equipment.

Table XI.7 Permeate concentration (w/w) of organic solvents using GFT 1000 and the feeds presented in Table XI.5. EtOH: ethanol; iPrOH: *i*-propanol; EtOAc: ethyl acetate; nPrOH: *n*-propanol; iBuOH: *i*-butanol; nBuOH: *n*-butanol; iAmOH: *i*-amyl alcohol; nd: not detected.

	1st. Run	2nd. Run	3rd. Run
water	99.8%	99.8%	99.7%
EtOH	0.20%	0.22%	0.26%
iPrOH	nd	nd	nd
EtOAc	29 ppm	nd	nd
nPrOH	14 ppm	13 ppm	12 ppm
iBuOH	5 ppm	nd	nd
nBuOH	88 ppm	24 ppm	32 ppm
iAmOH	nd	nd	nd

The flux through the membrane for runs 1 to 3 as presented in Table XI.7 was 0.37, 0.3 and 0.21 $kg.m^{-2}.h^{-1}$, respectively. These fluxes are similar to those shown in Figure XI.3 (Heintz & Stephan, 1994b) for an ethanol feed concentration of approximately 85% w/w and a feed temperature of 60°C. The water partial flux is reported as approximately 0.3 $kg.m^{-2}.h^{-1}$ and the total flux is mostly water.

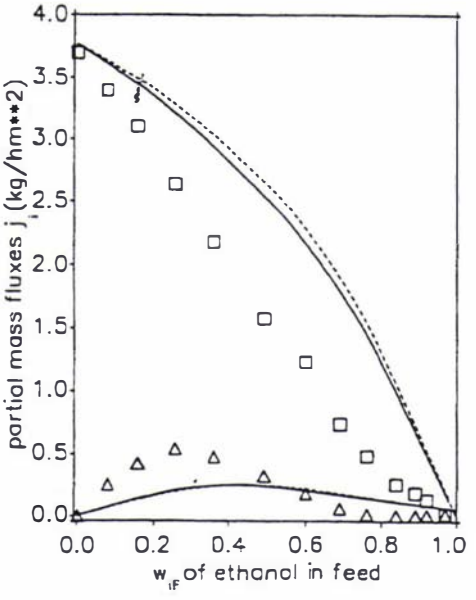

Figure XI.3 Partial fluxes for the system water-ethanol-PVA at 333K. □: water, Δ: ethanol.

For a similar concentration of water in the feed as that presented on Table X.5, Tarjus *et al.* (1996) reported the following fluxes: 0.2, 0.09 and 0.08 $kg.m^{-2}.h^{-1}$, respectively. These differences could be attributed to differences in flow type: Tarjus *et al.* (1996) used a dead-end filtration apparatus, whereas in this study the feed flowed across the membrane and was continuously renewed. Alternatively the difference could be attributed to differences in membrane production batch. Based on these results, it was chosen to use the equation developed by Tarjus *et al.* (1996) to calculate the membrane area required for the separation in equipment P1 (Figure XI.2), because it gave more conservative results and was in better agreement with industrial data:

$$\frac{dx}{dA} = \frac{x_w^2 (K_w + K_{eth}) + x_w (K_{eth0} - K_w)}{F} \qquad [XI.1]$$

$$K_w = k_w \, e^{\left[-\frac{E_w}{R}\left(\frac{1}{T} - \frac{1}{T_o}\right)\right]} \quad [XI.2]$$

$$K_{eth} = k_{eth} \, e^{\left[-\frac{E_{eth}}{R}\left(\frac{1}{T} - \frac{1}{T_o}\right)\right]} \quad [XI.3]$$

$$K_{eth0} = k_{eth0} \, e^{\left[-\frac{E_{eth}}{R}\left(\frac{1}{T} - \frac{1}{T_o}\right)\right]} \quad [XI.4]$$

where,

A	membrane area in m^2;
E	activation energy in $J.mol^{-1}$;
F	feed flow rate in $kg.h^{-1}$;
k	mass transfer coefficient in $kg.m^{-2}.h^{-1}$;
R	universal constant of gases in $J.mol^{-1}.K^{-1}$;
T	operation temperature in K;
T_o	reference temperature of 40°C;
x	mass fraction;

and the subscripts are:

w	water;
eth	ethanol;
0	reference.

Table XI.8 lists the values of the parameters used for Equations XI.1 to XI.4. The differential equation was solved using the function *ODE45* of MatLab®, which is a 4th order Runge-Kutta method (Appendix E *Tarjus1.m*).

Table XI.8 Experimental coefficients used in Equations XI.1 to XI.4 for the calculation of the membrane area required for the dehydration of an aqueous mixture of ethanol and fusel oils (Tarjus *et al.*, 1996).

	k (kg.m^{-2}.h^{-1})	k_w (kg.m^{-2}.h^{-1})	E (J.mol^{-1})
water	0.4365	0	46,370
ethanol	0.0146	4.234e-5	56,270

According to the data collected at the NZDCL during the 1995-1996 production season (Appendix A), the water concentration at the bottoms stream of the PC varied between 30 and 50% (w/w), the flow rate varied between 1350 and 1500 kg.h^{-1}, and the temperature of the stream was at approximately 80°C. In order to evaluate the effect of temperature, feed flow rate, and water concentration on the membrane area requirement Equations XI.1 to XI.4 were solved for a combination of the conditions listed in Table XI.9. These combinations were chosen based on the following reasoning:

- in a worst scenario, the water feed concentration could vary between 30 to 50% (w/w), as stated above. The plots generated in this study would also allow for an analysis of the membrane requirements at lower water concentrations;

- feed flow rates up to 4,500 kg.h^{-1} were evaluated in order to investigate the impact of an increase in the production rate in the operation and capital costs of the proposed pervaporation-aided distillation scheme;

- the effect of temperature changes also needed to be analysed, given the large impact of temperature in the membrane performance as identified in Section IV.4.

The reference condition was 1500 kg.h^{-1}, 80°C, and a water mass fraction of 0.5; each parameter was changed separately.

Table XI.9 Range of parameters evaluated in Equations XI.1 through XI.4.

Temperature (°C)	Feed flow rate ($kg.h^{-1}$)	mass fraction (water)
40	1500	0.3
60	2250	0.5
80	3000	0.7
	4500	

Figures XI.4 to XI.6 highlight the difference in membrane area required for the dehydration of an aqueous mixture of ethanol and fusels when the feed temperature, flow rate, and water mass fraction are varied separately.

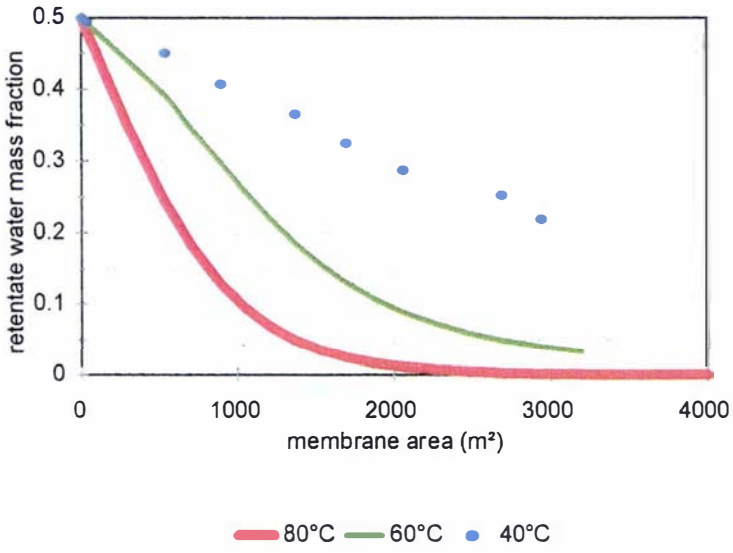

Figure XI.4 Influence of feed temperature on the membrane area required for the dehydration of an aqueous mixture of ethanol and water. The feed flow rate was 1500 $kg.h^{-1}$ and the water mass fraction was 0.5 for all cases evaluated.

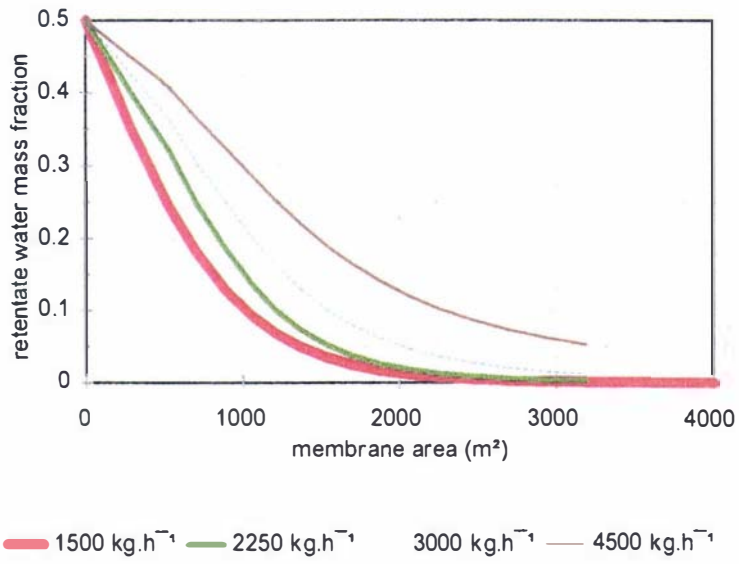

Figure XI.5 Influence of feed flow rate in the membrane area required for the dehydration of an aqueous mixture of ethanol and water. The feed temperature was 80°C and the water mass fraction was 0.5 for all cases evaluated.

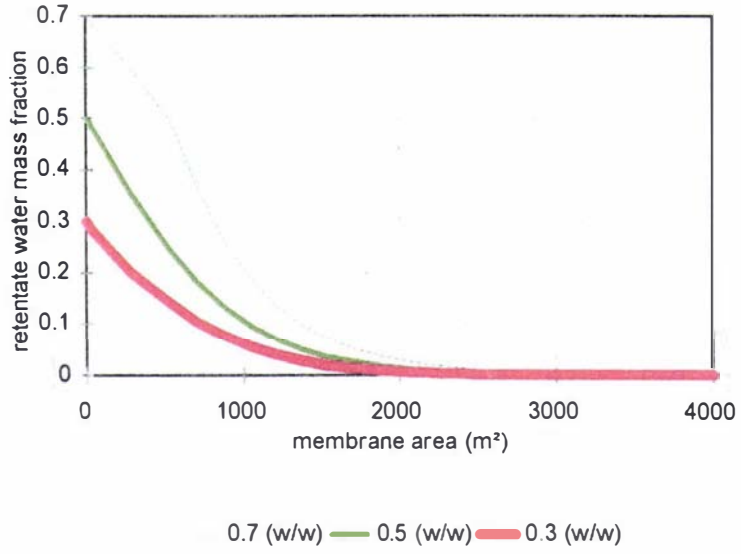

Figure XI.6 Influence of initial water mass fraction of the feed in the membrane area required for the dehydration of an aqueous mixture of ethanol and water. The feed flow rate was 1500 $kg.h^{-1}$ and the temperature was 80°C for all cases evaluated.

For dehydrating the feed stream down to 0.5% (w/w) of water or less, assuming that the conditions of the 1995-1996 production season did not change significantly (feed flow rate of 1500 $kg.h^{-1}$, temperature of 80°C, and water mass fraction of 0.5), it was estimated from Equations XI.1 through XI.4 that 1400 m^2 of membrane area would be required.

An increase in the feed flow rate or in the initial water mass fraction would result in a proportional increase in the membrane area required and a decrease in the feed temperature would result in an exponential increase in the membrane area required (Figure XI.7). As presented in Section XI.3.2.2, for the suggested, new production scheme, at today's rates, membrane replacement would correspond to approximately 20 to 30% of the total operation cost. In view of these trends and in order to keep operation costs to a minimum, it is recommended to operate the pervaporation unit at the highest possible temperature allowed by the process and membrane material, and at the lowest possible initial water mass fraction.

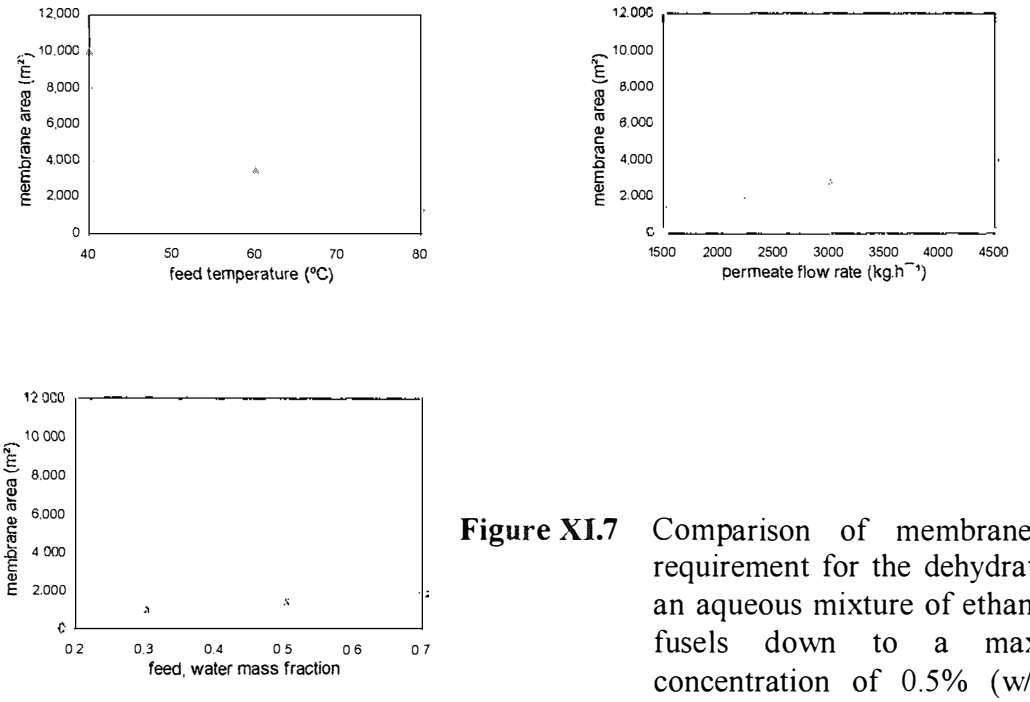

Figure XI.7 Comparison of membrane area requirement for the dehydration of an aqueous mixture of ethanol and fusels down to a maximum concentration of 0.5% (w/w) of water.

XI.3.2.2 Distillation of the dehydrated BC2 stream

The feed composition and operating parameters for the distillation of the dehydrated BC2 stream were presented in Table XI.6 The product composition (distillates) obtained with the pilot plant are presented in Table XI.10 together with the current product specification at the distillery.

Table XI.10 Product concentration (w/w) from distillation of dehydrated BC2 product stream, the balance is ethanol. iPrOH: *i*-propanol; EtOAc: ethyl acetate; nPrOH: *n*-propanol; iBuOH: *i*-butanol; nBuOH: *n*-butanol; iAmOH: *i*-amyl alcohol; nd: not detected.

	Product 1 (low reflux)	**Product 2 (high reflux)**	**Specification at the NZDCL**
iPrOH	<100 ppm	<100 ppm	<10 ppm
EtOAc	400 ppm	900 ppm	<10 ppm
nPrOH	200ppm	nd	<10 ppm
iBuOH	<100ppm	nd	<10 ppm
nBuOH	nd	nd	<10 ppm
iAmOH	nd	nd	<10 ppm

Assuming that the calculated HETP did not change with feed flow rate and ethanol concentration, the column used had only four theoretical trays in the enriching section. Using the Hysim® short cut distillation option (Appendix E: *Dehydr2.txt*), it was estimated that at least twelve theoretical trays would be required in the enriching section to achieve the desired separation. Therefore, it was chosen to operate the column at two extreme conditions. First, the separation ability of the column was investigated using a low reflux ratio that could provide a product flow rate similar to those of the simulated program, i.e., the distillate flow rate would be similar to the feed flow rate. As the column was undersized for the job proposed, it was also investigated whether distillation could achieve the separation required by increasing the reflux ratio to the maximum possible value allowed by the equipment at hand.

Product 1 was the result of operating the column with a reflux flow rate of 0.18 $l.min^{-1}$ and a reflux ratio of approximately 0.65. During operation, the bottoms flow rate was too low to be accurately measured and the distillate flow rate was close to the feed flow rate.

Product 2 was the result of operating the column with a reflux flow rate of 0.38 $l.min^{-1}$. At this condition, the product flow rate was minimal, about 20 $ml.h^{-1}$ ($R \approx \infty$) and there were problems keeping the level at the reboiler because of overflow. These problems frustrated attempts to measure the bottoms flow rate.

Although the pilot plant distillation column eliminated the higher alcohols (*n*-propanol, *i*-butanol, *n*-butanol, and *i*-amyl alcohol), the concentration of ethyl acetate in the product increased. Furthermore, the higher the reflux ratio, the higher the concentration of ethyl acetate and methanol in the distillate (the methanol concentration was not measured, but the peak was identified in the chromatogram and the conclusions drawn were based on visual analysis). Therefore, it would be necessary to remove ethyl acetate and other components, such as methanol, prior to pervaporation.

During pervaporation with hydrophilic membranes, ethyl acetate did not permeate. There is still some controversy about the ability of hydrophilic membranes to reduce the methanol concentration. Lochon (1998) suggested that methanol would generally permeate with water and it was shown in Section VII.2.2.3 that hydrophilic membranes are used for the separation of methanol from propanol. However, they are also used for the separation of methanol from water (Will & Lichtenthaler, 1992; Heintz & Stephan, 1994b), which suggests that the hydrophilic membrane would have a higher rejection for methanol than for water, and in consequence not all the methanol present in a mixture containing water would be eliminated. Furthermore, Bryan (1998) reports that Bend Research developed a hollow fibre, hydrophilic membrane that rejects methanol as well as higher alcohols. In view of these data, it was assumed for the purpose of this study that pervaporation would not be of any aid in the reduction of either methanol or ethyl acetate. Even if methanol could be eliminated from the process by pervaporation, it would still be necessary to use a stripping column to reduce the concentration of ethyl acetate .

In the new process, it should be possible to fine tune the operation of BC2 and PC, to allow the removal of ethyl acetate and methanol as a vapour product (Appendix E: *pc_dh3.sep*). The strategy to increase the methanol and ethyl acetate removal in PC would include:

- ❖ increasing the steam flow rate;
- ❖ increasing the reflux ratio;
- ❖ lowering the height of the feed entry;
- ❖ increasing the distillate flow rate.

Table XI.11 shows the product concentration obtained from the simulation of a column similar to the pilot plant, i.e. four ideal plates in the enriching section and a reflux ratio of 100 (Appendix E: *Pilotp.sep*), and the predicted product concentration obtained with a column of eighteen theoretical stages, feed entering on stage thirteen, and a reflux ratio of three (Appendix E: *c4_id.sep*). In both simulations, the feed conditions were similar to those used in the experiment

Table XI.11 Product concentration of the simulation of the pilot plant operation (*Pilot C*) and an ideal column with eighteen trays and a reflux ratio of three (*Ideal C*). MeOH: methanol; EtOH: ethanol; iPrOH: *i*-propanol; EtOAc: ethyl acetate; nPrOH: *n*-propanol; iBuOH: *i*-butanol; nBuOH: *n*-butanol; iAmOH: *i*-amyl alcohol.

	Pilot C	Ideal C (w/w)
water	0.04%	0.5%
EtOH	99.9%	99.9%
iPrOH	0.01%	0.01%
EtOAc	0.03%	0.03%
nPrOH	0.02%	7 ppm
iBuOH	50 ppm	<1 ppm
nBuOH	4 ppm	< 1 ppm
iAmOH	0.1 ppm	< 1 ppm

The pilot plant simulation results (Pilot C) compare well with the experimental results, thus improving confidence in the results obtained for "*Ideal C*". The product concentration predicted for the ideal column (*Ideal C*) would pass the required product specifications of the NZDCL except for the *i*-propanol and ethyl acetate concentrations (Table XI.10). These results highlight the need to reduce the concentration of ethyl acetate in the feed stream to the last column to the levels given in Table XI.10. If ethyl acetate is present in the feed stream at such levels, there would be more flexibility to reduce the concentration of *i*-propanol in the product stream. Provided that a real column can at least reproduce such behaviour, the new, dehydration scheme could be technically feasible.

XI.3.2.3 Comparison of operation costs

The dehydration scheme differs from the actual distillation process at NZDCL by the elimination of the ED and RC and the introduction of a pervaporation unit and a smaller column (C4) for the separation of fusel oils. For all other steps in the process, such as fermentation, remaining unchanged, the basis for comparing operation costs consists of the energy expenditure of the distillation columns and pervaporation unit to produce ethanol and the costs to replace membranes. Capital costs are not included.

The whole distillation process at NZDCL consumes approximately 7,500 kg of steam per hour, which results in an operation cost of NZ$ 201 per hour. If the new scheme was to be installed, the distribution of the operation costs would be similar to those presented in Table XI.12. The difficulty in separating propanols from ethanol is the major factor for the high energy consumption in column C4. However, in the new scheme the energy costs are still reduced by 10%. Nevertheless, a total operation cost between NZ$ 225 to 251 per hour is still too high in comparison to actual costs.

This new scheme only starts to become competitive when the membrane costs are reduced to less than NZ$ 200/m^2 or when their life expectancy is increased to over 6 years. Smaller

price reductions may also be advantageous if they are accompanied by an increase in life expectancy that would reduce the total cost of membrane replacement accordingly.

Table XI.12 Operation costs of the new production scheme. Cost data supplied by the NZDCL.

				Cost (NZ$.h^{-1})
Steam consumption	BC1, BC2	4.8	ton.h^{-1}	
	PC	0.2	ton.h^{-1}	
	C4*	1.6	ton.h^{-1}	
	total	6.6	ton.h^{-1}	177
Electricity		81.3	kW	4.27
Membrane[ε]		1400	m^2	44 to 71[†]
Total				225 to 251

* reboiler duty.
[ε] for a cost of NZ$ 500 to 800 per m^2 and a year of 330 days.
[†] for a membrane life expectancy of two years.

The major disadvantage of this process in comparison with distillation is the lack of economy of scale. Any increase in the production rate would immediately require a proportional increase in the membrane area. However, the modular nature of the membrane process makes these changes simple. Other advantages of this process are minor: reduction of the volume to be transported by approximately 5% and elimination of the existing pervaporation dehydration unit which has an area of approximately 100 m^2.

XI.4 Conclusion

The objectives of this chapter were:

- ❖ to evaluate the impact of pervaporation with hydrophobic membranes in the ethanol purification and concentration processes at NZDCL, in particular at BC1-BC2;
- ❖ to investigate any other viable alternatives for pervaporation-aided distillation.

The three organophilic membranes investigated had similar enrichment factors and did not improve the separation achieved by evaporation significantly. Therefore, the introduction of organophilic pervaporation would not be expected to have a positive impact in the ethanol purification process as conducted at NZDCL.

The energy spent on the purification of ethanol by distillation reflects the volume of water that needs to be eliminated and the difficulty of removing fusel oils. A simpler process has been developed that eliminated the ED and RC columns at the NZDCL. In this new strategy, the preliminary purification and concentration continues in the first two columns (*BC*) and the purifying column. The product is then dehydrated by pervaporation. In the absence of water, fusels are easily separated from ethanol. Product quality can be maintained, provided that methanol and ethyl acetate removal are accomplished in columns BC and PC.

A study of the influence of feed flow rate, feed temperature, and water concentration in the feed on this membrane process showed that the membrane area required is proportional to the feed flow rate or water concentration; there is an exponential relationship between temperature and the membrane area. Consequently, it is recommended that for a determined feed flow rate and water concentration, the membrane module should be operated at the maximum temperature allowed by the process and the membrane material.

The suggested, new production scheme achieved an estimated reduction in the energy consumption of approximately 10%. However, membrane replacement costs nullified this

benefit. In order for the new scheme to become competitive, the membrane costs should be reduced to a maximum of NZ$ 200/m^2 or the membrane life expectancy should be increased accordingly.

Other production schemes that include a review of the biological route in fermentation in order to reduce the concentration of methanol, ethyl acetate and fusel oils could improve the competitiveness of the proposed new scheme and should be investigated in the future.

Chapter XII

Discussion: Applications

In Chapters X and XI, alternatives that could reduce the energy expenditure or simplify the production layout of industrial ethanol were proposed. These proposals do not exhaust all the alternatives available for optimising or re-designing the process at the NZDCL. During this study, emphasis was given to schemes that included pervaporation since one of our main objectives was to improve the understanding of multicomponent pervaporation and the use of pervaporation in hybrid applications with distillation. Although the introduction of pervaporation to the distillation process at the NZDCL did not improve significantly the energy consumption and production costs, new developments in membrane material, module, or membrane type could rapidly change this scenario.

In the event of changes being implemented to the distillation process at the NZDCL, a careful analysis of the economics of MVR heat pumping and the evaluation of other traditional techniques for the separation of fusels, such as adsorption and selective extraction, should be conducted.

At the time this study was being completed, the ethanol production scenario at the NZDCL was about to undergo drastic changes. The distillery at Reporoa, NZ, was shut down and the whey processed at that site was to be diverted to Edgecumbe, to a distillation site beside the NZDCL. Furthermore, there was a proposal by the New Zealand Dairy Group, the parent company of Bay Milk, to acquire both ethanol production facilities. These changes create an opportunity for re-evaluation of the pinch analysis at the NZDCL, this time including the possibility of re-designing the whole production layout and to increase the ethanol production capacity at the NZDCL by incorporating the whey originally processed at Reporoa. There could also be an opportunity to improve the heat integration with the Bay Milk.

Pinch analysis has found wide use as a technique for heat integration and reduction of energy aquisition. In pinch analysis, the production pathway must be re-evaluated. In its narrower aspect, pinch analysis involves re-thinking the heat exchanger network of established plants. The solutions developed during pinch analsys must then be examined for their practicality. They must not impart plant flexibility and cannot be implemented for streams that are physically distant.

When a wider assessment of the production process is desired, pinch analysis can be used to spot process areas, such as process technologies, parameters, equipments, and production practices, that contribute most to production costs. This assessment is restricted to energy-related aspects, it does not include production requirements that impact product quality. However, once problem areas are pinpointed and solutions are generated, the suitability of each solution can be gradded by combining pinch technology with appropriate techniques that assess product quality and production feasibility.

Part Three

Conclusions

Chapter XIII

CONCLUSIONS

In this study, fundamental mechanisms of pervaporation and the technical and economical feasibility of using this new technology with distillation to produce high-grade, industrial ethanol were investigated. A pinch analysis of the NZDCL was performed to identify opportunities for energy savings.

During pervaporation, it was observed that the enrichment factor of alcohols was proportional to their molecular size and to their activity coefficient in the feed when organophilic membranes were used. A new, semi-empirical relationship was proposed. With this relationship, it is possible to rank the permeability of feed components during pervaporation before experiments are performed.

The overall pervaporation enrichment factor could also be determined by sorption alone and diffusion became significant only as the distribution of the molecular size of the feed components increased. The time spent in selecting and experimenting with the various membrane materials available every time a new application is proposed could be reduced if the behaviour of multicomponent solutions during sorption and diffusion was better understood.

For organophilic pervaporation membranes, it was observed that the temperature influence in the flux through the membrane could be successfully described by an Arrhenius-like relationship. Also, increases in temperature increased flux, without significantly changing the distribution of the components' concentration in the permeate. Therefore, pervaporation should be carried out at the highest possible temperature as permitted by the membrane material and the process requirements in order to reduce costs associated to membrane area.

In general, the flux of the minor organic components was not affected by the presence of other components and the solution-diffusion model described their flux satisfactorily. However, for systems in which the feed components tend to strongly associate it could be

essential to include flow coupling to correctly predict the flow of minor components. In the system studied, prediction of the flux of *i*-amyl alcohol could possibly benefit from including coupling with ethanol or total flux into the mathematical description. *i*-Amyl alcohol was not only preferentially sorbed into the membrane, it was also the minor component of highest concentration in the feed. Because the total flux and the flux of ethanol were highly correlated, it was not possible to distinguish between either mechanisms.

Organophilic pervaporation was investigated as an alternative method to remove fusels. Of the three commercial membranes investigated (GFT 1060, GFT 1070, GKSS PEBA) none had an enrichment factor that could challenge or improve the separation obtained by distillation alone for the range of concentrations tested.

An alternative process was proposed: first, water and the more volatile fractions (methanol, ethyl acetate, and aldehydes) would be eliminated or have their concentration reduced to acceptable levels by distillation with the BC and PC columns, followed by pervaporation with hydrophilic membranes to remove water. Finally, the fusels fraction would be removed from the ethanol mixture by a simple distillation. The proposed, new dehydration process eliminates the ED and RC columns, and gives a ten percent reduction in energy consumption. This benefit was unlikely to offset the cost of periodic membrane replacements. However, if the membrane price falls by over 60% or their life-expectancy is doubled, this alternative process should be revisited as a means to increase process capacity.

Purification of ethanol from whey fermentation is constrained by the removal of fusel alcohols. A pinch analysis of the NZDCL site confirmed that steam is the major contributor in the production cost of whey ethanol. The heating and cooling targets of NZDCL and the neighbouring Bay Milk also indicated that there was little practical scope left for further integration of the sites that could benefit NZDCL. However, small changes in the operation parameters, such as an increase in the feed temperature to BC1 or introduction of heat pumps could either reduce steam consumption by 1,600 $kg.h^{-1}$ or by approximately 6,500 $kg.h^{-1}$, respectively. In addressing such changes, strategies to compensate for an increase in the fusels content of the product stream of BC2, such as removal of a fusel-rich side

stream, strategies to provide for the heating needs of the fermentation site, and strategies to accommodate the increase in internal column flow rates must be carefully considered.

XIII.1 Recommendations for future work

During the investigations carried out in this study, traditional tools for the description of pervaporation and for the simulation of distillation were employed with varying levels of success. Shortcomings in these relationships were not unexpected.

In distillation, as in sorption of solvents into dense polymers, thermodynamic equilibrium is often described by semi-empirical relationships originally fitted for binary solutions and subsequently extended to multi-component solutions. Experimental data on multi-component vapour-liquid equilibrium is often nonexistent or of proprietary nature, which makes it difficult to evaluate the degree of accuracy of such relationships. Experimental data on sorption of liquid solutions into dense polymers are slowly becoming available. While much experimental data must still be generated in order to create a reliable data base and be able to extensively evaluate the adequacy of the existing thermodynamic relationships for the prediction of sorption, recent studies highlight the inability of the existing relationships, such as the Flory-Huggins, in predicting the sorption behaviour of poor solvents (polar molecules) into polymers such as PDMS (Favre *et al.*, 1993; 1996) and the need to develop relationships for prediction of sorption based on physical-chemical or structural properties of the molecules involved (Jonquières & Fane, 1997).

Regardless of the limitations of the thermodynamic models, they are the backbone of the simulation of distillation in the commercially available programs. According to Porter (1995), in designing distillation columns, doubts about the vapour-liquid estimates often reflect in a higher reflux ratio than necessary, leading to increased energy usage. Fundamental research on molecular forces are therefore needed in order to develop a molecular theory of phase equilibria. Kakhu & Homer (Porter, 1995) started development on the AGAPE (a generalized approach to phase-equilibria) method based on London dispersion forces. This theory aims at predicting both liquid-liquid and vapour-liquid equilibria from the molecular structure of the components of the mixture for freely rotating

molecules without need of experimental data. A similar approach for solid-liquid phase equilibria that can be applied to the sorption of solvents into dense polymers is still lacking.

Data measured from the BC columns suggested that the separation ability of this distillation column, was limited by the flow regime inside the column as much as the thermodynamic equilibrium. According to Porter (1995), a number of scale-up failures in distillation, due to the use of empirical correlations have lead to a renewed interest in the study of flow regimes. At present, design of distillation columns is based on correlations of experiments and of previous experience, and trial and error optimization. The relative success of this approach, the difficulty in accessing commercial scale columns, and the perception of distillation as a mature technology have hindered investment on fundamental science research and have also hindered the development and acceptance of new equipment design as there is no comprehensive theory of two-phase flow. The success of predicting single phase flow patterns by numerical solutions of the Navier-Stokes equation, turbulence equations, and the continuity equations by Computational Fluid Dynamics (CFD) has, in recent times, renewed the interest of engineers into investigating two-phase flow patterns and evaluating such influence in the mass transfer inside distillation columns (Porter, 1995).

Overall, it became apparent that membrane technology, though already an established separation technique, still faces a few challenges for future development and commercial acceptance.

- Pervaporation membranes have the ability of separating components using considerably less energy than traditional separation techniques, such as distillation, but the cost of membrane replacements makes then unsuitable for use on a large scale processes. There is a need to either decrease membrane and module production costs or to increase membrane life-expectancy. In recent years, the fast implementation of ultrafiltration serves as an example of the effect of cost reduction.

- Pervaporation membranes that have a high enrichment factor often present have low flux, which increase the membrane area required, consequently increasing the cost of the separation.

- There is no generalized theory of solid-liquid phase equilibria that can help predict the sorption of solvents into dense membranes. Such theory would facilitate the development of new membrane materials and the pairing of membrane - feed solution in assessing new applications.

- During pervaporation, a solution-diffusion model explains satisfactorily the transport of the liquid molecules through the membrane when they occur independently of the presence of other components. In highly swollen systems, the assumption of independent flow may not apply. So far, there is no theory for predicting the degree of membrane swelling or the level of interaction between solvent molecules occurring inside the polymer matrix.

- When using flat sheet membranes at laboratory scale, proper sealing of the membrane compartment and avoidance of membrane damaging were constant preocupations as such damages reduced the quality of the membrane performance and membrane life-expectancy. Since much of the information on the type of sealants used in industry and on the susceptibility of membranes to develop defects during their operation is of proprietary nature, it is only possible to expect that those issues are being addressed by the manufactures in order to reduce operation costs and improve separation performance.

- Confidence in pervaporation for the separation of organic components should increase with an enlargement of the "Applications List". Until then, investigation of new applications is still the responsibility of research centres, such as universities and research institutes, and membrane manufactures.

Overall, it is concluded that much investment is still needed in fundamental research and development of new applications for pervaporation to cement its place in the separation

industry. However, it is a technology that presents a recognised potential for energy savings and for challenging traditional process design.

Chapter XIV

NOTATION

Roman letters

a	activity	(-)
c	concentration	$kg.m^{-3}$
D	diffusion coefficient	$m^2.s^{-1}$
E	activation energy	$J.mol^{-1}$
f	fugacity	bar
f_c	friction coefficient	s^{-1}
G	Gibbs free energy	J
H	enthalpy	$J.mol^{-1}$
J	flux	$kg.m^{-2}.s^{-1}$
k	mass transfer coefficient	$kg.m^{-2}.s^{-1}$
K''	coefficient of proportionality	$m^{-3}.mol$
n	number of moles	mol
p	partial pressure	bar
P	pressure	bar
P	permeability	$kg.m^{-1}.s^{-1}$
Q	drag coefficient	(-)
R	solute rejection	(-)
R	universal gas constant	$J.mol^{-1}.K^{-1}$
R	resistance to transport	$kg^{-1}.m^2.s^1$
R_{TOT}	sum of all resistances to transport	$kg^{-1}.m^2.s^1$
R_{bl}	resistance to transport across the boundary layer	$kg^{-1}.m^2.s^1$
R_m	resistance to transport across the membrane	$kg^{-1}.m^2.s^1$
R_p	resistance to transport across the porous support	$kg^{-1}.m^2.s^1$
R_c	resistance to transport across the vacuum line	$kg^{-1}.m^2.s^1$
R_{ii}	straight coefficient in Onsager equation	(-)
R_{ij}	cross coefficient in Onsager equation	(-)

S	entropy	J
S	coefficient of solubility (sorption)	(-)
T	temperature	K
u	velocity	$m.s^{-1}$
V	molar volume	$m^3.mol^{-1}$
w	mass fraction	(-)
x	liquid molar fraction	(-)
y	vapour molar fraction	(-)
z	membrane thickness	m

Greek letters

α	separation factor, selectivity	(-)
β	enrichment factor	(-)
γ	activity coefficient	(-)
μ	driving force	N
μ	chemical potential	$J.mol^{-1}$
ρ	density	$kg.m^{-3}$
π	osmotic pressure	bar

subscripts

i	preferentially permeating species
j	non-preferentially permeating species

superscripts

f	feed
m	membrane
p	permeate

abbreviations of chemical names

H_2O	water
EtOH	ethanol
iPrOH	*i*-propanol
IPA	*i*-propanol
nPrOH	*n*-propanol
iBuOH	*i*-butanol
nBuOH	*n*-butanol
iAmOH	*i*-amyl alcohol
EtOAc	ethyl acetate

Chapter XV
REFERENCES

Abrams D.S., & Prausnitz J.M. (1975). Statistical thermodynamics of liquid mixtures: a new expression for the excess Gibbs energy of partly or completely miscible systems. *AIChE J.*, **21**(1), 116- 28.

Acharya H.R., & Stern S.A. (1990). Potential advantages and limitations of hybrid membrane processes for the separation of liquid mixtures. *ICOM 90.* Japan. (pp. 341-3).

Aptel P., Cuny J., Josefonvicz J., Morel G., & Néel J. (1974). Liquid transport through membranes prepared by grafting of polar monomers onto poly(tetrafluoroethylene) films. II. Steady-state distribution in membrane during pervaporation. *J.Appl.Polym.Sci.*, **18**, 365-78.

Bac A., Roizard D., Lochon P., & Ghanbaja J. (1996). Synthesis and characterization of new highly selective polyaryloxyphosphazene-polysiloxane crosslinked copolymer films. Application to the extraction of organic compounds from water by pervaporation. *Makromolekulare Chemie. Macromolecular Symposia*, **102**, 225-32.

Baker R.W. (1991). Pervaporation. In: Baker R.W., Cussler E.L., Eykamp W., Koros W.J., Riley R.L., & Strathmann H. (eds.), *Membrane separation systems.* (pp. 151-88). USA: Noyes Data Co.

Ballweg A.H., Brüschke H.E.A, Schneider W.H., Tusel G.F., Böddeker K.W., & Wenzlaff A. (1982). Pervaporation membranes - an economical method to replace conventional dehydration and rectification columns in ethanol distilleries. *Proceedings of the 5th International Alcohol Fuel Technology Symposium.* NZ. (pp. 97- 106).

Barber T.A., & Miller B.D. (1994). Pervaporation technology: fundamentals and environmental applications. *Chem. Eng.*, **9**, 88-90.

Bartels-Caspers C., Tusel-Langer E., & Lichtenthaler R.N. (1992). Sorption isotherms of alcohols in zeolite-filed silicone rubber and in PVA-composite membranes. *J. Membr. Sci.*, **70**, 75-83.

Baudot A., & Marin M. (1996). Dairy aroma compounds recovery by pervaporation. *J.Membr.Sci.*, **120**(2), 207-20.

Beaumelle D., & Marin M. (1994). Effect of transfer in the vapour phase on the extraction by pervaporation through organophilic membranes: experimental analysis on model solutions and theoretical extrapolation. *Chem. Eng. Proc.*, **33**, 449-58.

Beaumelle D., Marin M., & Gibert H. (1993). Pervaporation with organophilic membranes: state of the art. *Trans. I. Chem. E.*, **71** (Part C), 77-89.

Beaumelle D., Marin M., & Gibert H. (1992). Pervaporation of aroma compounds in water-ethanol mixtures: experimental analysis of mass transfer. *J.Food Eng.*, **16**, 293-307.

Bhargava R., & Hlavacek V. (1984). Experience with adopting one- parameter imbedding methods toward calculation of countercurrent separation processes. *Chem. Eng. Commun.*, **28**, 165-79.

Bitter J.G.A. (1991). *Transport mechanisms in membrane separation processes.* USA: Plenum Press.

Bitter J.G.A. (1987). Equilibrium sorption of semicrystalline and crosslinked polymer membranes in multicomponent permeant mixtures. *ICOM 87*, 520-1.

Bitter J.G.A. (1984). Effect of crystallinity and swelling on the permeability and selectivity of polymer membranes. *Desal.*, **51**, 19-35.

Blume I., Wijmans J.G., & Baker R.W. (1990). The separation of dissolved organics from water by pervaporation. *J.Membr.Sci.*, **49**, 253-86.

Bode E. (1990). A simple method to derive activity profiles and diffusivities of permeants in a membrane from steady state permeation measurements. *J.Membr.Sci.*, **50**, 1-17.

Bondi A. (1964). Van der Waals volumes and radii. *J.Phys.Chem.*, **68**(3), 441-451.

Böddeker K.W. (1990). Terminology in pervaporation. *J.Membr.Sci.*, **51**, 259-72.

Böddeker K.W., & Bengtson G. (1991). Selective pervaporation of organics from water. In: R.Y.M. Huang (ed.), *Pervaporation membrane separation processes.* (pp. 437-460). The Netherlands: Elsevier Science Pub. B.V.

Böddeker K.W., Bengtson G., & Pingel H. (1990). Pervaporation of isomeric butanols. *J.Membr.Sci.*, **54**, 1-12.

Brüschke H.E.A. (1990). Removal of ethanol from aqueous streams by pervaporation. *Desal.*, **77**, 323-9.

Bryan, P. F. (1998). *Private communication.*

Cartwright P. (1994). Membranes meet new environmental challenges. *Chem. Eng.*, **9**, 84-7.

Chamberlain R., Borges C.P., Habert A.C., & Nobrega R. (1995). Fractionation of fusel oil coupling pervaporation and distillation. *Proceedings of the 7th International Conference on Pervaporation Processes in the Chemical Industry*. Reno, Nevada. (pp. 271-85).

Chamberlain R., Habert A.C., & Nobrega R. (1994). Fuesel oil separation by pervaporation. *Anais do II CITEM*, 284-91.

Chen W.J., & Martin C.R. (1995). Highly methanol-selective membranes for the pervaporation separation of methyl t-butyl ether/methanol mixtures. *J.Membr.Sci.*, **104**, 101-8.

Cho Y.S., & Joseph B. (1984). Reduced-order models for separation columns - II. Application to columns with multiple feeds and sidestreams. *Comp. Chem. Eng.*, **8**(2), 81-90.

Cho Y.S., & Joseph B. (1983a). Reduced-order steady-state and dynamic models for separation processes. Part 1. Development of the model reduction procedure. *AIChE J.*, **29**(2), 261-9.

Cho Y.S., & Joseph B. (1983b). Reduced-order steady-state and dynamic models for separation processes. Part 2. Application to non-linear multicomponent systems. *AIChE J.*, **29**(2), 270-6.

Cleland, D. J. (1998). Lecture notes on Pinch Technology. Palmerston North: Massey University

Colman D.A., & Mitchell W.S. (1991). Enhanced mass transfer for membrane processes. *Trans. I. Chem. E.*, **69** (Part C), 91-96.

Comyn J. (1985). Introduction to polymer permeability and the mathematics of diffusion. In: J.Comyn (ed.), *Polymer permeability*. (pp. 1-10). UK: Elsevier Applied Science Publishers.

Crank J., & Park G.S. (1968). *Diffusion in polymers*. UK: Academic Press.

Crank J. (1956). *The mathematics of diffusion*. UK: Oxford University Press.

Dhole V., & Linnhoff B. (1992). Distillation targets. Part 2 . *Process Eng.*, **Jul**, 37-8.

Doghieri F., Nardella A., Sarti G.C., & Valentini C. (1993). Pervaporation of methanol - MTBE mixtures through modified polyphenylene-oxide membranes. *ICOM 93*. Heidelberg.

Douglas L., & Feinberg D. (1983). *Evaluation of nondistillation ethanol separation processes*. USA: Solar Energy Research Institute.

Drew, S. (1995). *Pinch technology - an introduction.* NZ: unpublished course material.

Drioli E., Zhang S., & Basile A. (1993). On the coupling effect in pervaporation. *J.Membr.Sci.*, **81**, 43-55.

Drucker D.B. (1981). *Microbiological applications of gas cromatography*. UK: Cambridge University Press.

Enneking L., Heintz A., & Lichtenthaler R.N. (1996). Sorption equilibria of the ternary mixture benzene/cyclohexene/cyclohexane in polyurethane- and PEBA-membrane polymers. *J.Membr.Sci.*, **115**(2), 161-70.

Enneking L., Stephan W., & Heintz A. (1993). Sorption and diffusivity measurements of cyclohexane + benzene and cyclohexane + toluene mixtures in polyurethane membranes. Model calculations of the pervaporation process. *Ber. Bunsenges. Phys. Chem.*, **97**(7), 912-22.

Fadeev A.G., Pavlova A.S., Voznjakovskiy A.P., & Volkov V.V. (1993). Pervaporation of organic-organic mixtures through fluorine-containing polymers. *ICOM 93.* Heidelberg.

Favre E. (1996). Extraction of 1-butanol from aqueous solutions by pervaporation. *J. Chem. Technol. & Biotechnol.*, **65**(3), 221-8.

Favre E., Nguyen Q.T., Sacco D., Moncuy A., & Clement R. (1996). Multicomponent polymer/solvents equilibria: an evaluation of Flory-Huggins theory for crosslinked PDMS networks swelled by binary mixtures. *Chem. Eng. Comm.*, **140**, 193-205.

Favre E., Schaetzel P., Nguygen Q.T., Clément R., & Néel J. (1994). Sorption, diffusion and vapour permeation of various penetrants through dense poly(dimethylsiloxane) membranes: a transport analysis. *J.Membr.Sci.*, **92**, 169-84.

Favre E., Nguyen Q.T., Schaetzel P., Clèment R., & Néel J. (1993). Sorption of organic solvents into dense silicone membranes. Part 1.-Validity and limitations of Flory-Huggins and related theories. *J.Chem.Soc.Faraday Trans.*, **89**(24), 4339-46.

Felder R.M., & Huvard G.S. (1980). Permeation, diffusion and sorption of gases and vapors. In: R.A. Fava (ed.), *Methods of experimental physics.* Vol. 16 . (pp. 315-378). USA: Academic Press, Inc.

Fell N. (1997). Spirits high in distillation. *The Chemical Engineer*, **11**, 23-4.

Fels M., & Huang R.Y.M. (1971). Theoretical interpretation of the effect of mixture composition on separation of liquids in polymers. *J.Macromol.Sci.-Phys.*, **B5**(1), 89-110.

Feng X., & Huang R.Y.M. (1996). Estimation of activation energy for permeation in pervaporation processes. *J.Membr.Sci.*, **118**, 127-31.

Feng X., & Huang R.Y.M. (1994). Concentration polarization in pervaporation separation processes. *J. Membr. Sci.*, **92**, 201-8.

Feng X., & Huang R.Y.M. (1992). Separation of isopropanol from water by pervaporation using silicone-based membranes. *J.Membr.Sci.*, **74**, 171-81.

Field R.W. (1993). Transport processes in membrane systems . In: J.A. Howell, V. Sanchez, & R.W. Field (eds.), *Membranes in bioprocessing: theory and applications*. (pp. 55-112). UK: Chapman & Hall.

Fleming H.L., & Slater C.S. (1992a). Definitions and background. In: W.S.W. Ho, & K.K. Sirkar (ed.), *Membrane Handbook*. (pp. 105- 16). USA: Van Nostrand Reinhold.

Fleming H.L., & Slater C.S. (1992b). Theory. In: W.S.W. Ho, & K.K. Sirkar (ed.), *Membrane Handbook*. (pp. 117-22). USA: Van Nostrand Reinhold.

Fleming H.L., & Slater C.S. (1992c). Applications and economics. In: W.S.W. Ho, & K.K. Sirkar (ed.), *Membrane Handbook*. (pp. 132- 59). USA: Van Nostrand Reinhold.

Fleming H.L., & Slater C.S. (1992d). Design. In: W.S.W. Ho, & K.K. Sirkar (ed.), *Membrane Handbook*. (pp. 123-31). USA: Van Nostrand Reinhold.

Flory P.J. (1953). *Principles of polymer chemistry*. USA: Cornell University Press.

Franken A.C.M., Mulder M., & Smolders C.A. (1990). Pervaporation process using a thermal gradient as the driving force. *J.Membr.Sci.*, **53**, 127-41.

Fredenslund A., Gmehling J., & Rasmussen P. (1977). *Vapor-liquid equilibria using UNIFAC*. The Netherlands: Elsevier.

Gmehling J., & Onken U. (1977). *Vapour liquid equilibrium data collection. Vol I.* Germany: DECHEMA.

Goto A., Takahashi M., Kuwahara N., & Kubota K. (1995). Numerical simulation of solvent diffusion for binary alcohol mixtures in polyacrylonitrile membrane. *J.Membr.Sci.*, **99**, 107-15.

Gref R., Nguyen Q.T, & Néel J. (1992). Influence of membrane properties on system performances in pervaporation under concentration polarization regime. *Sep. Sci. Technol.*, **27**(4), 467-91.

Hansen H.K., Rasmussen R., Fredenslund A., Schiller M., & Gmehling J. (1991). Vapor-liquid equilibria by UNIFAC group contribution. 5. Revision and extension. *Ind.Eng.Chem.Res.*, **30**(10), 2352-5.

Harders T., Sykes S.J., & Prince R.G.H. (1995). Spinning cone distillation in wine treatment. *CHEMECA 95*. **3**(pp. 32-6). Australia.

Hausen H. (1953). Zur Definition des Austauschgrades von Rektifizierböden bei Zwei- und Dreistoff-Gemischen. *Chem. -Ing. - Tech.*, **25**(10), 595-7.

Hauser J., Reinhardt G.A., Stumm F., & Heintz A. (1989a). Non- ideal solubility of liquid mixtures in poly(vinyl alcohol) and its influence on pervaporation. *J.Membr.Sci.*, **47**, 261-76.

Hauser J., Heintz A., Schmittecker B., & Lichtenthaler R.N. (1989b). Sorption equilibria and diffusion in polymeric membranes. *Fluid Phase Equilibria*, **51**, 369-81.

Hauser J., Reinhardt G.A., Stumm F., & Heintz A. (1989c). Experimental study of solubilities of water containing organic mixtures in polyvinylalcohol using gas chromatographic and infrared spectroscopic analysis. *Fluid Phase Equilibria*, **49**, 195- 210.

Heil J.F., & Prausnitz J.M. (1966). Phase equilibria in polymer solutions. *AIChE J.*, **12**(4), 678-685.

Heintz A., & Stephan W. (1994a). A generalized solution-diffusion model of the pervaporation process through composite membranes. Part I. Prediction of mixture solubilities in the dense active layer using the UNIQUAC model. *J. Membr. Sci.*, **89**, 143-51.

Heintz A., & Stephan W. (1994b). A generalized solution-diffusion model of the pervaporation process through composite membranes. Part II. Concentration polarization, coupled diffusion and the influence of the porous support layer. *J. Membr. Sci.*, **89**, 153- 69.

Heintz A., Funke H., & Lichtenthaler R.N. (1991). Sorption and diffusion in pervaporation membranes. In: R.Y.M. Huang (ed.), *Pervaporation membrane separation processes*. (pp. 279-319). The Netherlands: Elsevier Science Pub. B.V.

Hickey P.J., Juricic F.P., & Slater C.S. (1992). The effect of process parameters on the pervaporation of alcohols through organophilic membranes. *Sep. Sci. Technol.*, **27**(7), 843-61.

Holland C.D. (1981). *Fundamentals of multicomponent distillation*. USA: McGraw-Hill Book Co.

Howell J.A. (1993). Design of membrane systems. In: J.A. Howell, V. Sanchez, & R.W. Field (eds.), *Membranes in bioprocessing: theory and applications*. (pp. 141-202). UK: Chapman & Hall.

Huang R.Y.M., & Rhim J.W. (1991). Separation characteristics of pervaporation membrane separation processes. In: R.Y.M. Huang (ed.), *Pervaporation membrane separation processes.* (pp. 111-80). The Netherlands: Elsevier Science Publishers B.V.

Humphrey J.L., & Seibert A.F. (1992). Separation technologies: An opportunity for energy savings. *Chem. Eng. Progr.*, **Mar.**, 32-41.

Huss R.S., & Westerberg A.W. (1996a). Collocation methods for distillation design. 1. Model description and testing. *Ind.Eng.Chem.Res.*, **35**, 1603-10.

Huss R.S., & Westerberg A.W. (1996b). Collocation methods for distillation design. 2. Applications for distillation. *Ind.Eng.Chem.Res.*, **35**, 1611-23.

Ji W., Sikdar S.K., & Hwang S.T. (1994a). Modeling of multicomponent pervaporation for removal of volatile organic compounds from water. *J.Membr.Sci.*, **93**, 1-19.

Ji W., Hilaly A., Sikdar S.K., & Hwang S.T. (1994b). Optimization of multicomponent pervaporation for removal of volatile organic compounds from water. *J.Membr.Sci.*, **97**, 109-25.

Jonquières A., & Fane A. (1997). Filled and unfilled composite GFT PDMS membranes for the recovery of butanols from dilute aqueous solutions: influence of alcohol polarity. *J.Membr.Sci.*, **125**, 245-55.

Jonquières A., Roizard D., & Lochon P. (1996). Polymer design for pervaporation membranes: influence of the soft segment size of block copolymers (polyurethaneimides of polyurethaneamides) on pervaporation features. *J.Membr.Sci.*, **118**, 73-84.

Karlsson H.O.E. (1996). *Pervaporative aroma recovery during beverage processing.* Unpublished doctoral dissertation, Lund University, Sweden.

Karlsson H.O.E., Loureiro S., & Trägårdh G. (1995a). Aroma compound recovery with pervaporation - temperature effects during pervaporation of a muscat wine. *J.Food Eng.*, **26**, 177-91.

Karlsson H.O.E., & Trägårdh G. (1995b). Heat transfer and temperature polarization in pervaporation. *Proceedings of the 7th International Conference on Pervaporation Processes in the Chemical Industry.* Reno, Nevada. (pp. 171-181).

Kedem O. (1989). The role of coupling in pervaporation. *J.Membr.Sci.*, **47**, 277-84.

K.Engineering, Inc. (1993). Dehydrate ethanol without distillation. *Chem. Eng.*, **Oct.**, 155.

Kier L.B, & Hall L.H. (1976). *Molecular connectivity in chemistry and drug research.* USA: Academic Press.

Kober P.A. (1917). Pervaporation, perstillation and percrystallization. *J. Am. Chem. Soc.*, **39**, 944-50.

Koopmans L.H. (1987). *Introduction to contemporary statistical methods*. USA: PWS Publishers.

Koops G.H., Nolten J.A.M., Mulder M.H.V., & Smolders C.A. (1994). Selectivity as a function of membrane thickness: gas separation and pervaporation. *J.Appl.Polym.Sci.*, **53**, 1639-51.

Koops G.H., & Smolders C.A. (1991). Estimation and evaluation of polymeric materials for pervaporation membranes. In: R.Y.M. Huang (ed.), *Pervaporation membrane separation processes*. (pp. 235-78). The Netherlands: Elsevier Science Pub. B.V.

Kovach J.W., & Seider W.D. (1987). Heterogeneous azeotropic distillation: experimental and simulation results. *AIChE J.*, **33**(8), 1300-14.

Krishna R., & Taylor R. (1986). Multicomponent mass transfer: theory and applications. In: Cheremisinoff N.P. (ed.), *Handbook for heat and mass transfer operations*. Vol. II. (pp. 260-424). USA: Gulf Publishing Co.

Krishnamurthy R., & Taylor R. (1985a). A nonequilibrium stage model of multicomponent separation processes. *AIChE J.*, **31**(3), 449-56.

Krishnamurthy R., & Taylor R. (1985b). A nonequilibrium stage model of multicomponent separation processes. Part II: comparison with experiment. *AIChE J.*, **31**(3), 456-65.

Krishnamurthy R., & Taylor R. (1985c). A nonequilibrium stage model of multicomponent separation processes. Part III: The influence of unequal component-efficiencies in process design problems. *AIChE J.*, **31**(12), 1973-85.

Krishnamurthy R., & Taylor R. (1985d). Simulation of packed distillation and absorption columns. *Ind. Eng. Chem. Process Des. Dev.*, **24**, 513-24.

Kujawski W., Waczynski M, & Lasota M. (1996). Pervaporation properties of dense polyamide-6 membranes in separation of water- ethanol mixtures. *Sep. Sci. Technol.*, **31**(7), 953-63.

Kumins C.A., & Kwei T.K. (1968). Free volume and other theories. In: J.Crank, & G.S.Park (eds.), *Diffusion in Polymers*. (pp. 107- 40). UK: Academic Press.

Lamer T., Rohart M.S., Voilley A., & Baussart H. (1994). Influence of sorption and diffusion of aroma compounds in silicone rubber on their extraction by pervaporation. *J.Membr.Sci.*, **90**, 251-63.

Larsson M., & Zacchi G. (1996). Production of ethanol from dilute glucose solutions. A technical-economic evaluation of various refining alternatives. *Bioprocess Eng.*, **15**, 125-32.

Le Carbone-Lorraine. (1993). Membrane motivation with pervaporation. *Filtr. & Sep.*, **11**, 620-2.

Lee Y.M., Bourgeois D., & Belfort G. (1989). Sorption, diffusion, and pervaporation of organics in polymer membranes. *J.Membr.Sci.*, **44**, 161-81.

Leeper S.A. (1986). Membrane separations in the production of alcohol fuels by fermentation. In: W.C. McGregor (ed.), *Membrane separations in biotechnology*. (pp. 161-200). USA: Marcel Dekker, Inc.

Lewis W.K. (1922). The efficiency and design of rectifying columns for binary mixtures. *J. Ind. and Engng. Chem.*, **14**(6), 492-7.

Liang L., & Ruckenstein E. (1996). Pervaporation of ethanol-water mixtures through polydimethylsiloxane-polystyrene interpenetrating polymer network supported membranes. *J.Membr.Sci.*, **114**, 227-34.

Linnhoff B. (1995). *Hero 3.2 - the manual*. UK: IChemE.

Linnhoff B. (1993). Pinch analysis - a state of the art review. *Chem. Eng. Res. Des.*, **71**(A5), 503-22.

Linnhoff B., Dunford H., & Smith R. (1983). Heat integration of distillation columns into overall processes. *Chem.Eng.Sci.*, **38**(8), 1175-88.

Lochon P. (1998). *Private communication.*

Maiorella B.L., Blanch H.W., & Wilke C.R. (1984). Economic evaluation of alternative ethanol fermentation processes. *Biotech. Bioeng.*, **26**, 1003-25.

Mason E.A., & Lonsdale H.K. (1990). Statistical-mechanical theory of membrane transport. *J.Membr.Sci.*, **51**, 1-81.

Matsuura T. (1994). *Synthetic membranes and membrane separation processes*. USA: CRC Press, Inc.

Mawson J. (1994). Current status of the whey to ethanol fermentation in New Zealand. *Australasian Biotechnol.*, **4**, 24-5.

Mawson J. (1987). Ehtanol production from whey in New Zealand. *Austr. J. Biotechnol.*, **1**(3), 64-73.

Meares P. (1976). *Membrane separation processes*. The Netherlands: Elsevier Scientific Publishing Co.

Mix T.J., Dweck J.S., Weinberg M., & Armstrong R.C. (1978). Energy conservation in distillation. *Chem.Eng.Progr.*, **Apr.**, 49- 55.

Moganti S., Noble R.D., & Koval C.A. (1994). Analysis of a membrane/distillation column hybrid process. *J.Membr.Sci.*, **93**, 31-44.

Molina C., Steinchen A., Charbit G., & Charbit F. (1997). Model for pervaporation: application to ethanolic solutions of aroma. *J.Membr.Sci.*, **132**, 119-29.

Moutounet M., Escudier J.L., & Jouret C. (1992). Production of spirits by pervaporation. Comparison with still distillation. *Lebensm.- Wiss. u. -Technol.*, **25**, 71-3.

Mulder M. (1994). Energy requirements in membrane separation processes. In: J.G. Crespo, & Böddeker K.W. (ed.), *Membrane processes in separation and purification*. (pp. 445-475). The Netherlands: Kluwer Academic Publishers.

Mulder M. (1991). *Basic principles of membrane technology*. The Netherlands: Kluwer Academic Publications.

Mulder M., & Smolders C.A. (1991). Mass transport phenomena in pervaporation processes. *Sep. Sci. Technol.*, **26**(1), 85-95.

Mulder M., & Smolders C.A. (1986). Pervaporation, solubility aspects of the solution-diffusion model. *Sep. Pur. Meth.*, **15**(1), 1-19.

Mulder M.H.V., Franken A.C.M., & Smolders C.A. (1985a). Preferential sorption versus preferential permeability in pervaporation. *J.Membr.Sci.*, **22**, 155-73.

Mulder M.H.V., Franken A.C.M., & Smolders C.A. (1985b). On the mechanism of separation of ethanol/water mixtures by pervaporation. II. Experimental concentration profiles. *J.Membr.Sci.*, **23**, 41-58.

Mulder M.H.V., & Smolders C.A. (1984). On the mechanism of separation of ethanol/water mixtures by pervaporation. I. Calculations of concentration profiles. *J.Membr.Sci.*, **17**, 289- 307.

Mulder M.H.V., Hendrikman J.O., Hegeman H., & Smolders C.A. (1983). Ethanol-water separation by pervaporation. *J.Membr.Sci.*, **16**, 269-84.

Murphree E.V. (1925). Rectifying column calculations with particular reference to n component mixtures. *Ind. Eng. Chem.*, **17**(7), 747-50.

Naphtali L.M., & Sandholm D.P. (1971). Multicomponent separation calculations by linearization. *AIChE J.*, **17**(1), 148-53.

Néel J. (1991). Introduction to pervaporation. In: R.Y.M. Huang (ed.), *Pervaporation membrane separation processes.* (pp. 1-109). The Netherlands: Elsevier Science Publishers B.V.

Néel J. (1990). Fundamentals of pervaporation for ethanol/water separation. *The membrane alternative: energy implications for industry. The Watt Committee on energy.* Report no. 21. UK: Elsevier Applied Science.

Néel J., Aptel P., & Clément R. (1985). Basic aspects of pervaporation. *Desal.*, **53**, 297-326.

Nguyen Q.T. (1986). The influence of operation parameters on the performance of pervaporation processes. *AIChE Symposium Series 248*, **82**, 1-11.

Ognisty T.P. (1995). Analyse distillation columns with thermodynamics. *Chem.Eng.Progr.*, **Feb.**, 40-6.

Okada T., & Matsuura T. (1991). A new transport model for pervaporation. *J.Membr.Sci.*, **59**, 133-50.

Okada T., & Matsuura T. (1992). Predictability of transport equations for pervaporation on the basis of pore-flow mechanism. *J.Membr.Sci.*, **70**, 163-75.

Okushita H., Yoshikawa M., & Shimidzu T. (1995). Pervaporation of cyclohexane/cyclohexanone/cyclohexanol mixture through polyoxyethylene grafting nylon 6 membrane. *J.Membr.Sci.*, **105**, 51- 3.

Park G.S. (1968). The glassy state and slow process anomalies. In: J.Crank, & G.S.Park (eds.), *Diffusion in Polymers.* (pp. 141- 63). UK: Academic Press.

Paul D.R., & Ebra-Lima O.M. (1970). Pressure-induced diffusion of organic liquids through highly swollen polymer membranes. *J.Appl.Polym.Sci.*, **14**, 2201-24.

Pearce G.K. (1990). Hybrid pervaporation/distillation processes for alcohol dewatering. *ICOM 90.* Japan. (pp. 1011-3).

Pingel H. (1995). *Personal comunication.* : GKSS.

Porter K.E. (1995) Why research is needed in distillation. *Trans. I. Chem. Eng.*, **73** (Part A), 357-62.

Powers M.F., Vickery D.J., Arehole A., & Taylor R. (1988). A nonequilibrium stage model of multicomponent separation processes - V. Computational methods for solving the model equations. *Comp. Chem. Eng.*, **12** (12), 1229-41.

Prausnitz J.M. (1995). *Private comunication.*

Prausnitz J.M., Lichtenthaler R.N., & Azevedo E.G. (1986). *Molecular thermodynamics of fluid-phase equilibria.* USA: Prentice-Hall, Inc.

Pyke M. (1965). The manufacture of scoth grain whisky. *J. Inst. Brew.*, **71**, 209-18.

Radovanovic P., Thiel S.W., & Hwang S.T. (1990). Transport of ethanol-water dimers in pervaporation through a silicone rubber membrane. *J.Membr.Sci.*, **48**, 55-65.

Raghunath B., & Hwang S.T. (1992). Effect of boudary layer mass transfer resistance in the pervaporation of dilute organics. *J.Membr.Sci.*, **65**, 147-61.

Rautenbach R., & Vier J. (1995). Design and analysis of combined distillation/pervaporation processes. *Proceedings of the 7th International Conference on Pervaporation Processes in the Chemical Industry.* Reno, Nevada. (pp. 70-85).

Rautenbach R., & Helmus F.P. (1994). Some considerations on mass- transfer resistances in solution-diffusion-type membrane processes. *J. Membr. Sci.*, **87**, 171-181.

Rautenbach R., Herion C., & Meyer-Blumenroth U. (1991). Engineering aspects of pervaporation: calculation of transport resistances, module optimization and plant design. In: R.Y.M. Huang (ed.), *Pervaporation membrane separation processes.* (pp. 181-223). The Netherlands: Elsevier Science Pub. B.V.

Rautenbach R., & Albrecht R. (1989). *Membrane processes.* UK: John Wiley & Sons.

Rautenbach R., & Albrecht R. (1985). The separation potential of pervaporation. Part 1. Discussion of transport equations and comparison with reverse osmosis. *J.Membr.Sci.*, **25**, 1-23.

Rautenbach R., & Albrecht R. (1984). On the behaviour of asymmetric membranes in pervaporation. *J.Membr.Sci.*, **19**, 1-22.

Rautenbach R., & Albrecht R. (1980). Separation of organic binary mixtures by pervaporation. *J.Membr.Sci.*, **7**, 203-.

Reesen L. (1978). Alcohol production from whey. *Dairy Ind. Int.*, **1**, 9,16.

Reid R.C., Prausnitz J.M., & Poling B.E. (1987). *The properties of gases and liquids (4th. ed.).* USA: McGraw-Hill Book Co.

Rogers C.E. (1985). Permeation of gases and vapours in polymers. In: J.Comyn (ed.), *Polymer permeability.* (pp. 11-73). UK: Elsevier Applied Science Publishers.

Ruckenstein E., & Liang L. (1996). Poly(acrylic acid)-poly(vinyl alcohol) semi- and interpenetrating polymer network pervaporation membranes. *J.Appl.Polym.Sci.*, **62**, 673-87.

Ruckenstein E., & Sun F. (1995). Hydrophobic-hydrophilic composite membranes for the pervaporation of benzene-ethanol mixtures. *J. Membr. Sci.*, **103**(3), 271-83.

Ruston M. (1990). Recent advances in cellulosic membranes for gas separation and pervaporation. *The membrane alternative: energy implications for the industry. The Watt Committee on Energy.* Report no. 21. UK: Elsevier.

Ruzicka Jr. V., & Domalski E.S. (1993a). Estimation of the heat capacities of organic liquids as a function of temperature using group additivity. I. Hydrocarbon compounds. *J. Phys. Chem. Ref. Data*, **22**(3), 597-618.

Ruzicka Jr. V., & Domalski E.S. (1993b). Estimation of the heat capacities of organic liquids as a function of temperature using group additivity. II. Compounds of carbon, hydrogen, halogens, nitrogen, oxygen and sulfur. *J. Phys. Chem. Ref. Data*, **22**(3), 619-57.

Schäfer T., Pingel H., Kniebusch M.M., Böddekker K.W., & Crespo J.P.S.G. (1997). Recovery of aroma compounds from wine-must by pervaporation and sorption of selected compounds in poly-octyl- methyl-siloxane-membranes. Kemperman A.J.B., & Koops G.H., *Euromembrane 97.* The Netherlands. (pp. 323-5). The Netherlands.

Seader J.D. (1989). The rate-based approach for modeling staged separations. *C.E.P.*, **Oct.**, 40-49.

Shabtai Y., & Mandel C. (1993). Control of ethanol production and monitoring of membrane performance by mass-spectrometric gas analysis in the coupled fermentation-pervaporation of whey permeate. *Appl. Microbiol. Biotechnol.*, **40**, 470-6.

Shanley A. (ed.), Ondrey G., & Moore S. (1994). Pervaporation finds its niche. *Chem. Eng.*, **9**, 34-7.

Short J.L. (1978). Prospects for the utilization of deproteinated whey in New Zealand - A review. *N.Z.Jl.Dairy Sci. Technol.*, **13**, 191-94.

Simandl J., & Svrcek W.Y. (1991). Extension of the simultaneous- solution and inside-outside algorithms to distillation with chemical reactions. *Comp. Chem. Eng.*, **15**(5), 337-48.

Simmons V., Kaschemekat J., Jacobs M.L., & Dortmundt D.D. (1994). Membrane systems offer a new way to recover volatile organic air pollutants. *Chem. Eng.*, **9**, 92-4.

Smith J.M., & Van Ness H.C. (1980). *Introdução à termodinâmica da engenharia química (3rd. ed.).* Brazil: Ed. Guanabara Dois.

Sonntag R.E., & Van Wylen G. (1982). *Introduction to thermodynamics. (2nd ed.)*. USA: John Wiley and Sons, Inc.

Sorensen J.M., & Arlt W. (1980). Liquid-liquid equilibrium data collection. Ternary systems. **Vol. 5. Part 2**. In: D. Behrens, & R. Eckerman. *Chemistry Data Series*. BRD: DECHEMA.

Spitzen J.W.F., Elsinghorst E., Mulder M.H.V., & Smolders C.A. (1987). Solution-diffusion aspects in the separation of ethanol/ water mixtures with PVA membranes. R. Bakish (ed.), *2nd Internation Conference on Pervaporation Processes in the Chemical Industry*. Texas, USA. (pp. 209-24).

Stephan W., Noble R.D., & Koval C.A. (1995). Design methodology for a membrane/distillation column hybrid process. *J.Membr.Sci.*, **99**, 259-272.

Strathmann H., & McDonogh R.M. (1993). The use of pervaporation in biotechnology. In: J.A. Howell, V. Sanchez, & R.W. Field (eds.), *Membranes in bioprocessing: theory and applications*. (pp. 293-327). UK: Chapman & Hall.

Tanihara N., Tanaka K., Kita H., & Okamoto K. (1994). Pervaporation of organic liquid mixtures through membranes of polyimides containing methyl-substituted phenylenediamine moieties. *J. Membr. Sci.*, **95**, 161-9.

Tarjus H., Vauclair C., Remigy J.C., Niang M., & Schaetzel P. (1996). Fractionnement de mélanges aqueux d'alcools supérieurs par le couplage de la pervaporation et de la distillation. *Proceedings of the XIII Congress on Electricity Applications*. (pp. CC39-46). Birmingham, UK.

Taylor R. (1996). *Personal communication*,

te Hennepe H.J.C., Boswerger W.B.F., Bargeman D., Mulder M.H.V., & Smolders C.A. (1994). Zeolite-filled silicone rubber membranes. Experimental determination of concentration profiles. *J.Membr.Sci.*, **89**, 185-96.

te Hennepe H.J.C., Bargeman D., Mulder M.H.V., & Smolders C.A. (1987a). Pervaporation with zeolite filled silicone rubber membranes. *Proceedings of the Second International Conference on Pervaporation Processes in the Chemical Industry*. (pp. 71-8). Texas, USA: Bakish Materials Corporation.

te Hennepe H.J.C., Bargeman D., Mulder M.H.V., & Smolders C.A. (1987b). Zeolite-filled silicone rubber membranes. Part I. Membrane preparation and pervaporation results. *J.Membr.Sci.*, **35**, 39-55 .

Teo K.W., & Ruthven D.M. (1986). Adsorption of water from aqueous ethanol using 3-Å molecular sieves. *Ind. Eng. Chem. Process Des. Dev.*, **25**, 17-21.

Tioe, J. F. (1990). *A pinch technology analysis of energy integration in the Huntly power station.* Unpublished doctoral dissertation, masterate Massey University, NZ.

Tsujita Y. (1992). The physical chemistry of membranes. In: Y. Osada, & T.Nakagawa (eds.), *Membrane science and technology.* (pp. 3-60). USA: Marcel Dekker, Inc.

Tusel G.F., & Brüschke H.E.A. (1985). Use of pervaporation systems in the chemical industry. *Desal.*, **53**, 327-338.

Uragami T., Doi T., & Miyata T. (1996). Surface modification of poly[1-(trimethylsilyl-1-1propyne)] membrane by polymer additives and pervaporation property for aqueous ethanol solutions through their membranes. *IMSTEC 96.* (pp. 206-8). Australia.

van den Berg G.B., & Smolders C.A. (1992). Diffusional phenomena in membrane separation processes. *J.Membr.Sci.*, **73**, 103-18.

van Winden, W. (1997). *Production of volatiles during ethanolic fermentation of whey permeate by* Kluyveromyces marxianus. Report prepared for Massey University, NZ.

Vieth W.R. (1988). *Membrane systems: analysis and design.* BRD: Hanser Publishers.

Wagner W., & Pruss A. (1993). International equations for the saturation properties of ordinary water substance. *J. Phys. Chem. Ref. Data*, **22**(3), 783-7.

Watson J.M., & Payne P.A. (1990). A study of organic compound pervaporation through silicone rubber. *J.Membr.Sci.*, **49**, 171-205.

Wesselingh J.A., & Krishna R. (1990). *Mass transfer.* UK: Elis Horwood Ltd.

Wijmans J.G., Baker R.W., & Athayde A.L. (1994). Pervaporation: removal of organics from water and organic/organic separations. In: J.G. Crespo, & Böddeker K.W. (eds.), *Membrane processes in separation and purification.* (pp. 283-316). The Netherlands: Kluwer Academic Publishers.

Wijmans J.G., & Baker R.W. (1993). A simple predictive treatment of the permeation process in pervaporation. *J. Membr. Sci.*, **79**, 101-113.

Wiley, D. (1997). *Private communication.*

Will B., & Lichtenthaler R.N. (1992). Comparison of the separation of mixtures by vapor permeation and by pervaporation using PVA composite membranes. II. The binary systems ammonia- water, methylamine-water, 1-propanol-methanol and the ternary system 1-propanol-methanol-water. *J.Membr.Sci.*, **68**, 127-31.

Yoshikawa M., Wano T., & Kitao T. (1994). Specialty polymeric membranes. 2. Pervaporation separation of aqueous lower alcohol solutions through modified polybutadiene membranes. *J.Membr.Sci.*, **89**, 23-36.

Younaian L., Changluo Z., & Me'o L. (1990). Removal of ethanol from continuous fermentation broth by pervaporation. *ICOM 90.* Japan. (pp. 334-6).

Zadow J.G. (ed.) (1992). *Whey and lactose processing.* UK: Elsevier Applied Science.

Zhang S., & Drioli E. (1995). Pervaporation membranes. *Sep.Sci.Technol.*, **30**(1), 1-31.

Part Four

Appendices

Appendix A

COLLATION OF NZDCL DATA

Table A.1 Feed and product flow rates of NZDCL columns (Figure X.2).

date	11	09	95	22	11	95	05	03	96	25	04	96
shift	*1*	*2*	*3*	*1*	*2*	*3*	*1*	*2*	*3*	*1*	*2*	*3*
Steam (ton.day^{-1})		174.7			185.8			177.8			127.8	
Steam PC (kg.h^{-1})	300	280	280	220	220	220	300	300	300	300	300	300
Steam ED (kg.h^{-1})	1100	1100	1100	1000	1000	1000	1000	1000	1000	1000	1000	1000
Steam RC (kg.h^{-1})	1354	1374	1351	1371	1328	1377	1357	1362	1357	1364	1363	1373
Feed to BC1 (l.h^{-1})	45k	28.5k	43.9k	46k	45k	46k	40.6k	42k	44k	36.4k	36.4k	34k
Fusels to BC2 (l.h^{-1})	260	260	260	260	260	260	270	270	270	270	270	270
Feed to PC (l.h^{-1})	1200	1200	1206	1208	1200	1198	1192	1174	1172	1120	1103	1131
FI 10 (l.h^{-1})	5	5	5	5	5	5	10	10	10	10	10	10
FI 16 (l.h^{-1})	30	30	30	24	24	24	20	24	24	30	30	30
Pinch (l.h^{-1})	15	15	15	15	15	15	15	15	15	9	9	9
Water (l.h^{-1})	4920	4920	4920	3840	3840	3840	3840	3840	3840	3840	3840	3840
FI 21 (l.h^{-1})	100	100	100	100	100	100	100	100	100	100	100	100
FI 22 (l.h^{-1})	60	60	60	60	60	60	60	60	60	60	60	60
FI 23 (l.h^{-1})	60	60	60	60	60	60	60	60	60	60	60	60
FI 24 (l.h^{-1})	10	10	10	10	10	10	20	20	20	20	20	20
Product (l.h^{-1})	909	976	773	922	952	948	877	839	871	835	830	750

to drain: FI 10 and FI 16
to drums: Pinch and Base, FI 21, FI 22, FI 23, FI 24.

Table A.2 Concentration (w/w) of samples taken on the 11th of September 1995.

		methanol	ethanol	i-propanol	n-propanol	i-butanol	n-butanol	i-amyl acohol	ethyl acetate	water & other
Feed BC1	1	nd	1.82%	nd	nd	0.0019%	nd	0.0097%	0.0010%	98.16%
	2	nd	1.80%	nd	nd	0.0039%	nd	0.0069%	0.0010%	98.19%
	3	nd	1.84%	nd	nd	0.0029%	nd	0.0098%	0.0010%	98.15%
BC2 Prod.	1	0.0117%	59.41%	0.0012%	0.15%	0.0643%	nd	0.1941%	0.0456%	40.12%
	2	0.0120%	68.66%	0.0024%	0.16%	0.0371%	nd	0.0371%	0.0287%	31.06%
	3	0.0106%	74.42%	0.0047%	0.16%	0.0709%	nd	0.1429%	0.0343%	25.16%
FI-10	1	0.0124%	48.82%	nd	0.03%	0.0214%	nd	0.0056%	11.04%	40.07%
	2	0.0114%	54.88%	nd	0.04%	0.0206%	nd	nd	8.3240%	36.72%
	3	0.0124%	50.26%	nd	0.04%	0.0203%	nd	nd	12.15%	37.52%
PC Bottoms	1	nd	46.42%	0.0011%	0.12%	0.0507%	nd	0.1301%	0.0033%	53.27%
	2	nd	45.59%	0.0011%	0.11%	0.0356%	nd	0.0636%	0.0917%	54.11%
	3	0.0108%	42.69%	0.0022%	0.13%	0.0410%	nd	0.0550%	nd	57.07%
FI-16	1	nd	41.33%	0.1512%	1.65%	3.6621%	0.0154%	7.7281%	0.0607%	45.40%
	2	nd	37.24%	0.1083%	1.33%	2.8587%	0.0111%	5.4234%	0.0630%	52.96%
	3	nd	38.10%	0.1169%	1.41%	2.8936%	0.0234%	6.3082%	0.0813%	51.07%
ED Bottoms	1	nd	6.91%	nd	0.02%	0.0040%	nd	0.0181%	nd	93.05%
	2	nd	8.01%	0.0010%	0.04%	0.0373%	nd	0.0907%	nd	91.82%
	3	nd	8.04%	nd	0.02%	0.0031%	nd	0.0112%	nd	91.92%
ED Pinch	1	nd	16.10%	nd	0.04%	0.0113%	nd	0.0492%	nd	83.80%
	2	nd	12.64%	nd	0.03%	0.0041%	nd	0.0162%	nd	87.31%
	3	nd	23.53%	nd	0.07%	0.0143%	nd	0.0979%	nd	76.29%
FI-21	1	nd	80.43%	nd	2.21%	0.2965%	0.0080%	1.5659%	nd	15.48%
	2	nd	72.81%	nd	1.86%	0.2387%	0.0023%	0.5070%	nd	24.58%
	3	nd	66.09%	nd	1.82%	0.2443%	0.0091%	1.6025%	nd	30.23%
FI-22	1	nd	77.87%	nd	0.57%	0.0188%	nd	0.0047%	nd	21.54%
	2	nd	75.99%	nd	0.74%	0.0251%	nd	0.0048%	nd	23.24%
	3	nd	79.73%	0.0012%	0.69%	0.0283%	nd	0.0177%	nd	19.53%
FI-23	1	nd	74.29%	0.0000%	0.05%	nd	nd	nd	nd	25.66%
	2	nd	85.73%	0.0012%	0.06%	nd	nd	nd	nd	14.20%
	3	nd	89.59%	0.0024%	0.10%	nd	nd	nd	nd	10.30%
FI-24	1	0.0194%	74.98%	nd	nd	nd	nd	0.0242%	0.0036%	24.97%
	2	0.0146%	85.65%	nd	nd	nd	nd	nd	nd	14.34%
	3	0.0183%	91.84%	nd	nd	nd	nd	nd	nd	8.14%
RC Prod	1	nd	85.47%	nd	nd	nd	nd	nd	nd	14.53%
	2	nd	83.09%	nd	0.0048%	nd	nd	nd	nd	16.90%
	3	0.0133%	96.01%	nd	nd	nd	nd	nd	nd	3.98%

nd: not detected.

Table A.3 Concentration (w/w) of samples taken on the 22th of November 1995.

		methanol	ethanol	i-propanol	n-propanol	i-butanol	n-butanol	i-amyl acohol	ethyl acetate	water & other
Feed BC1	1	nd	1.38%	nd	nd	nd%	nd	0.0011%	nd	98.62%
	2	nd	2.29%	nd	0.0019%	0.0028%	nd	0.0032%	nd	97.70%
	3	nd	1.89%	nd	0.0062%	0.0024%	nd	0.0024%	nd	98.10%
BC2 Prod.	1	nd	79.12%	nd	0.1122%	0.0154%	nd	nd	0.0358%	20.76%
	2	nd	81.09%	nd	0.2694%	0.1227%	nd	0.0304%	0.0161%	18.48%
	3	nd	79.81%	nd	0.2419%	0.0870%	nd	0.0452%	0.0281%	19.82%
FI-10	1	0.0206%	59.39%	nd	0.0026%	nd	nd	nd	12.15%	40.59%
	3	nd	43.74%	nd	0.0051%	nd	nd	nd	8.5008%	56.25%
PC Bottoms	1	nd	42.59%	nd	0.1536%	0.0692%	0.0007%	0.1270%	0.0149%	57.06%
	2	0.0022%	52.04%	nd	0.2274%	0.0921%	0.0011%	0.1851%	0.0687%	47.45%
	3	nd	29.44%	nd	0.1932%	0.0739%	0.0008%	0.0786%	0.0088%	70.21%
FI-16	1	nd	27.45%	0.0609%	0.6705%	2.7006%	0.0038%	3.4894%	0.6943%	65.63%
	2	nd	39.28%	0.0578%	0.8296%	2.9460%	0.0047%	3.4387%	0.6537%	53.44%
	3	nd	39.63%	0.0579%	0.8738%	3.1045%	0.0059%	3.4126%	0.7166%	52.92%
ED Bottoms	1	nd	11.24%	nd	0.0345%	0.0074%	nd	0.0158%	nd	88.70%
	2	nd	12.23%	nd	0.0430%	0.0080%	nd	0.0440%	nd	87.68%
	3	nd	12.01%	nd	0.0444%	0.0087%	0.0013%	0.0220%	nd	87.91%
ED Pinch	1	nd	24.69%	nd	0.0663%	0.0209%	nd	0.0310%	nd	75.20%
	2	nd	23.88%	nd	0.0798%	0.0238%	nd	0.0436%	nd	75.97%
	3	nd	25.41%	nd	0.0826%	0.0273%	nd	0.0279%	nd	74.45%
FI-21	1	nd	58.82%	nd	1.7466%	0.5131%	0.0120%	2.7114%	nd	36.19%
	2	nd	59.22%	nd	2.0163%	0.4942%	0.0167%	2.9063%	nd	35.34%
	3	nd	62.50%	nd	2.1329%	0.5052%	0.0172%	1.6564%	nd	33.19%
FI-22	1	nd	83.07%	nd	0.7684%	0.0529%	nd	0.0117%	nd	16.10%
	2	nd	76.96%	nd	0.7281%	0.0428%	nd	0.0150%	nd	22.25%
	3	nd	58.45%	nd	0.5639%	0.0317%	nd	0.0023%	nd	40.95%
FI-23	1	0.0022%	83.24%	nd	0.0936%	0.0014%	nd	nd	nd	16.66%
	2	nd	81.92%	nd	0.0922%	0.0010%	nd	nd	nd	17.99%
	3	0.0031%	82.30%	nd	0.0906%	0.0026%	nd	nd	nd	17.61%
FI-24	1	0.0029%	93.95%	nd	0.0014%	nd	nd	nd	nd	6.05%
	2	0.0034%	68.65%	nd	nd	nd	nd	nd	nd	31.34%
	3	0.0028%	95.25%	nd	nd	nd	nd	nd	nd	4.75%
RC Prod	1	nd	95.71%	nd	nd	nd	nd	nd	nd	4.29%
	2	nd	93.96%	nd	nd	nd	nd	nd	nd	6.04%
	3	nd	70.64%	nd	nd	nd	nd	nd	nd	29.36%

nd: not detected.

Table A.4 Concentration (w/w) of samples taken on the 5th of March 1996.

		methanol	ethanol	i-propanol	n-propanol	i-butanol	n-butanol	i-amyl acohol	ethyl acetate	water & other
BC2 Prod.	1	nd	67.14%	nd	0.2993%	0.0839%	nd	0.2521%	0.0867%	32.22%
	2	nd	83.24%	nd	0.2986%	0.0819%	nd	0.1378%	0.0396%	16.25%
	3	nd	73.83%	nd	0.3301%	0.1299%	nd	1.2817%	0.0351%	24.43%
FI-10	1	nd	72.90%	nd	nd	nd	nd	0.0078%	4.7027%	27.10%
	2	nd	84.83%	nd	nd	nd	nd	nd	5.4864%	15.17%
	3	nd	79.17%	nd	nd	nd	nd	nd	6.4136%	20.83%
PC Bottoms	1	nd	71.51%	nd	0.3005%	0.1002%	nd	0.5765%	nd	27.51%
	2	nd	82.23%	nd	0.2611%	0.0827%	nd	0.3207%	nd	17.10%
	3	nd	85.81%	nd	0.3320%	0.1137%	nd	0.3370%	nd	13.41%
FI-16	1	nd	43.22%	0.0887%	1.5660%	4.2173%	nd	6.3551%	0.2683%	44.56%
	2	nd	42.56%	0.0900%	1.4345%	3.7569%	nd	6.2377%	0.2901%	45.92%
	3	nd	41.94%	0.0936%	1.4426%	3.7378%	nd	6.2127%	0.3376%	46.58%
ED Bottoms	1	nd	31.74%	nd	0.0534%	0.0374%	nd	0.0908%	nd	68.08%
	2	nd	33.32%	nd	0.0431%	0.0324%	nd	0.0652%	nd	66.53%
	3	nd	31.62%	nd	0.0394%	0.0069%	nd	0.0354%	nd	68.30%
ED Pinch	1	nd	40.34%	nd	0.0998%	0.0216%	nd	0.1029%	nd	59.44%
	2	nd	44.23%	nd	0.1044%	0.0334%	nd	0.0817%	nd	55.55%
	3	nd	38.10%	nd	0.1158%	0.0276%	nd	0.0767%	nd	61.68%
FI-21	1									
	2	nd	86.45%	nd	3.4863%	0.6584%	0.0242%	5.9013%	nd	3.48%
	3	nd	72.87%	nd	3.3563%	0.6082%	0.0192%	3.1669%	nd	19.98%
FI-22	1	nd	76.74%	nd	1.3371%	0.0615%	nd	0.0337%	nd	21.82%
	2	nd	79.80%	nd	1.2411%	0.0630%	nd	0.0618%	nd	18.84%
	3	nd	81.44%	nd	1.2656%	0.0469%	nd	nd	nd	17.25%
FI-23	1	nd	79.06%	nd	0.1443%	nd	nd	nd	0.0184%	20.79%
	2	nd	73.73%	nd	0.1170%	nd	nd	nd	nd	26.15%
	3	nd	76.72%	nd	0.1237%	nd	nd	nd	nd	23.16%
FI-24	1	nd	84.18%	nd	nd	nd	nd	nd	nd	15.82%
	2	nd	82.54%	nd	nd	nd	nd	nd	nd	17.46%
	3	nd	82.65%	nd	nd	nd	nd	nd	nd	17.35%
RC Prod	1	nd	86.48%	nd	nd	nd	nd	nd	nd	13.52%
	2	nd	82.81%	nd	nd	nd	nd	nd	nd	17.19%
	3	nd	82.09%	nd	nd	nd	nd	nd	nd	17.91%

nd: not detected.

Table A.5 Concentration (w/w) of samples taken on the 25th of April 1996.

		methanol	ethanol	i-propanol	n-propanol	i-butanol	n-butanol	i-amyl acohol	ethyl acetate	water & other
BC2 Prod.	1	nd	73.73%	nd	0.6614%	0.1078%	nd	0.3756%	0.0189%	25.13%
	2	nd	75.88%	nd	0.6884%	0.1126%	nd	0.3990%	0.0200%	22.92%
	3	nd	67.97%	nd	1.5205%	0.3772%	0.0300%	7.8547%	0.0138%	22.25%
FI-10	1	nd	82.90%	nd	nd	nd	nd	nd	3.1090%	17.10%
	2	nd	73.55%	nd	0.2562%	0.0886%	nd	0.3415%	0.0355%	25.76%
	3	nd	83.45%	nd	nd	nd	nd	nd	3.2233%	16.55%
PC Bottoms	1	nd	69.70%	nd	0.3466%	0.0891%	nd	0.4373%	0.0127%	29.43%
	2	nd	71.38%	nd	0.2221%	0.0772%	nd	0.3010%	nd	28.02%
	3	nd	68.26%	nd	0.8532%	0.1382%	nd	0.7854%	nd	29.96%
FI-16	1	nd	40.63%	0.0756%	1.6186%	2.0395%	nd	4.3375%	0.1243%	51.30%
	2	nd	42.98%	0.0783%	1.6512%	2.2744%	nd	4.7319%	0.1279%	48.29%
	3	nd	42.40%	0.0790%	1.5809%	2.3630%	nd	4.6530%	0.1377%	48.92%
ED Bottoms	1	nd	28.23%	nd	0.0555%	0.0147%	nd	0.0576%	nd	71.64%
	2	nd	27.06%	nd	0.0327%	0.0112%	nd	0.0351%	nd	72.86%
	3	nd	28.78%	nd	0.1053%	0.0062%	nd	0.0522%	nd	71.05%
ED Pinch	1	nd	39.28%	nd	0.1185%	0.0237%	nd	0.0794%	nd	60.49%
	2	nd	38.59%	nd	0.0610%	0.0177%	nd	0.0501%	nd	61.28%
	3	nd	38.73%	nd	0.1988%	0.0185%	nd	0.0423%	nd	61.01%
FI-21	1	nd	72.68%	nd	4.8859%	0.5352%	0.0191%	3.2318%	nd	18.65%
	2	nd	74.11%	nd	2.1982%	0.3630%	0.0112%	2.6682%	nd	20.65%
	3	nd	79.14%	nd	4.1432%	0.4192%	0.0128%	2.9507%	nd	13.34%
FI-22	1	nd	75.82%	nd	1.5182%	0.0430%	nd	0.0252%	nd	22.60%
	2	nd	74.74%	nd	0.6687%	0.0238%	nd	0.0136%	nd	24.55%
	3	nd	76.75%	nd	0.9965%	0.0219%	nd	0.0043%	nd	22.23%
FI-23	1	nd	77.05%	nd	0.1316%	nd	nd	nd	nd	22.81%
	2	nd	79.15%	nd	0.0543%	nd	nd	nd	nd	20.80%
	3	nd	83.46%	nd	0.0771%	nd	nd	nd	nd	16.46%
FI-24	1	nd	79.40%	nd	nd	nd	nd	nd	nd	20.60%
	2	nd	80.63%	nd	nd	nd	nd	nd	nd	19.37%
	3	nd	69.13%	nd	nd	nd	nd	nd	nd	30.87%
RC Prod	1	nd	89.67%	nd	nd	nd	nd	nd	nd	10.33%
	2	nd	72.33%	nd	nd	nd	nd	nd	nd	27.67%
	3	nd	76.31%	nd	nd	nd	nd	nd	nd	23.69%

nd: not detected.

Appendix B

TEMPERATURE EFFECT ON PERVAPORATION

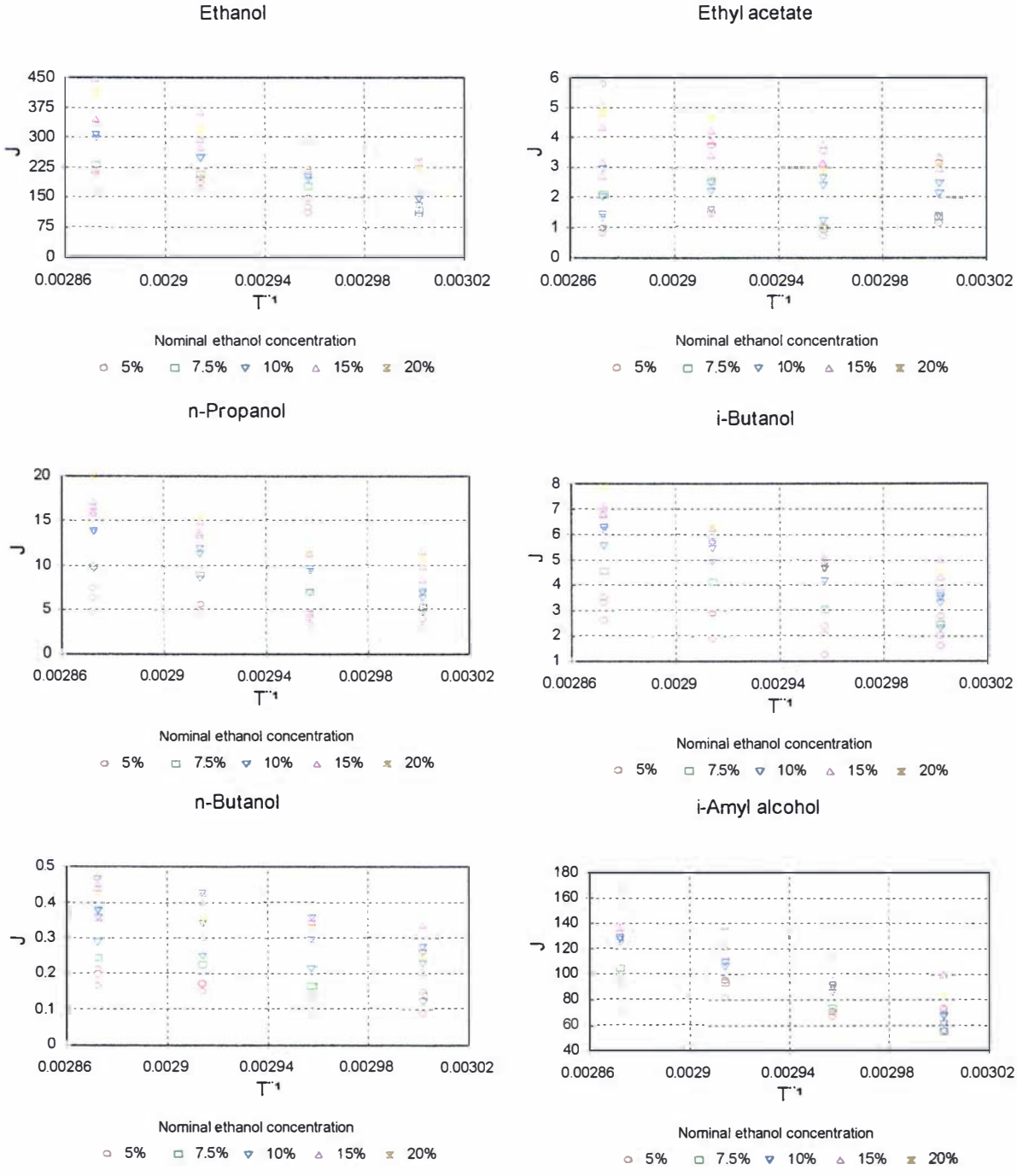

Figure B1 Relationship between partial flux (J in $g.m^{-2}.h^{-1}$) and the inverse of temperature (T^{-1} in K^{-1}) in Experiment II (Chapter IV).

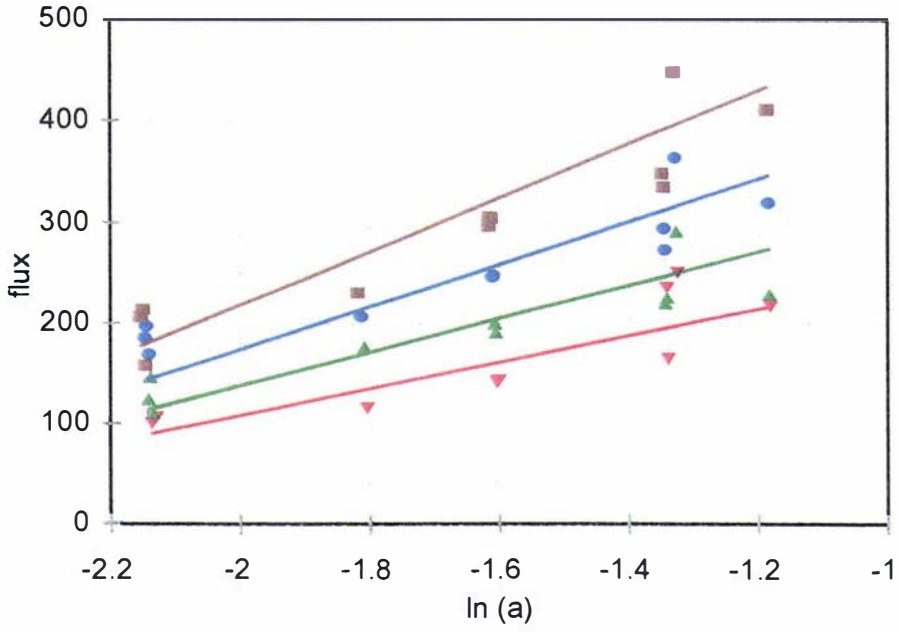

Figure B.2 Plot of ethanol partial flux (J in $g.m^{-2}.h^{-1}$) and feed activity at varying temperatures for Experiment II (Chapter IV). – 60°C; – 65°C; – 70°C; – 75°C. Discrete points represent experimental data.

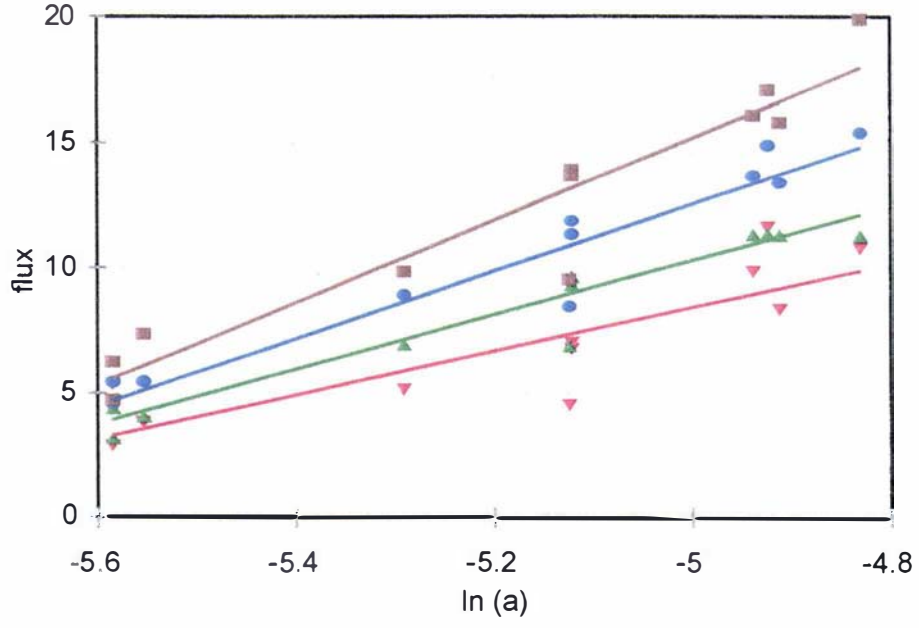

Figure B.3 Plot of *n*-propanol partial flux (J in $g.m^{-2}.h^{-1}$) and feed activity at varying temperatures for Experiment II (Chapter IV). – 60°C; – 65°C; – 70°C; – 75°C. Discrete points represent experimental data.

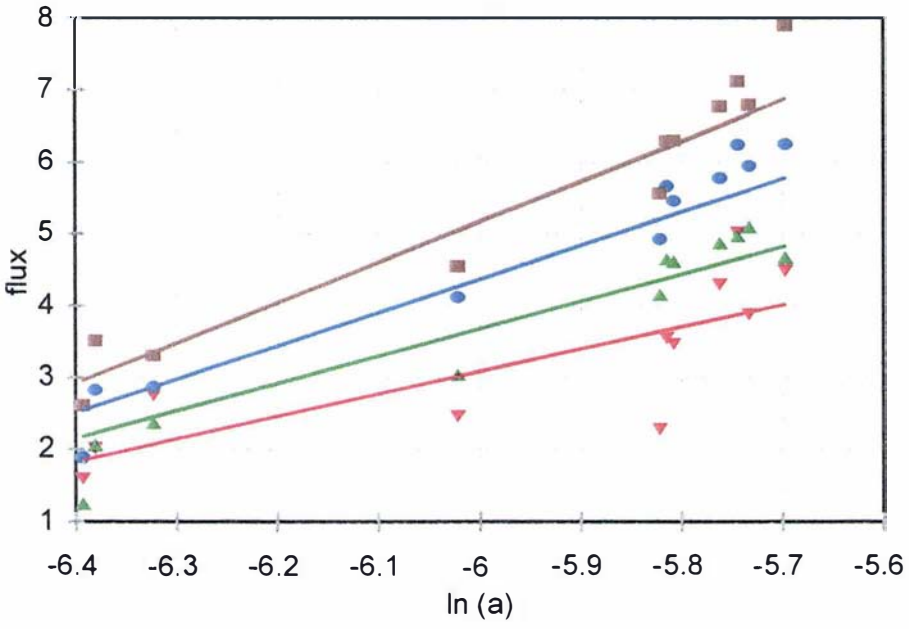

Figure B.4 Plot of *i*-butanol partial flux (J in $g.m^{-2}.h^{-1}$) and feed activity at varying temperatures for Experiment II (Chapter IV). – 60°C; – 65°C; – 70°C; – 75°C. Discrete points represent experimental data.

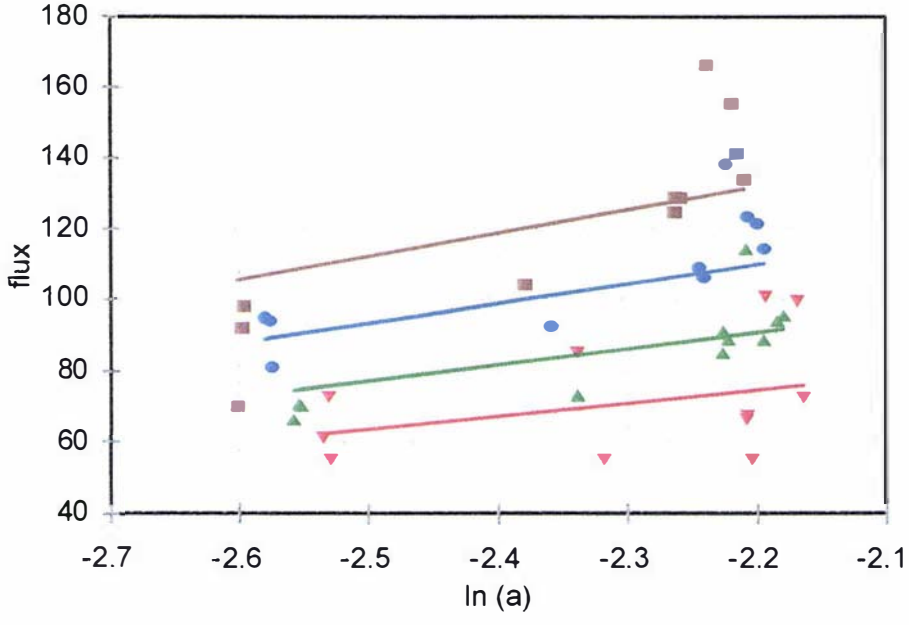

Figure B.5 Plot of *i*-amyl alcohol partial flux (J in $g.m^{-2}.h^{-1}$) and feed activity at varying temperatures for Experiment II (Chapter IV). – 60°C; – 65°C; – 70°C; – 75°C. Discrete points represent experimental data.

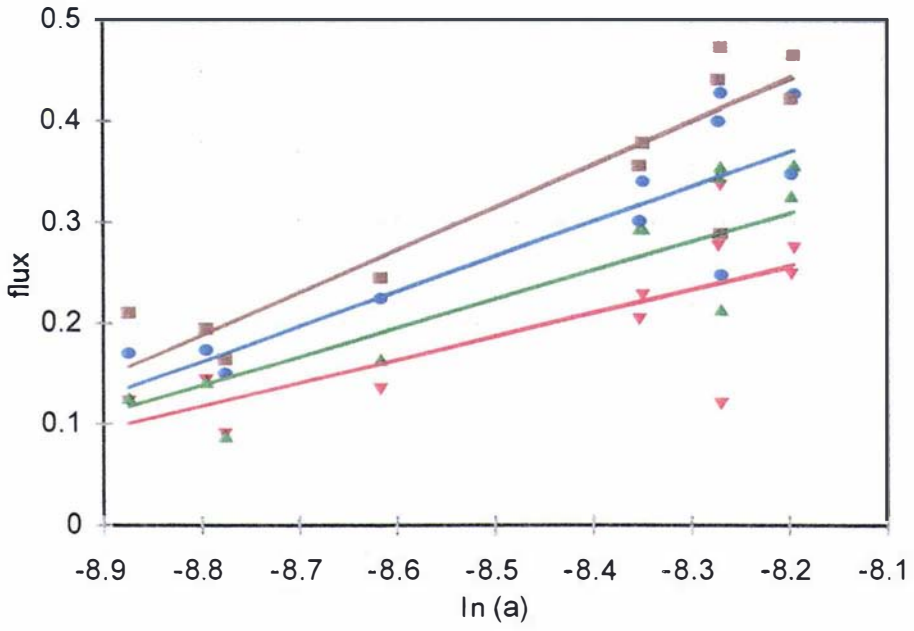

Figure B.6 Plot of *n*-butanol partial flux (J in $g.m^{-2}.h^{-1}$) and feed activity at varying temperatures for Experiment II (Chapter IV). – 60°C; – 65°C; – 70°C; – 75°C. Discrete points represent experimental data.

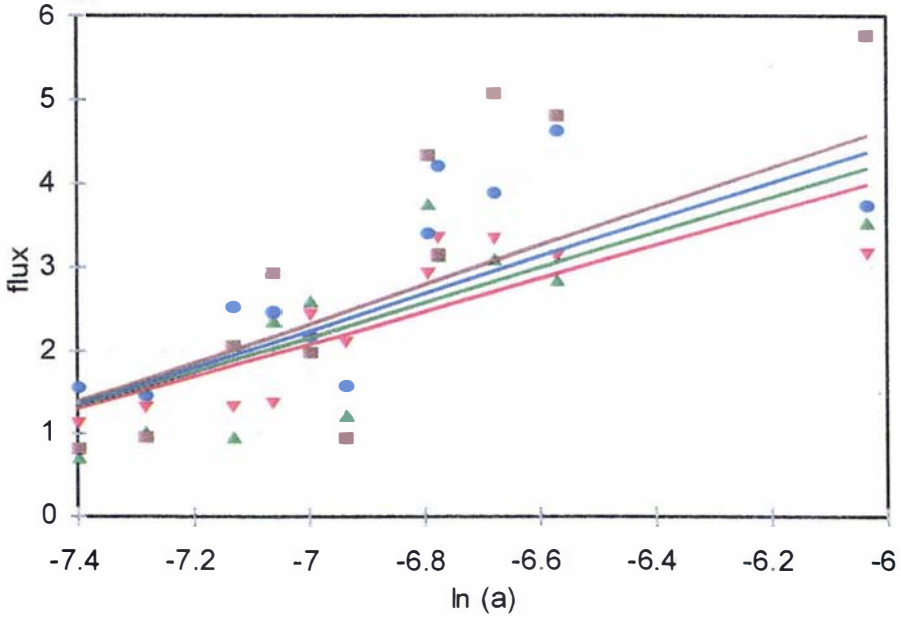

Figure B.7 Plot of ethyl acetate partial flux (J in $g.m^{-2}.h^{-1}$) and feed activity at varying temperatures for Experiment II (Chapter IV). – 60°C; – 65°C; – 70°C; – 75°C. Discrete points represent experimental data.

Appendix C

RESULTS OF DISTILLATION SIMULATIONS

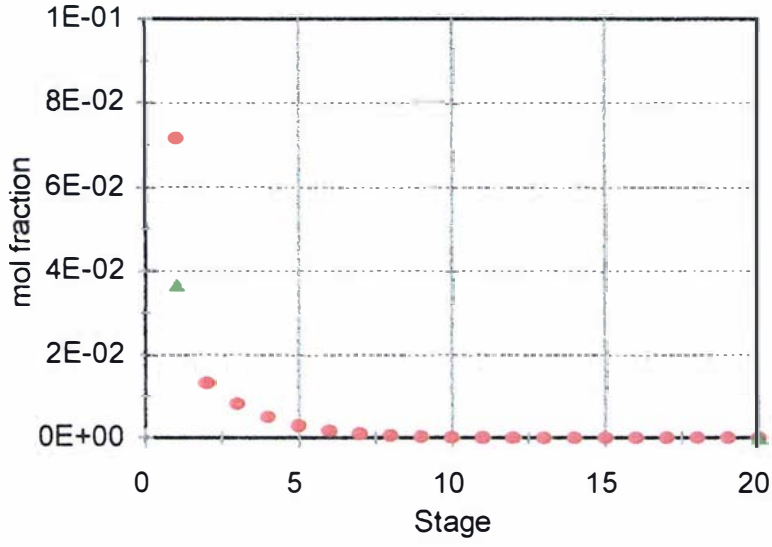

Figure C.1 Calculated concentration profile of ethyl acetate in the PC column (●) and experimental data from FI-10 (▲), set 1 from 11-Sep-95.

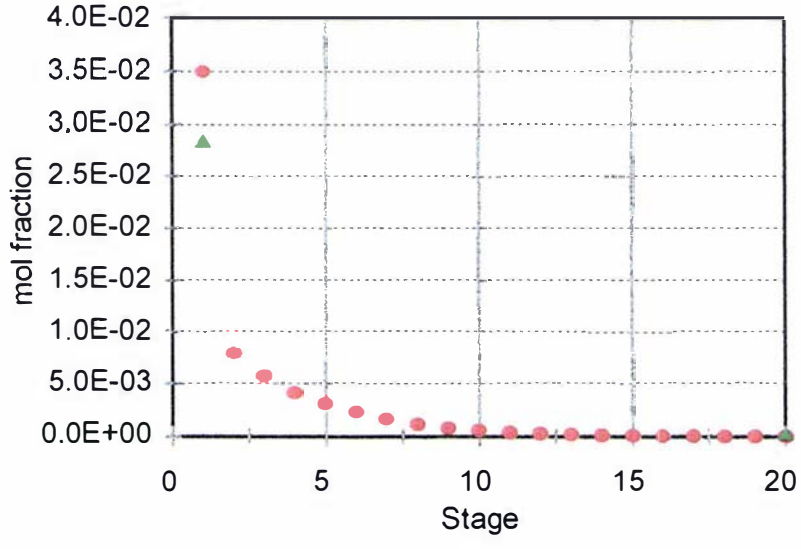

Figure C.2 Calculated concentration profile of ethyl acetate in the PC column (●) and experimental data from FI-10 (▲), set 2 from 11-Sep-95.

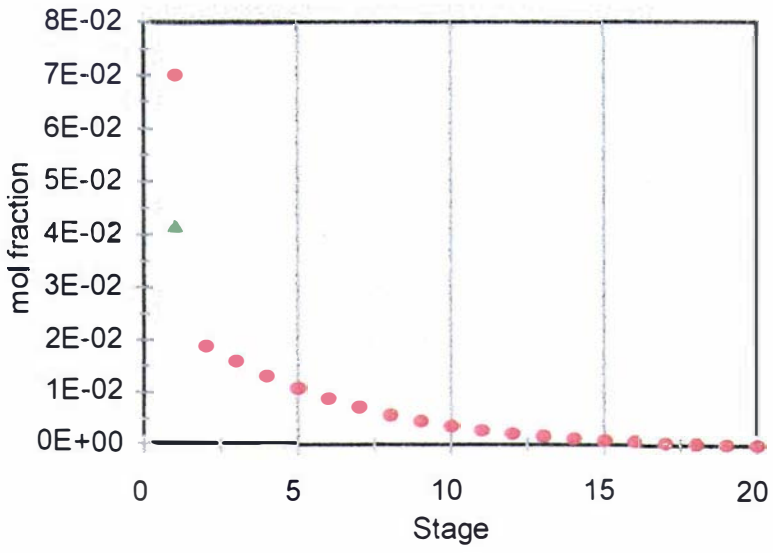

Figure C.3 Calculated concentration profile of ethyl acetate in the PC column (●) and experimental data from FI-10 (▲), set 3 from 11-Sep-95.

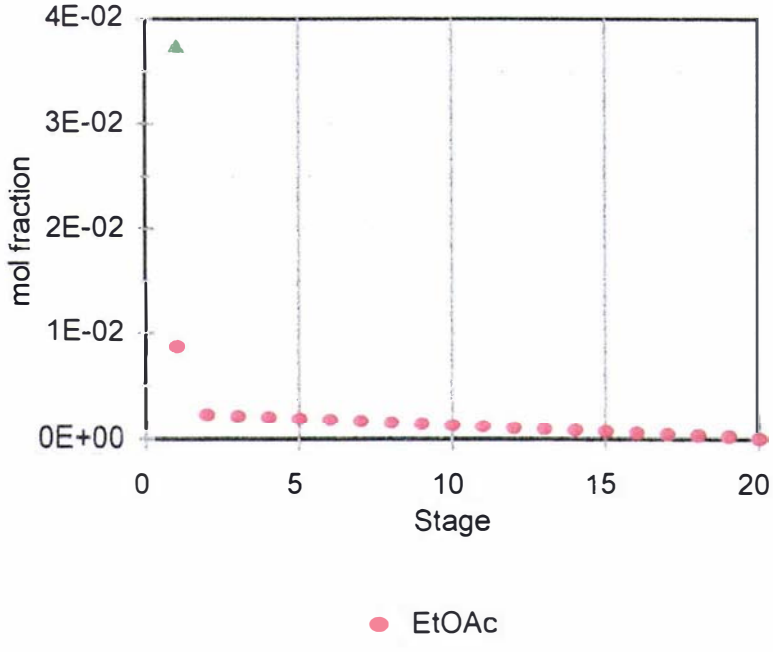

Figure C.4 Calculated concentration profile of ethyl acetate in the PC column (●) and experimental data from FI-10 (▲), set 4 from 22-Nov-95.

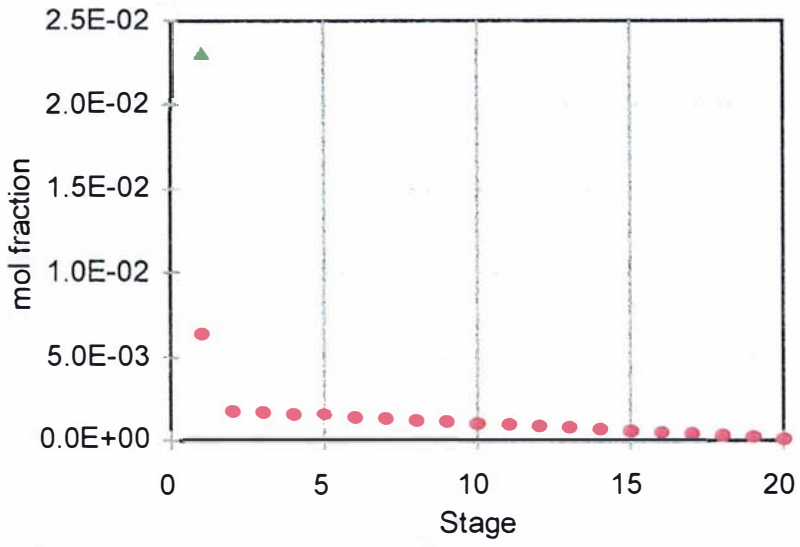

Figure C.5 Calculated concentration profile of ethyl acetate in the PC column (●) and experimental data from FI-10 (▲), set 5 from 22-Nov-95.

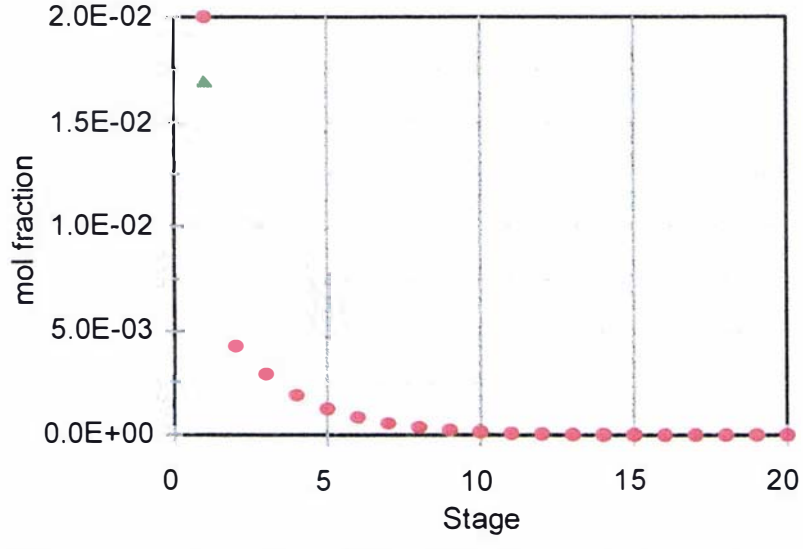

Figure C.6 Calculated concentration profile of ethyl acetate in the PC column (●) and experimental data from FI-10 (▲), set 7 from 05-Mar-96.

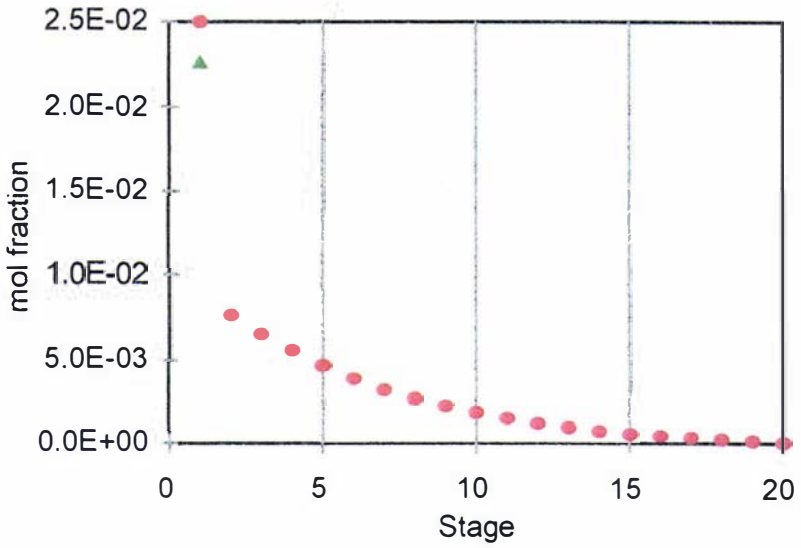

Figure C.7 Calculated concentration profile of ethyl acetate in the PC column (●) and experimental data from FI-10 (▲), set 8 from 05-Mar-96.

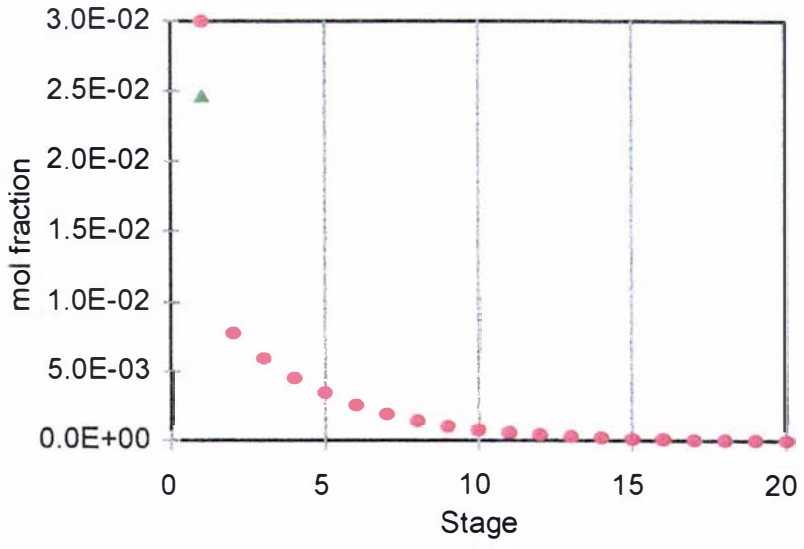

Figure C.8 Calculated concentration profile of ethyl acetate in the PC column (●) and experimental data from FI-10 (▲), set 9 from 05-Mar-96.

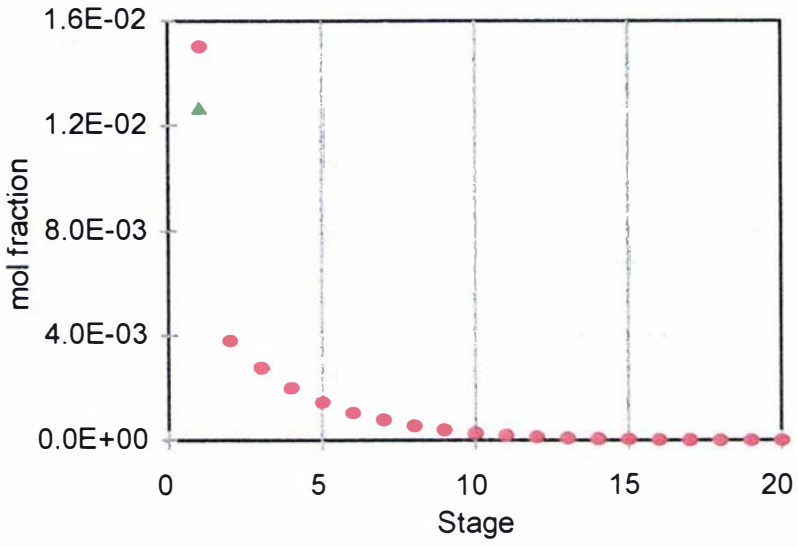

Figure C.9 Calculated concentration profile of ethyl acetate in the PC column (●) and experimental data from FI-10 (▲), set 10 from 25-Apr-96.

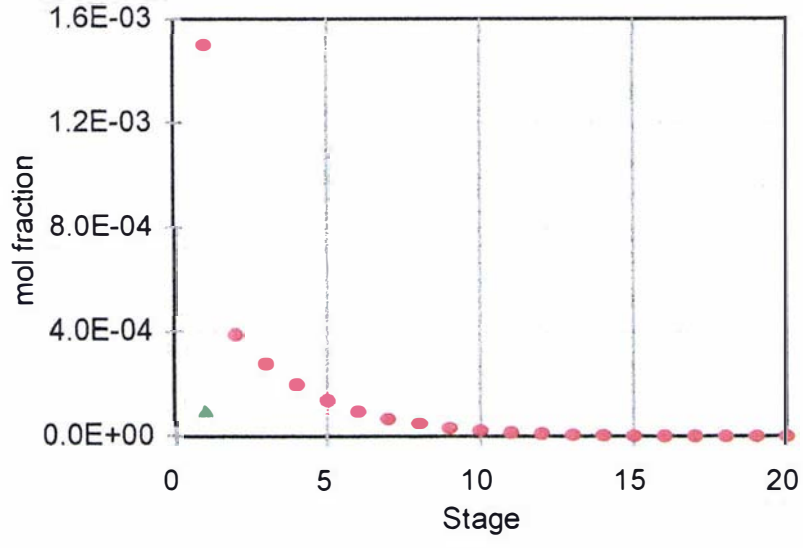

Figure C.10 Calculated concentration profile of ethyl acetate in the PC column (●) and experimental data from FI-10 (▲), set 11 from 25-Apr-96.

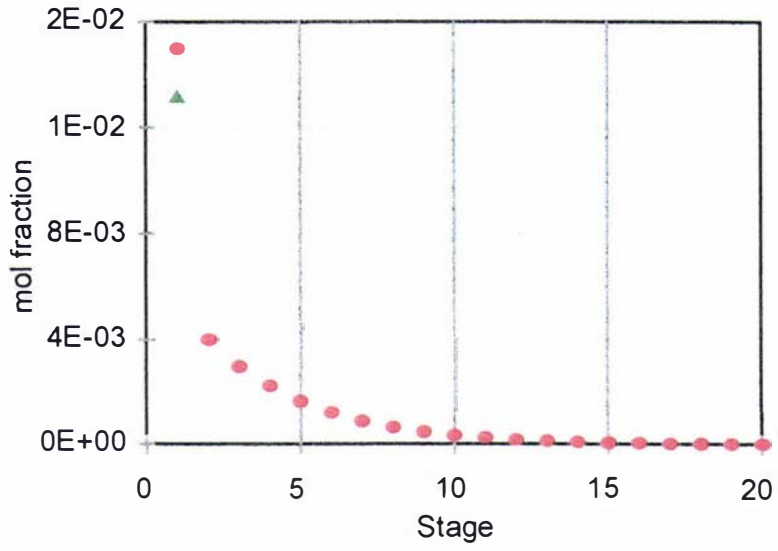

Figure C.11 Calculated concentration profile of ethyl acetate in the PC column (●) and experimental data from FI-10 (▲), set 12 from 25-Apr-96.

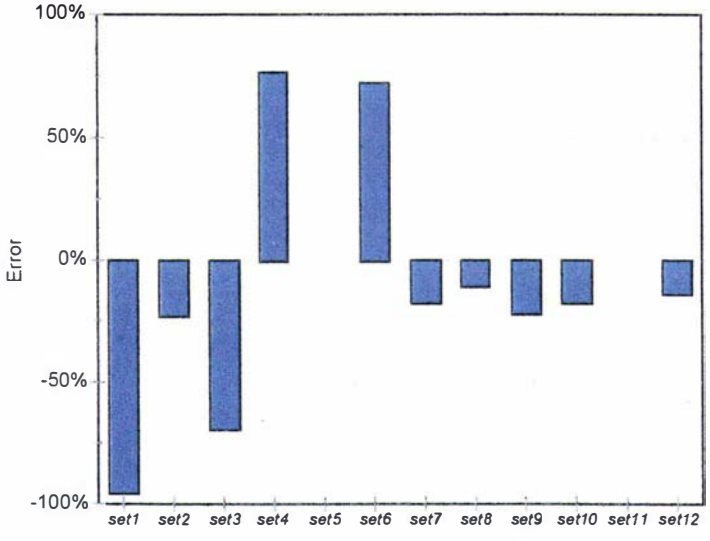

Figure C.12 Percentage error of predicted mol fraction of ethyl acetate at the distillation stream of column PC (FI-10). Percentage error defined as: [(experimental value - calculated value) / experimental value] × 100.

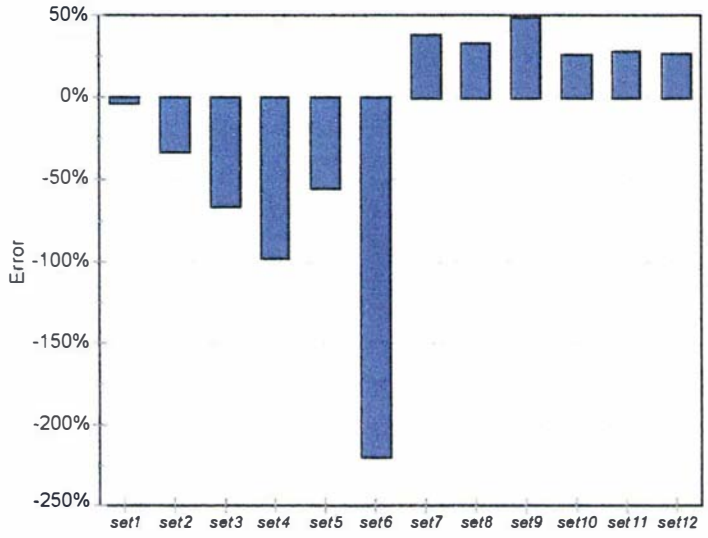

Figure C.13 Percentage error of predicted mol fraction of ethanol at the bottoms stream of column PC. Percentage error defined as: [(experimental value - calculated value) / experimental value] × 100.

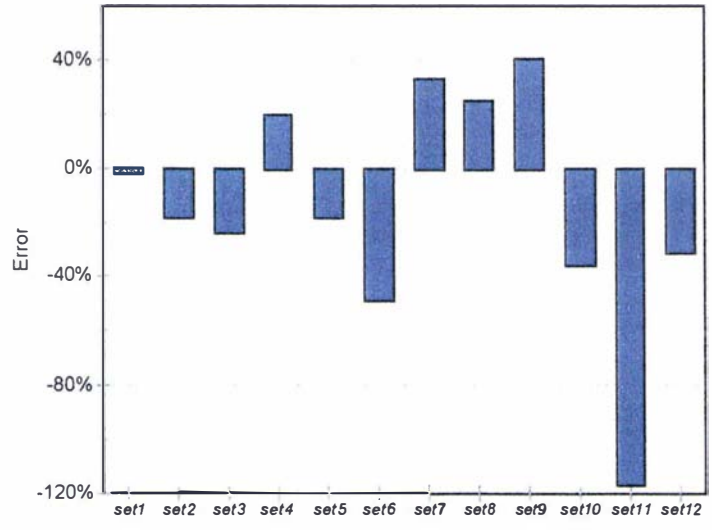

Figure C.14 Percentage error of predicted mol fraction of *n*-propanol at the bottoms stream of column PC. Percentage error defined as: [(experimental value - calculated value) / experimental value] × 100.

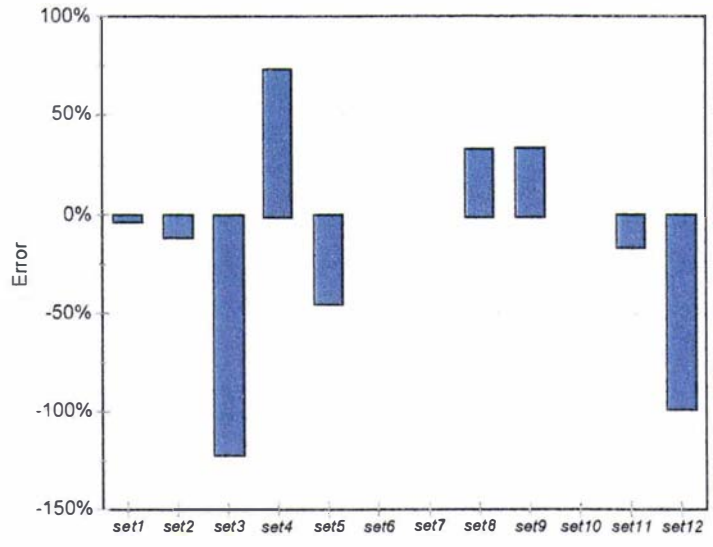

Figure C.15 Percentage error of predicted mol fraction of *i*-butanol at the bottoms stream of column PC. Percentage error defined as: [(experimental value - calculated value) / experimental value] × 100.

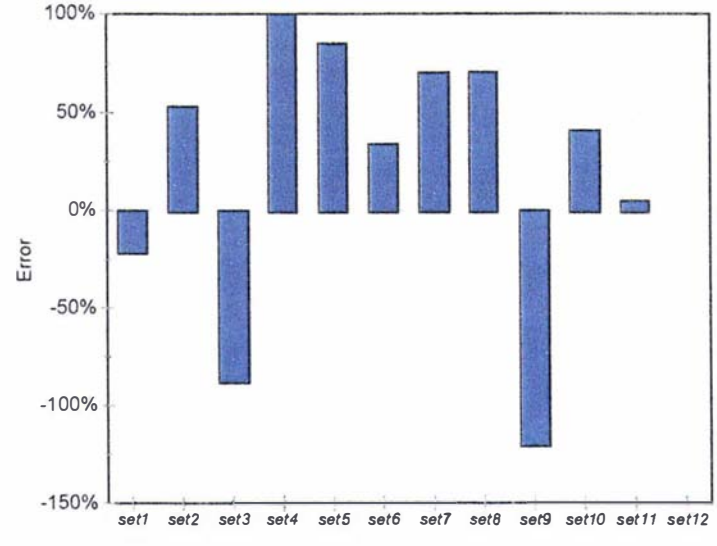

Figure C.16 Percentage error of predicted mol fraction of *i*-amyl alcohol at the bottoms stream of column PC. Percentage error defined as: [(experimental value - calculated value) / experimental value] × 100.

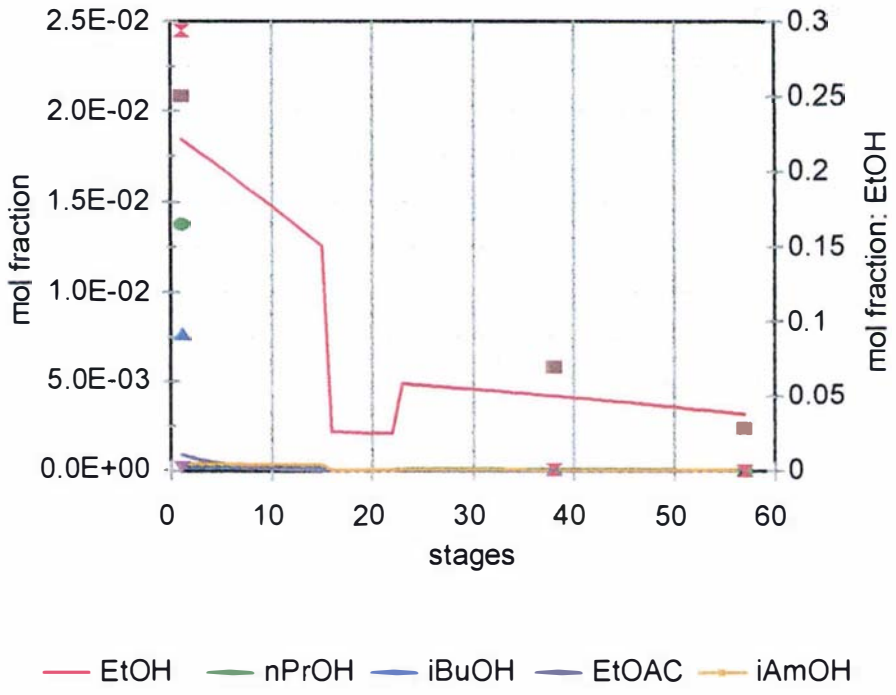

Figure C.17 Calculated concentration profile of ED column with ChemSep® and experimental values from 11-Sep-95, set 1. Experimental data: ■: EtOH; ▲: nPrOH; ●: iBuOH; ⧗: iAmOH; ▼: EtOAc. EtOH: ethanol; nPrOH: *n*-propanol; iBuOH: *i*-butanol; iAmOH: *i*-amyl alcohol; EtOAc: ethyl acetate.

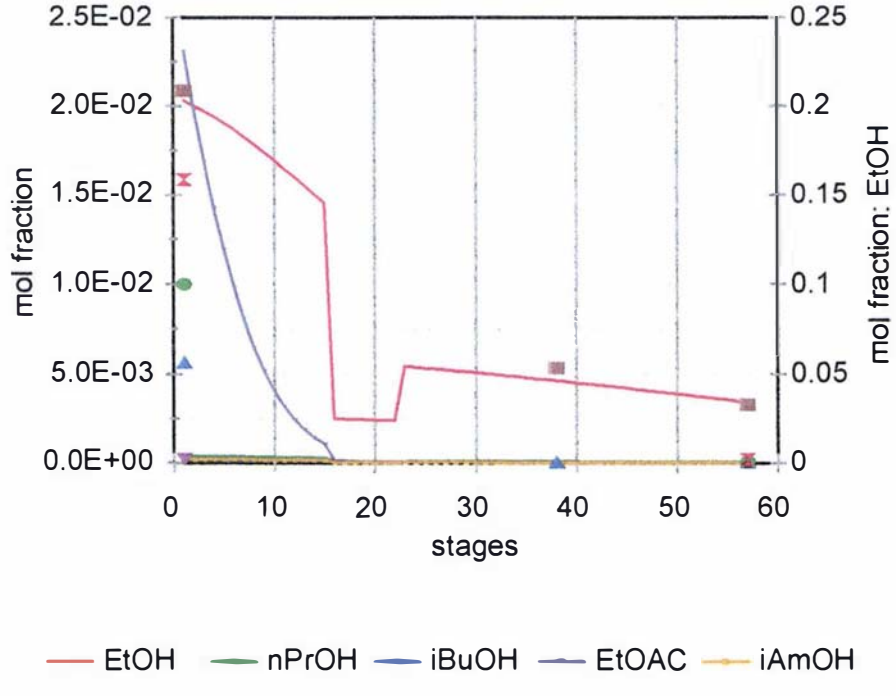

Figure C.18 Calculated concentration profile of ED column with ChemSep® and experimental values from 11-Sep-95, set 2. Experimental data: ■: EtOH; ▲: nPrOH; ●: iBuOH; ⧗: iAmOH; ▼: EtOAc. EtOH: ethanol; nPrOH: *n*-propanol; iBuOH: *i*-butanol; iAmOH: *i*-amyl alcohol; EtOAc: ethyl acetate.

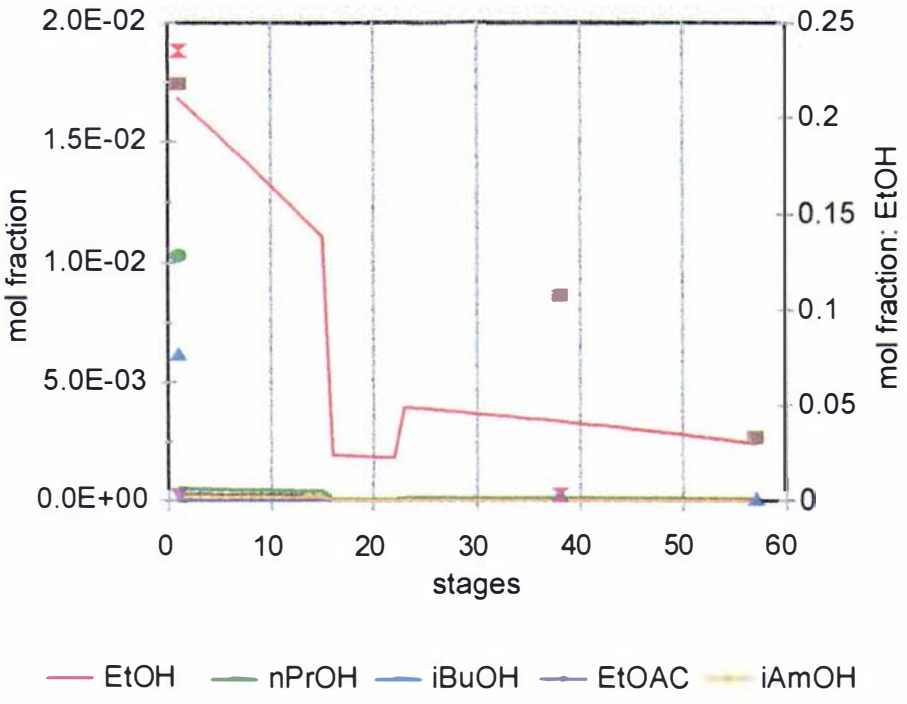

Figure C.19 Calculated concentration profile of ED column with ChemSep® and experimental values from 11-Sep-95, set 3. Experimental data: ■: EtOH; ▲: nPrOH; ●: iBuOH; ⧗: iAmOH; ▼: EtOAc. EtOH: ethanol; nPrOH: *n*-propanol; iBuOH: *i*-butanol; iAmOH: *i*-amyl alcohol; EtOAc: ethyl acetate.

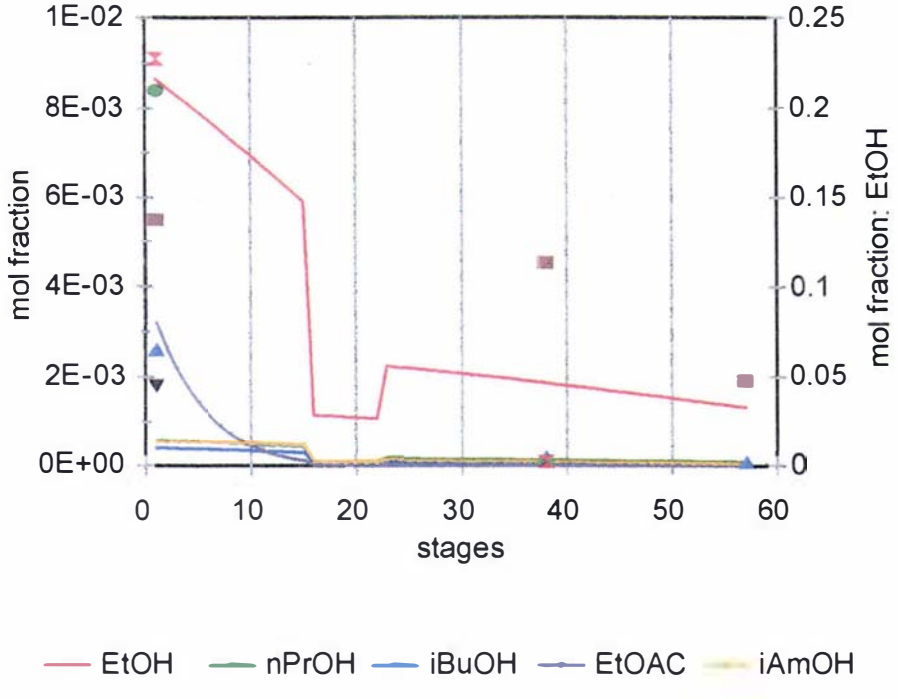

Figure C.20 Calculated concentration profile of ED column with ChemSep® and experimental values from 22-Nov-95, set 4. Experimental data: ■: EtOH; ▲: nPrOH; ●: iBuOH; ⧗: iAmOH; ▼: EtOAc. EtOH: ethanol; nPrOH: *n*-propanol; iBuOH: *i*-butanol; iAmOH: *i*-amyl alcohol; EtOAc: ethyl acetate.

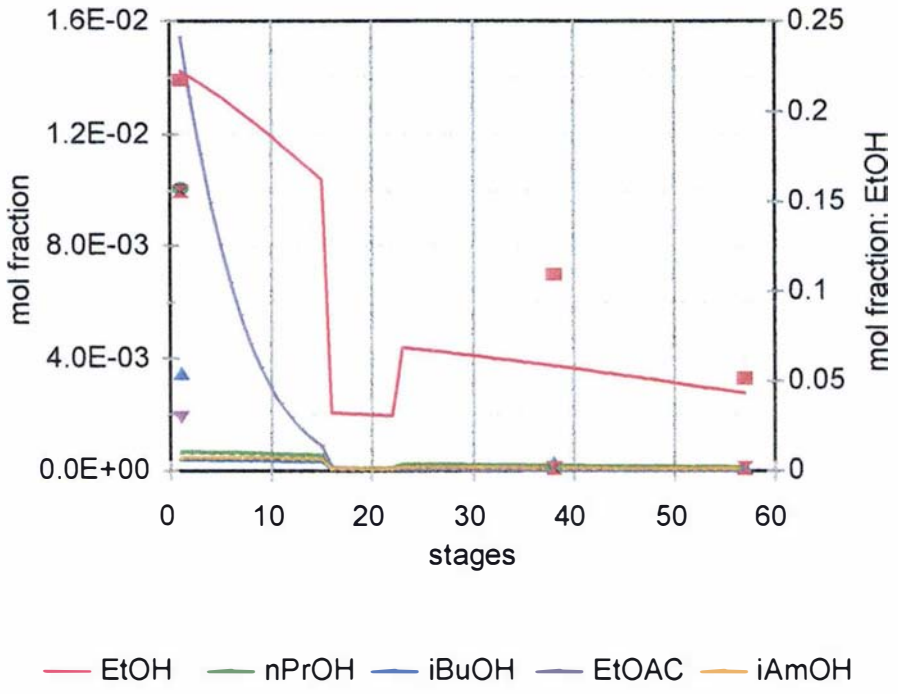

Figure C.21 Calculated concentration profile of ED column with ChemSep® and experimental values from 22-Nov-95, set 5. Experimental data: ■: EtOH; ▲: nPrOH; ●: iBuOH; ⧗: iAmOH; ▼: EtOAc. EtOH: ethanol; nPrOH: *n*-propanol; iBuOH: *i*-butanol; iAmOH: *i*-amyl alcohol; EtOAc: ethyl acetate.

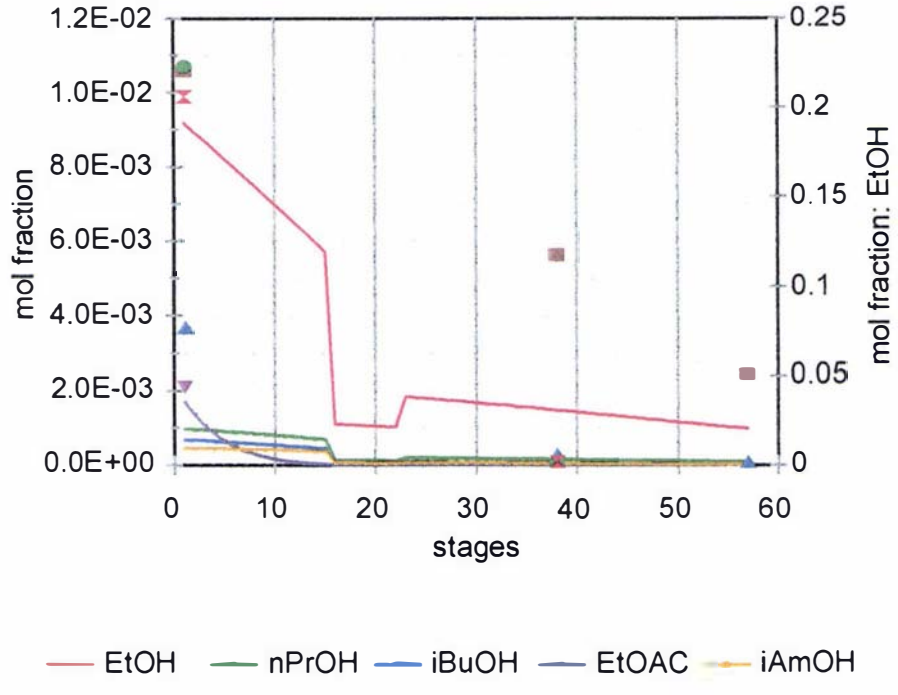

Figure C.22 Calculated concentration profile of ED column with ChemSep® and experimental values from 22-Nov-95, set 6. Experimental data: ■: EtOH; ▲: nPrOH; ●: iBuOH; ⧗: iAmOH; ▼: EtOAc. EtOH: ethanol; nPrOH: *n*-propanol; iBuOH: *i*-butanol; iAmOH: *i*-amyl alcohol; EtOAc: ethyl acetate.

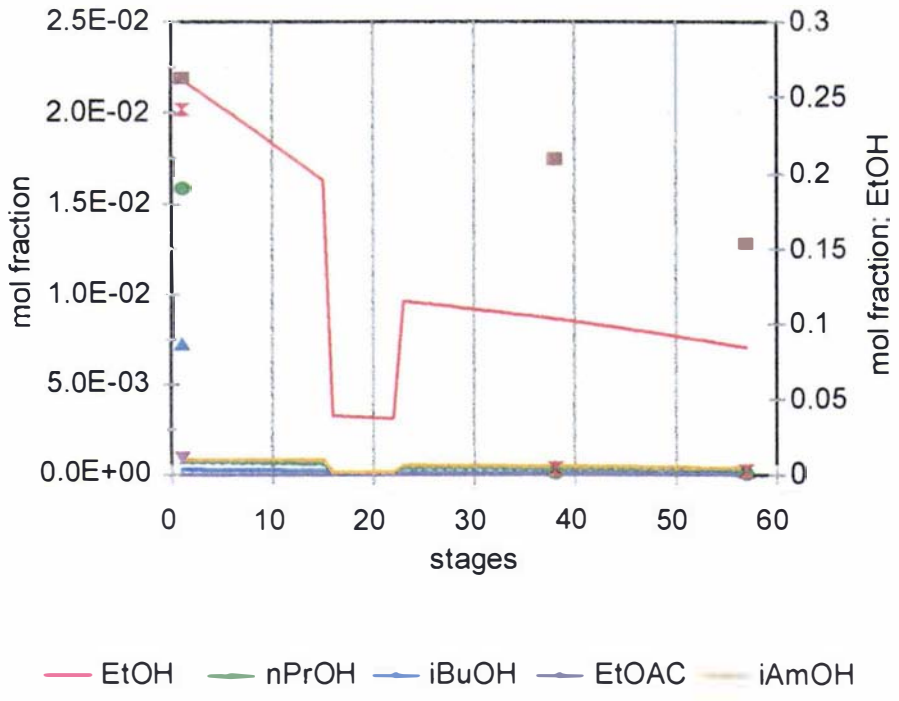

Figure C.23 Calculated concentration profile of ED column with ChemSep® and experimental values from 05-Mar-96, set 7. Experimental data: ■: EtOH; ▲: nPrOH; ●: iBuOH; ⧗: iAmOH; ▼: EtOAc. EtOH: ethanol; nPrOH: *n*-propanol; iBuOH: *i*-butanol; iAmOH: *i*-amyl alcohol; EtOAc: ethyl acetate.

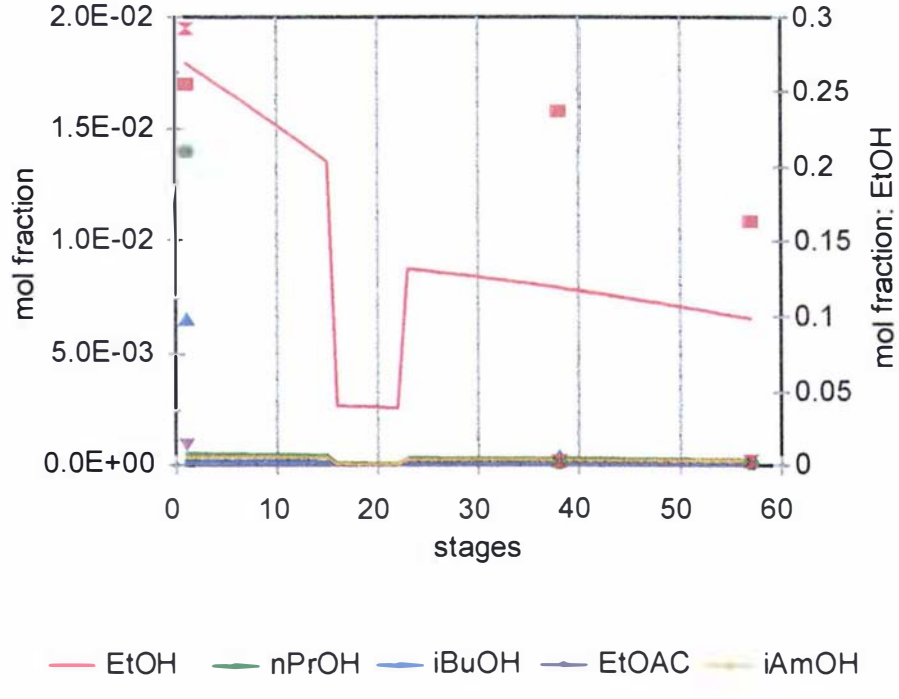

Figure C.24 Calculated concentration profile of ED column with ChemSep® and experimental values from 05-Mar-96, set 8. Experimental data: ■: EtOH; ▲: nPrOH; ●: iBuOH; ⧗: iAmOH; ▼: EtOAc. EtOH: ethanol; nPrOH: *n*-propanol; iBuOH: *i*-butanol; iAmOH: *i*-amyl alcohol; EtOAc: ethyl acetate.

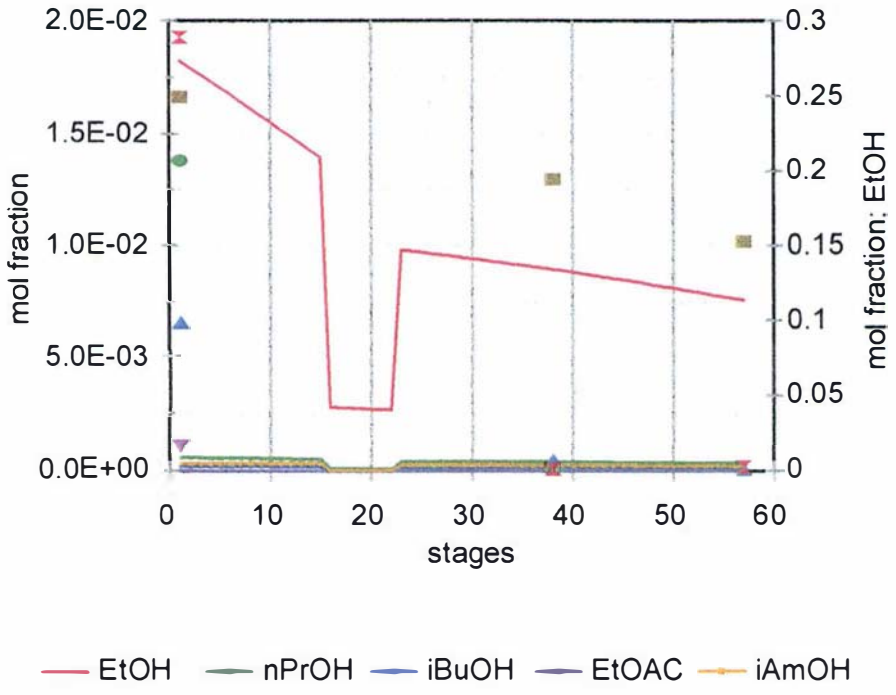

Figure C.25 Calculated concentration profile of ED column with ChemSep® and experimental values from 05-Mar-96, set 9. Experimental data: ■: EtOH; ▲: nPrOH; ●: iBuOH; ⧗: iAmOH; ▼: EtOAc. EtOH: ethanol; nPrOH: *n*-propanol; iBuOH: *i*-butanol; iAmOH: *i*-amyl alcohol; EtOAc: ethyl acetate.

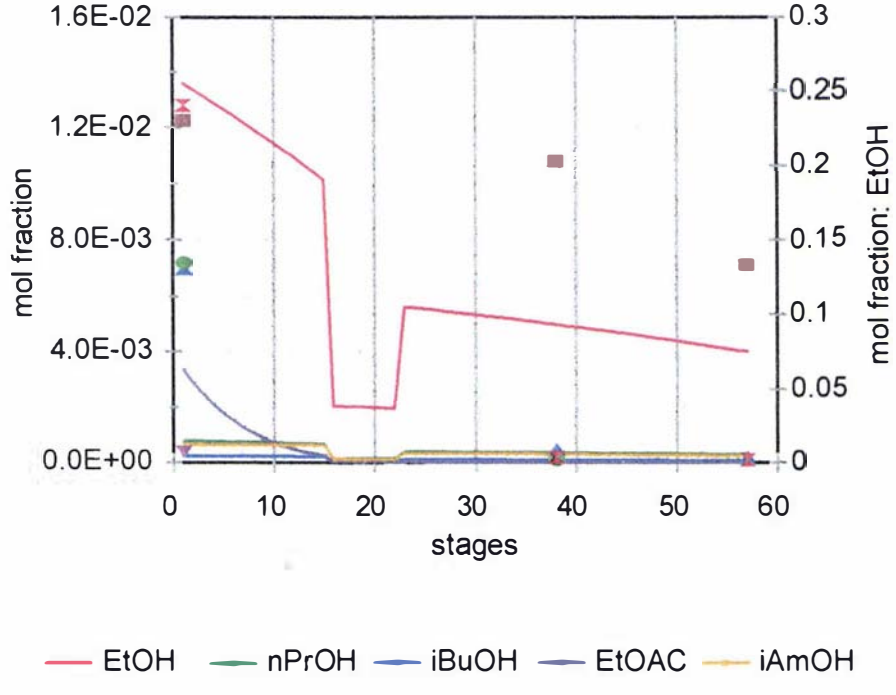

Figure C.26 Calculated concentration profile of ED column with ChemSep® and experimental values from 25-Apr-96, set 10. Experimental data: ■: EtOH; ▲: nPrOH; ●: iBuOH; ⧗: iAmOH; ▼: EtOAc. EtOH: ethanol; nPrOH: *n*-propanol; iBuOH: *i*-butanol; iAmOH: *i*-amyl alcohol; EtOAc: ethyl acetate.

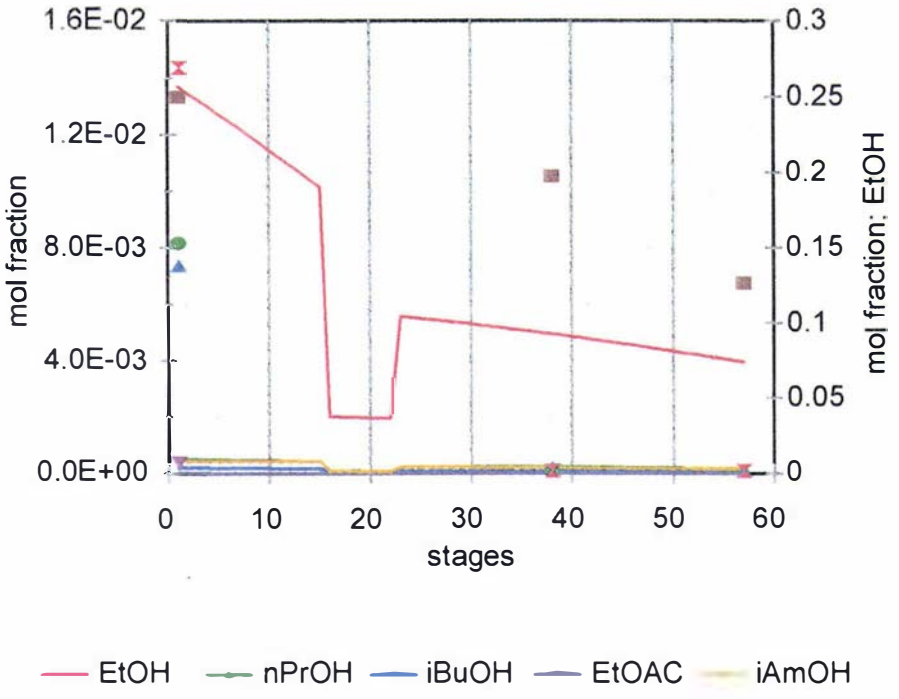

Figure C.27 Calculated concentration profile of ED column with ChemSep® and experimental values from 25-Apr-96, set 11. Experimental data: ■: EtOH; ▲: nPrOH; ●: iBuOH; ⧗: iAmOH; ▼: EtOAc. EtOH: ethanol; nPrOH: *n*-propanol; iBuOH: *i*-butanol; iAmOH: *i*-amyl alcohol; EtOAc: ethyl acetate.

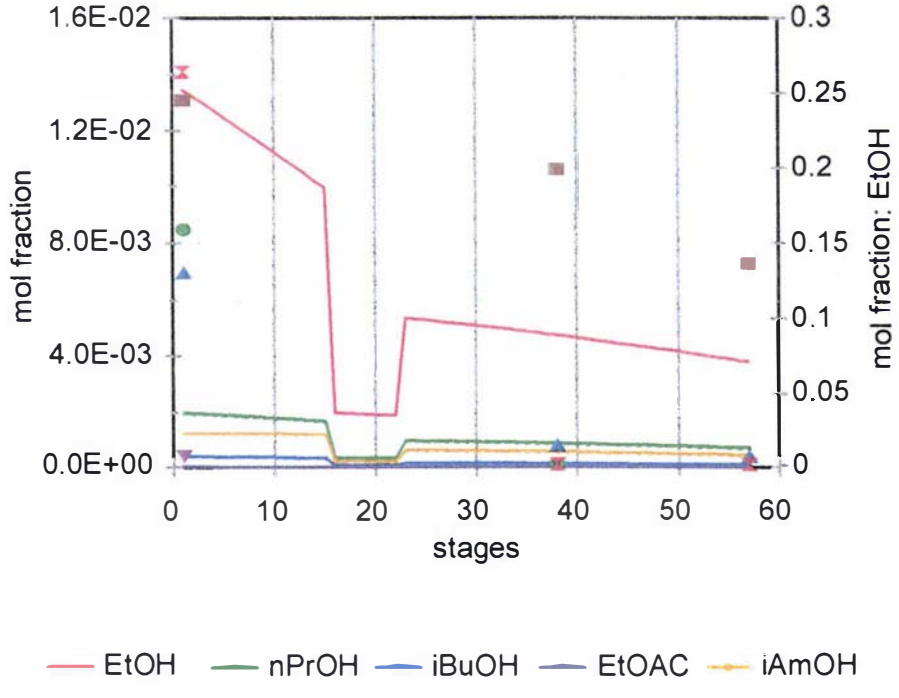

Figure C.28 Calculated concentration profile of ED column with ChemSep® and experimental values from 25-Apr-96, set 12. Experimental data: ■: EtOH; ▲: nPrOH; ●: iBuOH; ⧗: iAmOH; ▼: EtOAc. EtOH: ethanol; nPrOH: *n*-propanol; iBuOH: *i*-butanol; iAmOH: *i*-amyl alcohol; EtOAc: ethyl acetate.

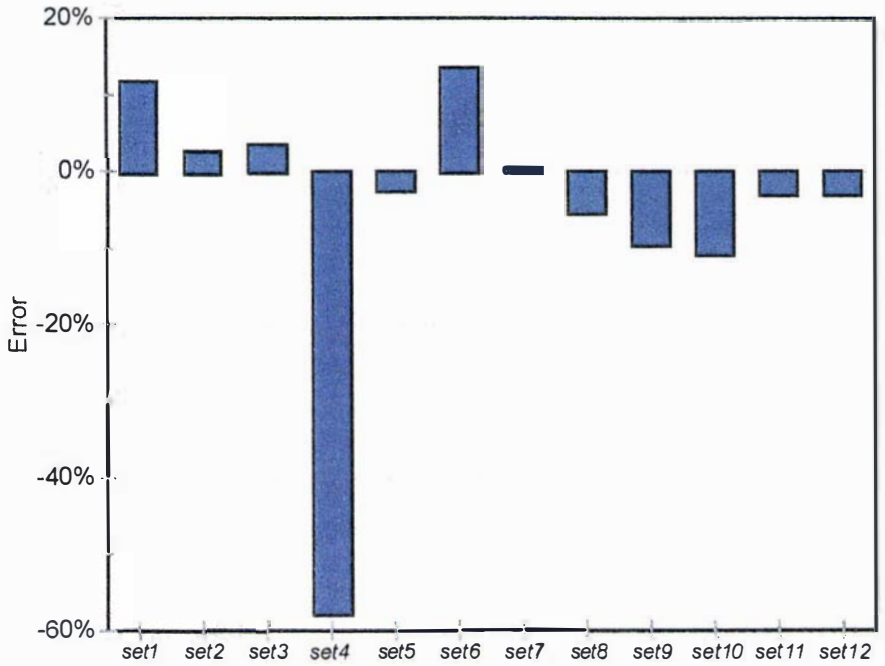

Figure C.29 Percentage error of predicted mol fraction of ethanol at the distillation stream of column ED (FI-16). Percentage error defined as: [(experimental value - calculated value) / experimental value] × 100.

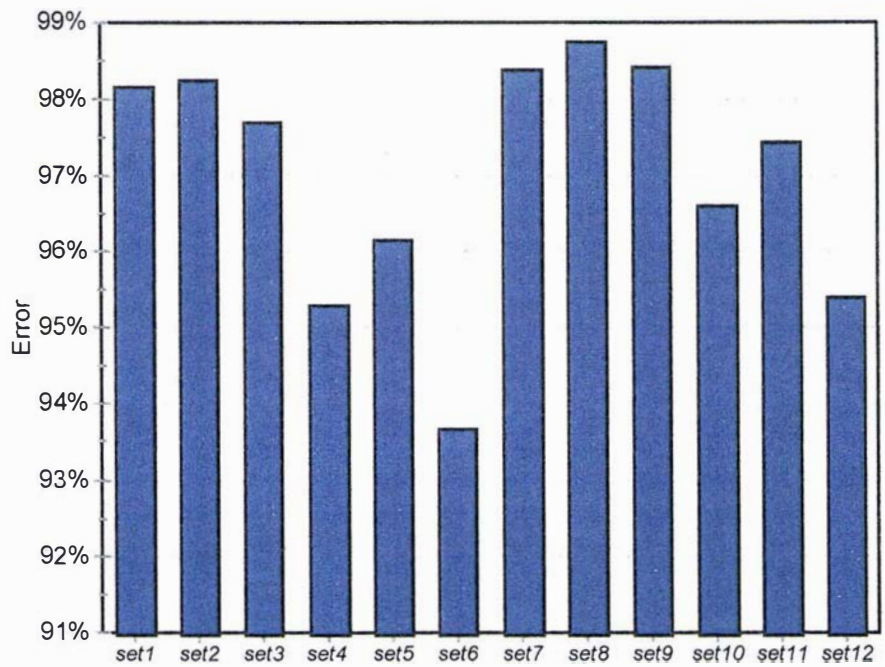

Figure C.30 Percentage error of predicted mol fraction of *i*-butanol at the distillation stream of column ED (FI-16). Percentage error defined as: [(experimental value - calculated value) / experimental value] × 100.

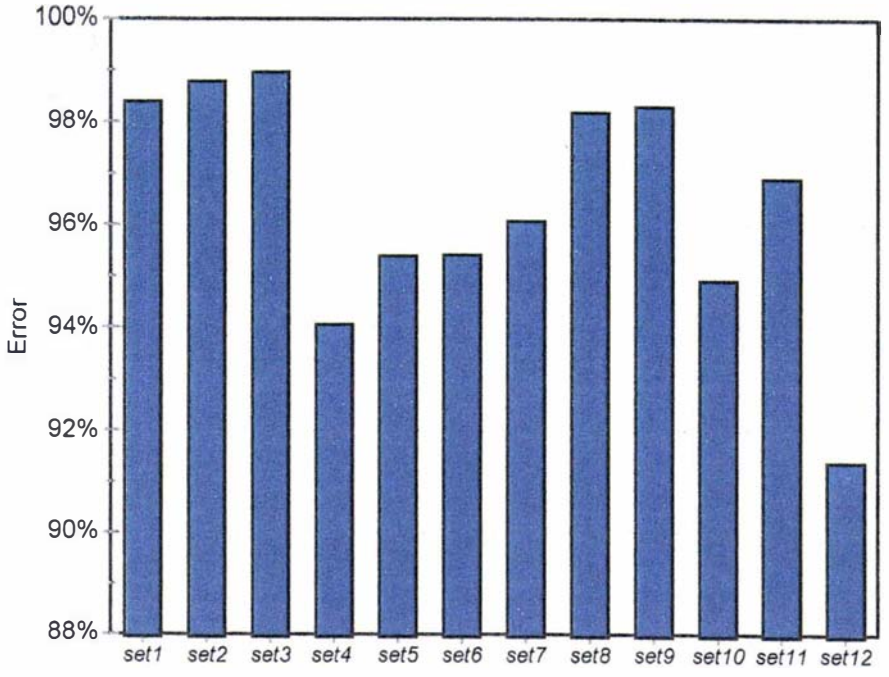

Figure C.31 Percentage error of predicted mol fraction of *i*-amyl alcohol at the distillation stream of column ED (FI-16). Percentage error defined as: [(experimental value - calculated value) / experimental value] × 100.

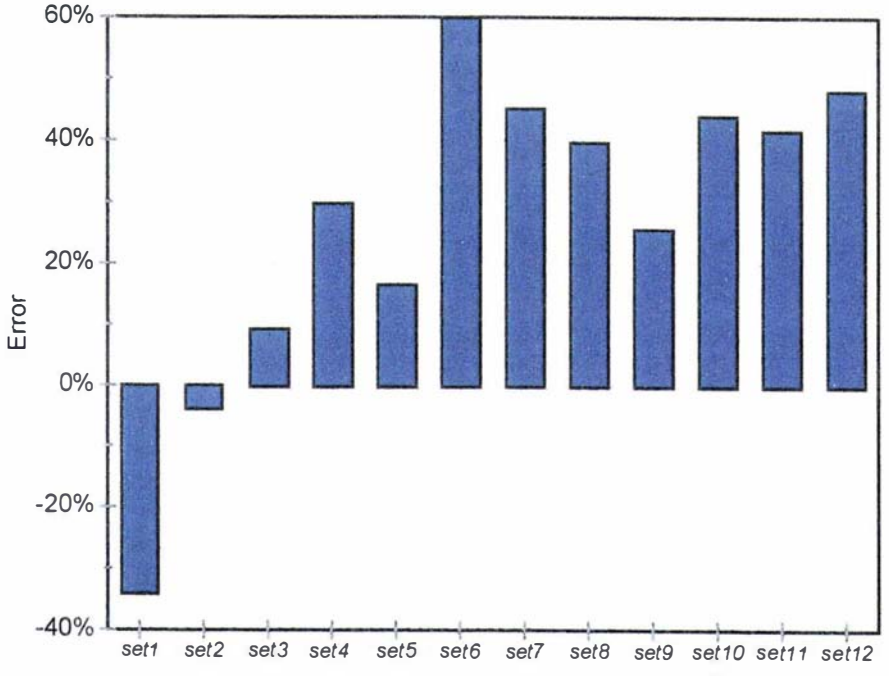

Figure C.32 Percentage error of predicted mol fraction of ethanol at the bottoms stream of column ED. Percentage error defined as: [(experimental value - calculated value) / experimental value] × 100.

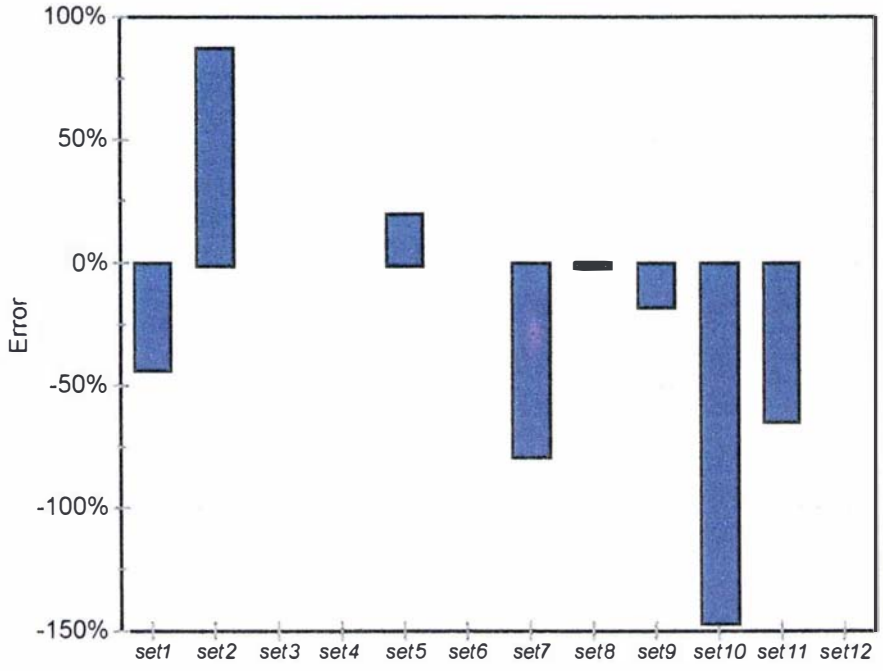

Figure C.33 Percentage error of predicted mol fraction of *i*-amyl alcohol at the bottoms stream of column ED. Percentage error defined as: [(experimental value - calculated value) / experimental value] × 100.

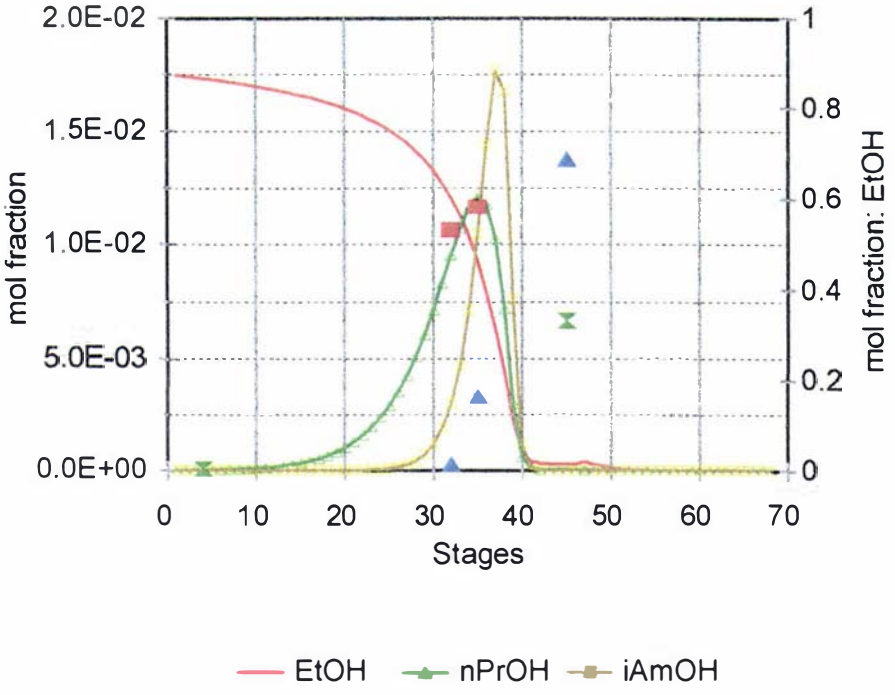

Figure C.34 Calculated concentration profile of RC column with ChemSep® and experimental values from 11-Sep-95, set 1. Experimental data: ■: EtOH; ▲: nPrOH; ⧗: iAmOH. EtOH: ethanol; nPrOH: *n*-propanol; iAmOH: *i*-amyl alcohol.

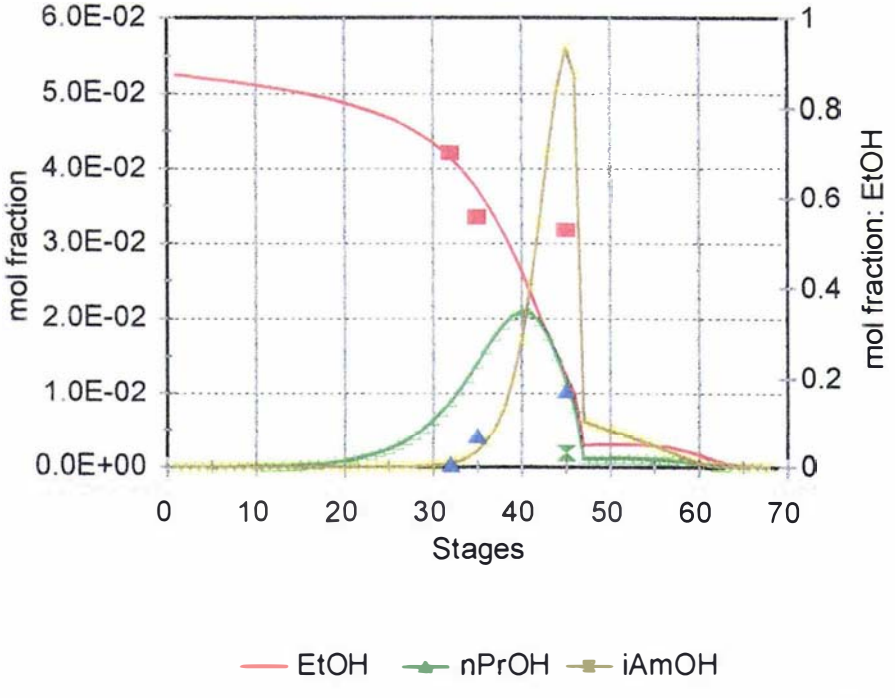

Figure C.35 Calculated concentration profile of RC column with ChemSep® and experimental values from 11-Sep-95, set 2. Experimental data: ■: EtOH; ▲: nPrOH; ⧗: iAmOH. EtOH: ethanol; nPrOH: *n*-propanol; iAmOH: *i*-amyl alcohol.

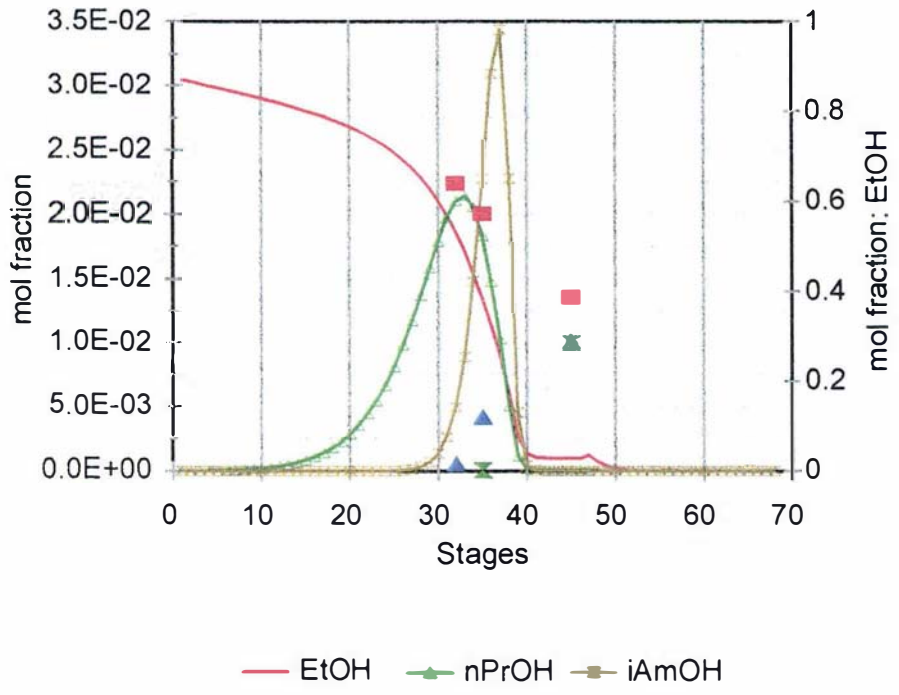

Figure C.36 Calculated concentration profile of RC column with ChemSep® and experimental values from 11-Sep-95, set 3. Experimental data: ■: EtOH; ▲: nPrOH; ⧗: iAmOH. EtOH: ethanol; nPrOH: *n*-propanol; iAmOH: *i*-amyl alcohol.

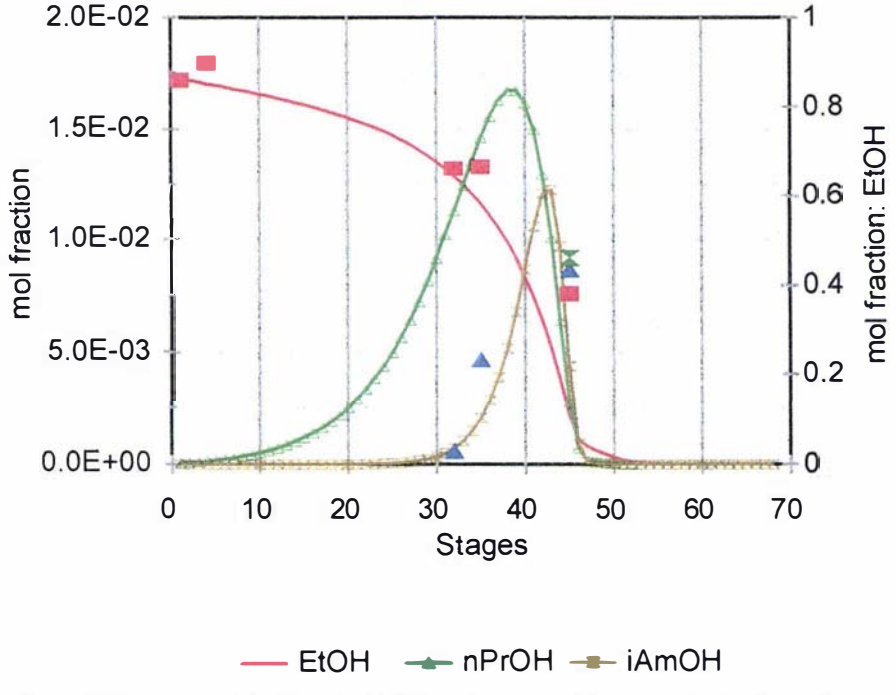

Figure C.37 Calculated concentration profile of RC column with ChemSep® and experimental values from 22-Nov-95, set 4. Experimental data: ■: EtOH; ▲: nPrOH; ⧗: iAmOH. EtOH: ethanol; nPrOH: *n*-propanol; iAmOH: *i*-

amyl alcohol.

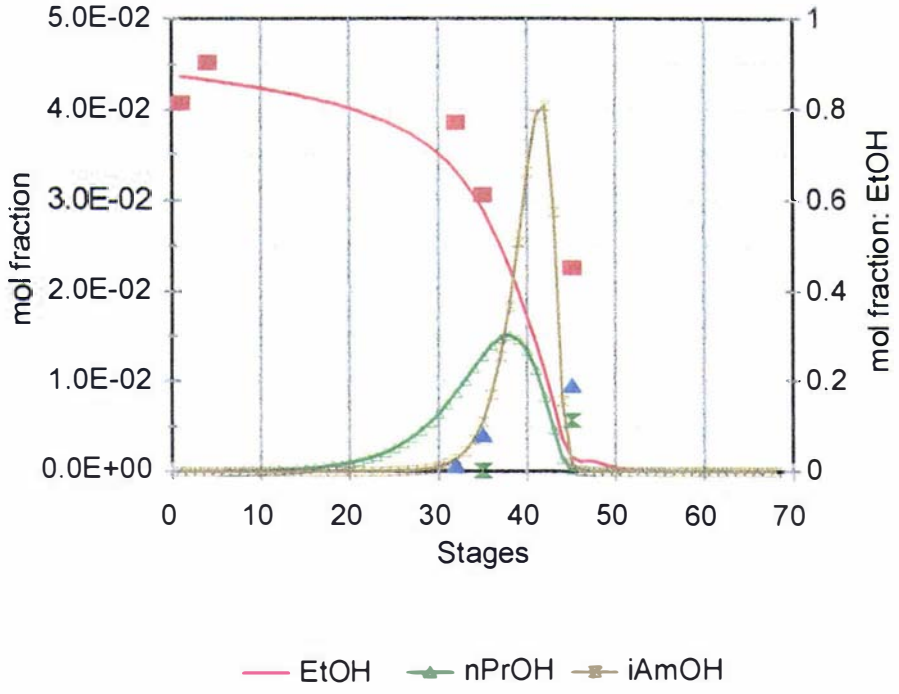

Figure C.38 Calculated concentration profile of RC column with ChemSep® and experimental values from 22-Nov-95, set 5. Experimental data: ■: EtOH; ▲: nPrOH; ⧗: iAmOH. EtOH: ethanol; nPrOH: *n*-propanol; iAmOH: *i*-amyl alcohol.

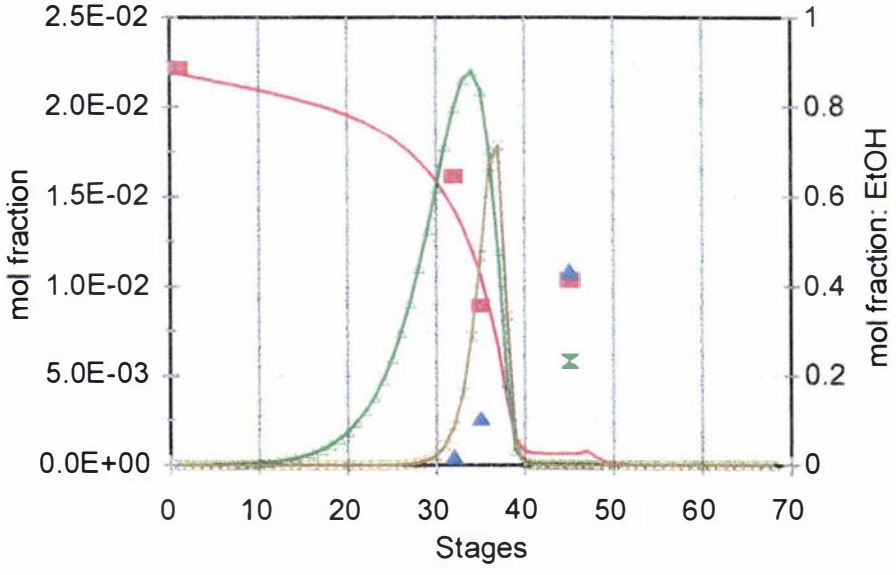

Figure C.39 Calculated concentration profile of RC column with ChemSep® and experimental values from 22-Nov-95, set 6. Experimental data: ■: EtOH; ▲: nPrOH; ⧗: iAmOH. EtOH: ethanol; nPrOH: *n*-propanol; iAmOH: *i*-amyl alcohol.

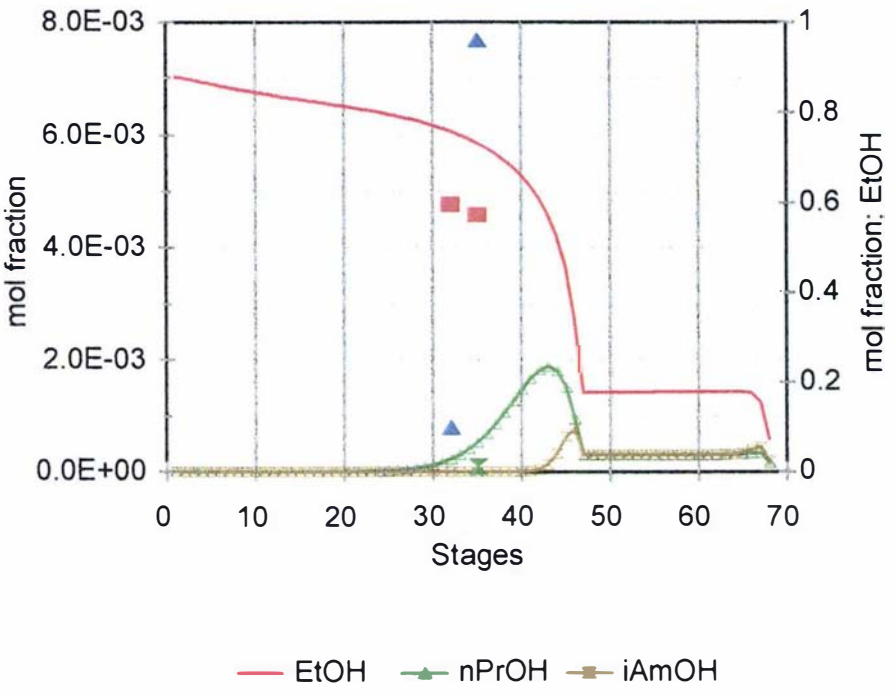

Figure C.40 Calculated concentration profile of RC column with ChemSep® and experimental values from 05-Mar-96, set 7. Experimental data: ■: EtOH; ▲: nPrOH; ⧗: iAmOH. EtOH: ethanol; nPrOH: *n*-propanol; iAmOH: *i*-amyl alcohol

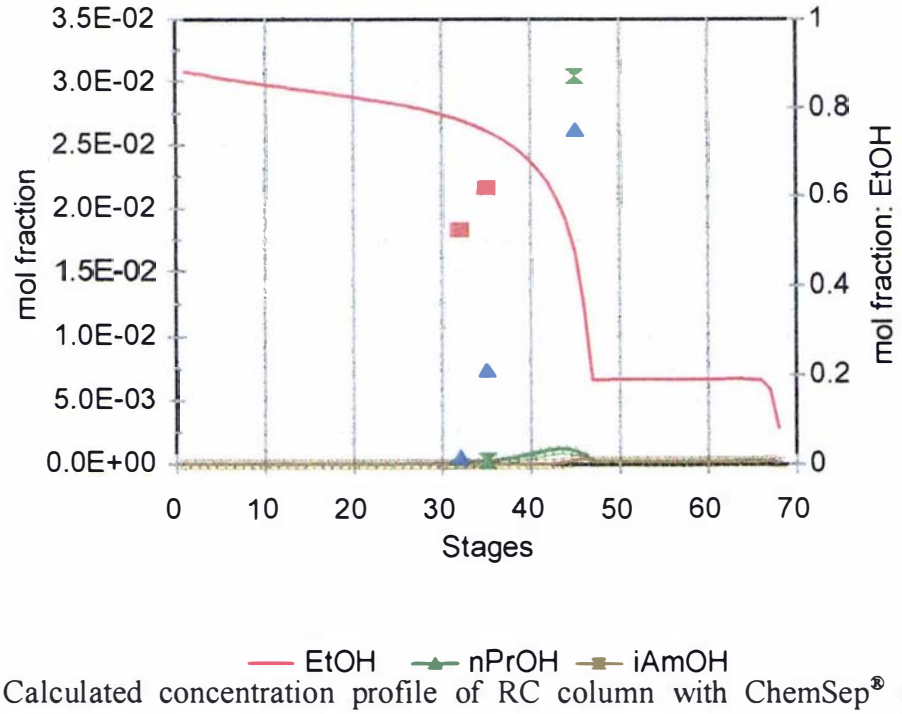

Figure C.41 Calculated concentration profile of RC column with ChemSep® and experimental values from 05-Mar-96, set 8. Experimental data: ■: EtOH; ▲: nPrOH; ⧗: iAmOH. EtOH: ethanol; nPrOH: *n*-propanol; iAmOH: *i*-amyl alcohol.

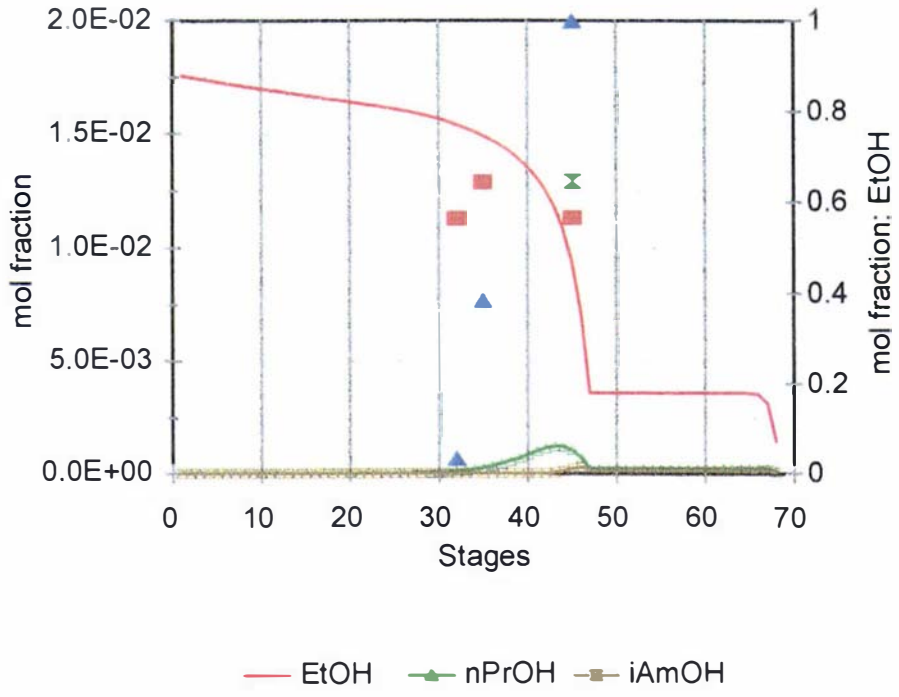

Figure C.42 Calculated concentration profile of RC column with ChemSep® and experimental values from 05-Mar-96, set 9. Experimental data: ■: EtOH; ▲: nPrOH; ⧗: iAmOH. EtOH: ethanol; nPrOH: *n*-propanol; iAmOH: *i*-amyl alcohol.

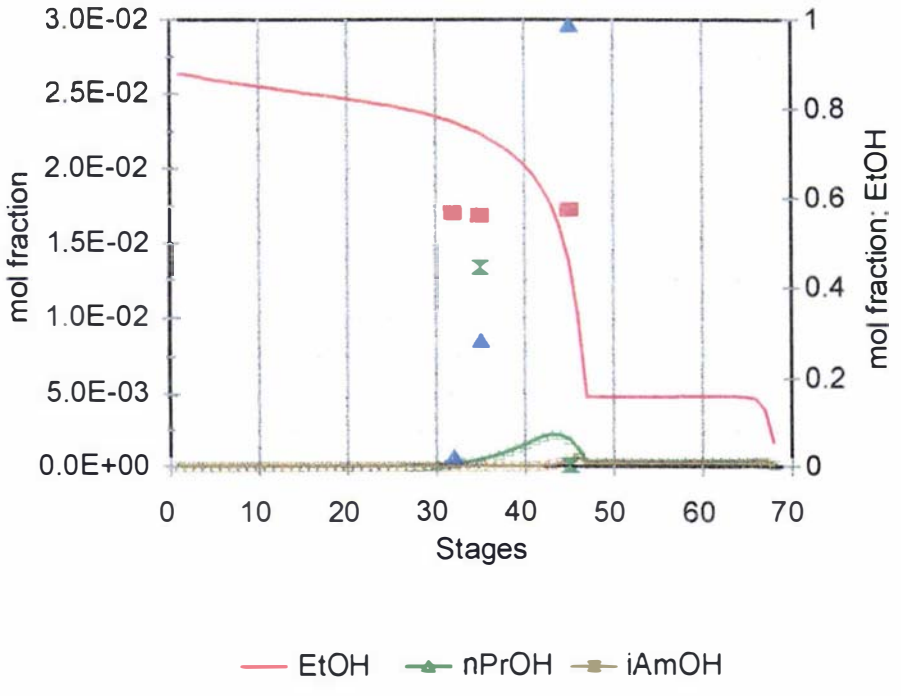

Figure C.43 Calculated concentration profile of RC column with ChemSep® and experimental values from 25-Apr-96, set 10. Experimental data: ■: EtOH; ▲: nPrOH; ⧗: iAmOH. EtOH: ethanol; nPrOH: *n*-propanol; iAmOH: *i*-amyl alcohol.

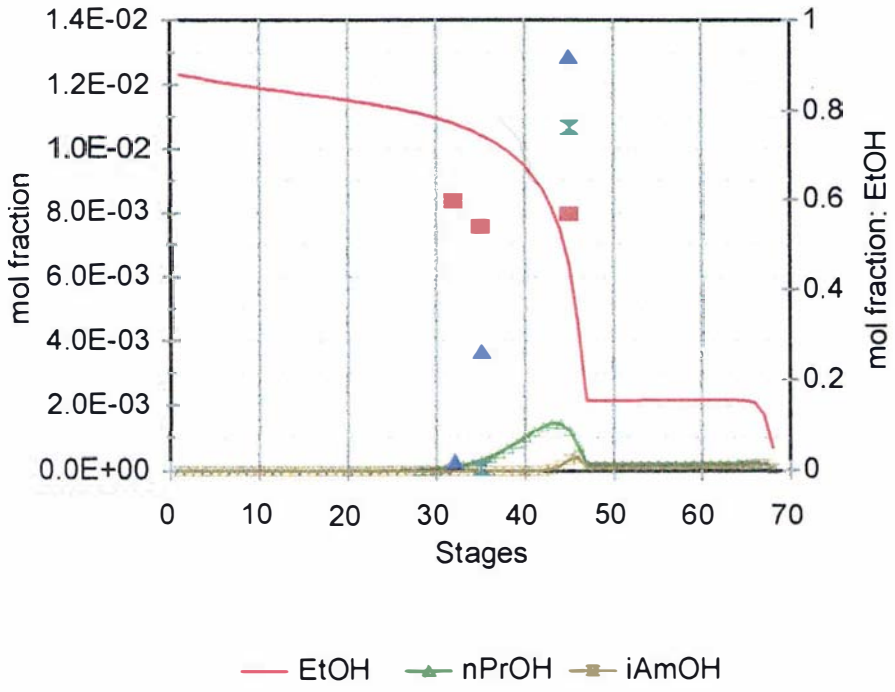

Figure C.44 Calculated concentration profile of RC column with ChemSep® and experimental values from 25-Apr-96, set 11. Experimental data: ■: EtOH; ▲: nPrOH; ⧗: iAmOH. EtOH: ethanol; nPrOH: *n*-propanol; iAmOH: *i*-amyl alcohol.

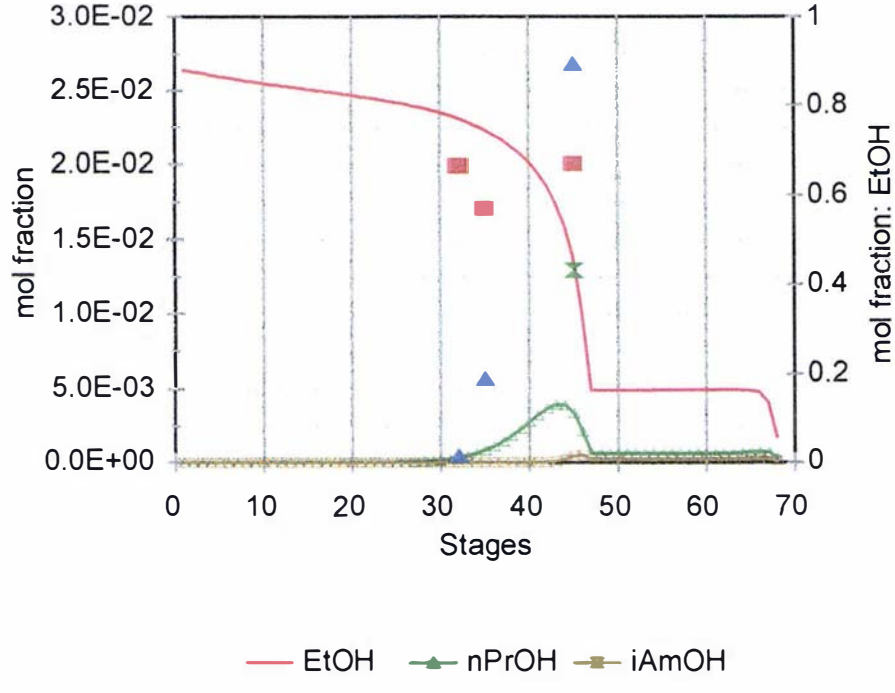

Figure C.45 Calculated concentration profile of RC column with ChemSep® and experimental values from 25-Apr-96, set 12. Experimental data: ■: EtOH; ▲: nPrOH; ⧗: iAmOH. EtOH: ethanol; nPrOH: *n*-propanol; iAmOH: *i*-amyl alcohol.

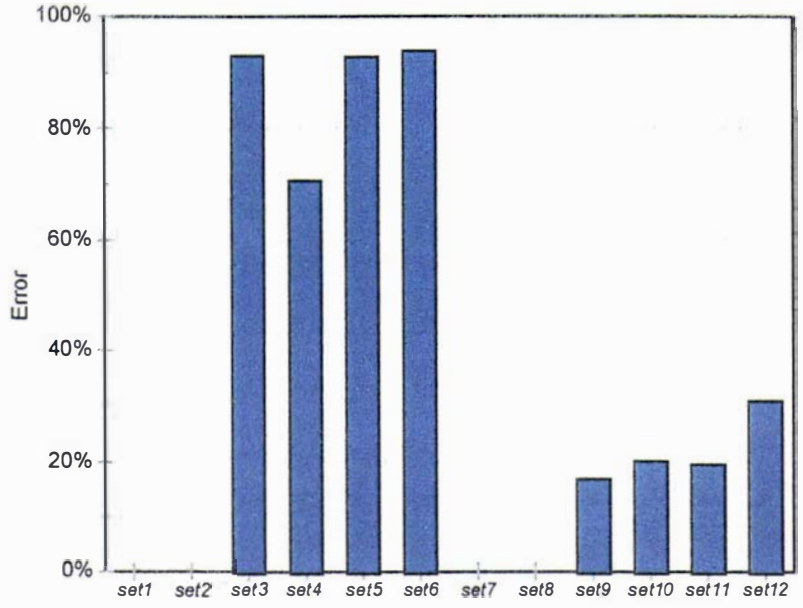

Figure C.46 Percentage error of predicted mol fraction of ethanol at the side stream of column RC (FI-21).

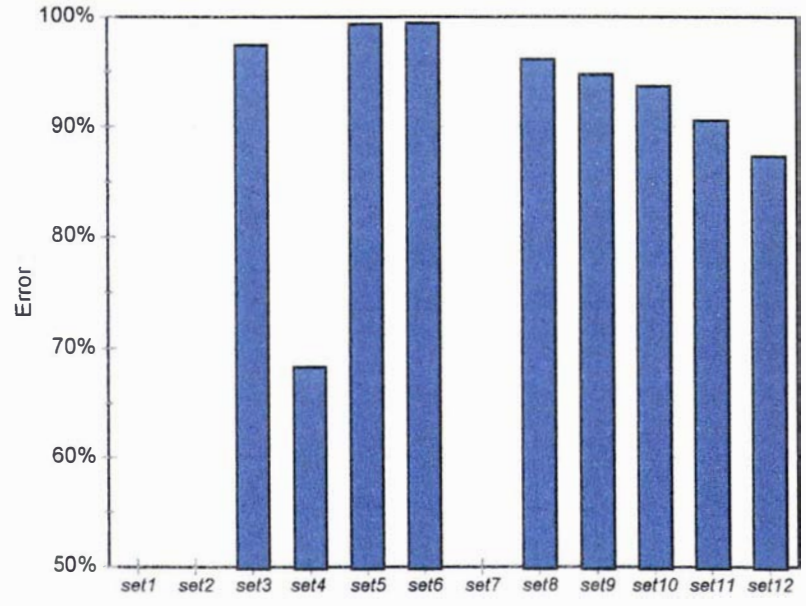

Figure C.47 Percentage error of predicted mol fraction of *n*-propanol at the side stream of column RC (FI-21). Percentage error defined as: [(experimental value - calculated value) / experimental value] × 100.

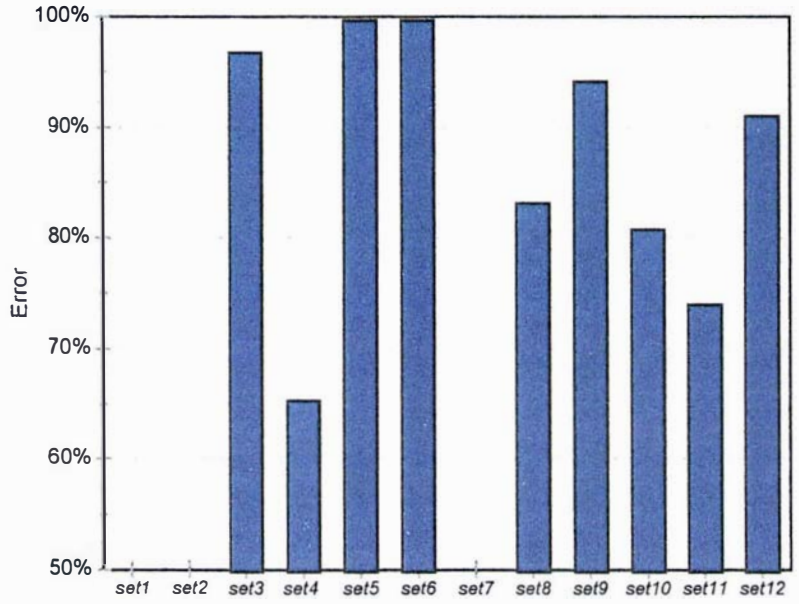

Figure C.48 Percentage error of predicted mol fraction of *i*-butanol at the side stream of column RC (FI-21). Percentage error defined as: [(experimental value - calculated value) / experimental value] × 100.

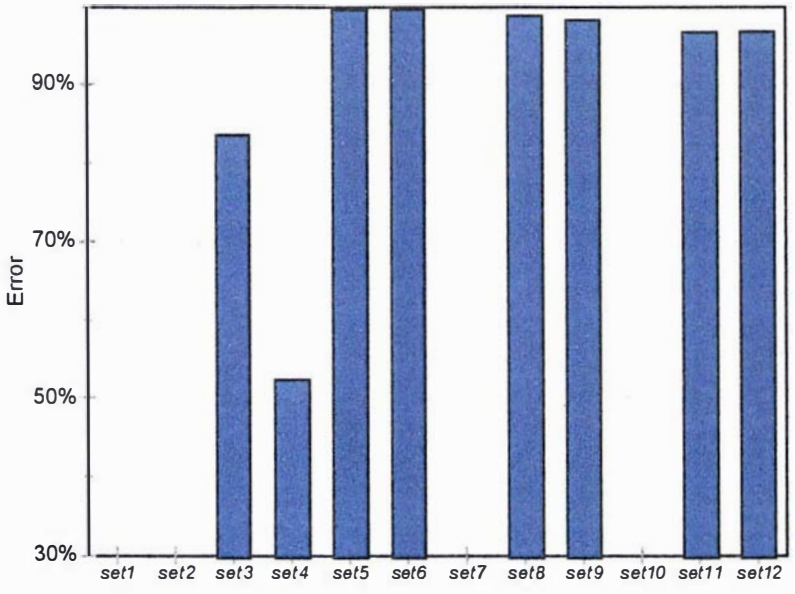

Figure C.49 Percentage error of predicted mol fraction of *i*-amyl alcohol at the side stream of column RC (FI-21). Percentage error defined as: [(experimental value - calculated value) / experimental value] × 100.

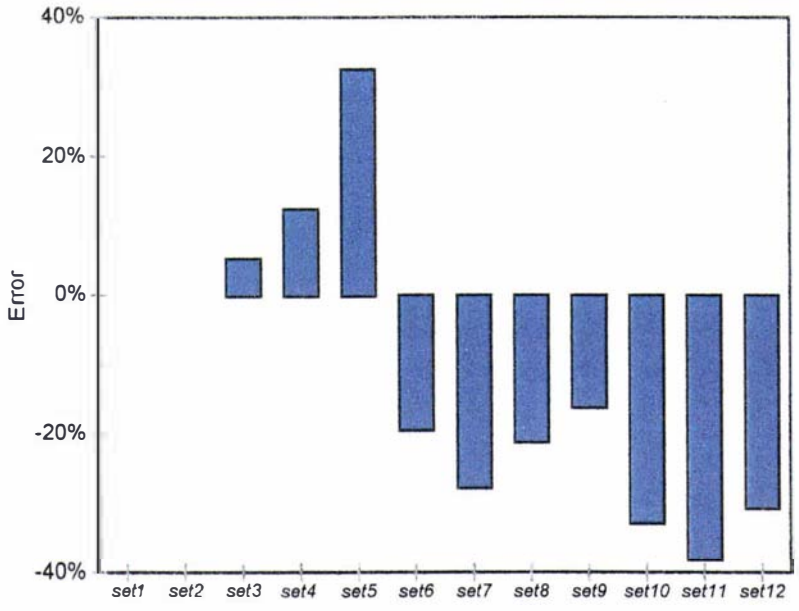

Figure C.50 Percentage error of predicted mol fraction of ethanol at the side stream of column RC (FI-22). Percentage error defined as: [(experimental value - calculated value) / experimental value] × 100.

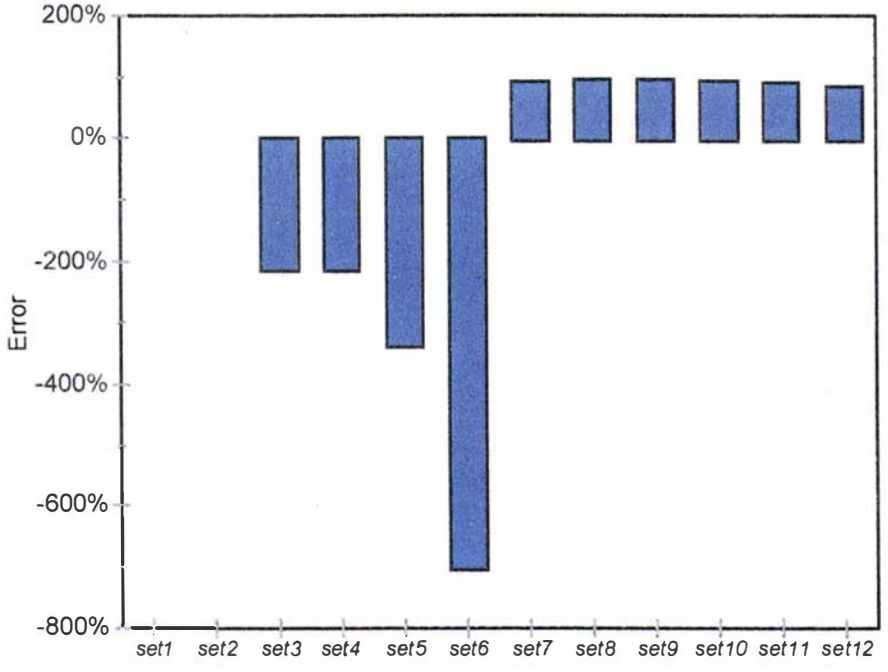

Figure C.51 Percentage error of predicted mol fraction of *n*-propanol at the side stream of column RC (FI-22). Percentage error defined as: [(experimental value - calculated value) / experimental value] × 100.

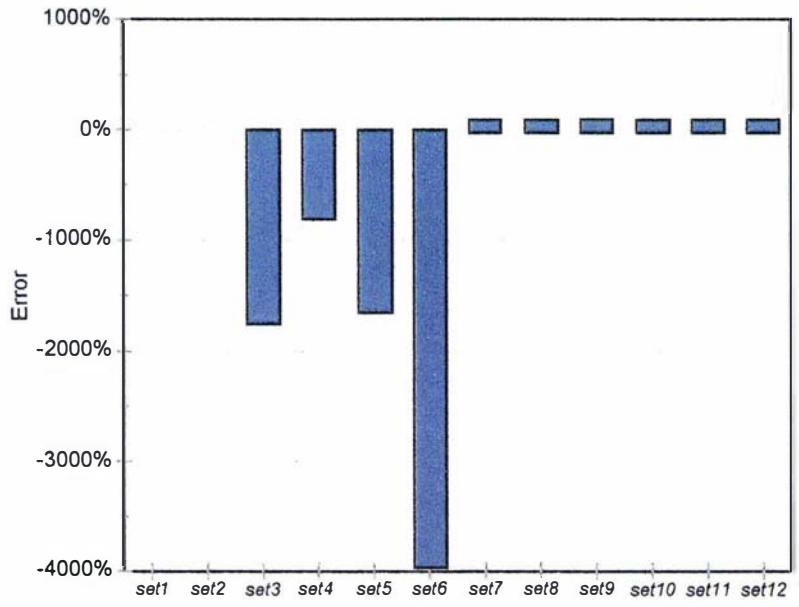

Figure C.52 Percentage error of predicted mol fraction of *i*-butanol at the side stream of column RC (FI-22). Percentage error defined as: [(experimental value - calculated value) / experimental value] × 100.

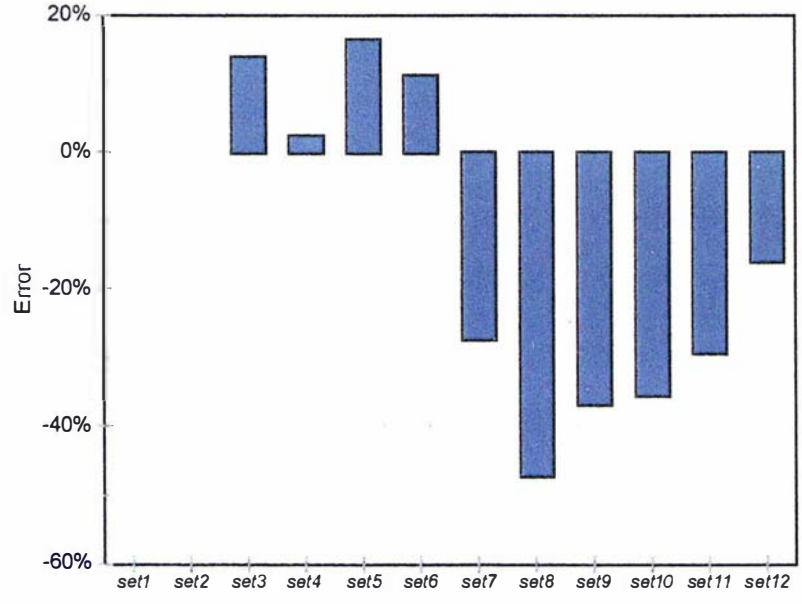

Figure C.53 Percentage error of predicted mol fraction of ethanol at the side stream of column RC (FI-23). Percentage error defined as: [(experimental value - calculated value) / experimental value] × 100.

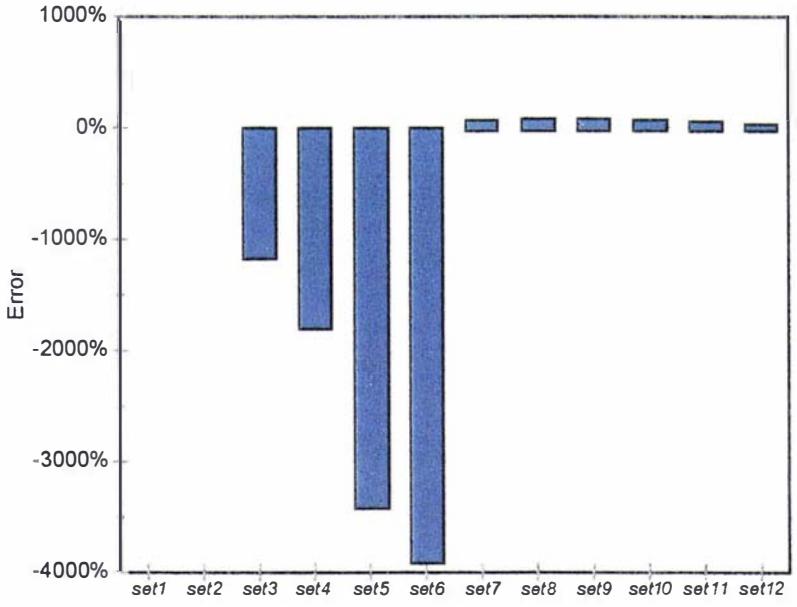

Figure C.54 Percentage error of predicted mol fraction of *n*-propanol at the side stream of column RC (FI-23). Percentage error defined as: [(experimental value - calculated value) / experimental value] × 100.

Appendix D

List of publications

Ferreira L.B., Mawson A.J. and Cleland D.J. (1997) *The role of sorption in the pervaporation of aqueous mixtures of alcohols and esters using poly-ether-block-amide membranes.* CHEMECA 97, Rotorua, N.Z.

Ferreira L.B., Mawson A.J. and Cleland D.J. (1997) *A study of pervaporation using organophilic membranes and aqueous solutions of alcohols and esters.* NAMS 97, Baltimore, U.S.A.

Ferreira L.B., Mawson A.J. and Cleland D.J. (1996) *Pervaporation with organophilic membranes.* Proceedings of the III NZ Conference of Postgraduate Students in Engineering and Technology, Christchurch, N.Z.

Appendix E

INDEX TO DISKS

Disk 1 contains all ChemSep® files for simulations of the RC column. These files can be opened with any word processor.

Disk 2 contains all ChemSep® files for simulations of the BC, PC, and ED columns. These files can be opened with any word processor.

Disk 3 contains all Hysim® (*.sim; *.txt), and all MatLab® program (*.m), results files (*.res) files, and spreasheets with summary of results (*.wb2).

Disk 4 contains all Hero® files (*.s) pertinent to pinch analysis.
contains all files pertinent to Chapter XI.

ERRATA

p.2, paragraph 3, line 4 "... feasible if membrane price ..." should read "...feasible if the membrane price..."

p.5, paragraph 2, line 6 "... and co-workers at the American ●il in the early ..." should read "... and co-workers in the early..."

p. 9, last line " ...of theorganic components..." should read "...of the organic components..."

p. 12, paragraph 3, line 5 "... is close its vapour equilibrium..." should read "... is close to its vapour equilibrium..."

p. 20 equation II.19

$$J_i = - D_i \, c_i^m \, \nabla(\ln \, a_i)$$

p. 61, line 4 "... of the permeability the membrane thickness..." should read "... of the permeability to the membrane thickness..."

p. 85, paragraph 2, line 3 "... opereating temperature..." should read "...operating temperature..."

p. 102, paragraph 1, line 4 "... Reid *et al.* (1986)..." should read "...Reid *et al.* (1987)..."

p. 103, last line "... of zeolites the enrichment factor..." should read "... of zeolites on the enrichment factor..."

p. 107, paragraph 1, line 1 "... reported a pervaporation enrichment factor..." should read "... reported pervaporation enrichment factor..."

p. 114, paragraph 1, line 3 "... van der Waal..." should read "...van der Waals..."

p. 120, paragraph 4, line 1 " postulate" should read "postulation"

p. 120, paragraph 4, line 2 "... using hydrophobic membrane..." should read "... using a hydrophobic membrane..."

p. 120, paragraph 4, line 3 "menat" should read "meant"

p. 121, paragraph 2, line 3 "... the external solvent solution..." should read "...the solvent solution at the interface..."

p. 129, Table V5 "... pencentage..." should read "... percentage..."

p. 129, paragraph 2, line 1 " ..., it would..." should read "...it might have been

anticipated that ..."

p. 146, line 2 "seeme" should read "seems"

p. 158, paragraph 1, line 5 "...Zadow, 1984..." should read "...Zadow, 1992..."

p. 168, paragraph 1, line 6 "... maximazing..." should read "... maximizing..."

p. 245, paragraph 2, line 1 "... the flux through the membrane..." should read "...the flux of water through the membrane..."

p. 251, paragraph 2, line 7 "... it is recommended to operate the pervaporation unit..." should read "... it is recommended that the pervaporation unit is operated at the highest possible temperature..."

p. 270

S entropy $J.mol^{-1}$

p. 275

Colman D., Naylor T., & Pearce G. (1990). *Alcohol dehydration by pervaporation*. UK: Elsevier.

p. 277

Fieldes (1990) *Untitled*, NZ. [internal report - The New Zealand Distillery Co. Ltd]

p. 284

Ray R., Friesen D., Newbold D., Anger L., Barss B., & McCray S. (1997). Distillation/membrane hybrid system for organic solvent dehydration. *Proceedings of the 9th Annual Meeting, North American Membrane Society* (p. C3). USA.

Rhim J.W. & Huang R.Y.M. (1989). On the prediction of separation factor and permeability in the separation of binary mixtures by pervaporation. *J.Membr.Sci.*, **46**, 335-48.